ETH
Eidgenössische Technische Hochschule Zürich
Swiss Federal Institute of Technology Zurich

Entrepreneurial Risks

Master Thesis
at the Department of Management Technology and Economics

Dragon-Kings in financial data - study at different time scales -

Xavier Meseguer

Advisor: Dr. Ryan Woodard
Professor: Prof. Dr. Didier Sornette

January 27, 2010

Abstract

Drawdowns (loss from the last local maximum to the next local minimum) offer a more natural measure of the financial market dynamics than fixed time-scale measures. We study the presence of *Dragon Kings* corresponding to meaningful outliers in the distribution of drawdowns at different time scales - from 1-min to daily. Our analysis comprises nine time series of prices of futures tracking major stock indexes (S&P, FT-SE, Nikkei), currencies (Yen, DM) and government bonds (Japan, US, Germany).

We find no empirical evidence of the presence of *Dragon-Kings* for high frequency data, 1-min resolution. Nevertheless, for the largest scales, namely daily, the statistical tests applied demonstrate that the 1% quantile of the largest events of the population of drawdowns belong to a distribution significantly different from the rest. For the other scales, the test results are inconclusive. This results suggest that the feedback mechanisms present in the *Dragon-Kings* require a certain time to build-up.

Contents

1

Introduction

Pervasive in our lives, natural systems (e.g. earthquakes) and social systems (e.g. stock market) exhibit *emergent* properties originating in the interconnections and relationships among the mutually interacting parts that form them. Often, these properties take the form of large events and have very little in common with the characteristics of the forming parts.

In a Gaussian world, using N.Taleb's [33] toponym "Mediocristan", large events are extremely rare and often neglected as too seldom to be taken into consideration, albeit they represent huge losses. These extreme events are quantified by heavy-tailed distributions of event sizes. In the literature, extreme events are treated from two opposing perspectives.

On the one hand, the concept of extreme events being rather frequent and resulting from the same organization principles as those generating other "mediocre" events, they belong to the same statistical distribution, often modeled as a power law. In this view, a DJIA fall of 50 bp dip belongs to the same family as the large "Black Monday" plunge and thereby the originating mechanisms are essentially akin. Inherent to this definition is the unpredictability of extreme events, since the search for a precursor is hampered by them sharing all characteristics (but the size) with their smaller siblings. This view reduces remarkable events to "unknown unknowables" with little or no human responsibility and more typical of the result of the "wrath of God". This vision is embraced by Bak and co-workers in their formulation of self-organized criticality [3] and by the so-called "Black Swan" concept popularized by N.A. Taleb [33].

In a shadow of stoic pessimism populated by "Black Swans" a new concept brings a new light to the problem of prediction. This concept termed by Sornette and collaborators as genuine "outliers" or even better

"kings" [13] or "Dragons" [29] seeks life beyond power laws. The concept of *Dragon-Kings* compiles instances in different realms suggesting that extreme events are even "wilder" than predicted by the extrapolation of the power law distributions in the tail and belong to a statistical population which is different from the bulk of the distribution of smaller events. Evidence points out that at the origin of these extreme events there are transient mechanisms of self-organization. Empirical evidence of the presence of *Dragon-Kings* has been found in the Zipf distribution of city sizes [13, 26], in material rupture processes [27], in epileptic seizures [21] and most interestingly for our study in the distribution of financial market drawdowns (runs of losses) [28, 11, 31].

It is now amply accepted that the distribution of asset returns is fat-tailed. More formally, it has been shown that the tails of the distribution of returns follows approximately a power law $P(return > x) \sim C/x^{\mu}$, with estimates of the 'tail indexes' μ falling in the range 2 to 4 [1, 8, 18, 6]. No trace of *Dragon-Kings* is apparent in the tail of the distribution.

But this is missing the forest for the trees! Fixed time scale measures fail to capture transient bursts of dependence that reside at the origin of large financial crashes. Let us take an example to clarify this claim. Consider a crash that unravels itself in a period of three successive drops of 10% each, summing up to a total of 30%. A, 10% market drop that occurs over one day can be seen in the data of the Nasdaq composite index to happen on average once every four years. According to this, how long do we have to wait for a crash such as the one described above to occur? Such an event has a recurrence of 4 million years! Hence, it should never be observed in our short available time series. However, there is ubiquitous evidence of such crashes occurring in the past century. How is this possible? Common reasoning is based on the assumption that consecutive drops are independent but this appears not to be always true. Hence, fixed time-scale measures that chop large crashes into small independent events will miss the underlying dynamics of the system [7]. Drawdowns will be presented in section 2 as a natural measure to capture these bursts of dependence.

There is ample empirical evidence of the presence of *Dragon-Kings* in the financial world; major indexes, currencies and market capitalization of the largest companies have been shown to exhibit clear "outlier" drawdowns [11]. This suggests that outliers constitute a ubiquitous feature of financial markets, independently of their underlyings.

Nevertheless, to our knowledge, the presence of *Dragon-Kings* was, at the time of writing, only tested at daily time scale. That is, drawdowns were solely composed of daily returns. In this paper we study the presence of *Dragon-Kings* in the distribution of drawdowns for different time scales, ranging from 1-minute up to daily. The research question

we are empirically seeking to answer is: are *Dragon-Kings* present at all time scales? If not, is there a threshold upon which they seem to emerge? The data sets used in our work are nine time series of prices of futures tracking major stock indexes (S&P, FT-SE, Nikkei), currencies (Yen, DM) and government bonds (Japan, US, Germany). These will be presented in section 3.

It is key to understand that diagnosing *DK* is a subtle problem that requires a battery of tools to pile up evidence of their presence. Our "toolbox" will be explained in section 4.

Section 5 presents the results and discussion and section 6 concludes.

2

Drawdowns in high-frequency data

2.1 Introduction

Drawdowns are relevant risk management tools for they present the cumulative loss that an investment may suffer. That is to say, they represent the worst case scenario of an investor buying at the local high and selling at the next minimum.

This chapter is an introduction to the concept of the "drawdown". This concept will be presented in its classic form in section 2.2 as a starting point for our analysis. In section 2.3 this first definition will be extended to deal with the inherent stronger fluctuations in our high-frequency data. Section 2.4 and 2.5 motivates the study of drawdowns before other classic metrics and introduces a theoretical approach to the expected distribution of drawdowns, respectively.

2.2 The *pure* drawdowns

In early works by Johansen and Sornette [10] drawdowns were simply defined as persistent decrease in the price at the close of each successive trading day (daily close). A drawdown was thus the cumulative loss from the last maximum to the next minimum. Notice that a drawdown was always composed of returns of negative sign and its duration is a random variable.

This definition is highly exposed to noise and fails to account for the full intensity of the market cumulative drop. This short-coming is particularly sensitive for our purpose *à cause* of the noisy nature of our high-frequency data.

2.3 The coarse-grained drawdowns

The *pure* drawdown is terminated by *any* increase in the price (positive return) no matter how small. This definition is very sensitive to noise, *i.e.*, to random uncorrelated as well as correlated fluctuations in the price. We now take this definition a step further and present price coarse-grained drawdowns, more specifically, "ϵ-drawdowns".

"ϵ-drawdowns" as defined by J&S in [12] ignore increases below a certain magnitude, ϵ, which would traditionally terminate the drawdown. Notice that for $\epsilon = 0$, we obtain the "pure" drawdown. Per contra, for non-zero ϵ, we allow the drawdown to progress if the amplitude of the fluctuations remains below the threshold, ϵ.

2.3.1 The fixed $\epsilon-$drawdowns

In the spirit of Johansen and Sornette [12] we extend the definition of the *pure* drawdown and introduce a parameter ϵ that ignores fluctuations below a certain threshold. This threshold is fixed throughout the time series and is defined relative to the standard deviation of returns as,

$$\epsilon = \epsilon_0 \cdot \sigma_{ret} \tag{2.1}$$

The threshold is proportional to the standard deviation of the returns calculated for the entire series, σ_{ret}. The coefficient ϵ_0 is chosen from the observation of data.

2.4 Motivation for the study of drawdowns

The distribution of drawdowns captures the way successive drops can influence each other and construct in this way a persistent process. This persistence is not measured by the distribution of returns because, by its very definition, it neglects the relative position of the returns as they unravel themselves as a function of time by only counting their frequency. Akin, two point correlation is a mere linear dependency average incapable of grasping the subtleties of these interdependencies as the examples in section 2.4.1 and 2.4.2 exhibit.

2.4.1 A nonlinear model with zero correlation but strong dependence

To better elucidate the importance of drawdowns in capturing successive price variations, we propose an example, borrowed from [25, 9] and studied in depth in [32], which shows how two-point correlation, unlike drawdowns, washes out important burst of dependence.

Let us consider the process, in which price movements $r(t)$ are constructed in the following fashion:

$$r(t) = \epsilon(t) + \epsilon(t-1)\epsilon(t-2), \tag{2.2}$$

where $\epsilon(t)$ is a white noise process with zero mean and unit variance $N(0,1)$. The process described by Eq.:2.2 is also a white noise process since both mean $E(r(t) = 0)$ and two-point correlation $E(r(t)r(t'))$ for $t \neq t'$ are zero. Despite the nonexistence of a serial correlation there is potential for non-linear predictability since the three point correlation function is nonzero and equal to 1. That is, $E(r(t)r(t-1)r(t-2)) = 1$. This implies that it should be possible to predict in part the next return $r(t)$ already from the knowledge of the two past returns $r(t-1)$ and $r(t-2)$.

Where frequency distribution and two-point correlation have failed, the distribution of drawdowns will succeed! Following the example, table 2.4.1 presents the value that a price variation $r(t)$ may take corresponding to $\epsilon(t)$.

$\epsilon(t-2), \epsilon(t-1), \epsilon(t)$	$\rightarrow$	$r(t)$
$+++$	$\rightarrow$	+2,
$++-$	$\rightarrow$	0,
$+-+$	$\rightarrow$	0,
$+--$	$\rightarrow$	-2,
$-++$	$\rightarrow$	0,
$-+-$	$\rightarrow$	-2,
$--+$	$\rightarrow$	+2,
$---$	$\rightarrow$	0,

Tab. 1: Increments in price ($r(t)$) corresponding to the last three realizations of $\epsilon(t)$, as defined in Eq.:2.2. (+) means $\epsilon(\tau) = 1$, (-) means $\epsilon(\tau) = -1$.

A close inspection reveals that there is room for prediction if we look at the distribution of drawdowns. There are no drawdowns of duration larger than two. Indeed, the worst scenario corresponds to the sequence for ϵ: $--+--$. This forms the sequence of price increments: $+2, -2, -2$ which is interrupted by +2 after $\epsilon(t+1) = +1$ either immediately or

after an undefined sequence of $\epsilon = -1$. While the drawdowns of the process $\epsilon(t)$ can in principle be of infinite duration, the drawdowns of the price cannot. This shows that the structure of the process $r(t)$ defined by Eq.:2.2 has a clear signature in the distribution of price drawdowns. This example illustrates how the distribution of drawdowns grasps the subtle dependencies of the process $r(t)$ described by equation 2.2 better than two-point correlation or any other fixed time scale measures.

2.4.2 Drawdowns capture serial information

By looking only at daily returns we destroy the information that daily returns may be correlated at special times, the so-called burst of dependence. However, variable-time measures (i.e. distribution of drawdowns) will capture the information of these happening sequentially.

Let us consider the example of a hypothetical fall of 15% occurring over five consecutive days with losses of 3% each day. In a Bachelier-Samuelson [2] world modeled by a Gaussian bell-shaped distribution, the event of a 3% loss in DJIA occurs once every 1.5 years (P(x>3%)=0.0027), relatively frequently. However, if we apply elementary probability theory, under the assumption of independence, to finding out what the probability of five such events taking place: $(0.0027)^5 \cong 1.4 \cdot 10^{-}13$ or which is the same a recurrence time of 27,876 million years, about twice the age of the universe.

History proves this estimation wrong, with many instances where such drops occurred. Hence, the flaw in the argument lies on the assumption of these events being independent, we indeed experience *bursts of dependence*. Evidently, drawdowns will keep the information in the sequence and will not dissect a singular event into several 'mediocre' small occurrences. In the words of Sornette [29] "by cutting the mammoth in pieces, we only observe mice".

2.5 Expected distribution of drawdowns for independent price variations

Drawdowns may be composed of negative price returns of similar size contributing alike, what we call the *democratic* case, or may be ruled by a few large losses, the *tyrannic* regime. This composition is characterized by the size distribution of the negative returns.

The *tyrannic* regime will appear when negative returns decay slower than exponential *i.e.*, belong to the class of sub-exponential distributions

(such as the power law or stretched exponential), and will lead to the tail of the distribution of drawdowns asymptotically being the same as the distribution of the individual price variations.

In contrast, under the null hypothesis of (*i*) independent and identically distributed consecutive price returns[1] and (*ii*) pdf of returns no fatter than exponential, the probability density function of dd is expected to be exponential. Hence, following [12, 11], the probability $P(D)$ to observe a drawdown of size D is

$$P(D) = \frac{p_+}{p_-} \sum_{n=1}^{\infty} \int_{-\infty}^{0} dx_1 p(x_1) \cdots \int_{-\infty}^{0} dx_n p(x_n) \delta(D - \sum_{j=1}^{n} x_j) \tag{2.3}$$

where

$$p_+ = 1 - p_- \equiv \int_0^{+\infty} dx p(x) \tag{2.4}$$

is the probability to observe a positive return and the term p_+/p_- ensures the normalization of $P(D)$. The sum over n in Eq.:2.3 takes into consideration all n possible lengths that sum up to be a drawdown of size D. Deriving from this expression we come to the conclusion that, under the assumptions (*i*) and (*ii*), the tail of the drawdown distribution is generically an exponential function

$$P(D) = \frac{e^{\frac{-|D|}{D_0}}}{D_0} \tag{2.5}$$

where $D_0 > 0$ is the typical amplitude of the drawdown. For approximately symmetric distributions of daily returns, $p_+ = p_- = 1/2$, the typical drawdown has an amplitude of 4 times the average daily drop.

On the other hand, if we look at the duration of drawdowns, we also expect them to be exponentially distributed stemming from the assumed independence of signs of successive returns. The probability of a drawdown lasting n consecutive price variations is $p_+ p_-^n$ which can be rewritten using logarithms as

$$P(n \, price \, variations) = p_+ \exp(n \ln p_-) \tag{2.6}$$

which may be identified as an exponential distribution, thus, the typical duration is

$$n_0 = \frac{1}{\ln \frac{1}{p_-}} \tag{2.7}$$

[1] The condition of *iid* returns can be weakened and still lead to an exponentially decaying pdf of drawdons if the pdf of returns is not fatter than exponential

Since most markets can be characterized almost symmetrically, the probability of a loss p_- is close to 1/2 leading to a typical drawdown duration of $n_0 = 1/\ln 2 \approx 1.44$ consecutive downward price movements[2]. Notice that this process is memoryless since the occurrence of an arbitrary number n of successive negatives does not modify the probability of the new event, and illustrates the fact that increasing a drawdown by a time unit, halves its probability of occurrence. Any deviation from this behavior would indicate traces of correlation and, thus, room for prediction.

Previous studies [1] suggest that for time scales from 5 min up to approximately 16 days, the tails of the distributions of returns can be well described by a power law decay, characterized by an exponent $\alpha \approx 3$. As a consequence, it is reasonable to expect the drawdowns to be ruled by a *tyrannic* regime and, hence, its distribution to belong to the sub-exponential class.

It has been demonstrated that the stretched exponential can provide any desired approximation to the Pareto distribution [30]. For its generality and the fact that it has been successfully used as a model for the distribution of DD for larger scale, the SE emerges as an adequate preliminary candidate for the distribution of drawdowns.

[2] An estimate for the typical DD size, D_o, can be derived from this expression. Still, this estimate will lead to smaller results than using expression 2.3 since it restricts the fluctuations of DD to only their length

3

Data

3.1 Description

In this paper we used high-frequency data prepared by Matt Lee as described in [15]. Our data set consists of nine time series of prices of futures tracking major stock indexes (S&P, FT-SE, Nikkei), currencies (Yen, DM) and government bonds (Japan, US, Germany).

Name	Data set	From	to	Size
IA	German Government Bond	29/09/88	30/09/97	1,059,343
IX	FTSE 100	02/01/86	30/09/97	857,479
DM	Deutschmark	02/12/74	26/02/99	1,415,007
JY	Japanese Yen	03/03/77	26/02/99	1,352,201
SP	SP 500	21/04/82	26/02/99	1,664,104
US1	T-Bonds	22/08/77	25/10/79	22,105
US3	T-Bonds	13/02/81	29/01/82	62,672
IJ	Japanese Government Bonds	10/07/87	31/07/97	178,971
NK	Nikkei 225	25/09/90	26/02/99	135,220

Tab. 2: Data set descriptions including time span and sample size

3.1.1 Handling of Tick data

Originally tick data, which records every transaction, was smoothed over 1-min time length. Gaps in time due to weekends and evenings were collapsed assuming a negligible volatility change over the gaps and that prices do not evolve nearly as fast when not traded. Furthermore, since several contracts can be traded simultaneously, data was prepared to ensure that only one price is considered at a time and that the transition to the next contract is done 'smoothly'.

3.1.2 Time-scale conversion

A rolling average algorithm was applied to the high-resolution data to smooth out high-frequency fluctuations and convert into larger scales. The algorithm uses a non-overlapping window of size corresponding to the target scale,*i.e.* 15-min, 1-hour or 1-day.

The algorithm calculates the average price value of the interval $[t[iW], t[(i+1)W]]$ where W is the size of the window wich corresponds to the scale we want to convert the data into.

4

Testing for Dragon-Kings: Methods

4.1 Testing drawdown distributions for Dragon-Kings

The goal of this study is to present evidence of the existence of the so-called *Dragon-Kings* in the distribution of drawdowns at different time scales. *DK* in financial markets are extreme events belonging to a different regime resulting from time dependence that may only appear at special times. For this purpose, as explained in Chap. 2, classical tools like distribution of returns or two-point correlation will fail to identify these bursts of dependence. Actually, testing for *DK* or more generally for a change of population in a distribution is a subtle new problem that requires clever new tools and there is no single methodology. In this section we present our toolset and methodology to approach the problem.

4.2 Complementary Cumulative Distribution Function (ccdf) of Drawdowns

Dragon-Kings can be diagnosed sometimes directly, in the form of obvious "breaks" or "bumps" in the tail of the distribution. We study the complementary cumulative distribution function (ccdf) of the absolute value of drawdowns which expresses how often the random variable of

the DD size is *above* a particular level. The ccdf is defined as,

$$F_c(dd) = P(DD > dd) = 1 - F(dd) \tag{4.1}$$

where $F(dd)$ is the cumulative distribution function of drawdowns. This function ($F_c(dd)$) is monotonically decreasing and, since the absolute size of a DD is necessarily positive, $F_c(0) = P(DD > 0) = 1$.

The logarithmic plot of the ccdf can be a very powerful tool to give a first indication of the distribution of drawdowns and, as mentioned above, suspicious deviations and "bumps" may be symptoms of a change of regime.

The visual inspection of the distribution provides a fast and useful tool to classify "unknown" distributions and decide which tests are more appropriate for each case. A Pareto distribution will appear as a straight line in the log-log plot and as a convex curve in the log-linear plot [30]. An exponential distribution will appear as a straight line in the log-linear plot and as a concave curve in the log-log plot.

4.3 T-statistics

Demonstrating that data do indeed follow a power law or an exponential distribution requires more complex techniques than a log-log or log-lin plot of the distribution. Indeed, several alternative functions can present similar forms, thus validating that a given data follows a certain distribution might not be trivial.

Several statistical tests are available to make a more quantitative study of the nature of the distribution (Kolmogorov-Smirnov) [6]. Still these tools only address the question of what is the average representation of the tail of the PDF (in some range predefined rather arbitrarily) and fail to test the adequacy of a given model as a function of the depth (quantile) in the tail of the PDF, [30, 17].

In [22] Pisarenko and Sornette present a new statistical tool (T-statistic) designed specifically to describe the behavior of the sample tail as compared with power-like and exponential tails as a function of the lower threshold u. Specifically, they introduce two statistics: *TP(u)* and *TE(u)*. The former, *TP(u)*, asymptotically converges to zero *for the power law tail described by the Pareto distribution:* $1 - F(x) = (u/x)^b : x \geq u$ *with arbitrary power index b.* The latter, *TE(u)*, has a similar behavior *for the exponential tail* $1 - F(x) = exp(-(x - u)/d) : x \geq u$ *with arbitrary form parameter d.* At the same time, both statistics deviate from zero for distributions different from the target one.

Hence, these statistics shall help answer what part of the tail may be

described by a Pareto (or exponential) distribution and which may not. Evidence of a different regime will be found if the largest part of the distribution of drawdowns is well described by either an exponential or Pareto decay and, upon a certain threshold u, if $TE(u)$ or $TP(u)$ is correspondingly significantly different from zero.

Implied from the above, this test is strongly *parametric*, *i.e.* reliable results for the diagnosis of *DK* may only be obtained if, indeed, the analyzed distribution follows either an exponential or a Pareto behavior.

These statistics and their properties are presented in Appendix B. Also in the Appendix, *TP*- and *TE*- statistics are applied on synthetically generated data belonging to known distributions to illustrate their behavior.

4.4 Surrogate data analysis

To further establish the statistical confidence with which we can conclude that the largest drawdowns are outliers, for each financial time series, we have reshuffled the return time series 500 times and hence generated the corresponding 500 synthetic data sets [11, 31]. These data sets will have *exactly* the same distribution of returns as each original series, by definiton. Nevertheless, high order correlations apparently present in the largest drawdowns are destroyed by the reshuffling. These synthetic data sets are used to construct drawdown distributions and these are compared with the DD distribution resulting from the original return series. Hence, if the original DD distribution does not exhibit a significant departure from the synthetic data sets, it fails to reject the hypothesis of order of returns not being paramount in the creation of the observed DD.

Furthermore, this surrogate data analysis of the distribution of drawdowns has the advantage of being *non-parametric, i.e.* independent of the quality of fits with a model. The drawback is that this kind of bootstrap analysis is "negative", we use these tests to *reject* a given null-hypothesis, not to *confirm* a given hypothesis.

4.5 Nested hypothesis testing

In the spirit of [11] we propose another test that aims to answer the question of whether there is a threshold quantile below which the null stretched exponential hypothesis cannot be rejected and beyond which it can.

Let us formally introduce the framework of the hypothesis testing. We consider a drawdown sample $X_1, \ldots, X_n$ with a probability density

function (pdf) $p(x|a)$, where a is some vector corresponding to the set of parameters in the pdf. This is to say, that the respective cumulative distribution is

$$P(x|a) = P(x = 0)\exp(-Bx^z + Cx^{2z}) \tag{4.2}$$

where a=(B,C,z). Taking C = 0 we obtain the "pure" stretched exponential (SE). The generic case of C $\neq$ 0, corresponds to the introduction of a non-linear term that represents the curvature or deviation from the straight line in the log-linear plot of $\ln P$ versus x^z that would qualify the stretched exponential as a straight line. This new candidate function will be referred to as the modified stretched exponential (MSE).

For the purpose of our study we will consider two hypotheses.

- H_1: the parametrical set a=(B,C,z) may take any real value in a three dimensional space I_1.
- H_0: is the particular case of H_1 in which C is fixed to 0, resulting in a parametrical subset of two dimensions, I_0. No need to say, that I_0 is a subset contained in I_1

Let us denote the maximum likelihood estimator under H_i as L_i, where $i = 0, 1$

$$L_0 = MAX_0[p(X_1|a)\ldots p(X_n|a)] \tag{4.3}$$

where 'MAX_0' is taken over a in the parametric interval I_0, and

$$L_1 = MAX_1[p(X_1|a)\ldots p(X_n|a)] \tag{4.4}$$

where 'MAX_1' in this case is obtained using the parametric interval I_1. By contruction the likelihood values of $L_1 \geq L_0$ since any additional parameters cannot but increase the fit to the data. In order to compare the two likelihood values we use the following ratio,

$$T = -2\log\frac{L_0}{L_1} \tag{4.5}$$

which according to the theorem by Wilks [24], as n tends to infinity is asymptotically distributed as Chi-square with one degree of freedom (obtained as the difference between the space dimensions of I_1 and I_0).

To proceed with the hypotheses analysis we will first have to define the maximum likelihood function corresponding to the ccdf candidates, namely

$$P_{SE}(x) = A_{SE}(u)\exp(-Bx^z) \tag{4.6}$$

$$P_{MSE}(x) = A_{MSE}(u)\exp(-Bx^z + Cx^{2z}) \tag{4.7}$$

where $A_{SE}(u) = \frac{1}{1-\exp(-Bu^z)}$ and $A_{MSE}(u) = \frac{1}{1-\exp(-Bu^z+Cu^{2z})}$ were obtained as normalizing factors in the interval [0,u].

Technically , the maximum likelihood determination of the best parameters of the two condidate models is done by the minimization of:

$$-ln(L_1) = -\sum_{i=1}^{N}(-lnA_{MSE}(u) - ln(BzX_i^{z-1} - 2zCX_i^{2z-1}) + BX_i^z - CX_i^{2z}) \quad (4.8)$$

$$-ln(L_0) = -\sum_{i=1}^{N}(-lnA_{SE}(u) - ln(BzX_i^{z-1}) + BX_i^z) \quad (4.9)$$

with respect to the parameters B, C and z, using the downhill simplex minimization algorithm [23]. In order to secure that the MLE indeed retains the parameter values of the global minimization, the downhill simplex minimization algorithm uses a wide range of start value in the search, in our case we used 1000 starting values randomly distributed in the interval [0,5] for each parameter. The next step is to ask whether these results allow us to reject C=0 for this particular threshold u. This test is based on the statistics of T (Eq.:4.5) that compares the likelihood values for both hypotheses (Eq.:4.6,4.7): a large T indicates that L_1 is significantly larger than L_0 which implies that the MSE is a much better model for the distribution than the SE. Conversely, if T is small (by definition it is always positive), L_1 is not much larger than L_0 which means that adding an additional parameter C $\neq$ 0 does not provide a significantly better fit. Hence, the pure stretched exponential can be accepted as an adequate model.

The aim of this test is to show that the empirical ccdf can be described by the stretched exponential model up to a certain threshold u, beyond which the null hypothesis of C=0 (the SE model) may be rejected with a certain significance level. Practically what we would like to observe is small values of T for a large proportion of the drawdowns (indicating that adding an additional parameter to the model does not significantly increase the fit). For the last thresholds, however, we would like to obtain large T meaning that the null hypothesis can be rejected which is to say that the curvature in the plot lnP versus x^z is significant, hence, qualifying these last samples as outliers.

This is a very powerful method which allows us to test for significant departures from our candidate distribution, the stretched exponential. However, by construction it is a joint test of both the adequacy of the SE model and the change of regime. Therefore, if tested with a distribution the "bulk" of which is significantly different from the SE, the ML analysis

will reject the change of regime, while actually it is the model of the distribution which is rejected.

4.6 Comparing distributions at different scales

Evidence for outliers and extreme events does not require the existence of a break in the event size distribution, *e.g.* a deviation in the tail, and the possible appearance of a "bump". Actually, dragon-kings do not always lead to this diagnostic and, sometimes, their presence can only be identified in more subtle ways.

L'vov et al. [16] identified the presence of Dragon-King events in the distribution of turbulent velocity fluctuations relying on the comparison between distributions of event sizes obtained at different resolution scales. They have shown that they can collapse the distribution of velocity fluctuations for different scales only for the small velocity fluctuations. This suggests that the distributions of velocity fluctuations are composed of two regions, a part corresponding to the so-called normal scaling and a domain of extreme events.

Applied to the study of the distribution of DD this translates to comparing the ccdf of drawdowns at different time scales (1 min, 15 min, 1 hour and 1 day) and rescaling both axes in the logarithmic plots in an effort to collapse the curves. Provided that we, indeed, observe two discernable regimes, one that may be collapsed and one that may not, we will have evidence of the existence of Dragon-Kings.

5

Results and discussion

5.1 Introduction

Our study included nine different data sets that show a broad perspective of different asset markets, including government bonds, currencies and stock indexes. In the following section we present a detailed analysis of the results of applying our methodology in seeking evidence of *DK* to one of the data sets. A thorough presentation of all results and the pertinent discussions may be found in Appendix C.

5.2 German Government Bonds

The complementary cumulative distribution of the $\epsilon-$drawdowns at the studied time scales are presented in figures 1 to 4. Fig.:1 and 3 show the logarithmic plots of the distributions of *pure* drawdowns and $\sigma/2-$drawdowns, respectively. For the 1-min time scale, the distribution follows a straight line in the logarithmic plot giving first evidence of a power law behavior of index $\mu_{\epsilon=0} = 2.77$ and $\mu_{\epsilon=\sigma/2} = 2.85$ for the *pure* and $\epsilon = \sigma/2$ cases, respectively. This PL behavior is confirmed by the $TP-$statistics in Fig.:9(a) and Fig.:10(a) in which the $TP(u)$ does not significantly deviate from zero at the tail. Indeed, if we compare the resulting $TP-$statistics with the one obtained by applying the $TP-$statistic to a synthetically generated PL (Fig.:**??**) we obtain similar results. The remaining figures also reveal a consistent convergence at the highest thresholds towards a PL behavior for the other studied scales. The indexes

for these cases are of the same order throughout the scales and DD type.

Fig.:2 and Fig.:4 shows the log-lin plots of the distributions of *pure* drawdowns and $\sigma/2-$drawdowns, respectively. For the scales above 15-min, the distributions show signs of a convergence to a plain exponential for the tail. These are qualified by a straight line in the semilog plot. Nevertheless, the $TE-$test in Fig.:7 and 8 are not conclusive in this aspect since the oscillations around zero are too wild to assert or reject the hypothesis of an exponential behavior at the tail.

The surrogate data analysis reshuffles the return time series 500 times and generates 500 synthetic data sets. These data sets will, by definition, have exactly the same distribution of returns as the original series but any high order correlations and time dependencies will be destroyed. These synthetic data sets are used to construct drawdown distributions and these are compared with the DD distribution resulting from the original return series. Hence, if the original DD distribution does not exhibit a significant departure from the synthetic data sets, it fails to reject the hypothesis of order of returns not being paramount in the creation of the observed DD. In Fig.:5 and Fig.:6 the 500 synthetic drawdown distributions are plotted together with a 95% confidence interval of a random realization falling into that interval. Superposed to that, the original DD distribution is plotted.

We see that for the 1-min scale and $\sigma/2-$DD the original distribution lies inside the 95% confidence interval for the most part, particularly, for the tail. For the *pure* drawdown distribution at the 1-min scale, we only see a significant departure for the the intermediate regime of distribution, not for the tail. Original distributions for the 15-min, hourly and daily scale for both types of DD significantly deviate from the synthetically generated ones for the body of the distribution but converge to barely border the 95% confidence interval at the tail. The only exception to the previous statement is the $\sigma/2-$DD distribution at the 15-scale for which the original distribution lies within the 95% confidence interval for the tail of the distribution. These results suggest that high order correlations play a significant role in the creation of the observed drawdowns for the larger scales, beyond 15-min, and more clearly at the intermediate regime of the distribution. Only for the largest scales, namely hourly and daily, the largest drawdowns (the ones at the tail) are significantly larger from the synthetic ones, there is less than a 5% probability of a synthetically generated drawdown being larger than the original ones.

The nested hypothesis statistical test compares, for each quantile, the fit of the drawdown distribution with a stretched exponential model (C=0) versus that of a more sophisticated model that allows for an upward curvature in the lnP and x^z plot (C≠0). In Tab.:5.3 we present the probability that C=0 for each quantile and time scale. This probability

is calculated considering the T-values that compare the fits (Eq.:4.5) distributed as a chi-square with one degree of freedom. This test is strongly *parametric* and the result are strongly conditioned by the fit to our candidate distribution.

There is evidence of a change of regime for largest 1% of the 0−DD at the daily scale. In order to obtain this result we verified that for the *pure* drawdowns at the daily scale, for the 80%, 90% and 95% smallest DD, corresponding to drawdowns smaller than 0.69%, 0.95% and 1.53%, respectively, the probability of C=0 was larger than 5%. However, for drawdowns larger than 2.62%, this is the largest 1% events, the hypothesis of C=0 may be rejected at a 95% confidence level. In other words, the test shows two population, the first integrated by 99% of the *pure*-DD at the daily scale, those smaller than 2.62%, that can be well described by a stretched exponential (C=0), and the largest 1% that show a significant upward curvature in the lnP and x^z plot (C≠0). To support this result we present Fig.:12(c) and Fig.:12(d). These figures show the SE and MSE maximum likelihood estimates of the *pure* drawdown distributions for the daily scale superposed to the actual distribution. We observe that for cutoffs above 1% the MSE yields a better fit to the distribution, however, this does not become significant at a 95% level until larger thresholds.

The nested hypothesis test has been similarly performed for each scale and drawdown type obtaining the following results:

1. for the hourly scale and *pure*-DD distribution, the test shows evidence of two populations, the first integrated by 90% of the drawdowns and the second by 10%-largest, namely above the 0.32% threshold.

2. for the daily scale and the $\sigma/2$-DD distribution, the test shows of a change of regime for thresholds above 1.69% ($P_9 0$).

3. the test results inconclusive for the rest of scales and DD types

As above mentioned, this test is strongly *prametric* and therefore, its results also depend on the fit of our candidate distribution. Fig.:12 to what extend this is key in this test. Results 1 and 2 become questionable since our best ML estimates fail to capture the real behavior of the tail.

Finally, in the spirit of L'vov et al. [16] we compare the ccdf of drawdowns at different time scales (from 1-min to daily) and rescale both axes in the logarithmic plot in an effort to collapse the curves. Provided that we, indeed, are capable of collapsing the curves and we observe two differentiated regimes we will have evidence of a change of regime. In Fig.:11 we show the logarithmic plots of the distribution at all time scales for both types of $\epsilon-$DD. On the left side, they are simply superposed and, on the right side, the axes are normalized to obtain a collapse. The

collapsing is obtained and the departures at the tail result inconclusive since they are not pervasive across all scales.

5.3 Discussion

The essential results from our analysis seem to be pervasive in the majority of datasets under study. These results are:

1. Six out of nine datasets show clear evidence of a power law behavior of the distribution of $\epsilon-$drawdowns (both $\epsilon = 0$ and $\epsilon = \sigma/2$) for high frequency data (1 min scale). The exponents lie in the range $2 \leq \mu \leq 3$. This evidence has been observed in the logarithmic plots of the distribution in which the distribution describes a straight line qualifying the PL and, subsequently, tested with the $TP-$statistics obtaining values very close to zero.

2. Log linear plots of the distribution of $\epsilon-$drawdowns at larger scales (1-hour and 1-day) converge to a straight line in the semilogarithmic plot qualifying the exponential as an adequate candidate for the tail of the distribution. However, by applying the $TE(u)$ to validate our observations, we obtain inconclusive results characterized by wild but bounded oscillations around zero.

3. The surrogate data test finds no significant deviations of the original $\epsilon-$DD distribution from the synthetic distributions for the 1-min resolution. However, for larger scales (15-min to daily) the original $\epsilon-$DD distribution significantly deviates from the synthetically generated DD distributions. This is particularly obvious for the intermediate regime of the distribution and, only for the hourly and daily scales, can the deviations at the tail be considered significant. This result indicates that high-order correlations and time dependencies are paramount in the creation of the observed drawdowns.

4. Nested hypothesis tests our candidate distribution, namely the stretched exponential, against the modified stretched exponential which integrates a parameter to capture the upward curvature of the tail in the lnP versus x^z plot. This test is strongly *parametric* and therefore is inconclusive if the distribution cannot be approximated by a stretched exponential in its largest part. This limitation affected most of our distribution for which the SE was not a good candidate. Nevertheless, for five of our datasets, for the daily scales we were able to accept the stretched exponential model for the vast majority

of drawdowns and rejected it in front of the MSE for the largest quantiles. Hence, certifying a change of regime.

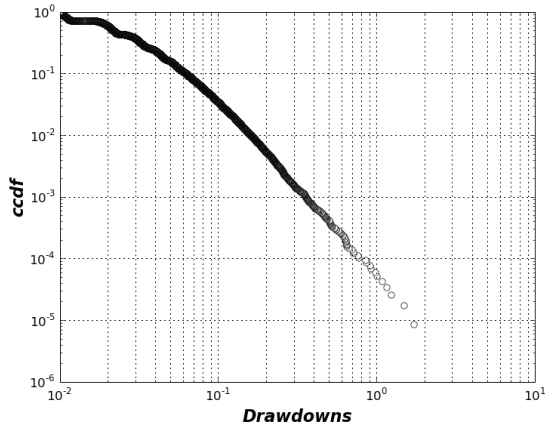

(a) German Government Bonds at 1-min scale

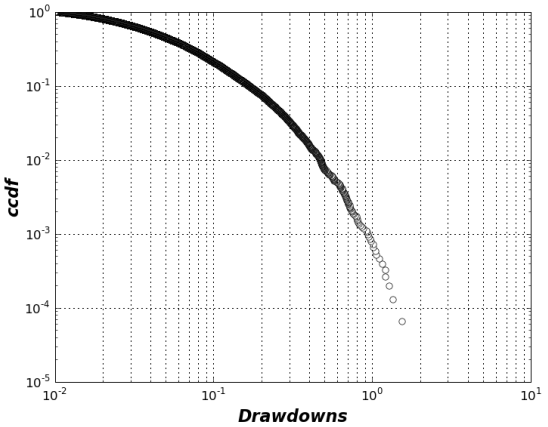

(b) German Government Bonds at 15-min scale

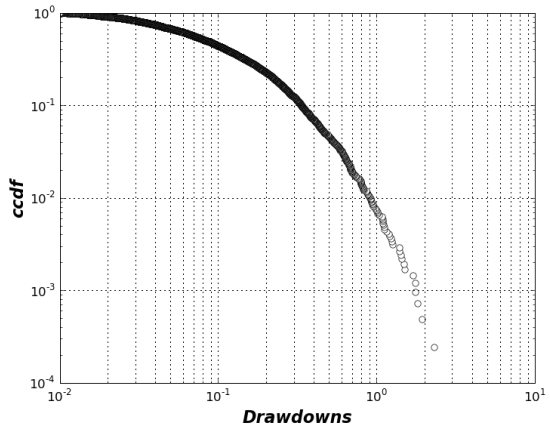

(c) German Government Bonds at 1-hour scale

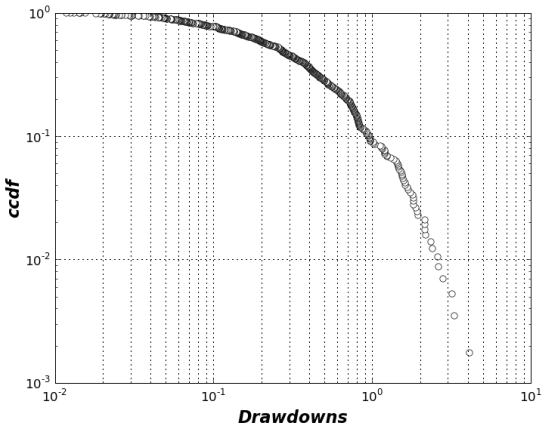

(d) German Government Bonds at 1-day scale

Fig. 1: Logarithmic plots of the complementary cumulative distribution of *pure* drawdowns ($\epsilon = 0$) for the price of futures on the German Government Bonds at different time scales (from 1-min to 1-day).

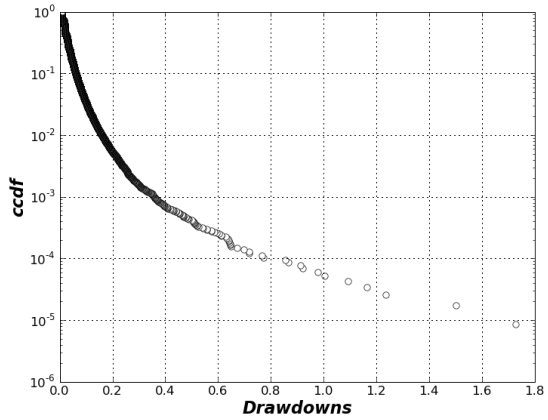

(a) German Government Bonds at 1-min scale

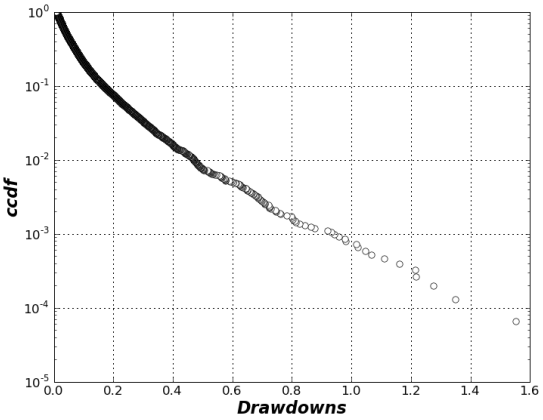

(b) German Government Bonds at 15-min scale

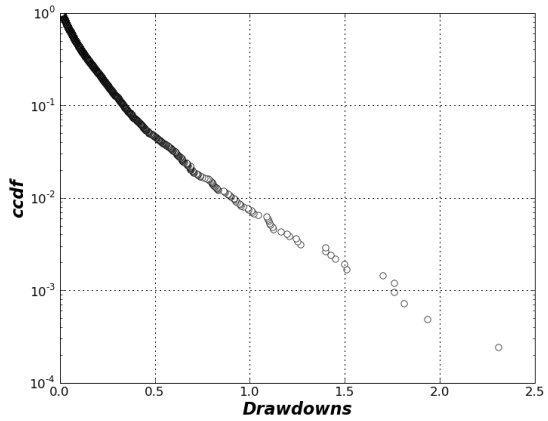

(c) German Government Bonds at 1-hour scale

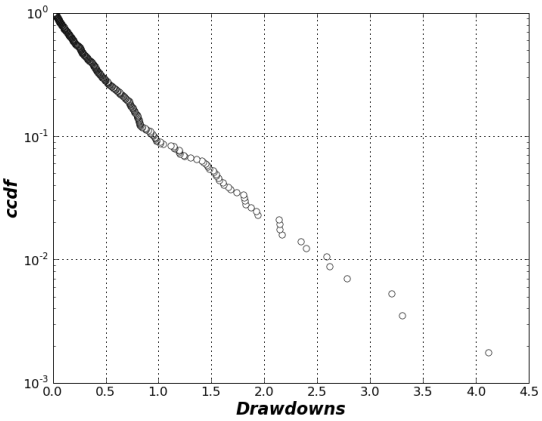

(d) German Government Bonds at 1-day scale

Fig. 2: Log-linear plots of the complementary cumulative distribution of *pure* drawdowns ($\epsilon = 0$) for the price of futures on the German Government Bonds at different time scales (from 1-min to 1-day).

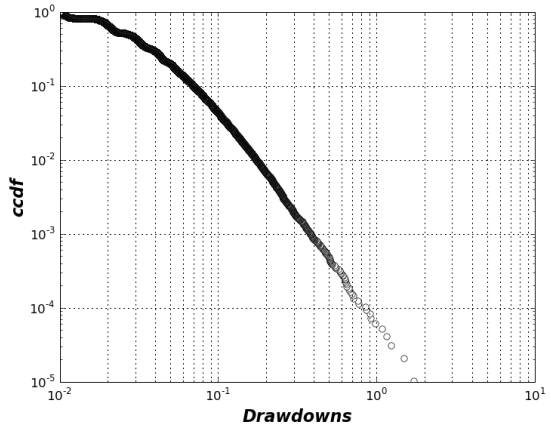

(a) German Government Bonds at 1-min scale

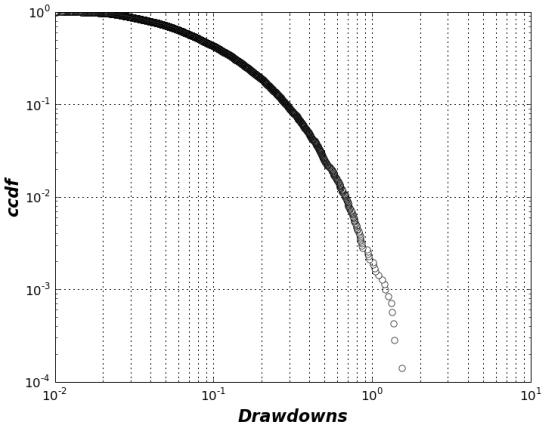

(b) German Government Bonds at 15-min scale

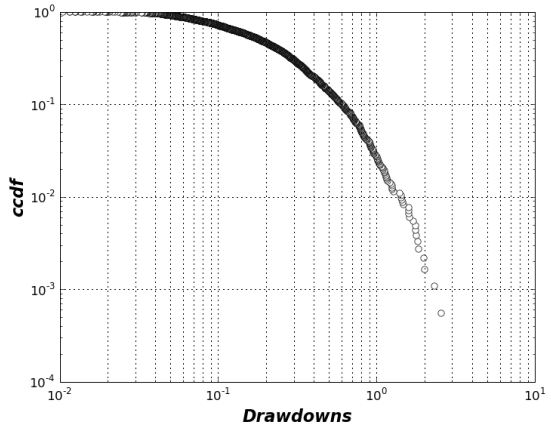

(c) German Government Bonds at 1-hour scale

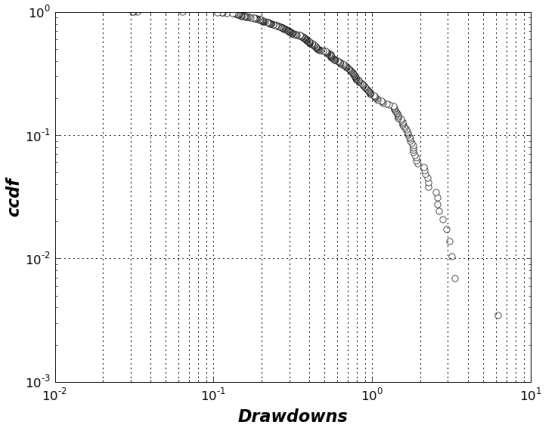

(d) German Government Bonds at 1-day scale

Fig. 3: Logarithmic plots of the complementary cumulative distribution of $\epsilon-$drawdowns ($\epsilon = 0.5\sigma$) for the price of futures on the German Government Bonds at different time scales (from 1-min to 1-day).

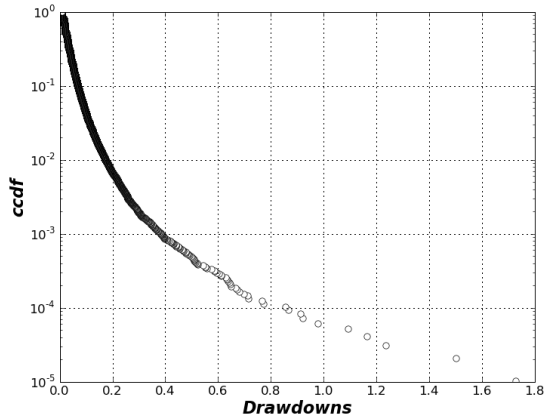

(a) German Government Bonds at 1-min scale

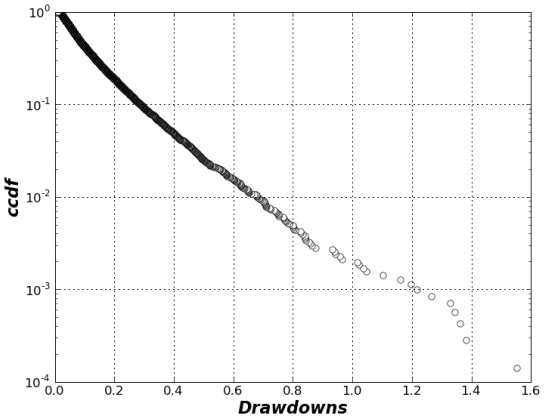

(b) German Government Bonds at 15-min scale

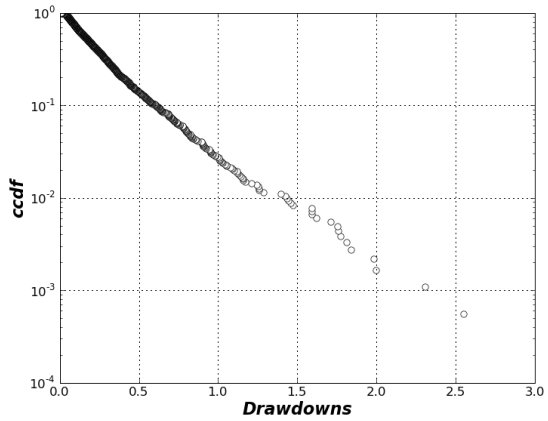

(c) German Government Bonds at 1-hour scale

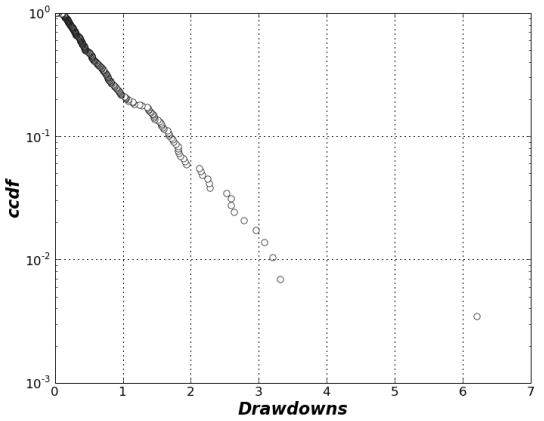

(d) German Government Bonds at 1-day scale

Fig. 4: Log-linear plots of the complementary cumulative distribution of $\epsilon-$drawdowns ($\epsilon = 0.5\sigma$) for the price of futures on the German Government Bonds at different time scales (from 1-min to 1-day).

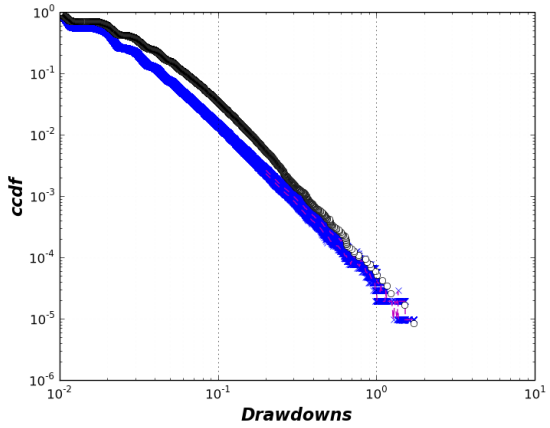

(a) German Government Bonds at 1-min scale

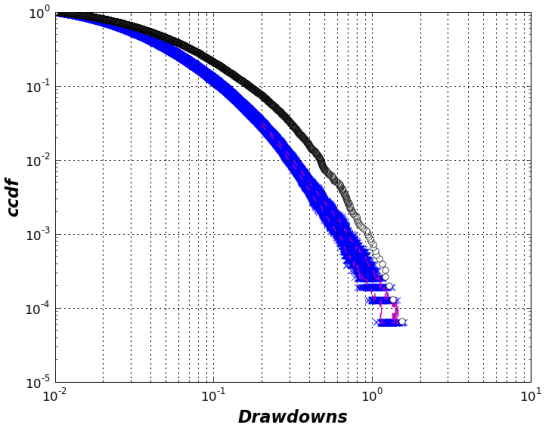

(b) German Government Bonds at 15-min scale

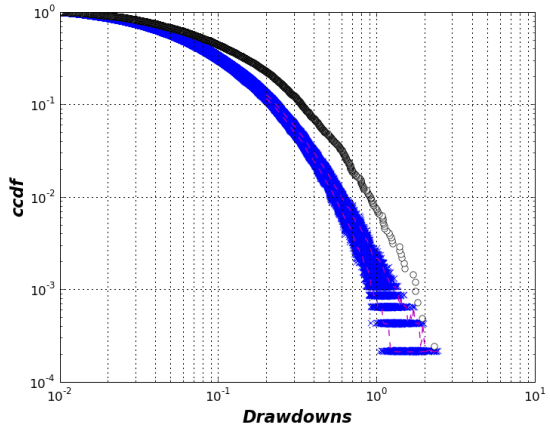

(c) German Government Bonds at 1-hour scale

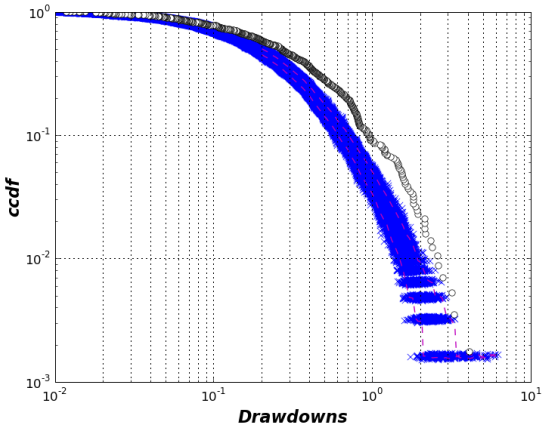

(d) German Government Bonds at 1-day scale

Fig. 5: Logarithmic plots of the complementary cumulative distribution of *pure* drawdowns ($\epsilon = 0$) for the German Government Bonds time series at different time scales (from 1-min to 1-day). Plotted are: (x) the 0-DD ccdf of 500 samples of the reshuffled return time series, (-) the 95% confidence interval of the reshuffled realizations, namely the interval for which there is 95% probability of a randomly generated DD with exactly the same return distribution lying within, (o) the 0-DD ccdf of the time series of the original German Government Bonds dataset.

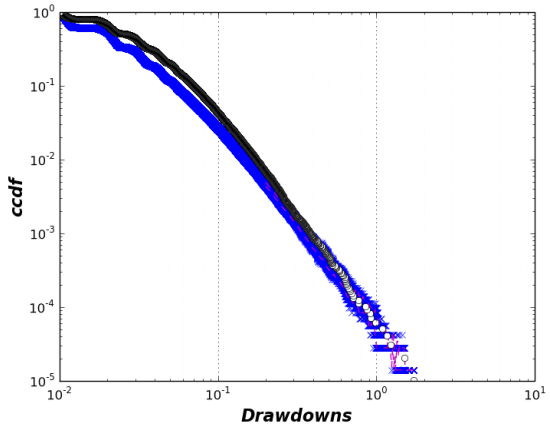

(a) German Government Bonds at 1-min scale

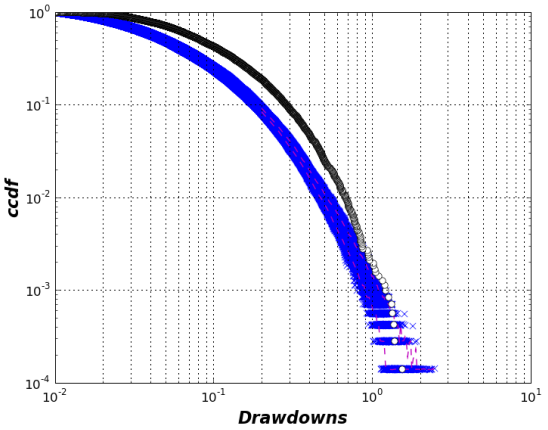

(b) German Government Bonds at 15-min scale

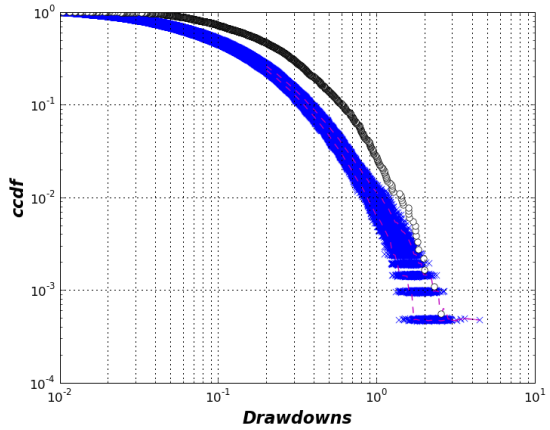

(c) German Government Bonds at 1-hour scale

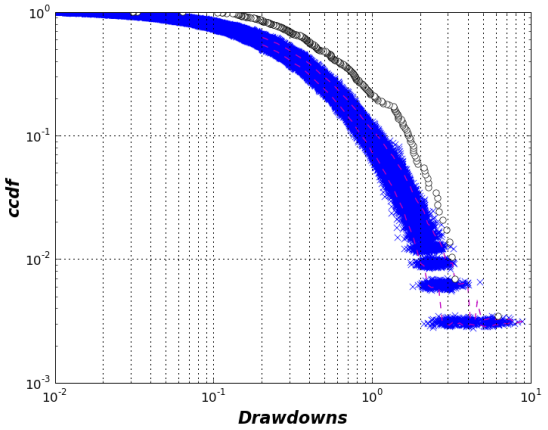

(d) German Government Bonds at 1-day scale

Fig. 6: Logarithmic plots of the complementary cumulative distribution of $\sigma/2$-Drawdowns ($\epsilon = 0.5\sigma$) for the German Government Bonds time series at different time scales (from 1-min to 1-day). Plotted are: (x) the $\sigma/2$-DD ccdf of 500 samples of the reshuffled return time series, (-) the 95% confidence interval of the reshuffled realizations, namely the interval for which there is 95% probability of a randomly generated DD with exactly the same return distribution lying within, (o) the $\sigma/2$-DD ccdf of the time series of the original German Government Bonds dataset.

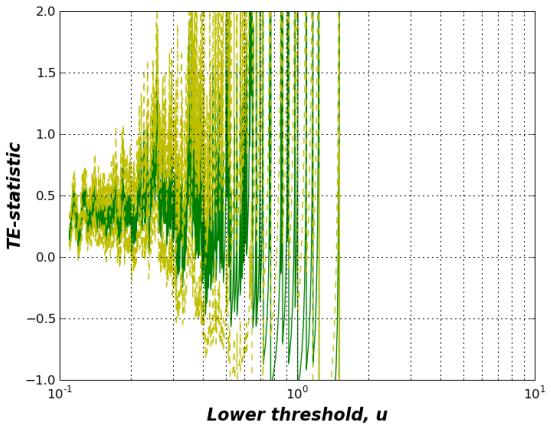

(a) German Government Bonds at 1-min scale

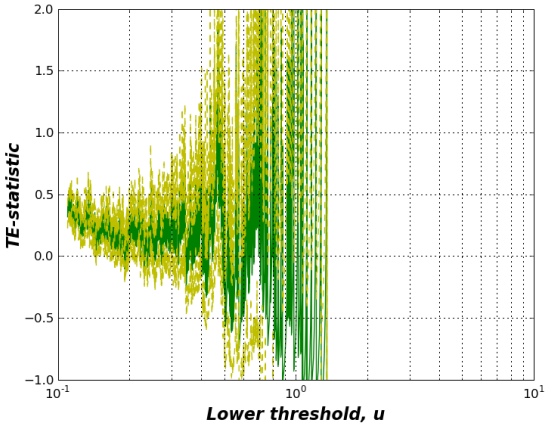

(b) German Government Bonds at 15-min scale

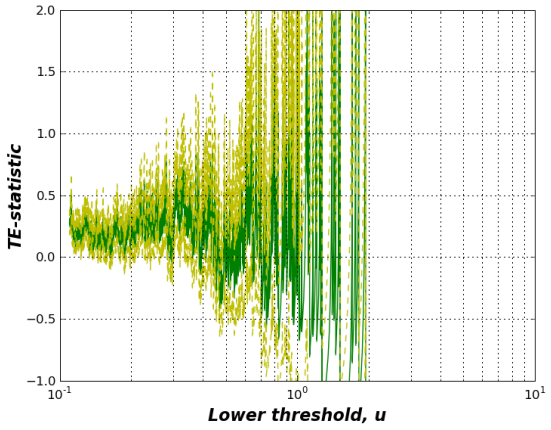

(c) German Government Bonds at 1-hour scale

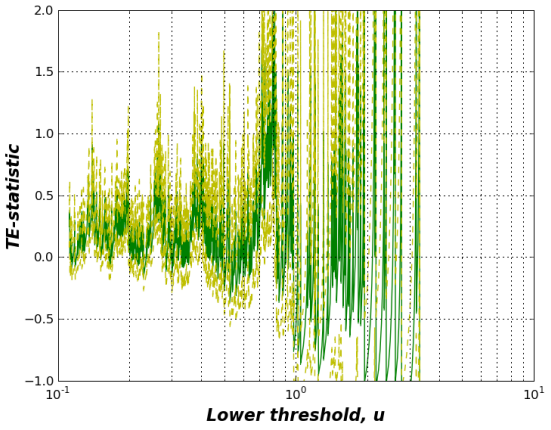

(d) German Government Bonds at 1-day scale

Fig. 7: *TE*−statistic (Eq.B.5) as a function of the lower threshold u, applied to the distribution of *pure*-drawdowns of the German Government Bonds dataset for each of the studied time scales (from 1-min to 1-day). The two dashed lines represent plus and minus one standard deviation from the statistic, defined as Eq.:B.6.

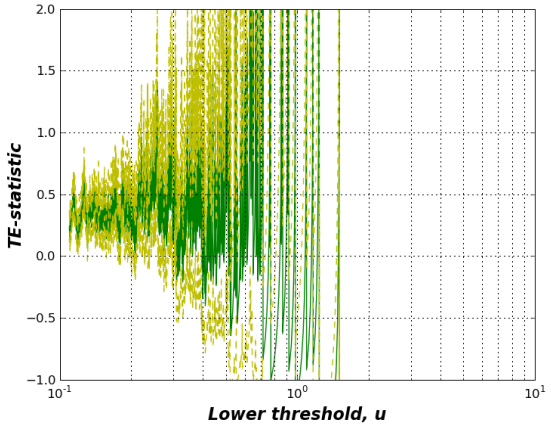

(a) German Government Bonds at 1-min scale

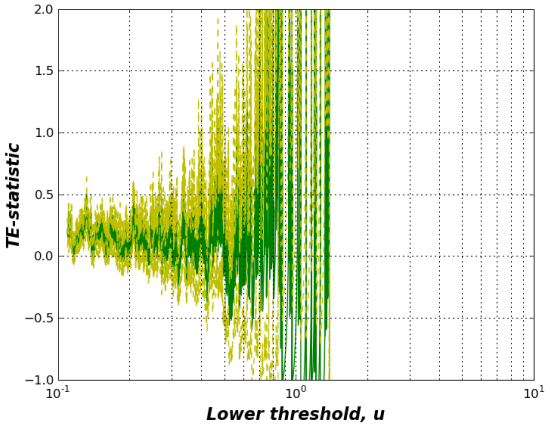

(b) German Government Bonds at 15-min scale

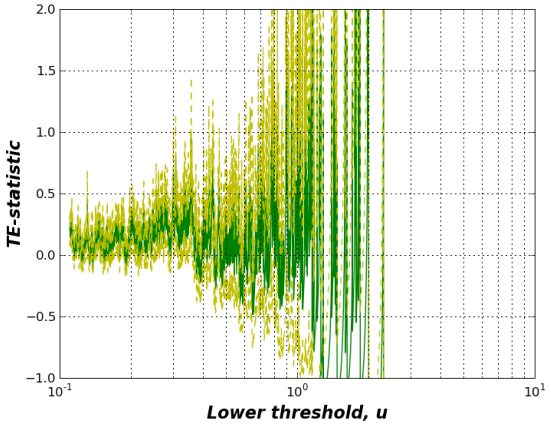

(c) German Government Bonds at 1-hour scale

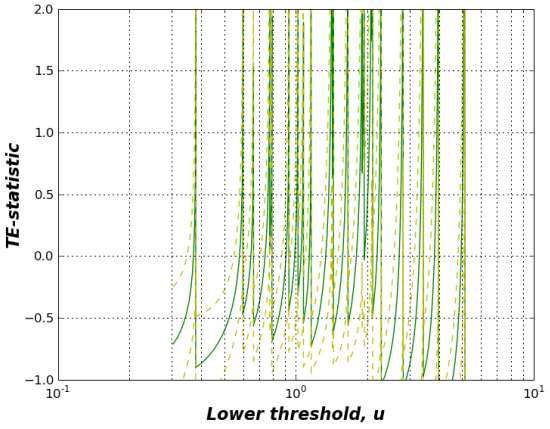

(d) German Government Bonds at 1-day scale

Fig. 8: $TE-$statistic (Eq.B.5) as a function of the lower threshold u, applied to the distribution of $\sigma/2$-drawdowns of the German Government Bonds dataset for each of the studied time scales (from 1-min to 1-day). The two dashed lines represent plus and minus one standard deviation from the statistic, defined as Eq.:B.6.

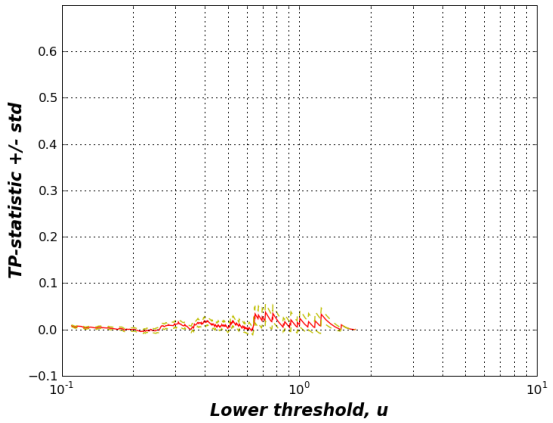

(a) German Gov Bonds at 1-min scale

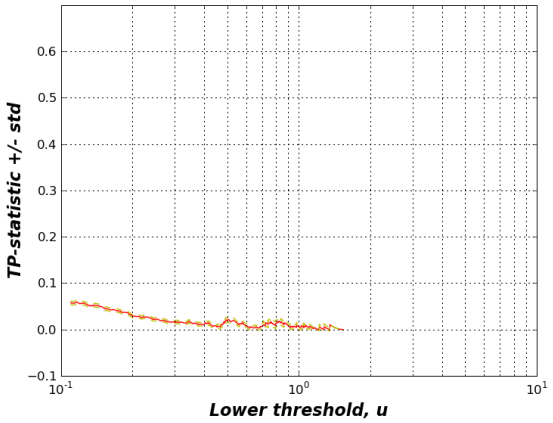

(b) German Gov Bonds at 15-min scale

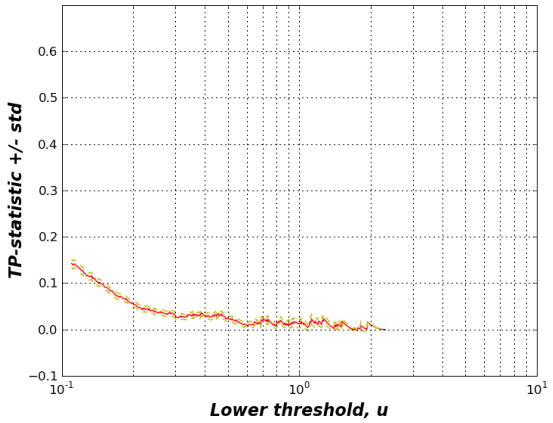

(c) German Gov Bonds at 1-hour scale

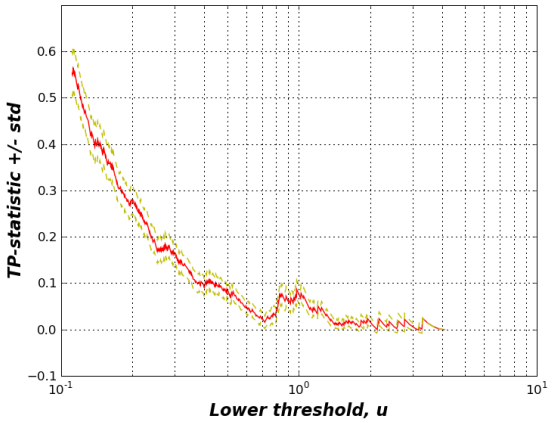

(d) German Gov Bonds at 1-day scale

Fig. 9: *TP*−statistic (Eq.B.2) as a function of the lower threshold u, applied to the distribution of *pure*-drawdowns of the German Government Bond dataset for each of the studied time scales (from 1-min to 1-day). The two dashed lines represent plus and minus one standard deviation from the statistic, defined as Eq.:B.3.

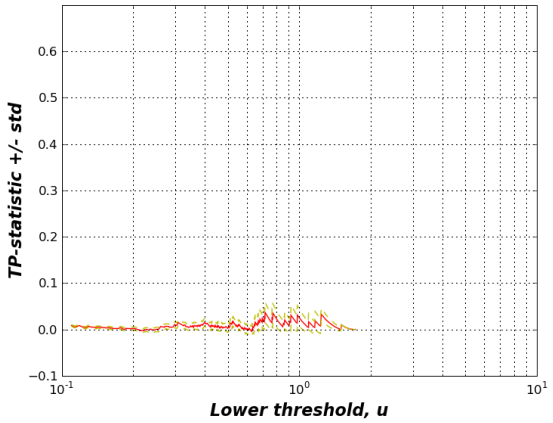

(a) German Gov Bonds at 1-min scale

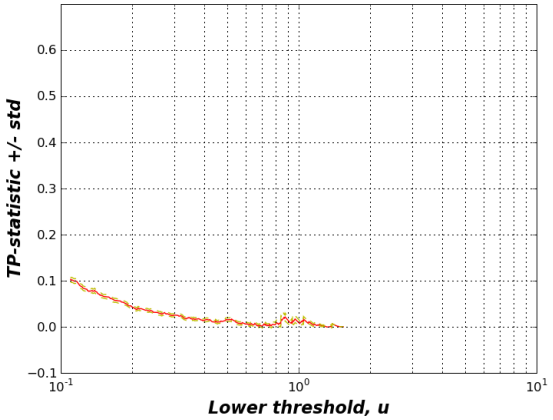

(b) German Gov Bonds at 15-min scale

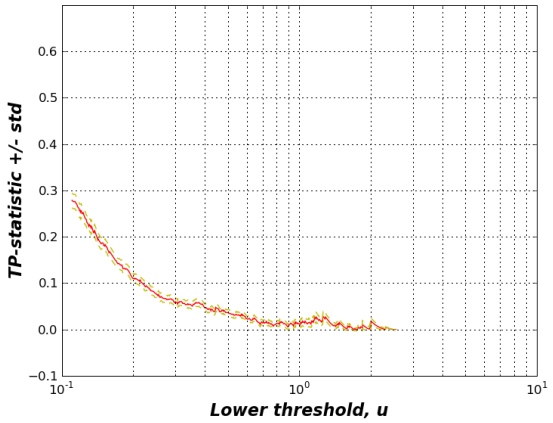

(c) German Gov Bonds at 1-hour scale

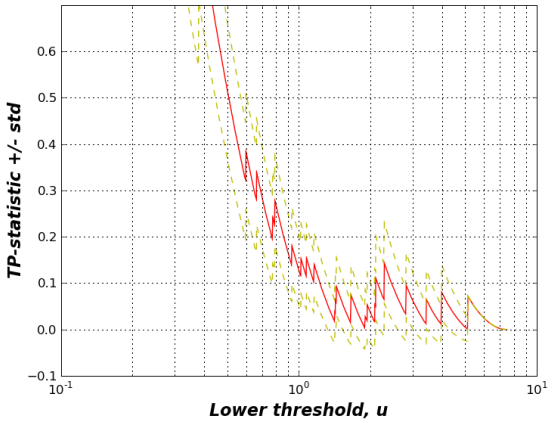

(d) German Gov Bonds at 1-day scale

Fig. 10: $TP-$statistic (Eq.B.2) as a function of the lower threshold u, applied to the distribution of $\sigma/2$-drawdowns of the German Government Bond dataset for each of the studied time scales (from 1-min to 1-day). The two dashed lines represent plus and minus one standard deviation from the statistic, defined as Eq.:B.3.

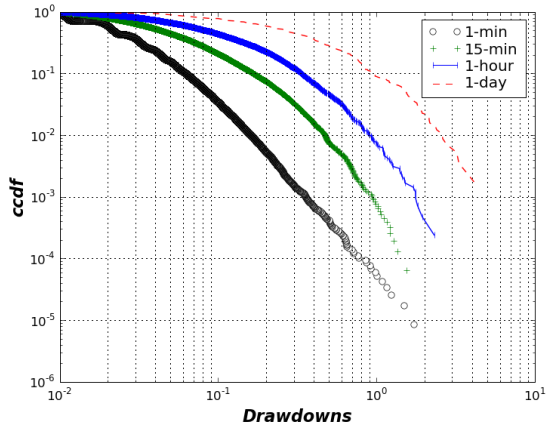

(a) IA *pure*-DD, no normalization

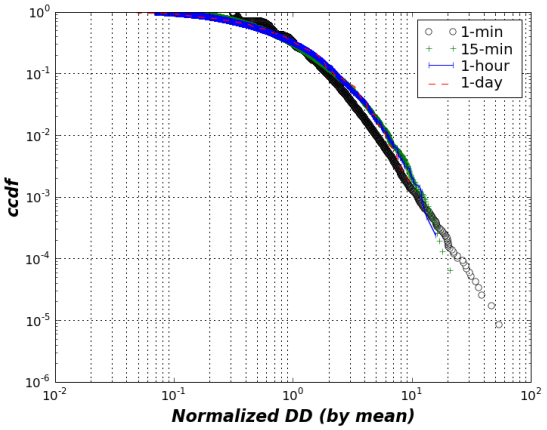

(b) IA *pure*-DD, normalized

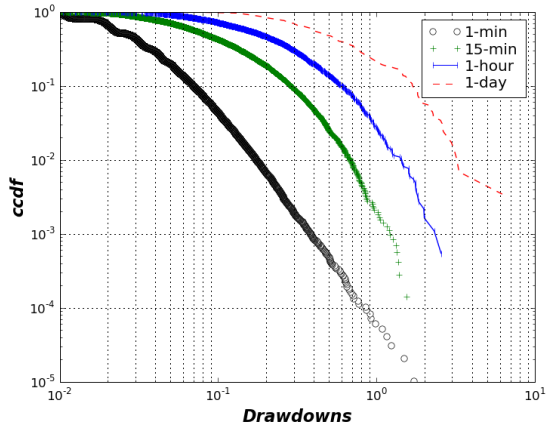

(c) IA $\sigma/2$-DD, no normalization

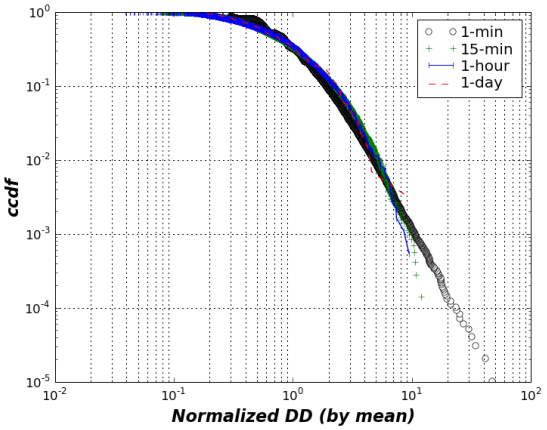

(d) IA $\sigma/2$-DD, normalized

Fig. 11: Distributions of ϵ-drawdown ($\epsilon = 0, \sigma/2$) at all studied scales were collapsed to identify dissident behaviors in the tail. The left panels show the superposed original distributions and the right panels normalize the ϵ-DD by their mean.

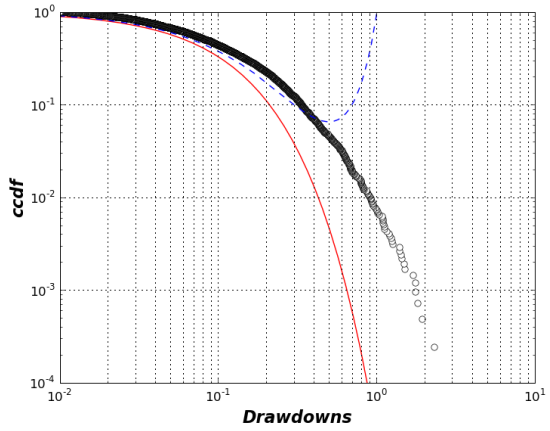

(a) IA hourly, *pure*-DD (log-log)

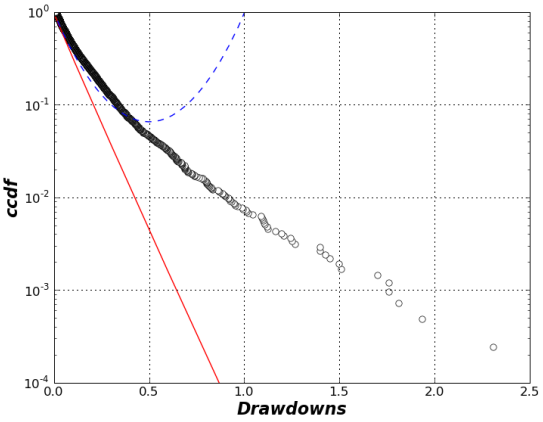

(b) IA hourly, *pure*-DD (semilog)

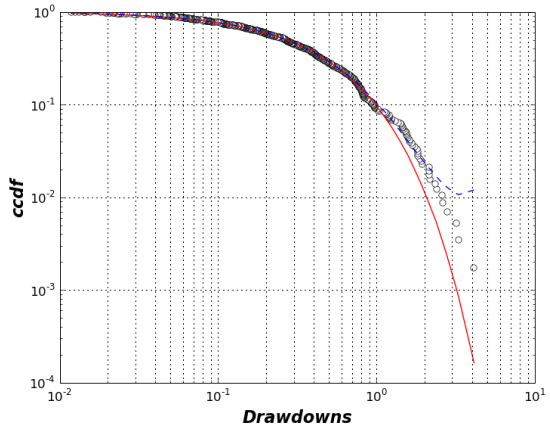

(c) IA daily, *pure*-DD (log-log)

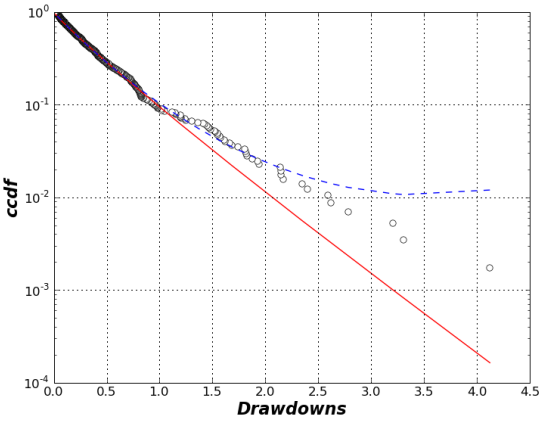

(d) IA daily, *pure*-DD (semilog)

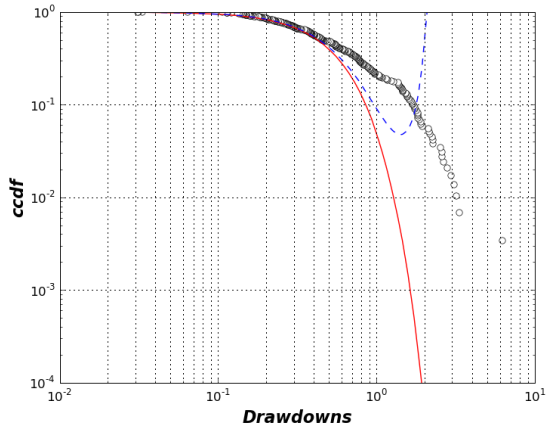

(e) IA daily, $\sigma/2-$DD (log-log)

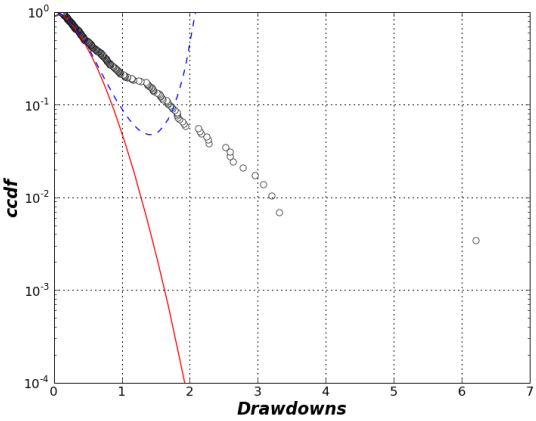

(f) IA daily, $\sigma/2-$DD (semilog)

Fig. 12: Plotted are the logarithmic and semilogarithmic plots of: (o) the complementary cumulative distribution of *pure* drawdowns ($\epsilon = 0$) for the price of futures on the German Government Bonds at the hourly and daily scales. The same for the $\sigma/2-$DD at a daily scale. (-) The ML fit of the stretched exponential to the original distribution. (- -) The ML fit of the modified stretched exponential to the original distribution.

	$\epsilon = 0.0$				
Scales	$\mathbf{P}_{80}$	$\mathbf{P}_{90}$	$\mathbf{P}_{95}$	$\mathbf{P}_{99}$	$\mathbf{P}_{99.5}$
1-min	NS	NS	NS	NS	NS
15-min	NS	0.12%	<0.01%	<0.01%	<0.01%
1-hour	9.78%	0.14%	0.01%	<0.01%	<0.01%
1-day	45.02%	23.84%	26.93%	1.45%	0.77%

Tab. 3: German Government Bonds, probability that C=0 for each quantile, time scale and drawdown type. This probability is calculated considering that the T-values follow a chi-square distribution with one degree of freedom [24]. T-values (defined as Eq.4.5) result from comparing the two competing candidates (SE and MSE) at different fraction 'quantiles' of the ϵ-DD belonging to [0,u] for each of the studied scales. Results are obtained for $\epsilon = 0.0$. "NS" indicates not significant as it results from a very poor fit of both candidates distributions, hence, rendering the test indecisive.

	$\epsilon = 0.5$				
Scales	$\mathbf{P}_{80}$	$\mathbf{P}_{90}$	$\mathbf{P}_{95}$	$\mathbf{P}_{99}$	$\mathbf{P}_{99.5}$
1-min	<0.01%	<0.01%	NS	NS	NS
15-min	<0.01%	<0.01%	<0.01%	<0.01%	<0.01%
1-hour	0.66%	0.03%	<0.01%	<0.01%	<0.01%
1-day	13.36%	1.61%	1.16%	0.42%	0.42%

Tab. 4: German Government Bonds, probability that C=0 for each quantile, time scale and drawdown type. This probability is calculated considering that the T-values follow a chi-square distribution with one degree of freedom [24]. T-values (defined as Eq.4.5) result from comparing the two competing candidates (SE and MSE) at different fraction 'quantiles' of the ϵ-DD belonging to [0,u] for each of the studied scales. Results are obtained for $\epsilon = 0.5$. "NS" indicates not significant as it results from a very poor fit of both candidates distributions, hence, rendering the test indecisive.

6

Conclusions

We started the study with the aim of empirically answering the question of whether *Dragon-Kings* were a pervasive idiosyncrasy of the financial market drawdowns not only across asset types, as it has already been demonstrated by J&S [11], but also across *times scales*.

The approach utilized to diagnose the existence of *DK* consisted in piling up evidence resulting from statistical tests. One of them, the "$T-$statistics" represents the *state of the art* in testing for the behavior of the tail of a distribution. Others like the "nested hypothesis test", the "surrogate data analysis" or the "collapsing the distribution at different scales" are tools that were cleverly designed to test for *DK* at the tail of the distribution. Finally, "Visual inspection of the ccdf" is the most common and least quantitative.

Our analysis comprised nine time series of prices of futures tracking major stock indexes (S&P, FT-SE, Nikkei), currencies (Yen, DM) and government bonds (Japan, US, Germany) at different time scales ranging from 1-min to 1-day.

No evidence of a change of regime was found for the smallest time scale, 1-min. The surrogate data analysis was not able to certify the importance of high-order correlation in the creation of the observed drawdowns and the $TP-$test revealed a power like decay in the distribution for most datasets but was unable to certify a significant departure of this behavior in the tail that would qualify for different regime. Furthermore, the nested hypothesis test yielded inconclusive results.

On the other hand, evidence for the existence of *Dragon-Kings* was found for the largest time scale, daily. A result that goes hand in hand with previous results by J&S [28, 11, 31]. Surrogate data analysis

lead to conclude that the largest market events are to be characterized by the presence of higher order correlations. Additionally, the nested hypothesis test confirms our proposed picture of a significant change of regime between "normal" drawdowns (above 99% of the total data set) to "anomalous" large drawdowns that we dubbed here "genuine outliers" corresponding to less than 1% of the total number of events.

For the 15-min and 60-min time scales, the results are less conclusive. The surrogate data analysis rejects the hypothesis of high-order correlations being at the origin of the largest observed drawdowns at the 15-min scale but fails to reject it for the hourly scale. The nested hypothesis test yields inconclusive results linked to the poor fit of the data to our candidate distribution.

The fact that no evidence of a change of regime was found for high-frequency data and that this seems to emerge upon the daily scales suggest that the positive feedback mechanisms that allegedly lie at the origin of the largest drawdowns require a certain time to build up and their results cannot be observed at high levels of granularity. This conclusion presents an open door to the understanding of this mechanisms such as the "herding behaviors".

Notwithstanding the importance of the results presented in this work, there are still questions that remain unanswered. Here we propose several lines of work to continue this study:

- To our knowledge the surrogate analysis test was never perfomed on the intermediate regime of the distribution. For our datasets it revealed that for scales beyond 15-min, that high-order correlations and time dependencies are paramount in the creation of the observed drawdowns both, in the tail and in the intermediate regime. This is indeed a very important result since it extents the role of correlations to other sizes and questions the *uniqueness* of this quality of the *Dragon-Kings*. The explanation we propose takes into consideration the slow decay of the volatily in the financial markets [5]. In this view, destroying time dependencies would modify the distribution of the synthetic drawdowns. We, however, encourage the study of this behavior in other data sets to proof or rebate this view.

- Drawdowns in high-frequency are more exposed to noise than at larger scales. We propose a new definition of the $\epsilon-$drawdown were ϵ-threshold is not fixed throughout the sample but dependent on the absolute size of the ongoing drawdown, namely $\epsilon(DD_i)$.

  A reverse price movement has a different impact depending on the size of the DD. This is to say, larger DD are more resilient to fluctuations than smaller ones. Hence, ϵ may be defined as:

$$\epsilon(DD_i) = \epsilon_0 \cdot DD_i \tag{6.1}$$

where DD_i is the size of the ongoing DD and ϵ_0 is chosen from the observation of the data.

- Le Bris [14] has recently proposed a new methodology to adjust returns to account for the volatility of the market. The parting idea is that a drop in the market will not have the same impact in a stable market as for a highly volatile one. This adjustment of the returns can lead to a more accurate capturing of the crash and have a significant impact in the study of *DK*

- *Parametric* tests are a double-edged sword. On the one side they provide clear results but on the other side these are always bound to the adequacy of the model. To circumvent this problem, we need new non-parametric test of a change of regime.

The problem of testing for different regimes in the tail of a distribution is still in its adolescence, even more so for intra-day data. We hereby encourage the new generations to think creatively and create clever new tools that give a new light to this problem.

A

Power-Laws

A.1 PL fundamentals

A probability distribution function $P(x)$ exhibiting a power law tail is such that (further mathematical details on the mathematics of PL can be found in [30, 20, 19])

$$P(x) \propto \frac{L(x)}{x^{1+\mu}} \tag{A.1}$$

Clearly this distribution diverges as $x \to 0$ so Eq.A.1 cannot for all $x \geq 0$: there must be some lower bound,x_{min}, and possibly, also, some large limiting cut-off. The exponent μ (also referred to as the "index") characterizes the nature of the tail: for $\mu < 2$, one speaks of "heavy tail" for which the variance is not theoretically defined. $L(x)$ is a slowly varying function defined by $lim_{x\to\infty} L(tx)/L(x) = 1$ for any finite t.

Power laws are scale invariant, this is, for an arbitrary real number λ, there exists γ such that, $P(x) = \gamma P(\lambda x) \forall x$. This relation means that the ratio of probability of occurrence of events x_1 and x_2 depends only in the relation x_1/x_2 and not on the actual values. As a consequence, a power-law distribution will show a straight line in a log-log plot.

A.2 Generating power-law distributed random numbers

There is a variety of methods available for generating PL-distributed random numbers. Perhaps the simplest and most elegant method is the

transformation method [23, 6]. Suppose $p(x)$ is a continuous distribution with Cumulative Distribution Function like,

$$P(x) = P(X \leq x) = \int_x^{\infty} p(x')dx' = (\frac{x}{x_{min}})^{-\alpha+1} \tag{A.2}$$

from which we wish to draw random reals $x \leq s_{min}$. We first generate n uniformly distributed reals r in the interval $0 \leq r \leq 1$. The probability densities $p(x)$ and $p(r)$ are related by

$$p(x) = p(r)\frac{dr}{dx} = \frac{dr}{dx} \tag{A.3}$$

where the second equality follows because $p(r) = 1$ over the interval 0 to 1. Integrating w.r.t x we find,

$$P(x) = \int_x^{\infty} p(x')dx' = \int_r^1 dr' = 1 - r \tag{A.4}$$

and taking the functional inverse of P as in A.2 we obtain,

$$x = x_{min}(1 - r)^{-1/(\alpha-1)} \tag{A.5}$$

which can be implemented easily in most programming languages.

A.3 Fitting power laws to empirical data

A power-law as described in A.2 is univocally described by the lower-bound upon which a PL behavior is observed, namely x_{min}, and the scaling parameter α. The former can be guessed by close inspection of the logarithmic plot of the distribution. The latter, however, will be fitted using the *method of maximum likelihood*, which gives asymptotically accurate results [4, 6].

The maximum likelihood estimator (MLE) for the continuous case is [6],

$$\hat{\alpha} = 1 + n[\sum_{i=1}^{n} ln\frac{x_i}{x_{min}}]^{-1} \tag{A.6}$$

where x_i, $i = 1, \ldots, n$ are the observed values upon the threshold, $x_i \leq x_{min}$. Equation A.6 is equivalent to the Hill estimator, which is known to be asymptotically normal and consistent (*i.e.*, $\hat{\alpha} \to \alpha$ in the limit of large n, x_{min} and n/x_{min})

B

T-statistics

B.1 TP-statistics

Considering the Pareto distribution $F(x)$, conditioned on the semi-axis $x \geq u$:

$$F(x) = 1 - (u/x)^b, \quad x \geq u, \quad b > 0. \tag{B.1}$$

where u is a lower threshold, and b is a power index of the distribution. In [22] the following statistic $TP = TP(x_1, \ldots, x_n)$ was presented:

$$TP(u) = [(1/n_u) \sum_{k=1}^{n_u} log(x_k/u)]^2 - (0.5/n_u) \sum_{k=1}^{n_u} log^2(x_k/u) \tag{B.2}$$

where u is the lower threshold of x_k. TP tends to zero as $n \to \infty$ for a sample $x_1, \ldots, x_n$ whose distribution follows Eq.B.1 and at the same time will deviate from zero for others.

The standard deviation $std(TP)$ of the statistic TP can be estimated by:

$$n_u^{-0.5} std[2E_1 \, log(x_k/u) - 0.5 \, log^2(x_k/u)] \tag{B.3}$$

where E_1 can be replaced by $(1/n_u) \sum_{k=1}^{n_u} log(x_k/u)$.

A close inspection of Eq.B.3 confirms the suspicion that the further we go to the higher quantiles, the more we increase the lower threshold u, less samples conform the statistic resulting in larger confidence intervals and less reliable results. Hence, statistical significance of the results should and will be taken into account.

B.2 TE-statistics

Let us consider the exponential distribution $F(x)$, conditioned on the semi-axis $x \geq u$:

$$F(x) = 1 - exp(-(x-u)/d), \quad x \geq u, \quad d > 0. \tag{B.4}$$

where u is a lower threshold, and d is the form parameter of the distribution. Also in [22] the statistic $TE = TE(x_1, \ldots, x_n)$ was introduced:

$$TE(u) = (1/n_u) \sum_{k=1}^{n_u} log^2(x_k/u - 1) - [(1/n_u) \sum_{k=1}^{n_u} log(x_k/u - 1)]^2 - \pi^2/6 \tag{B.5}$$

where u is the lower threshold of x_k. TE converges to zero as $n \to \infty$ for a sample $x_1, \ldots, x_n$ whose distribution follows Eq.B.4 and at the same time will deviate from zero for others.

Let us now, estimate the standard deviation $std(TP)$ of the statistic TE:

$$n_u^{-0.5} std[log(x_k/u - 1) - E\, log(x/u - 1)]^2 \tag{B.6}$$

where E is the symbol for the mathematical expectation and can be substituted by its sample analog $(1/n_u) \sum_{k=1}^{n_u} log(x_k/u - 1)$.

Akin to the TP statistic, the deeper we move along the u axis, the less samples conform our static and thus, the poorer the statistic becomes.

B.3 Application of the $TP-$ and $TE-$statistics to data sets generated from known distributions

With the aim of showing to which extend are the above described statistical tools capable of identifying Pareto and Exponential distributions, we present a series of figures plotting the $TP-$ and $TE-$statistics as a function of the lower threshold – this is, $TP(u)$ and $TE(u)$ – on data sets generated upon known distributions; the pure Pareto and Exponential samples.

B.3.1 Pareto distribution

A Pareto sample of size $n = 20,000$ was generated with power index $b = 3$ and $u = 27.14$ as defined in Eq.B.1. Fig.13.a shows its cumulative distribution which shows the distinguishing sign of the straight line in the log-log plot.

$TP-$ and $TE-$ are applied to this sample as a function of its lower threshold u obtaining respectively the plots a) and b) in Fig.14. We see

that $TP-$statistic is very close to zero till thresholds $u \cong 7$ beyond which random oscillation become starker. $TE-$statistic, on the other hand, presents a clear positive shift that veils under vehement fluctuations. $TP-$ and $TE-$ statistics presented, respectively, clear signs of Pareto distribution and rejected the possibility of this data being described by an exponential distribution.

B.3.2 Exponential distribution

An exponential sample of size $n = 20,000$ was generated with form parameter $d = 4$ and $u = 39.61$ as defined in Eq.B.4. Fig.13.b shows its cumulative distribution. The unmistakable form of an inverse exponential in the log-log plot points the finger at the exponential distribution.

$TP-$ and $TE-$ are applied to this sample as a function of its lower threshold u obtaining respectively the plots a) and b) in Fig.15. $TP-$statistic shows a clear positive bias that is reduced with larger thresholds. This is a clear trait of $TP-$statistic applied to exponential samples. More interesting is the $TE-$ statistic that is presents mild oscillations around the zero line up to thresholds $u \cong 10$. Beyond this point fluctuations become stronger. These results are typical of an exponential sample confronted with the $T-$statistics.

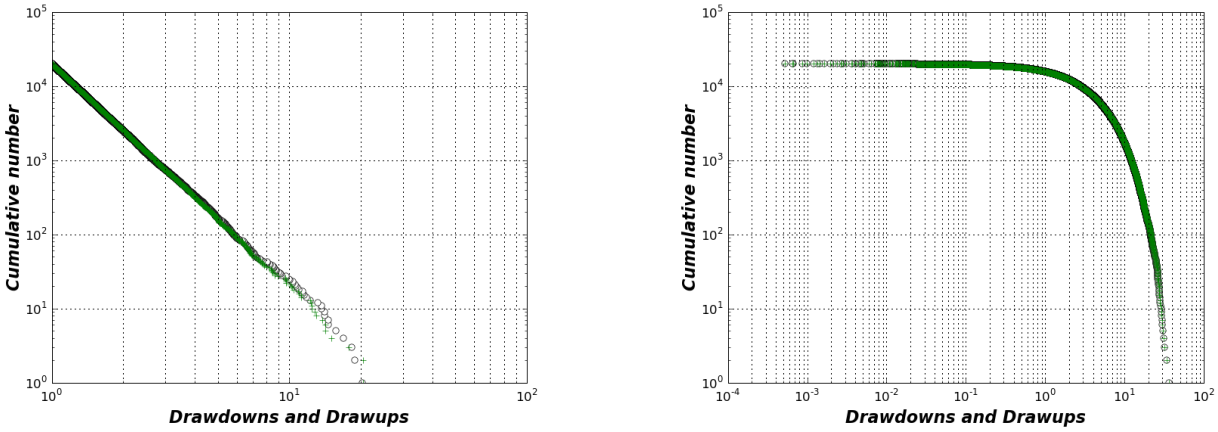

(a) dist PL (b) dist EXP

Fig. 13: (a) distribution of a simulated Pareto sample of size $n = 20,000$ with power index $b = 3$ generated with $u = 27.14$ as defined in Eq.(B.1).(b) distribution of a simulated exponential sample of size $n = 20,000$ with form parameter $d = 4$ generated with $u = 39.61$ as defined in Eq.B.4

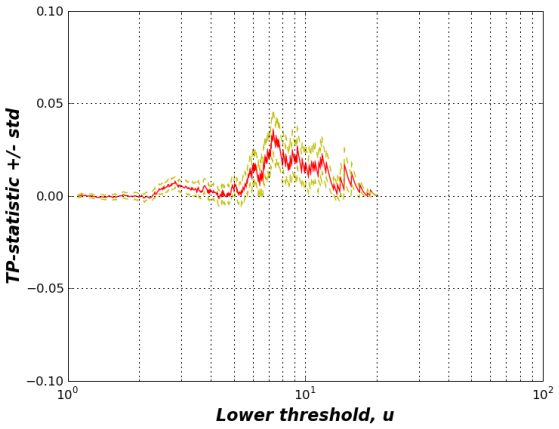

(a) $TP-$statistic

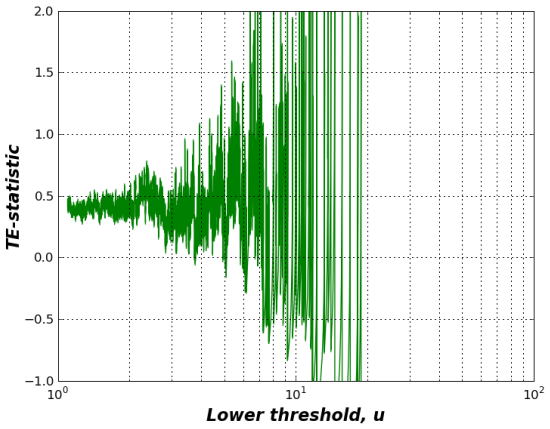

(b) $TE-$statistic

Fig. 14: (a) $TP-$ statistic as a function of the lower threshold u, applied to a simulated Pareto sample of size $n = 20,000$ with power index $b = 3$ generated with $u = 27.14$ as defined in Eq.(B.1). Increasing u decreases the number of data values used in the calculation of the statistic TP, thus enhancing the fluctuations around 0. The two dashed lines show plus or minus one standard deviation, estimated as exposed in the text Eq.B.3. (b) $TE-$ statistic of the same synthetic data

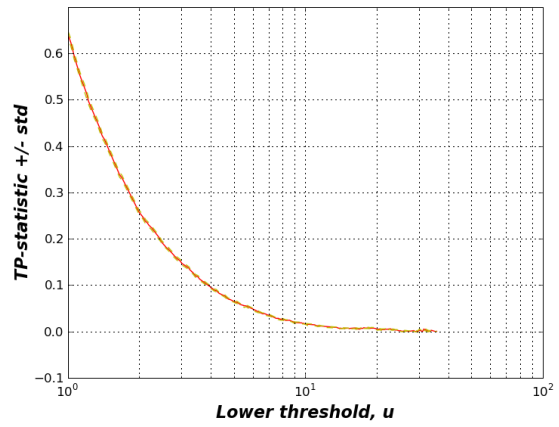

(a) $TP-$statistic

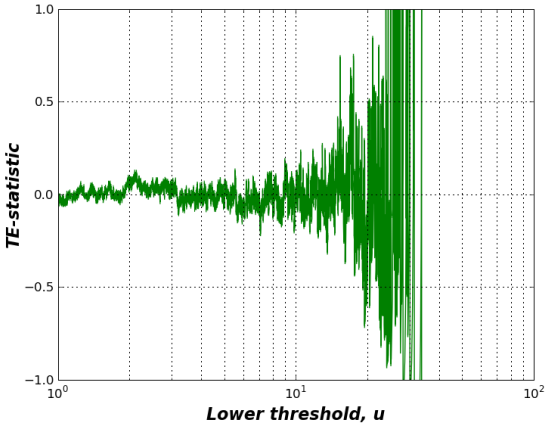

(b) $TE-$statistic

Fig. 15: (a) $TP-$statistic as a function of the lower threshold u, applied to a simulated exponential sample of size $n = 20,000$ generated with form parameter $d = 4$ and $u = 39.61$ as defined in Eq.B.4. Increasing u decreases the number of data values used in the calculation of the statistic TP, thus enhancing the fluctuations around 0. The two dashed lines show plus or minus one standard deviation, estimated as exposed in the text Eq.B.3. (b) $TE-$statistic of the same synthetic data

C

Results of the tests

C.1 Introduction

This document compiles all the results obtained from applying the methods described in Chapter 4 to our data sets. Our approach to diagnose the existence of *Dragon-Kings* at different time scales consists of piling up results from different methods to give sufficient proof of the existence of such events.

Section C.2 describes the results of the tests classified by data set. Section C.3 presents the results of each test.

C.2 Analysis of the results

C.2.1 Drawdowns in financial indexes

This section presents the results for three of the world's major financial indexes: S&P 500 (US), FTSE 100 (UK), Nikkei 225 (Jap).

C.2.1.1 S&P 500

For small time scales -1-min to 15-min-, Fig.16 and 18 depict a straight line of the ccdf in a loglog plot for the most part of the distribution, serving this as a first indication of PL behavior for the bulk of the distribution. Furthermore, a "bump" in the distribution can be appreciated for the 15-min time scale for DD larger than 3%. $TP-$statistics reinforces this first evidence for the minute scale (Fig.88) in which up until $u \approx 5\%$ the

drawdown distribution can be described as a PL, upon this point we see a clear deviation from this behavior. For the quarterly scale, the $TP-$statistic does not qualify as a PL up until thresholds $u \approx 0.4\%$ and upon $u \approx 3\%$ the test shows significant departure from that behavior.

For larger time scales, Fig.17 and 19 give primary evidence of an exponential behavior. In this case the "break" in the distribution is even more obvious and can be located around 5% and 7% for the hourly and daily scale respectively. The $TE-$statistic as a function of the lower threshold presented in Fig.70 and 71 concur with our previous evidence, since they show very little departure from zero up until the above mentioned thresholds, thus, qualifying the exponential as a candidate for the most part of the distribution and giving evidence of a significant departure from this behavior for the largest drawdowns. Results of the Maximum Likelihood test listed in Tab.C.3.6.1 confirm our proposed picture for the daily scale; the hypotheses of C=0 cannot be rejected for the first thresholds *i.e.* the probability of C=0 is as high as 27% for the 80% of the drawdowns. However, for thresholds upon 7% the SE model can be rejected at the 95% confidence level. Hence, larger drawdowns that represent about 1% of the sample require a different model as there is a statistically significant upward curvature. Reshuffling the daily returns we observe that, for the largest part, the top 1% DD lie above the 95% confidence interval of the synthetic time series, strengthening our hypotheses of time dependencies being at the origin of the largest DD.

C.2.1.2 FT-SE 100

Fig.20 and 22 show the survival function of ϵ-drawdowns in the price of futures of the FTSE-100 index for different levels of granularity in the data - 1-min to 1-day scales- and values of ϵ corresponding to 0 and 0.5σ as defined in Sec.2.3. All distribution seem to present a distinct change of regime at the naked eye.

The results from reshuffling the returns are shown in Fig.54 and Fig.55. We reject the hypotheses of time dependencies not being at the origin of the creation of DD at a 95% confidence level for all scales but 1-min.

TE-statistics (Fig.72) show a significant departure from an exponential behavior for the minutely and quarterly scales. The hourly scale has a behavior that reminds us of the Stretched Exponential as shown in [22]. The hourly scale cannot be qualified as an exponential but for the interval $0.5 \leq u \leq 3\%$. The $TP-$statistics are unable to validate the PL model but for small portions of the distribution.

The nested hypothesis test (see Tab.C.3.6.2) fails to reject the SE hypotheses for the daily scale. For the hourly scale, the Stretched

Exponential model is already strongly rejected for thresholds upon 2% ($P_{90\%}$).

Collapsing all the statistics does not reveal any special behavior at the tail that would be a syntom of a group of drawdowns belonging to a different family as it can be seen in Fig.107.

C.2.1.3 Nikkei 225

The distribution of $\epsilon-$drawdowns obtained for the Nikkei 225 data set (Fig.25 and Fig.27) do not show obvious evidence of a break in the tail of the distribution for high-frequency data, namely 1-min and 15-min scales. However, for hourly and daily scales and $\epsilon = 0$ the largest three drawdowns lie above the straight line depicted by the rest of their smaller siblings. This is not clearly observed for the hourly and daily $\sigma/2-$DD distributions.

Returns for the Nikkei 225 were reshuffled 500 times and the $\epsilon-$DD recalculated, this time, extracting any time dependencies. The results in Fig.56 and 57 show no large deviations of the reshuffled time series with the original one for the high-frequency data. Nontheless, for larger time scales, the tail of the original distribution clearly deviates from the synthetic data, hereby, showing symptoms of the importance of the time dependencies that presumably lie at the origine of the largest DD in the tail.

Oscillations of the $TE-$statics do not allow us to assert nor reject an exponential model. For the highest quantiles, however, $TP-$statistics reveal a convergency towards a PL.

The ML and scale collapsing tests are undecisive, the three largest events that for the hourly and daily time scales seem appear as a break in the distribution were not captured by these tests.

C.2.2 Drawdowns in currencies

The following sections study the existence of *Dragon-Kings* in the distribution of drawdowns of the price of futures of the Japanese Yen and the now disappeared Deutschmark.

C.2.2.1 Japanese Yen

Reshuffling the returns of the original dataset eliminates any high order correlation. Hence, observing that the original DD distribution lies within the 95% confidence interval does not allow us to reject the hypotheses of time dependencies being at the origin of the larger DD. This is what we observe for the Japanese Yen dataset at the minute scale in Fig.58. *Par contre*, for all other scales the larger part of the original distribution lies

significantly above the synthetic distributions giving a first indication of time dependencies playing a key role in the DD creation.

Fig.29 shows for the quarterly, hourly and daily scale a shape that resseambles that of a straight line that would qualify the DD-distributions as an exponential in a semilog plot. In the above mentioned cases a trained eye can detect a break in the distribution, being specially obvious for the hourly scale at about 2%. In Fig.76, $TE-$test concurs with the naked eye in envisaging a deviation from the exponential behavior for drawdowns larger than 2% for the hourly and daily scale and at the 1% threshold for the quarterly scale. The nested hypothesis test applied to the daily distribution rejects the C=0 hypothesis at a 95% confidence level for thresholds upon 2.66%, this implies that 90% of the sample is well described by the SE whereas the 10% largest DD are significantly better described by the MSE. Furthermore, the collapsing of the distributions at different scales in figure 109 reveals a special behavior at the tail of the distribution.

C.2.2.2 Deutschmark

The surrogate data analysis consisting of reshuffling the return time series destroys any high order correlations. Hence, if the original DD distribution does not exhibit a significant departure from the synthetic data sets, it fails to reject the hypotheses of order of returns not being paramount in the DD distribution. This conclusion can be drawn from observing Fig.60 for the 1-min and 15-min scales. On the other hand, distributions for the hourly and daily scale significantly deviate from that of the synthetic data.

Nested hypothesis test is not conclusive for the hourly scale. Nevertheless, for the daily scale, the probability of C=0 for 95% of the sample is 13.7%. The Stretched Exponential hypotheses is only rejected at a 95% confidence level for DD sizes larger than 6.5%, including in this latter group 1% of the drawdowns. T-statistcs do not reveal neither a TE nor a PL behavior for any of the studied scales.

C.2.3 Drawdowns in Government Bonds

This section investigates the presence of *DK* in the distribution of DD in the price of futures on the Government Bonds of Japan, the US and Germany.

C.2.3.1 Japanese Government Bonds

Fig.62 shows the original DD distribution superposed on five hundred distributions of DD constituted by reshuffling the returns. Only for

the daily scale lies the original distribution significantly above the synthetic distributions. There is a negligible probability of a DD of that size occurring by randomly concatenating returns. This test reject the hypotheses of order of returns not being a generating mechandism for the DD and qualifies the existence of *DK* in the low-frequency scales.

Nested hypothesis test (Tab.C.3.6.6) gives evidence of two a change of regime in the distribution of DD occurring for drawdowns larger than 1.86% ($P_{99.5}$), below that, namely 99.5% of the DD, the SE hypothesis (C=0) cannot be rejected at a 95% confidence level.

In Fig.80, $TE-$statistics dismiss the possibility of the distribution behaving as exponential at any scale. $TP-$statistics, however, show a convergence to a PL (Fig.98) for all scales.

C.2.3.2 US Treasury Bonds

US Treasury Bonds is composed by two datasets: US1 and US3. A preliminary observation of Fig.40 and 44 suggests that distribution for high frequency data converge to a PL-like behavior. This is partially reinforced by the $TP-$statistic in Fig.100 where, certain intervals, can be described by a PL and asserted in Fig.102 in which the PL seems to describe well the distribution. The TE-test clearly rejects the exponential hypotheses.

Nested hypothesis test indicates that for the hourly time scale, the stretched exponential can be accepted to describe 99% of the drawdowns in the distributions and it is only upon drawdowns larger than 3% that the upward curvature described by the empirical distribution becomes significant at a 95% level.

C.2.3.3 German Government Bonds

$TP-$statistics in Fig.104 gives evidence of a power law behavior of the distribution of DD for the minute scale. For larger scales, however, the distribution in Fig.49 can be better described by an exponential, in line with the results of the $TE-$test in Fig.86.

In Fig.68, original distributions for the quaterly, hourly and daily scale clearly deviate from the synthetically generated ones. This tests gives evidence of time dependencies and high order correlations playing a key role in the creation of drawdowns. Collapsing the distributions of DD at different is possible and there is no obvious signature of a different regime.

The nested hypothesis test (Tab.C.3.6.9) gives evidence of a change of regime for DD larger than 2.62 % at the daily scale. Below this threshold (99% of the drawdowns), the distribution is well described

by a SE exponential. Upon this threshold, the hypothesis of C=0 may be rejected at a 95% confidence level.

C.3 Figures

C.3.1 Distributions of ϵ-DD for different scales

C.3.1.1 SP 500

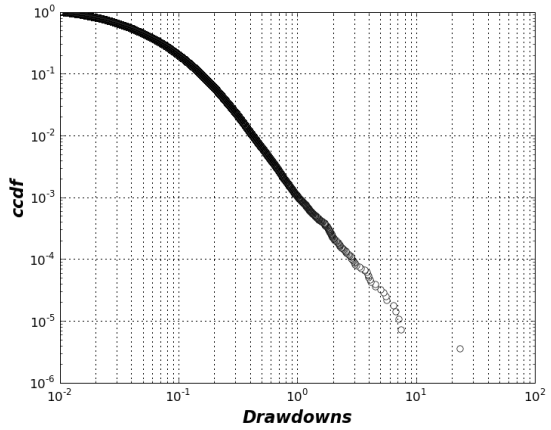

(a) SP 500 at 1-min scale

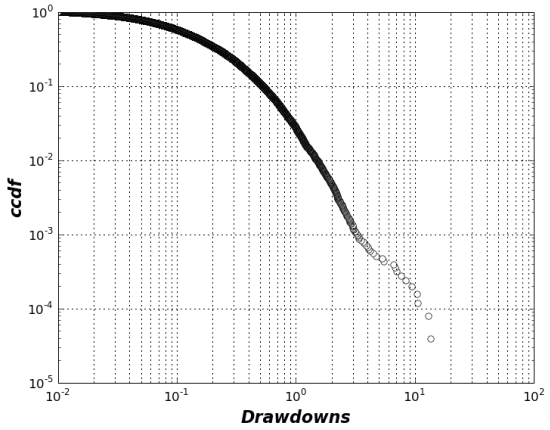

(b) SP 500 at 15-min scale

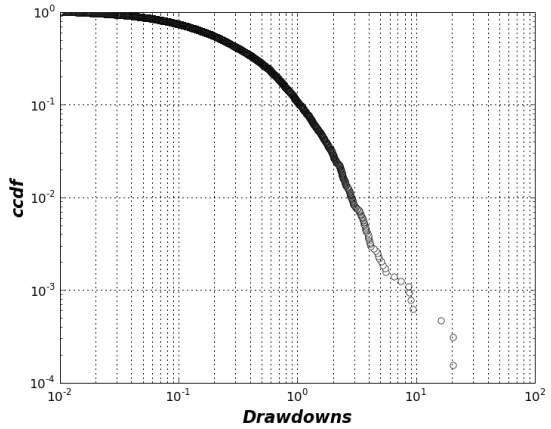

(c) SP 500 at 1-hour scale

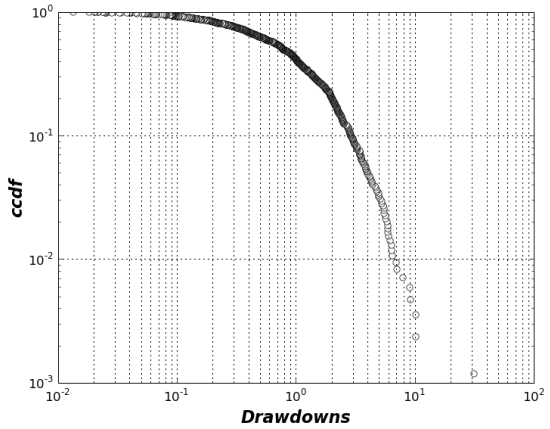

(d) SP 500 at 1-day scale

Fig. 16: Logarithmic plots of the complementary cumulative distribution of *pure* drawdowns ($\epsilon = 0$) for the price of futures on the SP 500 index at different time scales -from 1-min to 1-day-.

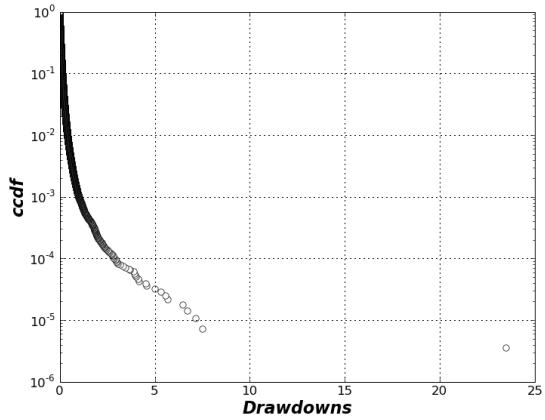

(a) SP 500 at 1-min scale

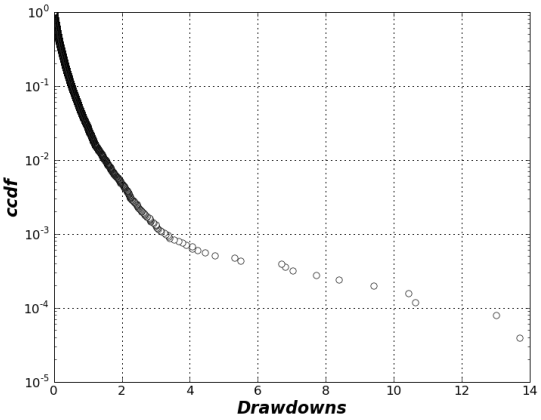

(b) SP 500 at 15-min scale

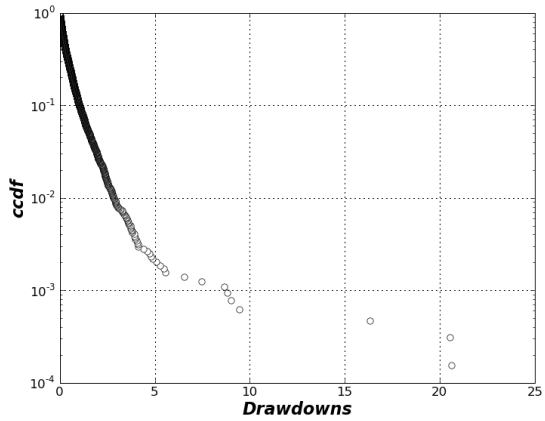

(c) SP 500 at 1-hour scale

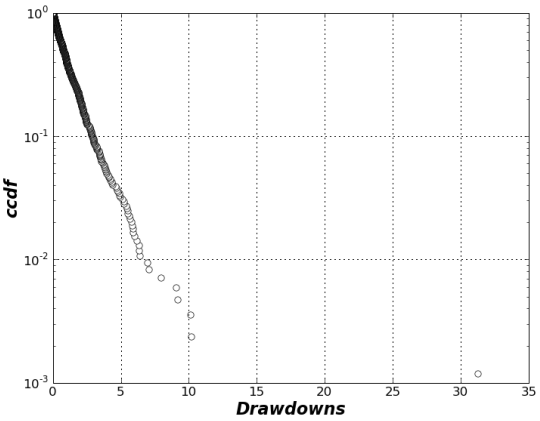

(d) SP 500 at 1-day scale

Fig. 17: Log-linear plots of the complementary cumulative distribution of *pure* drawdowns ($\epsilon = 0$) for the price of futures on the SP 500 index at different time scales -from 1-min to 1-day-.

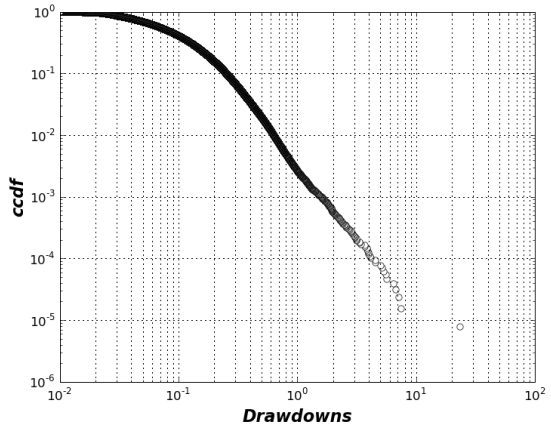

(a) SP 500 at 1-min scale

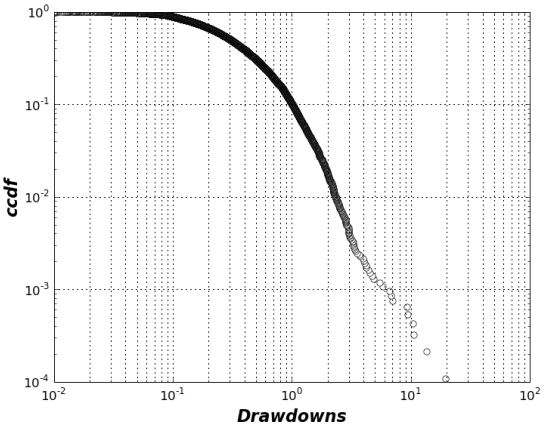

(b) SP 500 at 15-min scale

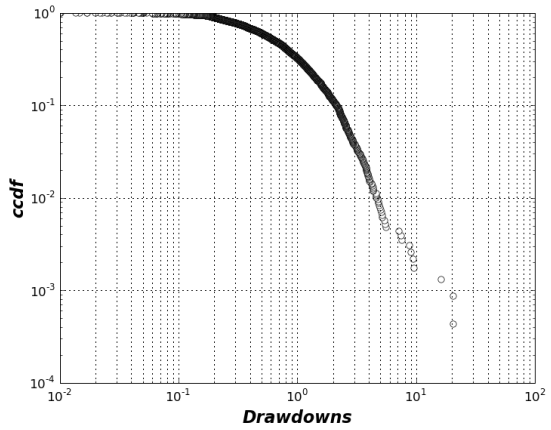

(c) SP 500 at 1-hour scale

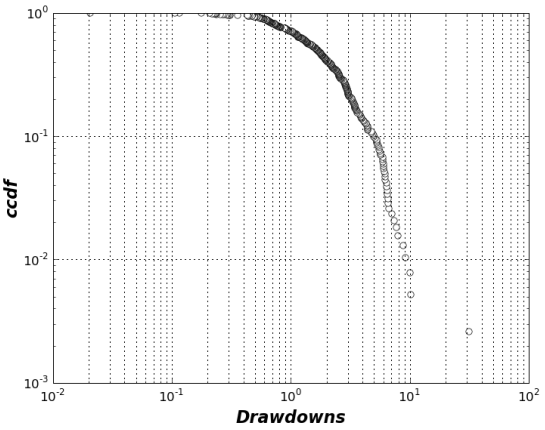

(d) SP 500 at 1-day scale

Fig. 18: Logarithmic plots of the complementary cumulative distribution of $\epsilon-$drawdowns ($\epsilon = 0.5\sigma$) for the price of futures on the SP 500 index at different time scales -from 1-min to 1-day-.

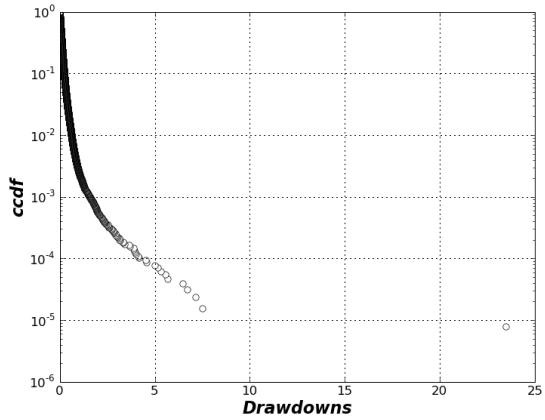

(a) SP 500 at 1-min scale

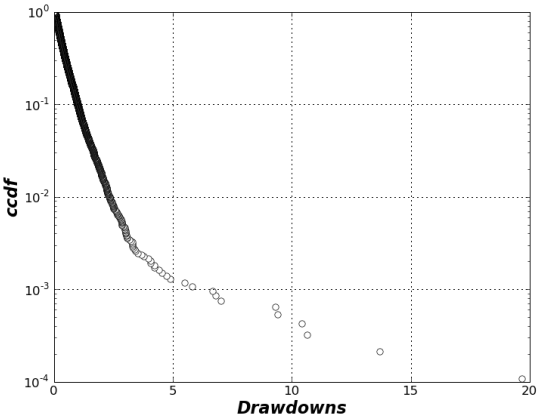

(b) SP 500 at 15-min scale

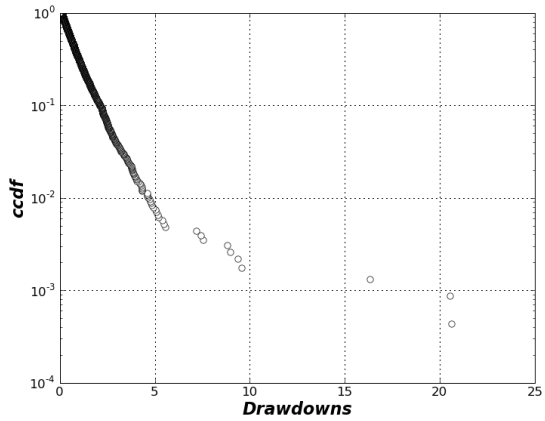

(c) SP 500 at 1-hour scale

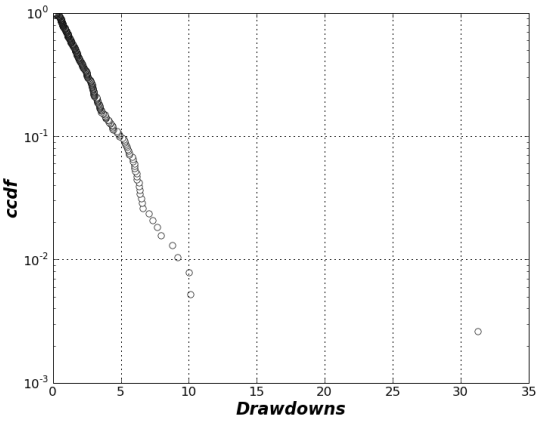

(d) SP 500 at 1-day scale

Fig. 19: Log-linear plots of the complementary cumulative distribution of $\epsilon-$drawdowns ($\epsilon = 0.5\sigma$) for the price of futures on the SP 500 index at different time scales -from 1-min to 1-day-.

C.3.1.2 FTSE 100

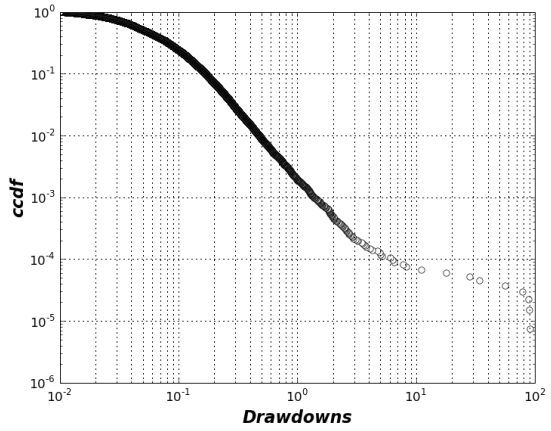

(a) FTSE 100 at 1-min scale

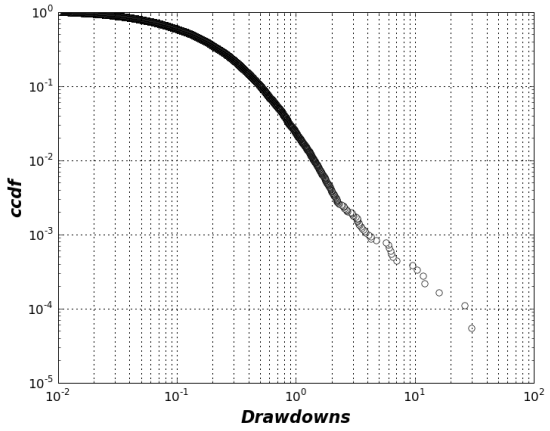

(b) FTSE 100 at 15-min scale

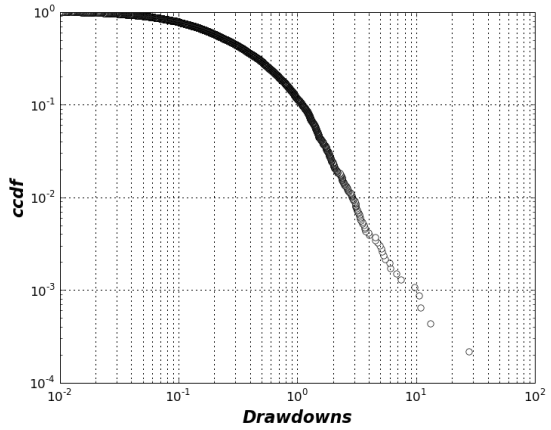

(c) FTSE 100 at 1-hour scale

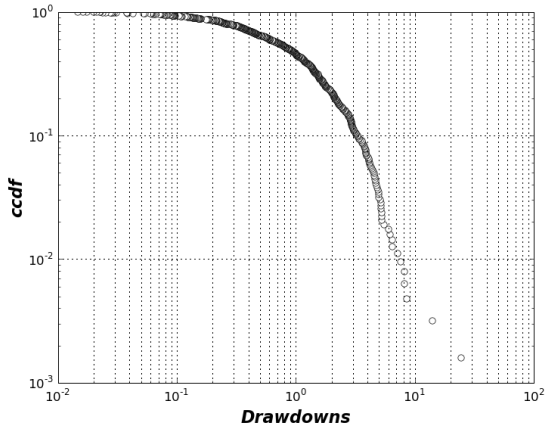

(d) FTSE 100 at 1-day scale

Fig. 20: Logarithmic plots of the complementary cumulative distribution of *pure* drawdowns ($\epsilon = 0$) for the price of futures on the FTSE 100 index at different time scales -from 1-min to 1-day-.

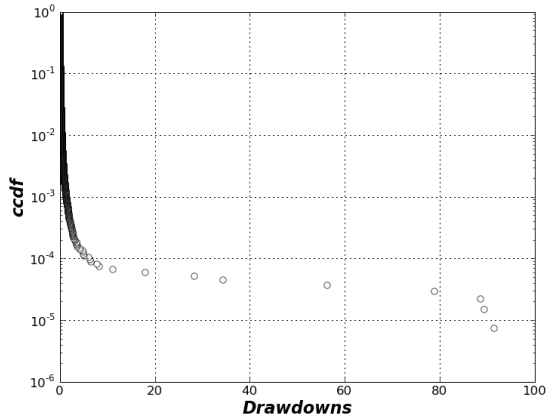

(a) FTSE 100 at 1-min scale

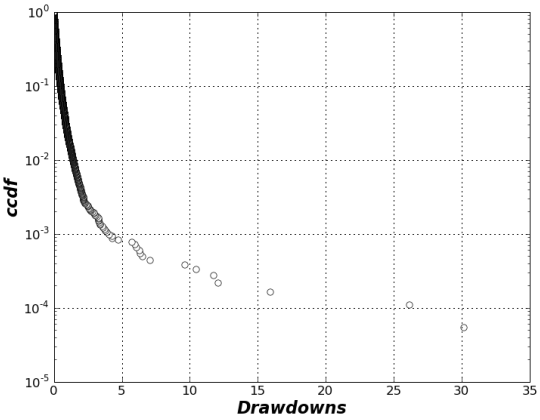

(b) FTSE 100 at 15-min scale

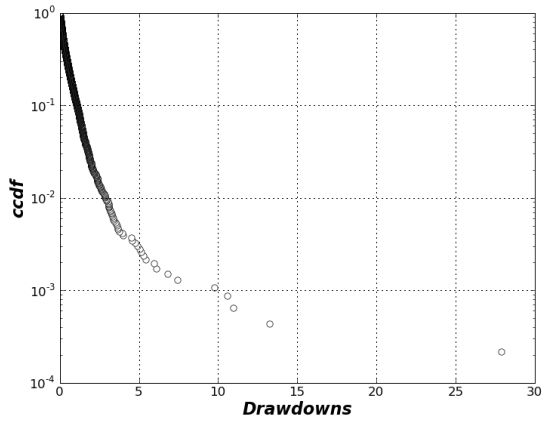

(c) FTSE 100 at 1-hour scale

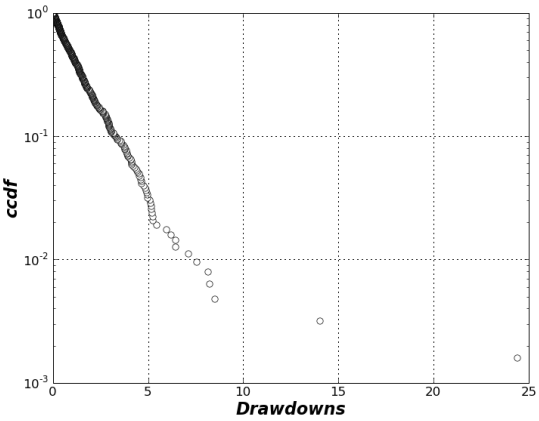

(d) FTSE 100 at 1-day scale

Fig. 21: Log-linear plots of the complementary cumulative distribution of *pure* drawdowns ($\epsilon = 0$) for the price of futures on the FTSE 100 index at different time scales -from 1-min to 1-day-.

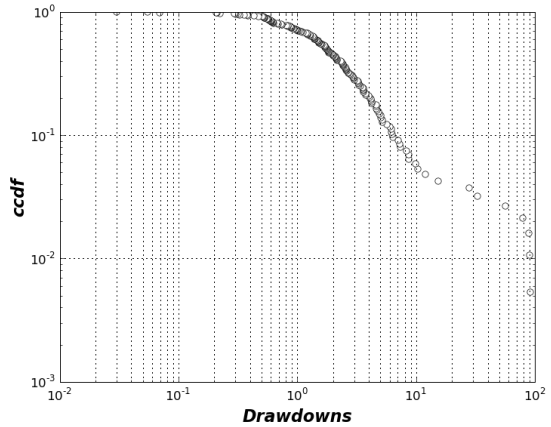

(a) FTSE 100 at 1-min scale

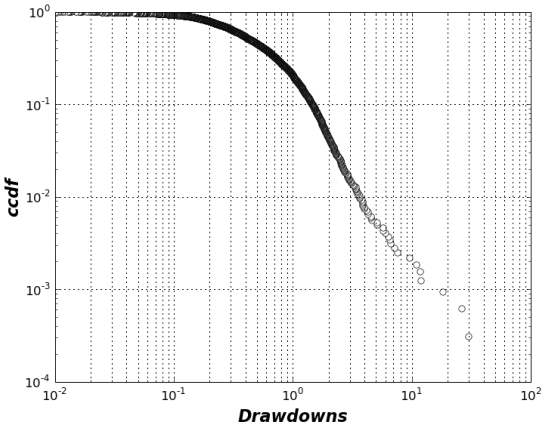

(b) FTSE 100 at 15-min scale

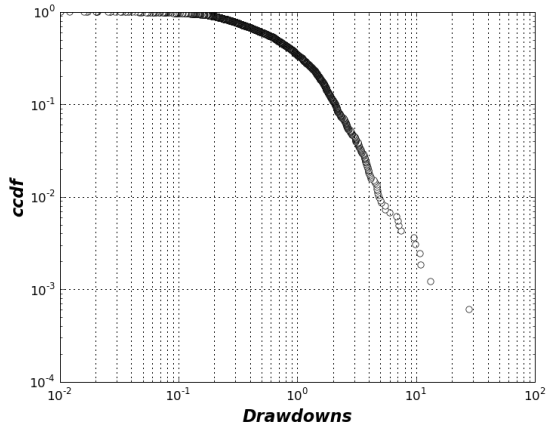

(c) FTSE 100 at 1-hour scale

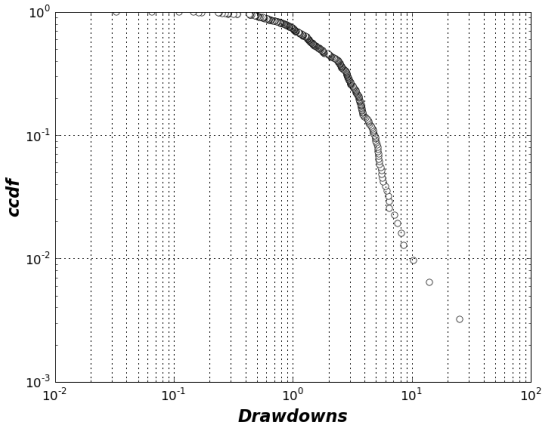

(d) FTSE 100 at 1-day scale

Fig. 22: Logarithmic plots of the complementary cumulative distribution of $\epsilon-$drawdowns ($\epsilon = 0.5\sigma$) for the price of futures on the FTSE 100 index at different time scales -from 1-min to 1-day-.

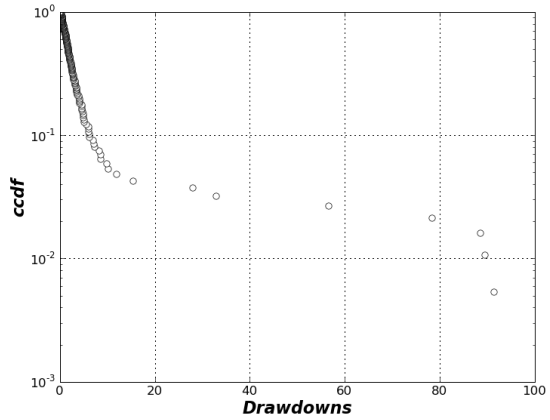

(a) FTSE 100 at 1-min scale

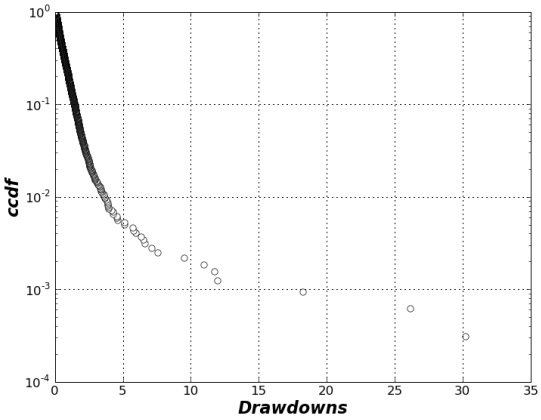

(b) FTSE 100 at 15-min scale

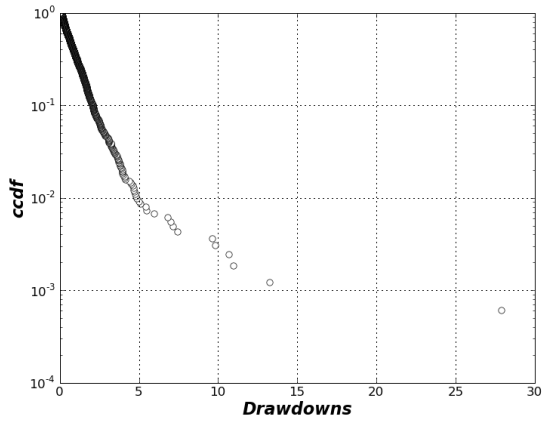

(c) FTSE 100 at 1-hour scale

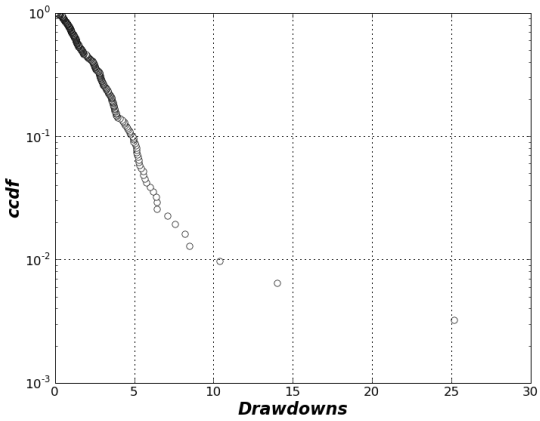

(d) FTSE 100 at 1-day scale

Fig. 23: Log-linear plots of the complementary cumulative distribution of $\epsilon-$drawdowns ($\epsilon = 0.5\sigma$) for the price of futures on the FTSE 100 index at different time scales -from 1-min to 1-day-.

C.3.1.3 Nikkei 225

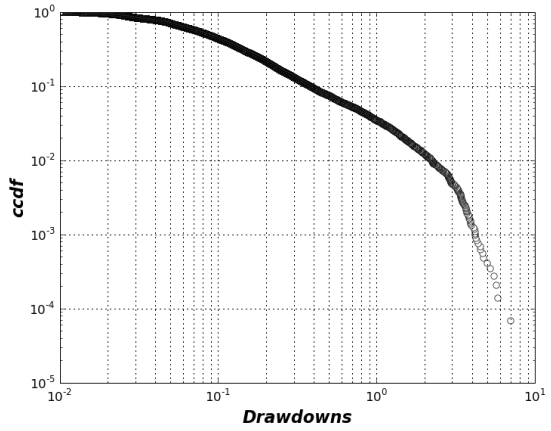

(a) Nikkei 225 at 1-min scale

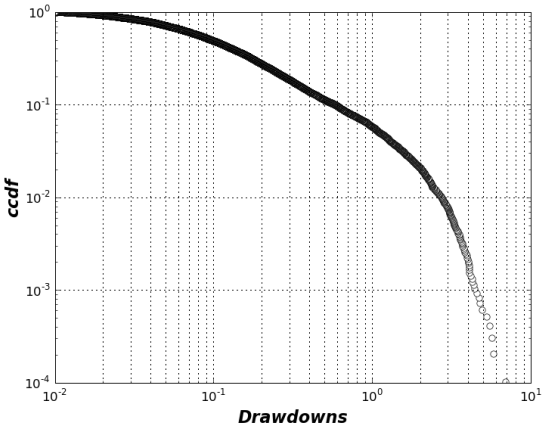

(b) Nikkei 225 at 15-min scale

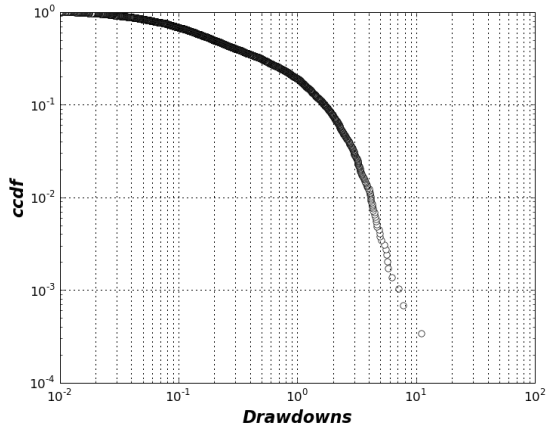

(c) Nikkei 225 at 1-hour scale

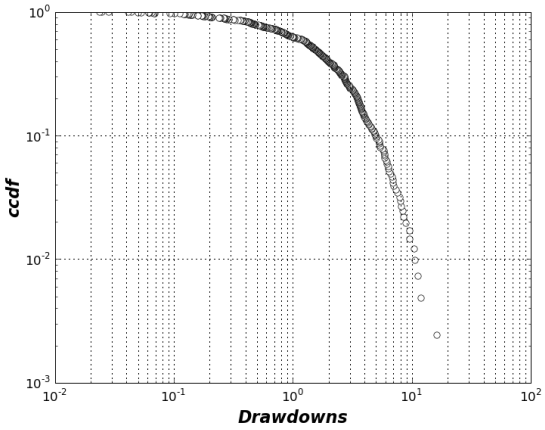

(d) Nikkei 225 at 1-day scale

Fig. 24: Logarithmic plots of the complementary cumulative distribution of *pure* drawdowns ($\epsilon = 0$) for the price of futures on the Nikkei 225 index at different time scales -from 1-min to 1-day-.

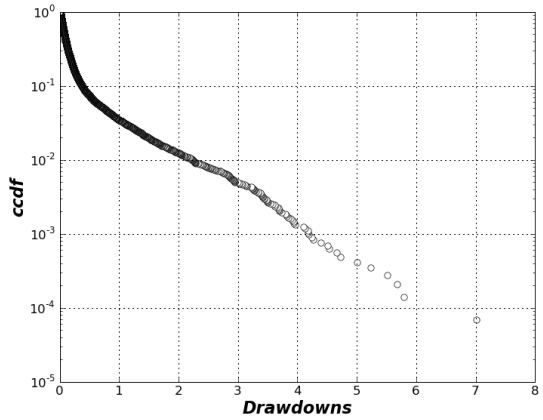

(a) Nikkei 225 at 1-min scale

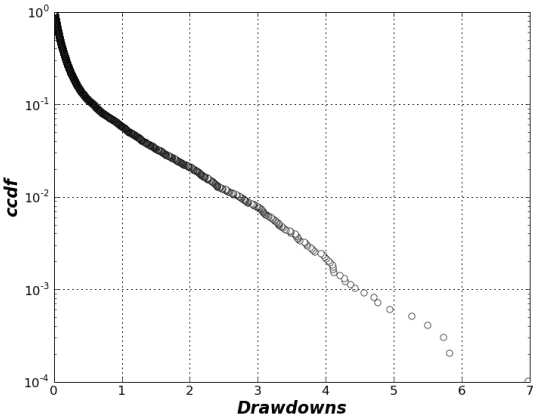

(b) Nikkei 225 at 15-min scale

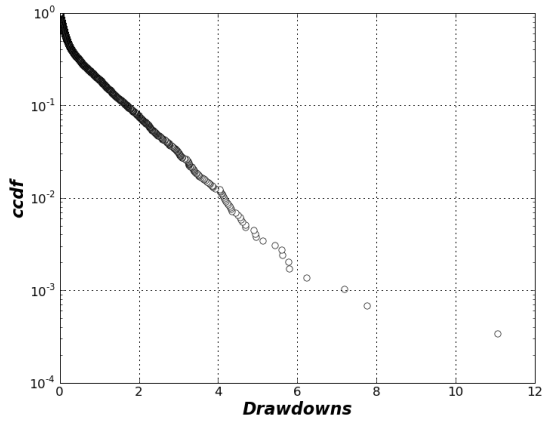

(c) Nikkei 225 at 1-hour scale

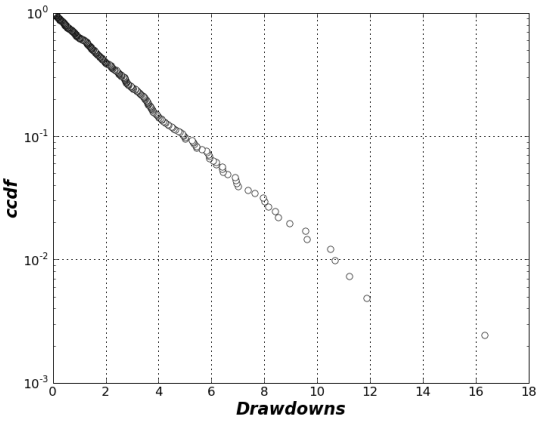

(d) Nikkei 225 at 1-day scale

Fig. 25: Log-linear plots of the complementary cumulative distribution of *pure* drawdowns ($\epsilon = 0$) for the price of futures on the Nikkei 225 index at different time scales -from 1-min to 1-day-.

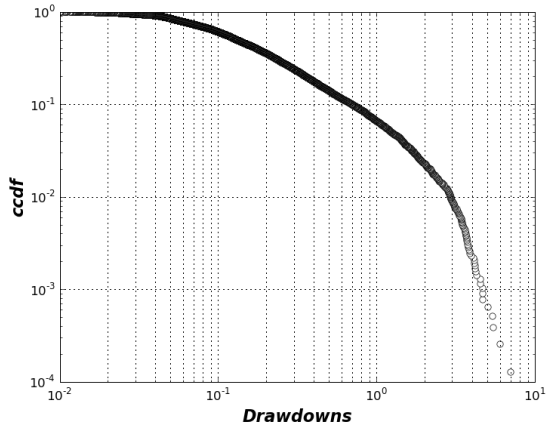

(a) Nikkei 225 at 1-min scale

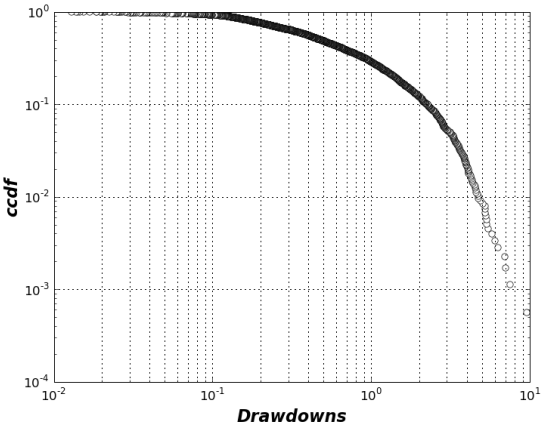

(b) Nikkei 225 at 15-min scale

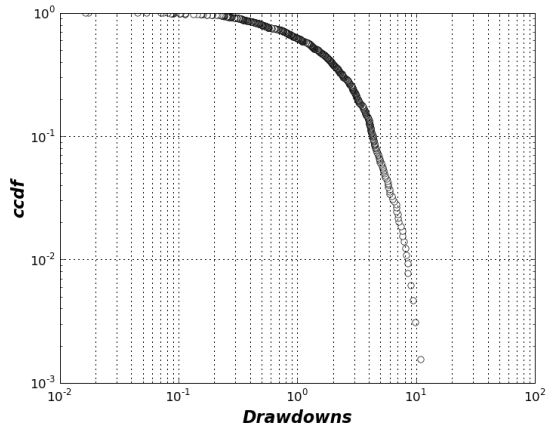

(c) Nikkei 225 at 1-hour scale

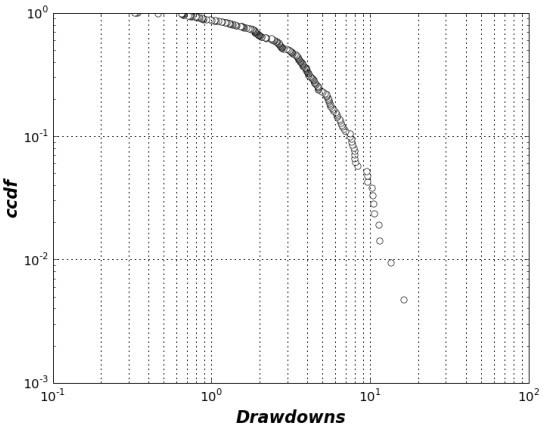

(d) Nikkei 225 at 1-day scale

Fig. 26: Logarithmic plots of the complementary cumulative distribution of $\epsilon-$drawdowns ($\epsilon = 0.5\sigma$) for the price of futures on the Nikkei 225 index at different time scales -from 1-min to 1-day-.

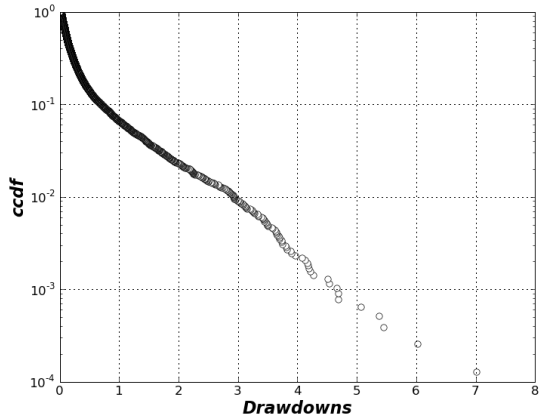

(a) Nikkei 225 at 1-min scale

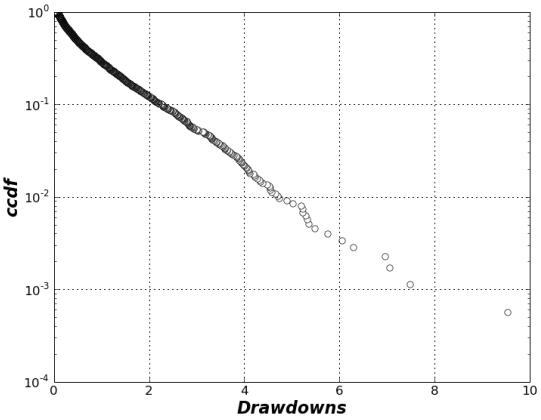

(b) Nikkei 225 at 15-min scale

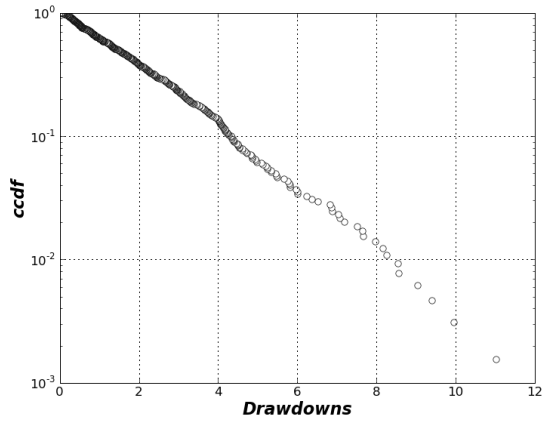

(c) Nikkei 225 at 1-hour scale

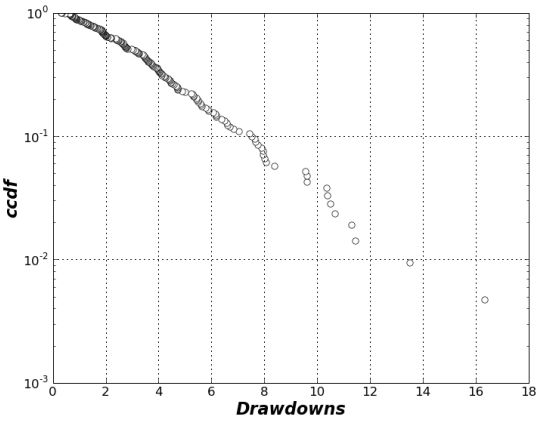

(d) Nikkei 225 at 1-day scale

Fig. 27: Log-linear plots of the complementary cumulative distribution of $\epsilon-$drawdowns ($\epsilon = 0.5\sigma$) for the price of futures on the Nikkei 225 index at different time scales -from 1-min to 1-day-.

C.3.1.4 Japanese Yen

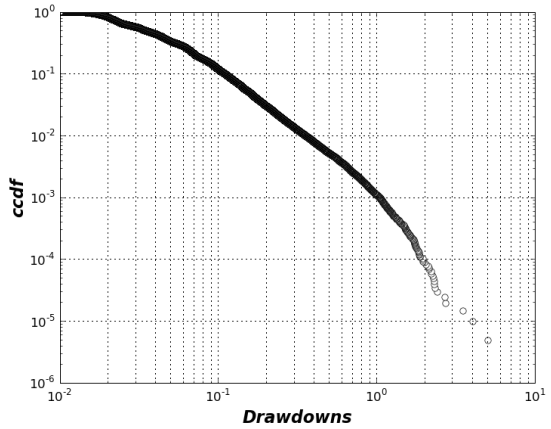

(a) Japanese Yen at 1-min scale

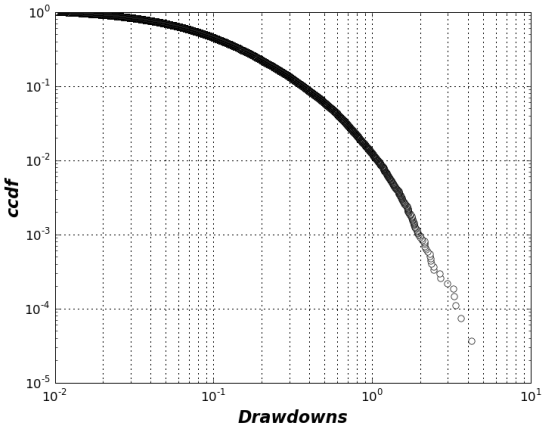

(b) Japanese Yen at 15-min scale

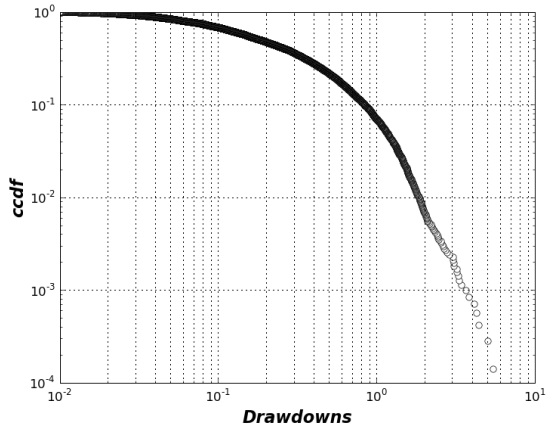

(c) Japanese Yen at 1-hour scale

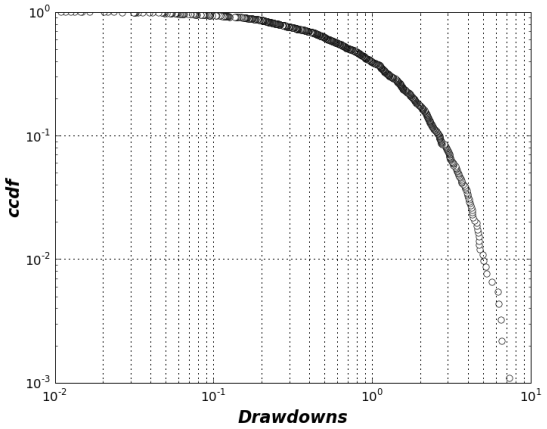

(d) Japanese Yen at 1-day scale

Fig. 28: Logarithmic plots of the complementary cumulative distribution of *pure* drawdowns ($\epsilon = 0$) for the price of futures on the Japanese Yen index at different time scales -from 1-min to 1-day-.

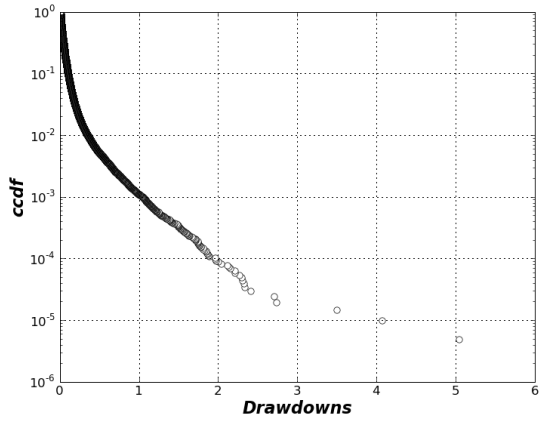

(a) Japanese Yen at 1-min scale

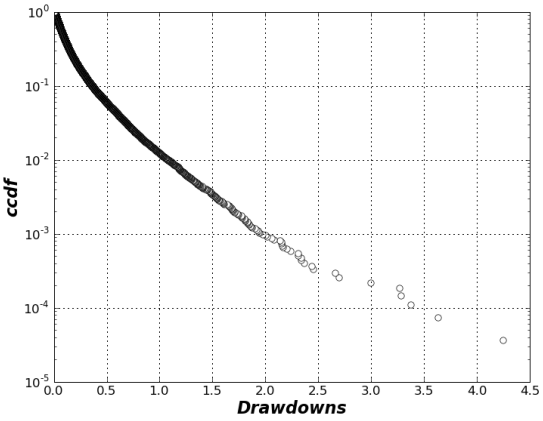

(b) Japanese Yen at 15-min scale

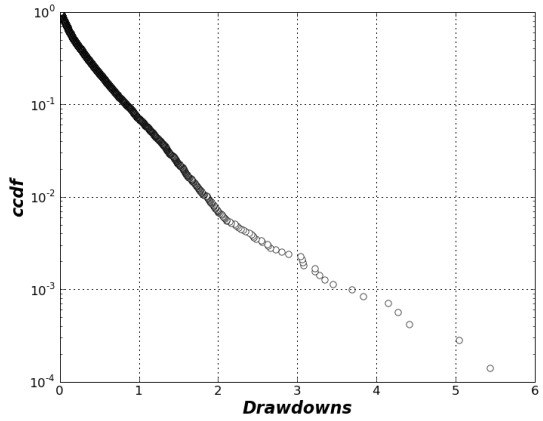

(c) Japanese Yen at 1-hour scale

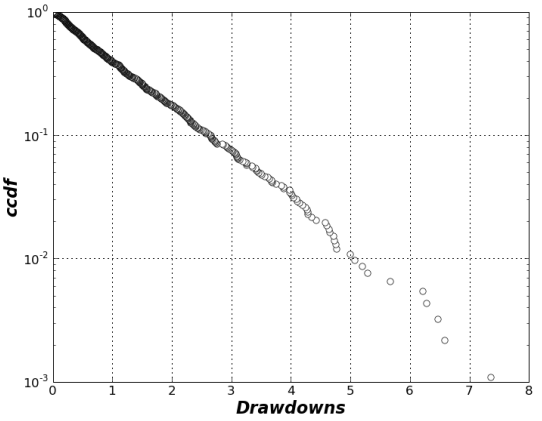

(d) Japanese Yen at 1-day scale

Fig. 29: Log-linear plots of the complementary cumulative distribution of *pure* drawdowns ($\epsilon = 0$) for the price of futures on the Japanese Yen index at different time scales -from 1-min to 1-day-.

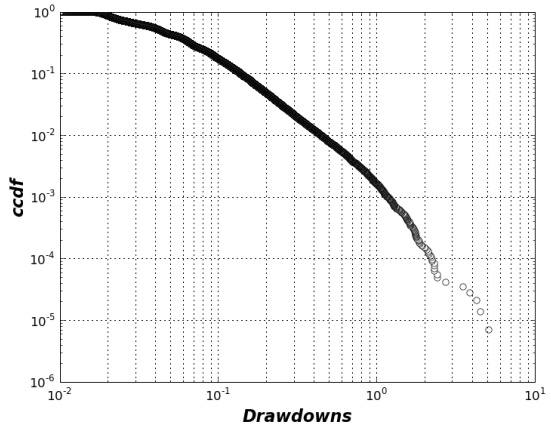

(a) Japanese Yen at 1-min scale

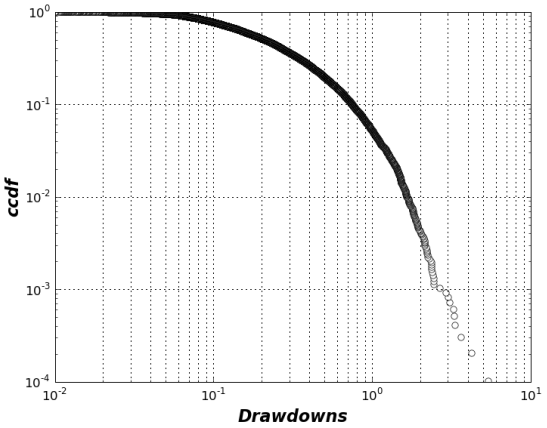

(b) Japanese Yen at 15-min scale

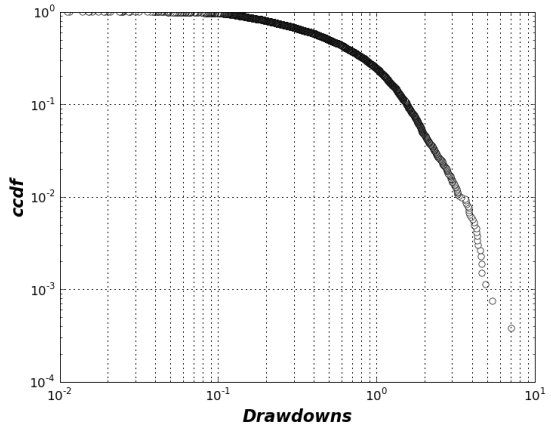

(c) Japanese Yen at 1-hour scale

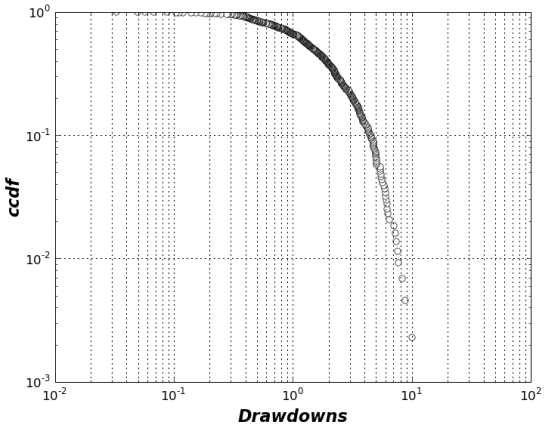

(d) Japanese Yen at 1-day scale

Fig. 30: Logarithmic plots of the complementary cumulative distribution of $\epsilon-$drawdowns ($\epsilon = 0.5\sigma$) for the price of futures on the Japanese Yen index at different time scales -from 1-min to 1-day-.

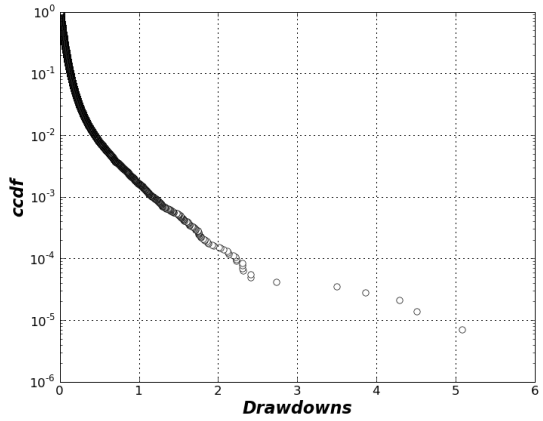

(a) Japanese Yen at 1-min scale

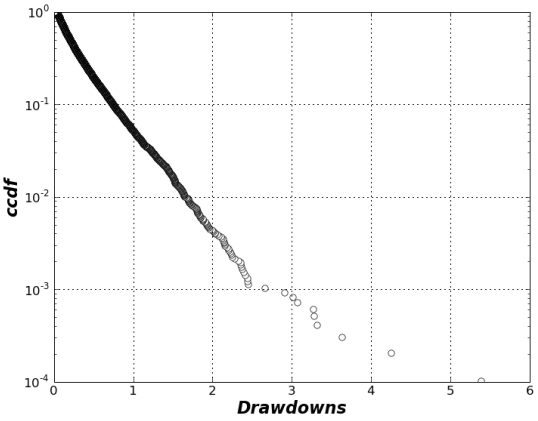

(b) Japanese Yen at 15-min scale

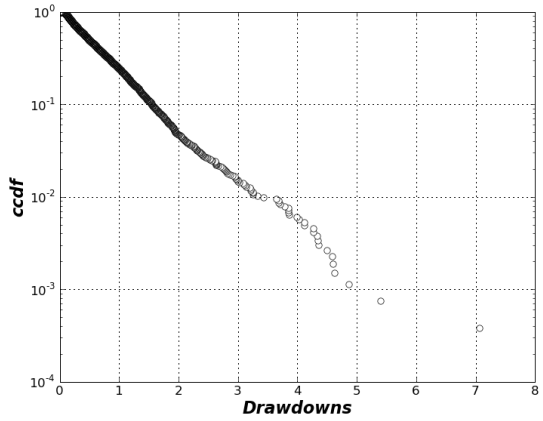

(c) Japanese Yen at 1-hour scale

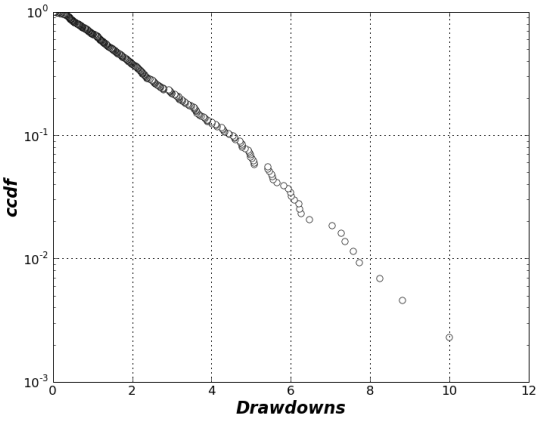

(d) Japanese Yen at 1-day scale

Fig. 31: Log-linear plots of the complementary cumulative distribution of $\epsilon-$drawdowns ($\epsilon = 0.5\sigma$) for the price of futures on the Japanese Yen index at different time scales -from 1-min to 1-day-.

C.3.1.5 Deutschmark

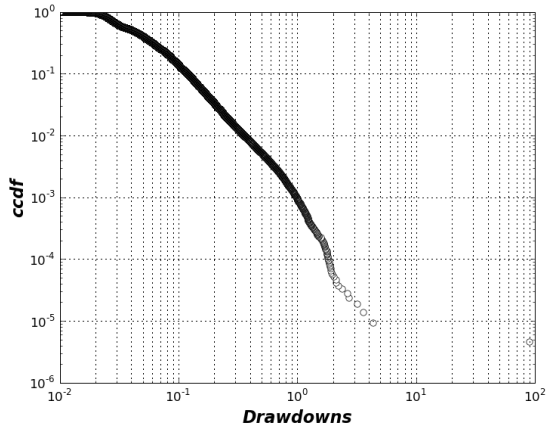

(a) Deutschmark at 1-min scale

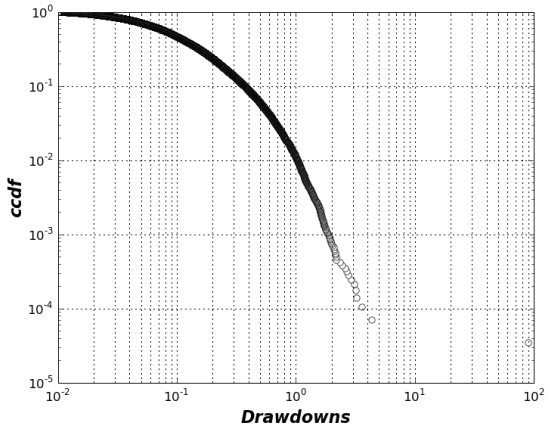

(b) Deutschmark at 15-min scale

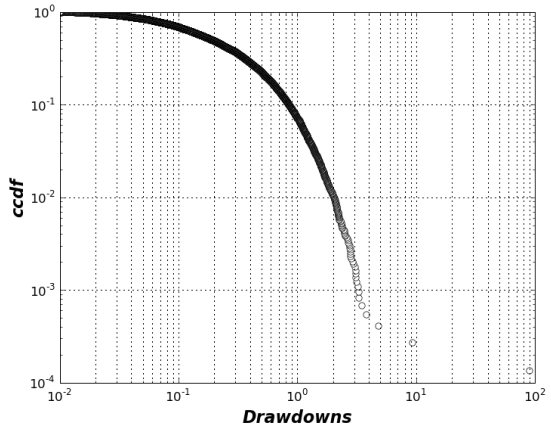

(c) Deutschmark at 1-hour scale

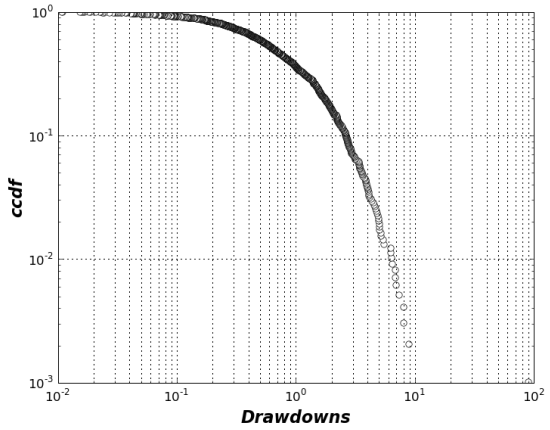

(d) Deutschmark at 1-day scale

Fig. 32: Logarithmic plots of the complementary cumulative distribution of *pure* drawdowns ($\epsilon = 0$) for the price of futures on the Deutschmark index at different time scales -from 1-min to 1-day-.

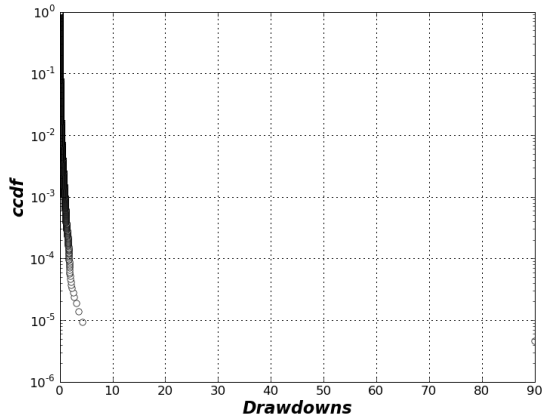

(a) Deutschmark at 1-min scale

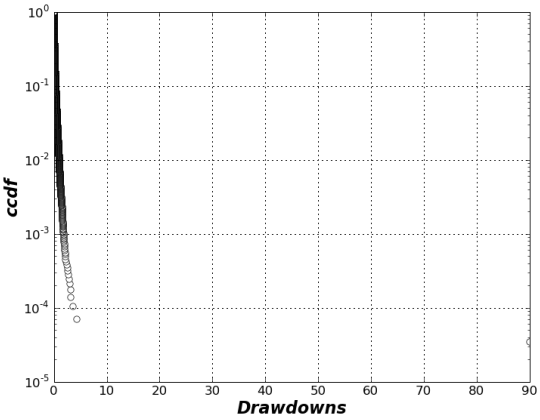

(b) Deutschmark at 15-min scale

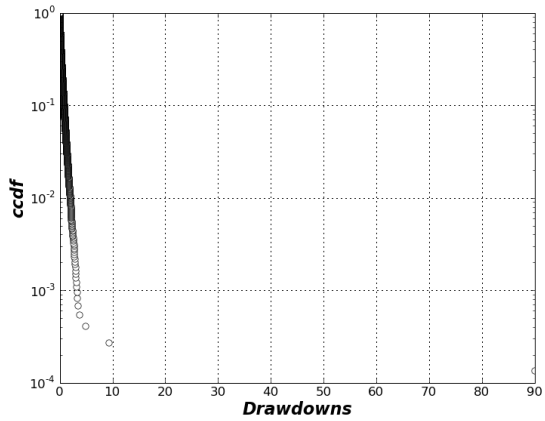

(c) Deutschmark at 1-hour scale

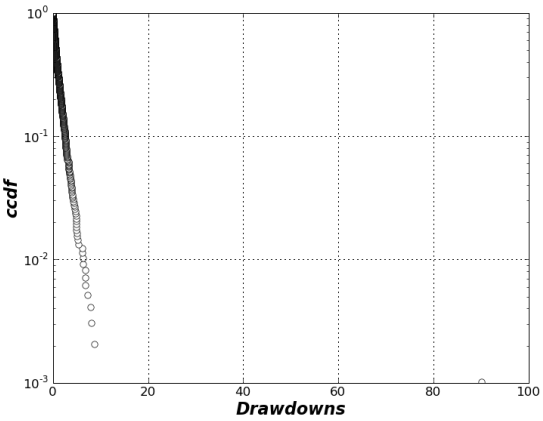

(d) Deutschmark at 1-day scale

Fig. 33: Log-linear plots of the complementary cumulative distribution of *pure* drawdowns ($\epsilon = 0$) for the price of futures on the Deutschmark index at different time scales -from 1-min to 1-day-.

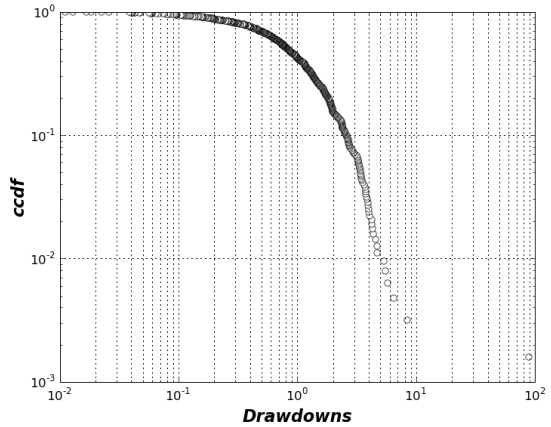

(a) Deutschmark at 1-min scale

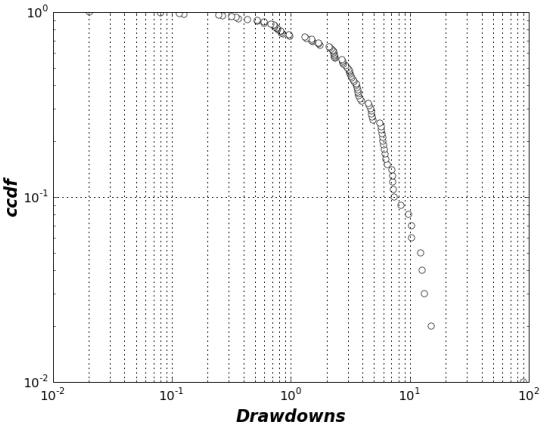

(b) Deutschmark at 15-min scale

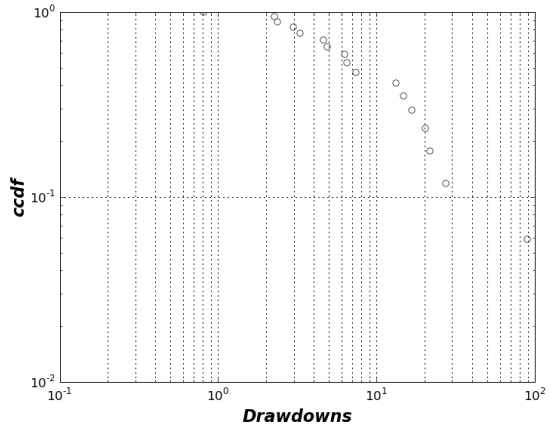

(c) Deutschmark at 1-hour scale

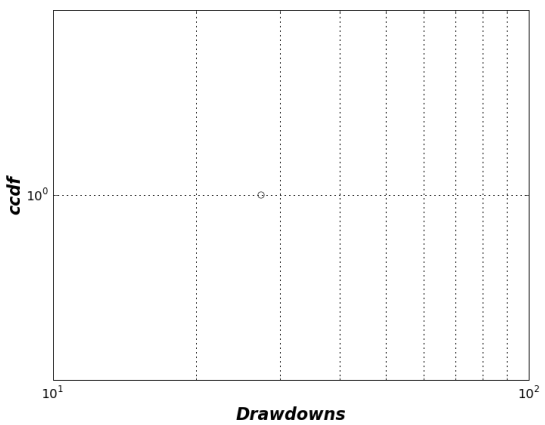

(d) Deutschmark at 1-day scale

Fig. 34: Logarithmic plots of the complementary cumulative distribution of $\epsilon-$drawdowns ($\epsilon = 0.5\sigma$) for the price of futures on the Deutschmark index at different time scales -from 1-min to 1-day-.

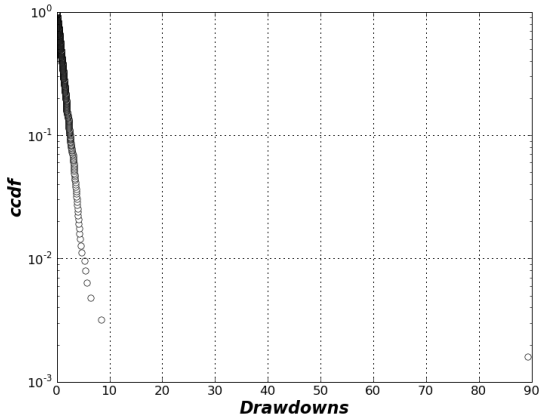

(a) Deutschmark at 1-min scale

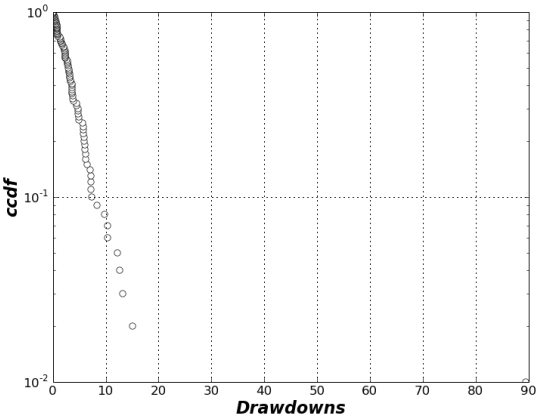

(b) Deutschmark at 15-min scale

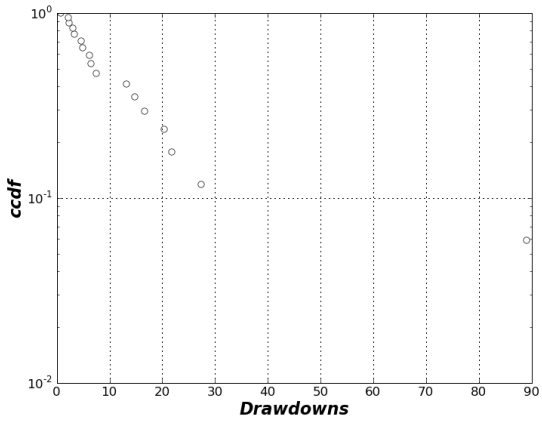

(c) Deutschmark at 1-hour scale

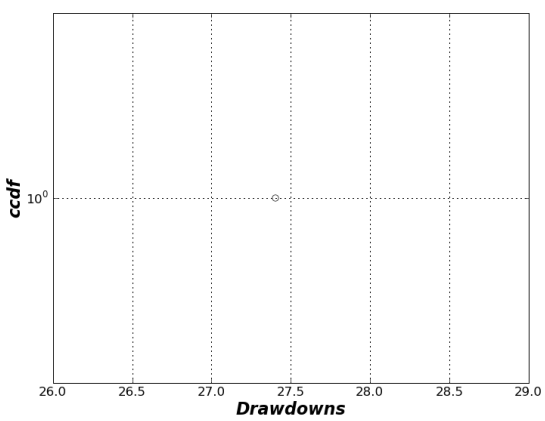

(d) Deutschmark at 1-day scale

Fig. 35: Log-linear plots of the complementary cumulative distribution of $\epsilon-$drawdowns ($\epsilon = 0.5\sigma$) for the price of futures on the Deutschmark index at different time scales -from 1-min to 1-day-.

C.3.1.6 Japanese Government Bonds

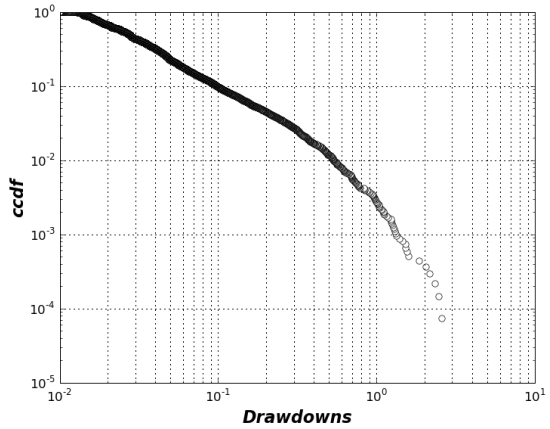

(a) Jap Government Bonds at 1-min scale

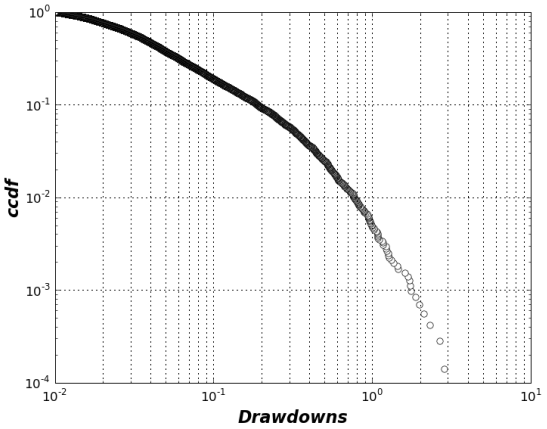

(b) Jap Government Bonds at 15-min scale

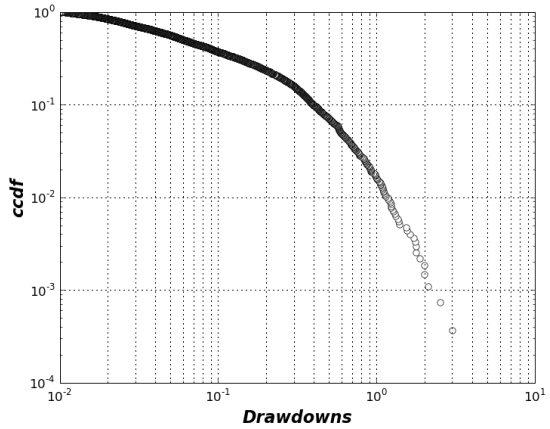

(c) Jap Government Bonds at 1-hour scale

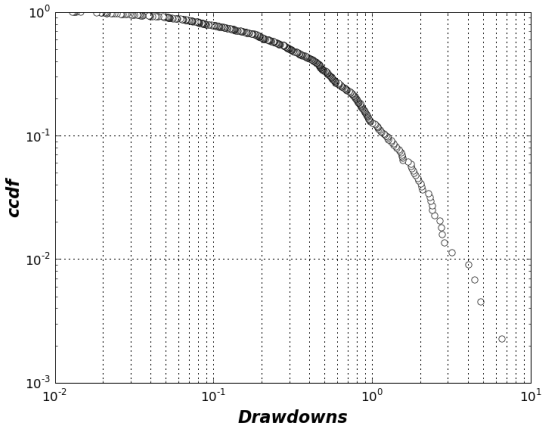

(d) Jap Government Bonds at 1-day scale

Fig. 36: Logarithmic plots of the complementary cumulative distribution of *pure* drawdowns ($\epsilon = 0$) for the price of futures on the Jap Government Bonds index at different time scales -from 1-min to 1-day-.

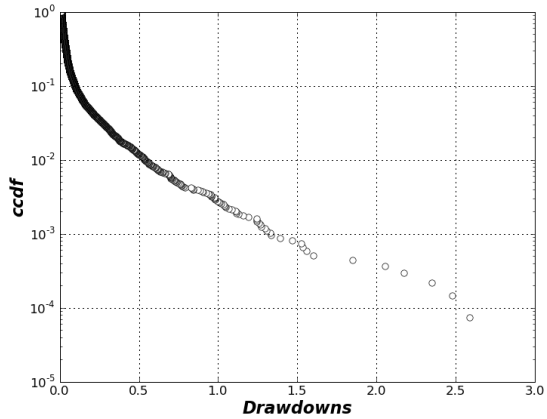

(a) Jap Government Bonds at 1-min scale

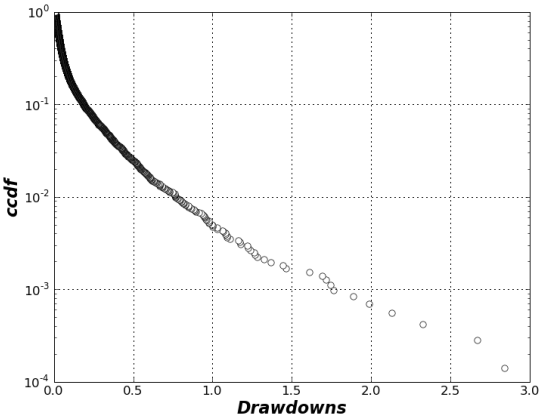

(b) Jap Government Bonds at 15-min scale

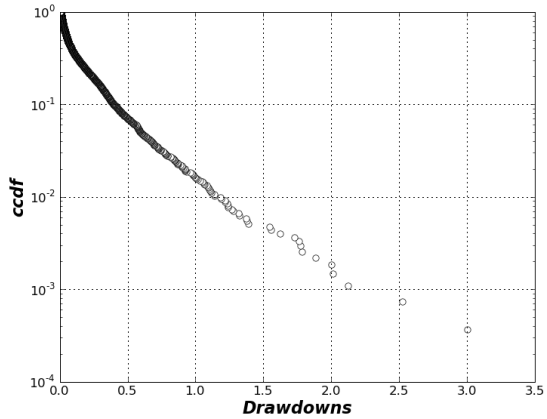

(c) Jap Government Bonds at 1-hour scale

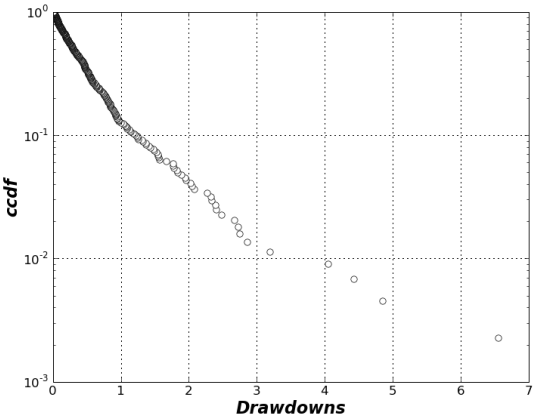

(d) Jap Government Bonds at 1-day scale

Fig. 37: Log-linear plots of the complementary cumulative distribution of *pure* drawdowns ($\epsilon = 0$) for the price of futures on the Jap Government Bonds index at different time scales -from 1-min to 1-day-.

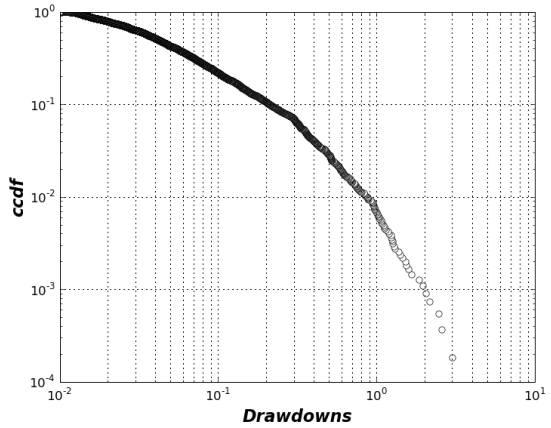

(a) Jap Government Bonds at 1-min scale

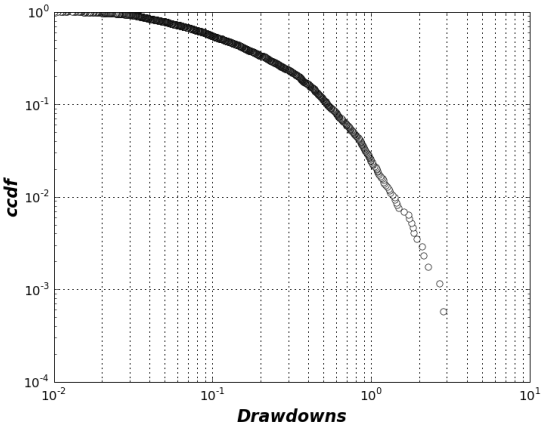

(b) Jap Government Bonds at 15-min scale

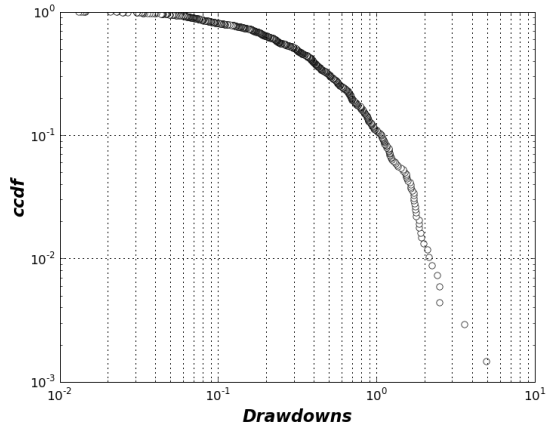

(c) Jap Government Bonds at 1-hour scale

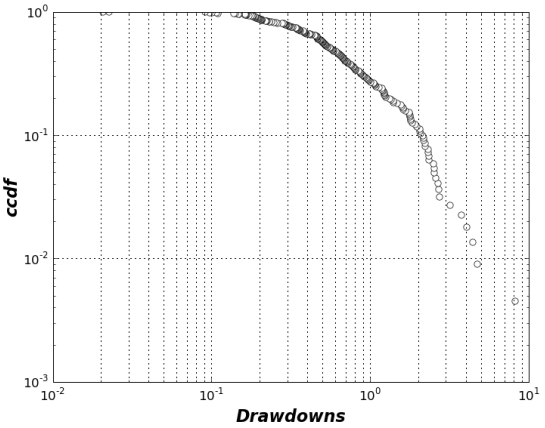

(d) Jap Government Bonds at 1-day scale

Fig. 38: Logarithmic plots of the complementary cumulative distribution of $\epsilon-$drawdowns ($\epsilon = 0.5\sigma$) for the price of futures on the Jap Government Bonds index at different time scales -from 1-min to 1-day-.

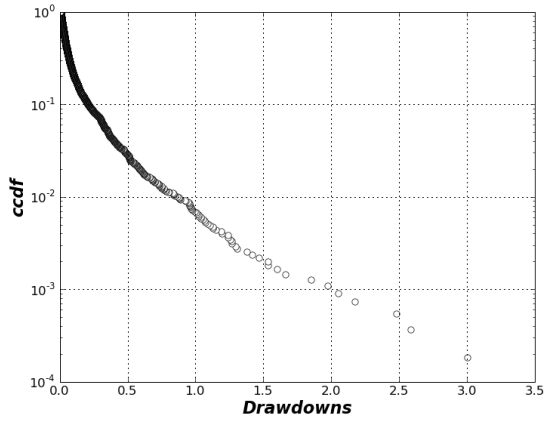

(a) Jap Government Bonds at 1-min scale

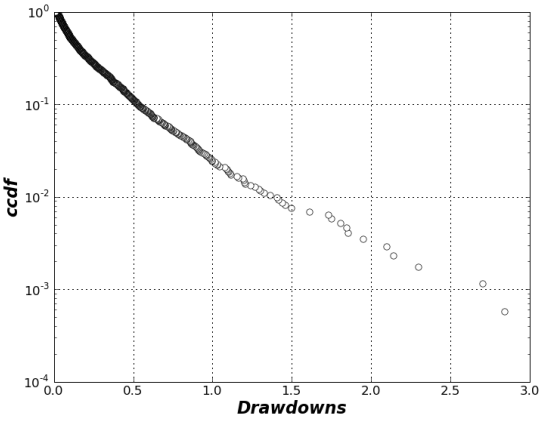

(b) Jap Government Bonds at 15-min scale

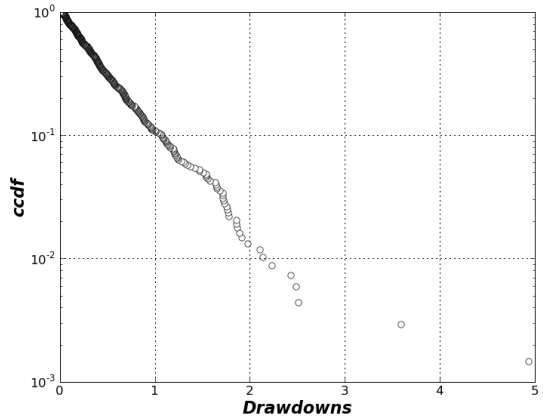

(c) Jap Government Bonds at 1-hour scale

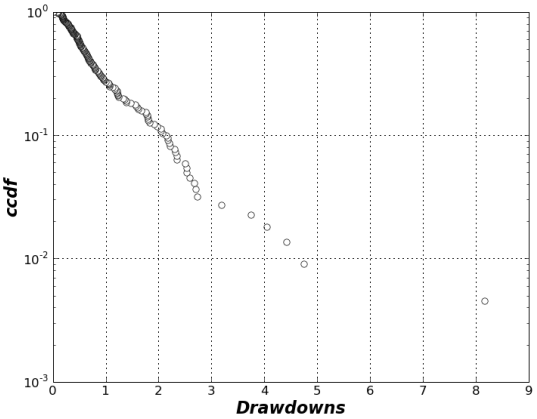

(d) Jap Government Bonds at 1-day scale

Fig. 39: Log-linear plots of the complementary cumulative distribution of $\epsilon-$drawdowns ($\epsilon = 0.5\sigma$) for the price of futures on the Jap Government Bonds index at different time scales -from 1-min to 1-day-.

C.3.1.7 US Treasury Bonds I

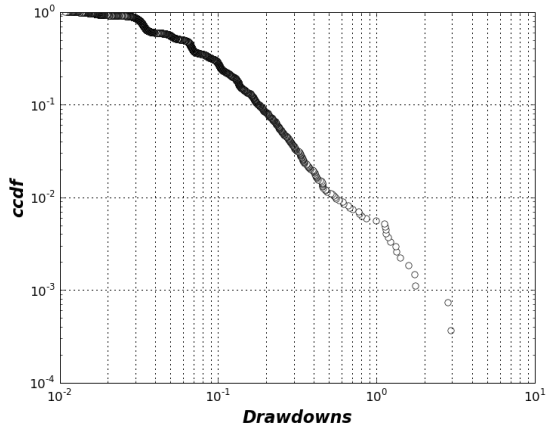

(a) US T-Bonds I at 1-min scale

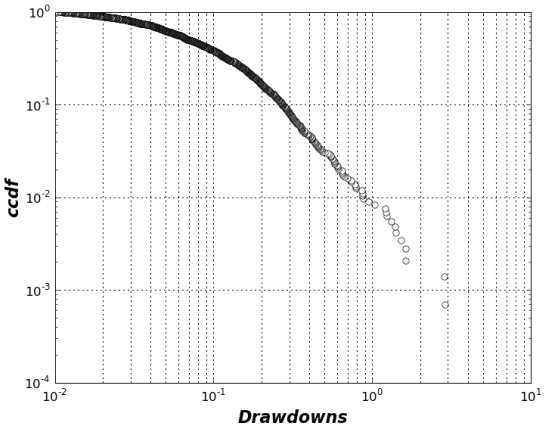

(b) US T-Bonds I at 15-min scale

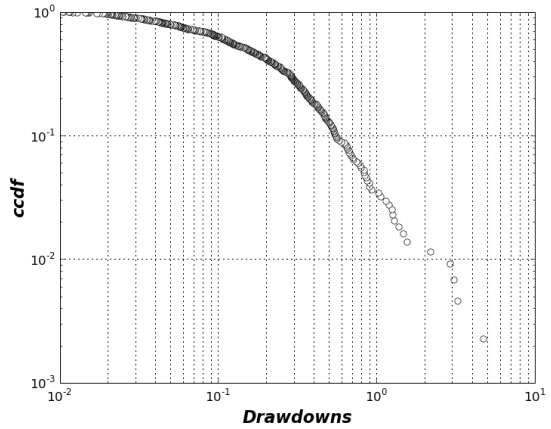

(c) US T-Bonds I at 1-hour scale

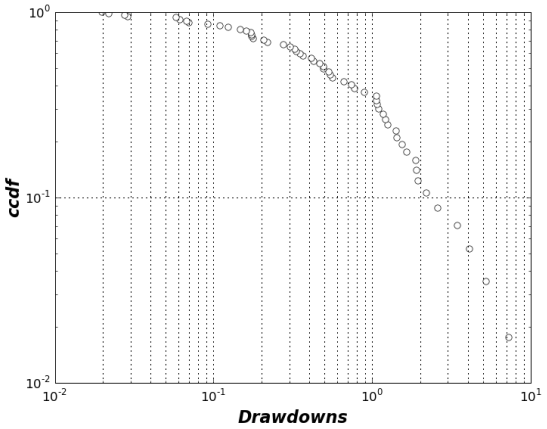

(d) US T-Bonds I at 1-day scale

Fig. 40: Logarithmic plots of the complementary cumulative distribution of *pure* drawdowns ($\epsilon = 0$) for the price of futures on the US T-Bonds I index at different time scales -from 1-min to 1-day-.

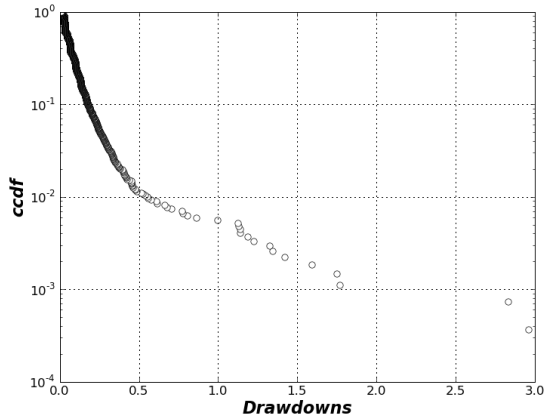

(a) US T-Bonds I at 1-min scale

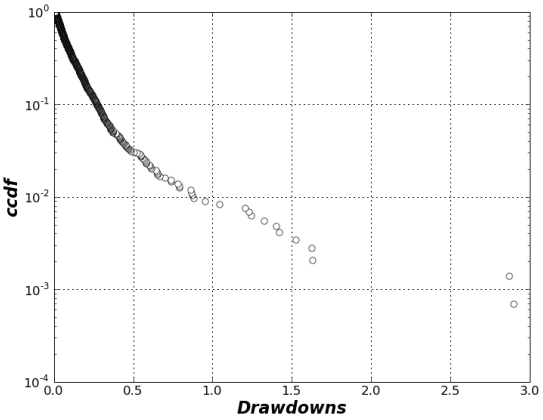

(b) US T-Bonds I at 15-min scale

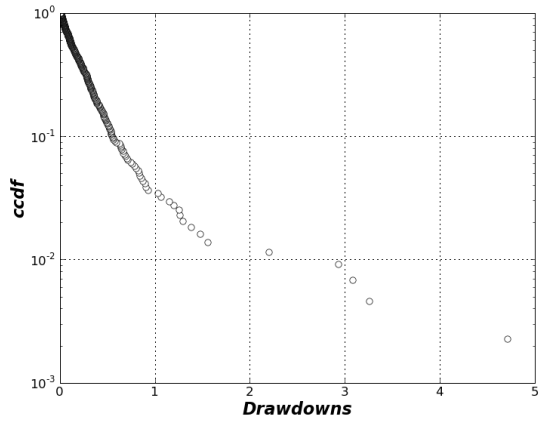

(c) US T-Bonds I at 1-hour scale

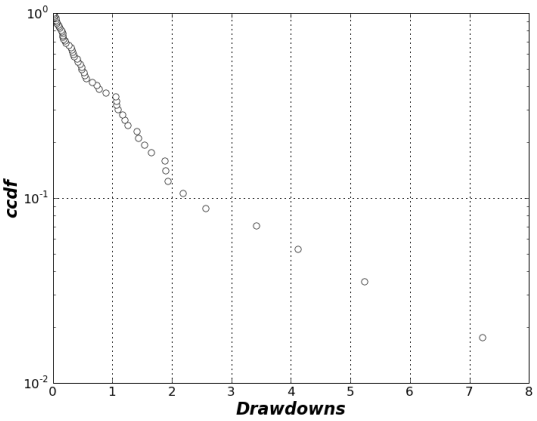

(d) US T-Bonds I at 1-day scale

Fig. 41: Log-linear plots of the complementary cumulative distribution of *pure* drawdowns ($\epsilon = 0$) for the price of futures on the US T-Bonds I index at different time scales -from 1-min to 1-day-.

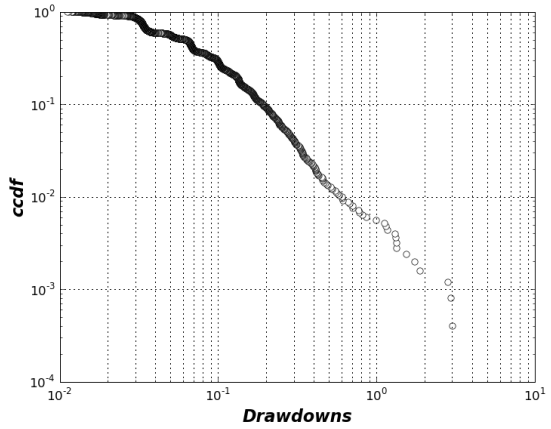

(a) US T-Bonds I at 1-min scale

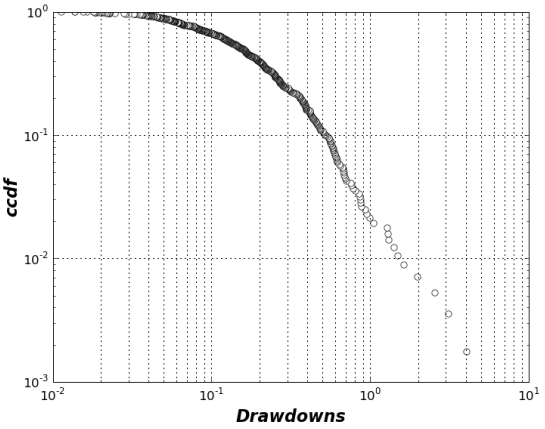

(b) US T-Bonds I at 15-min scale

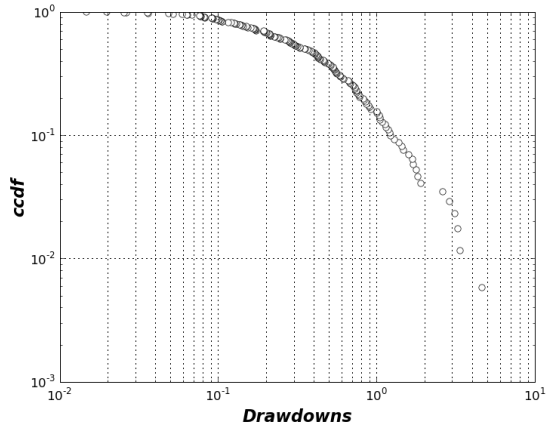

(c) US T-Bonds I at 1-hour scale

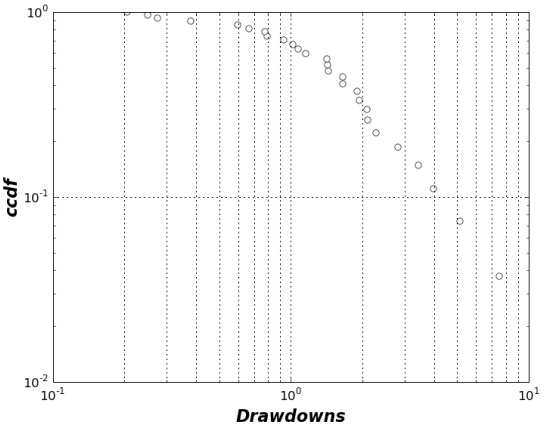

(d) US T-Bonds I at 1-day scale

Fig. 42: Logarithmic plots of the complementary cumulative distribution of $\epsilon-$drawdowns ($\epsilon = 0.5\sigma$) for the price of futures on the US T-Bonds I index at different time scales -from 1-min to 1-day-.

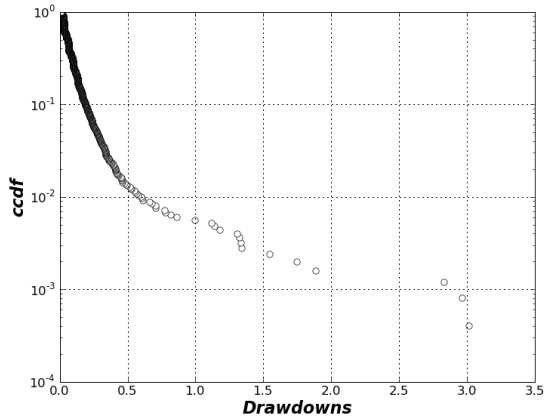

(a) US T-Bonds I at 1-min scale

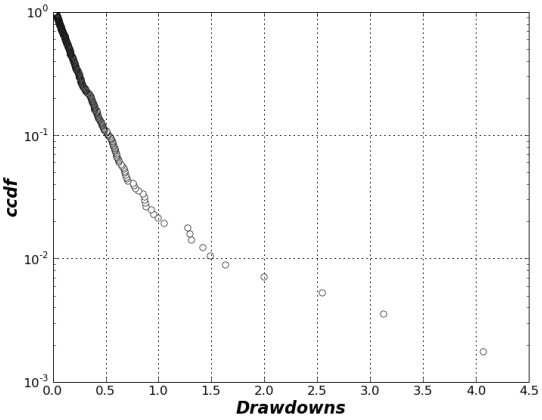

(b) US T-Bonds I at 15-min scale

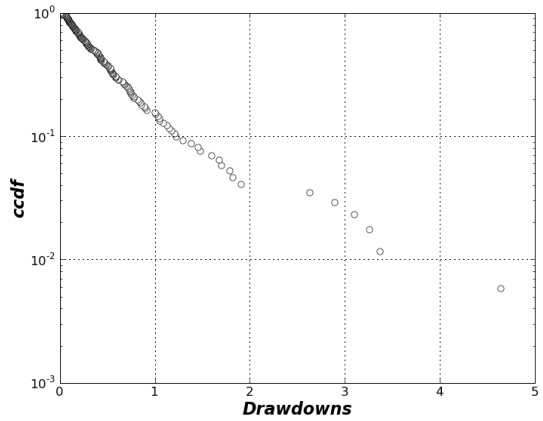

(c) US T-Bonds I at 1-hour scale

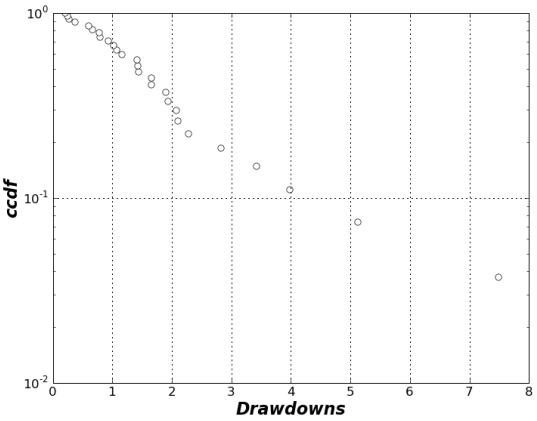

(d) US T-Bonds I at 1-day scale

Fig. 43: Log-linear plots of the complementary cumulative distribution of $\epsilon-$drawdowns ($\epsilon = 0.5\sigma$) for the price of futures on the US T-Bonds I index at different time scales -from 1-min to 1-day-.

C.3.1.8 US Treasury Bonds III

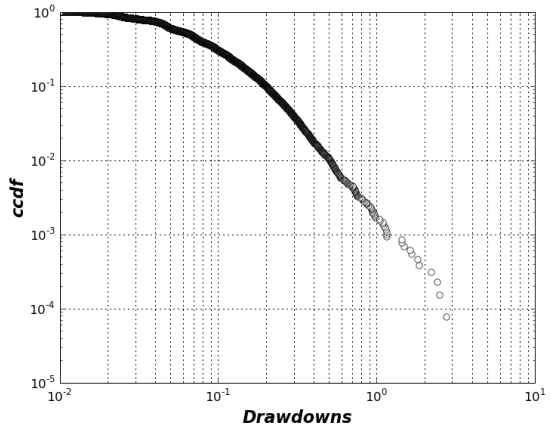

(a) US T-Bonds III at 1-min scale

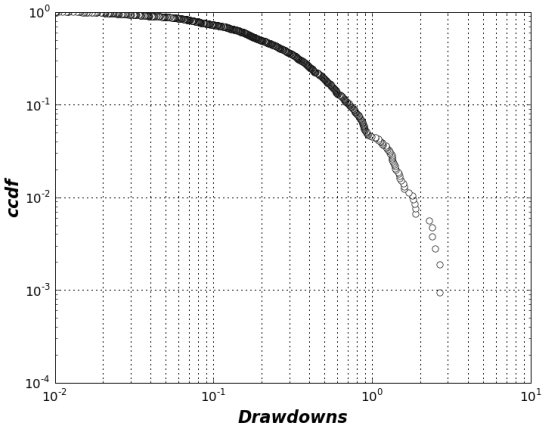

(b) US T-Bonds III at 15-min scale

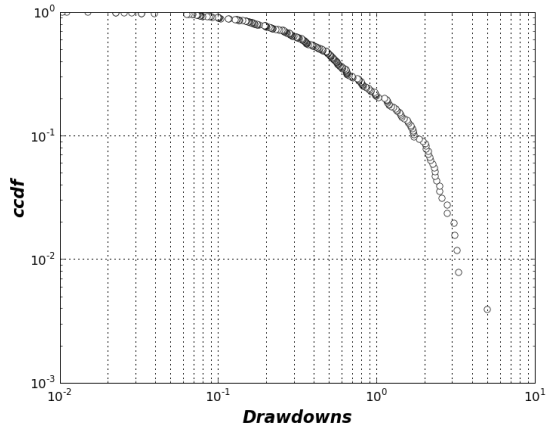

(c) US T-Bonds III at 1-hour scale

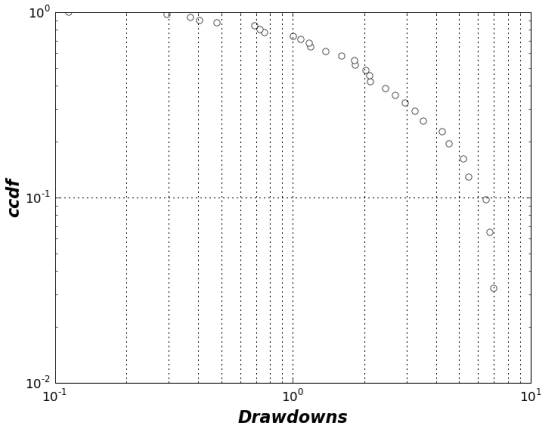

(d) US T-Bonds III at 1-day scale

Fig. 44: Logarithmic plots of the complementary cumulative distribution of *pure* drawdowns ($\epsilon = 0$) for the price of futures on the US T-Bonds III index at different time scales -from 1-min to 1-day-.

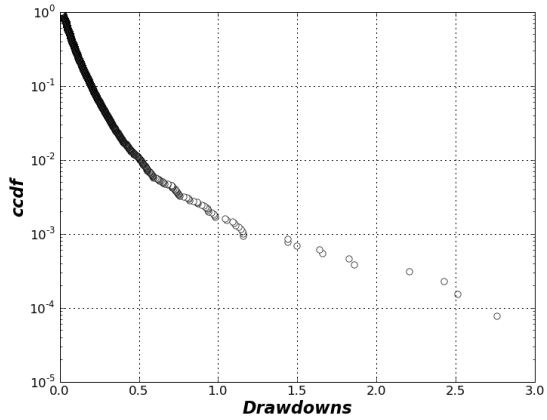

(a) US T-Bonds III at 1-min scale

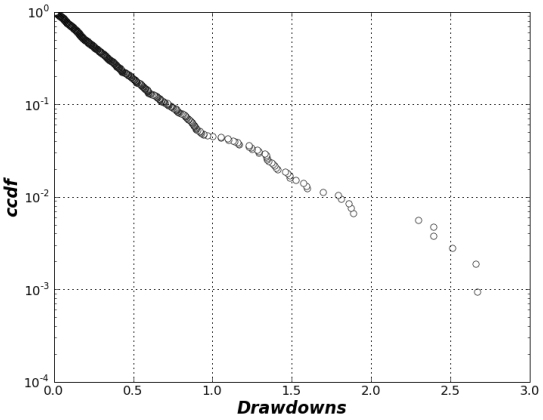

(b) US T-Bonds III at 15-min scale

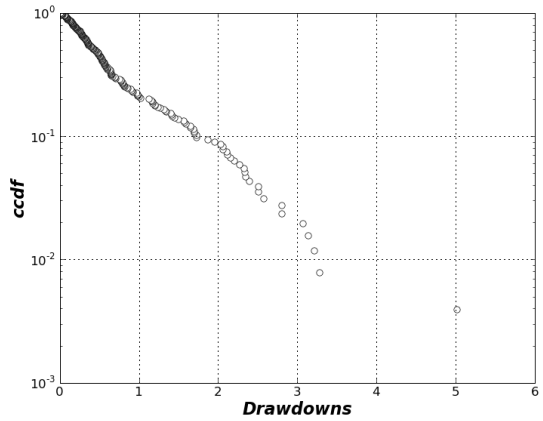

(c) US T-Bonds III at 1-hour scale

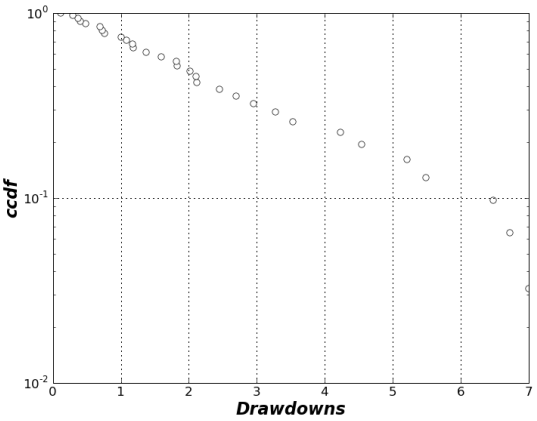

(d) US T-Bonds III at 1-day scale

Fig. 45: Log-linear plots of the complementary cumulative distribution of *pure* drawdowns ($\epsilon = 0$) for the price of futures on the US T-Bonds III index at different time scales -from 1-min to 1-day-.

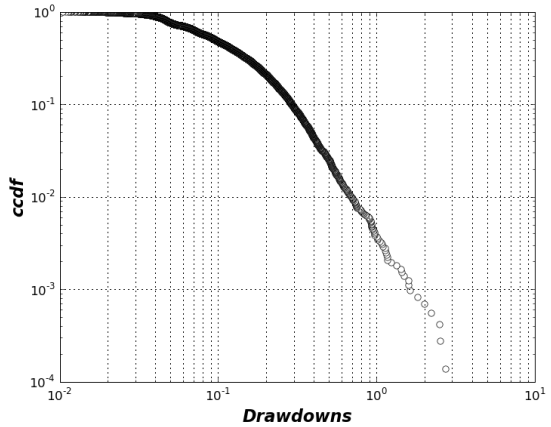

(a) US T-Bonds III at 1-min scale

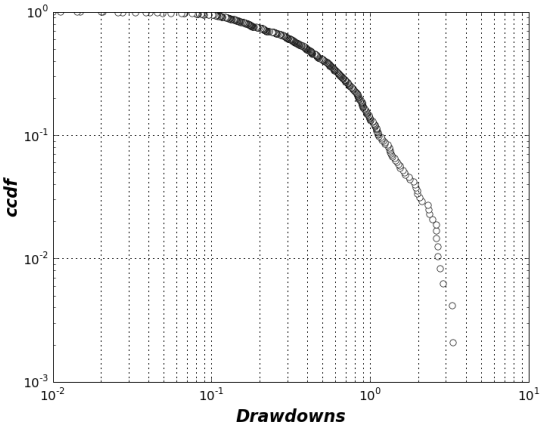

(b) US T-Bonds III at 15-min scale

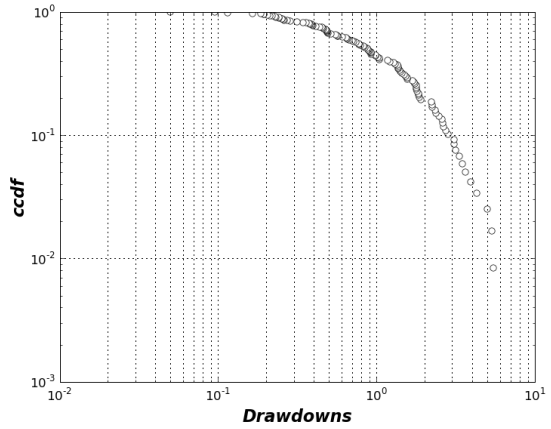

(c) US T-Bonds III at 1-hour scale

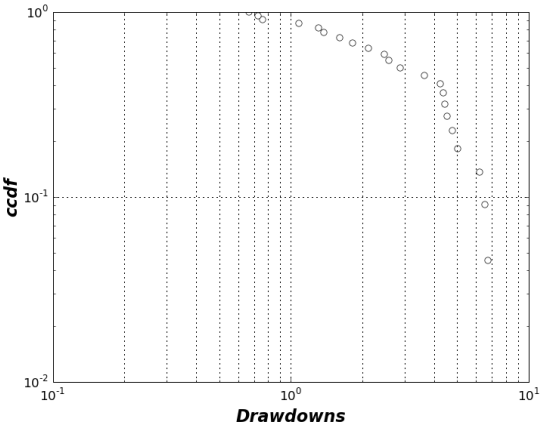

(d) US T-Bonds III at 1-day scale

Fig. 46: Logarithmic plots of the complementary cumulative distribution of $\epsilon-$drawdowns ($\epsilon = 0.5\sigma$) for the price of futures on the US T-Bonds III index at different time scales -from 1-min to 1-day-.

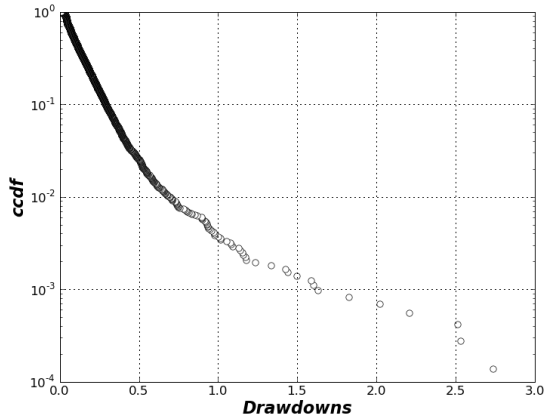

(a) US T-Bonds III at 1-min scale

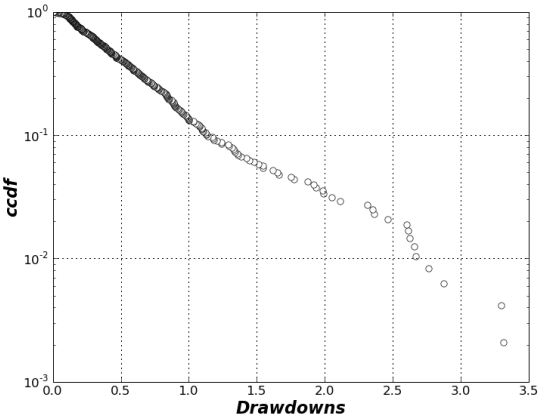

(b) US T-Bonds III at 15-min scale

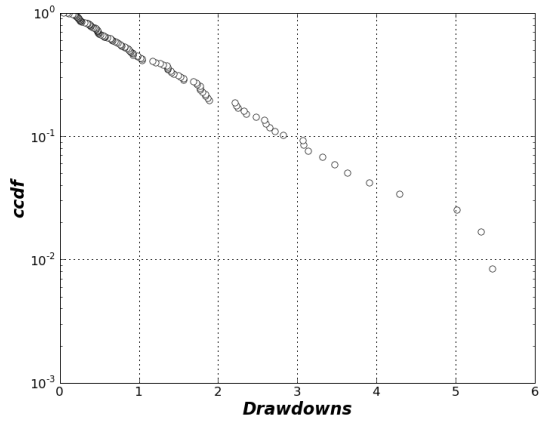

(c) US T-Bonds III at 1-hour scale

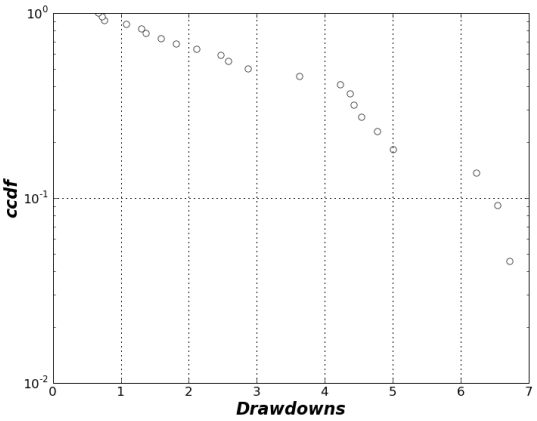

(d) US T-Bonds III at 1-day scale

Fig. 47: Log-linear plots of the complementary cumulative distribution of $\epsilon-$drawdowns ($\epsilon = 0.5\sigma$) for the price of futures on the US T-Bonds III index at different time scales -from 1-min to 1-day-.

C.3.1.9 German Government Bonds

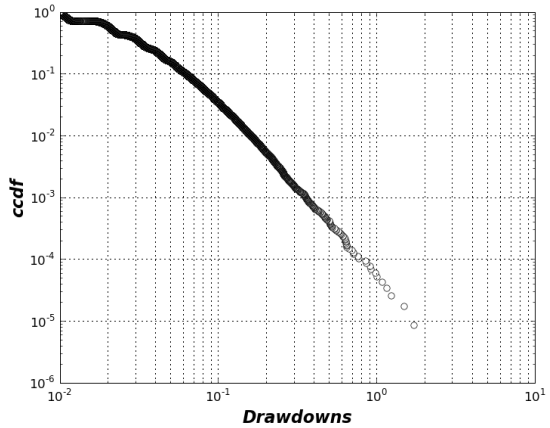

(a) German Government Bonds at 1-min scale

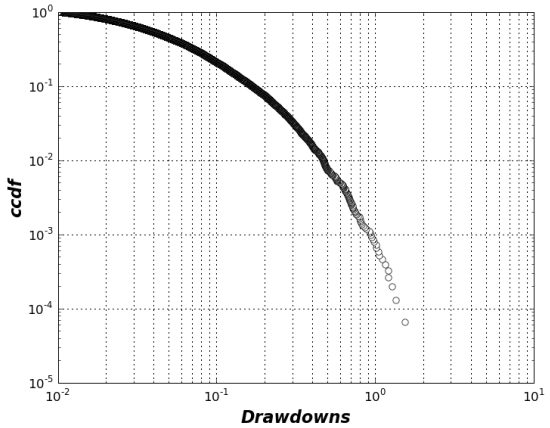

(b) German Government Bonds at 15-min scale

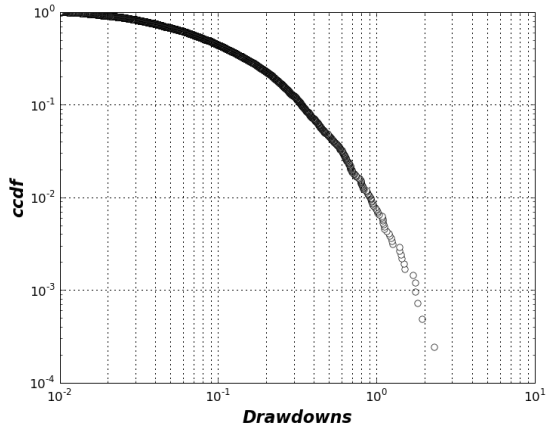

(c) German Government Bonds at 1-hour scale

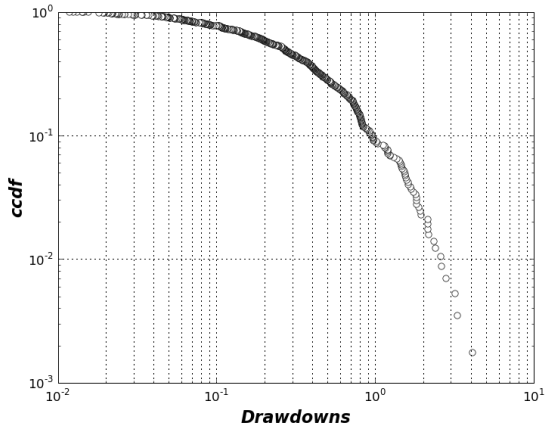

(d) German Government Bonds at 1-day scale

Fig. 48: Logarithmic plots of the complementary cumulative distribution of *pure* drawdowns ($\epsilon = 0$) for the price of futures on the German Government Bonds index at different time scales -from 1-min to 1-day-.

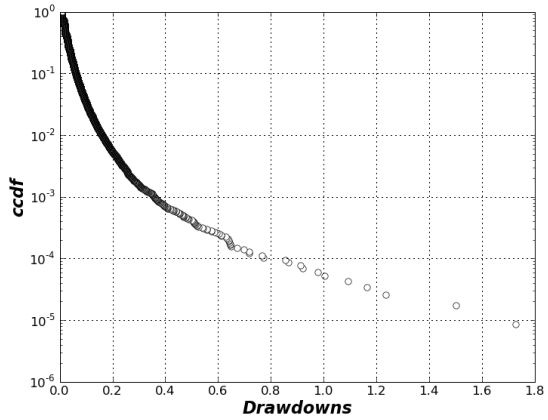

(a) German Government Bonds at 1-min scale

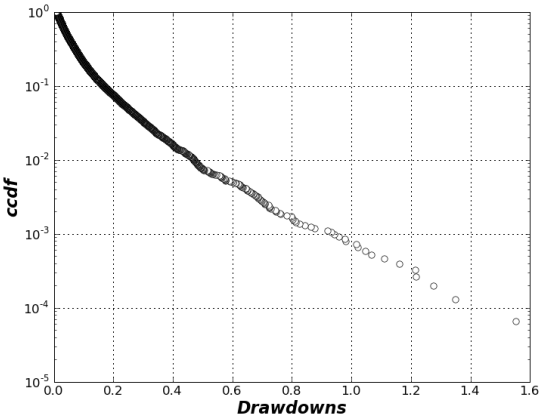

(b) German Government Bonds at 15-min scale

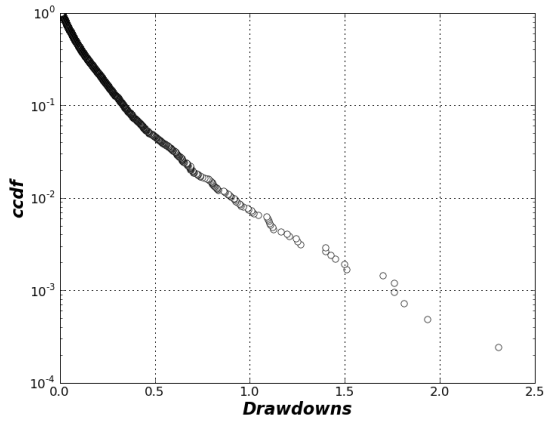

(c) German Government Bonds at 1-hour scale

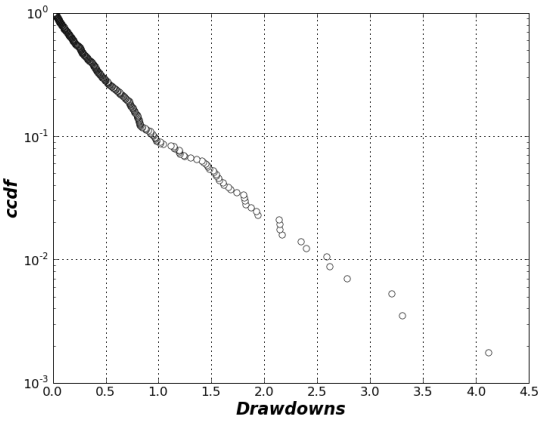

(d) German Government Bonds at 1-day scale

Fig. 49: Log-linear plots of the complementary cumulative distribution of *pure* drawdowns ($\epsilon = 0$) for the price of futures on the German Government Bonds index at different time scales -from 1-min to 1-day-.

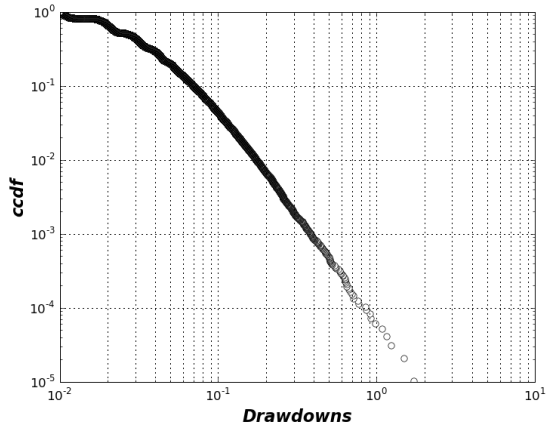

(a) German Government Bonds at 1-min scale

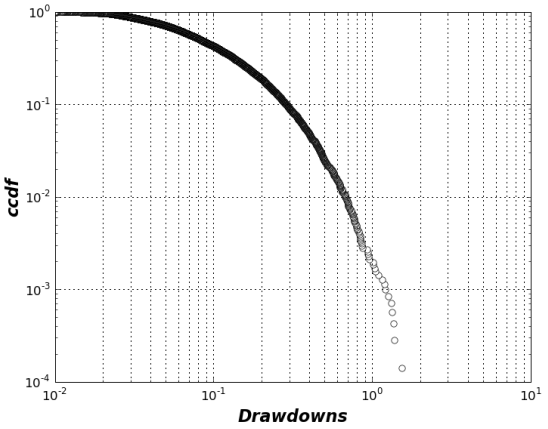

(b) German Government Bonds at 15-min scale

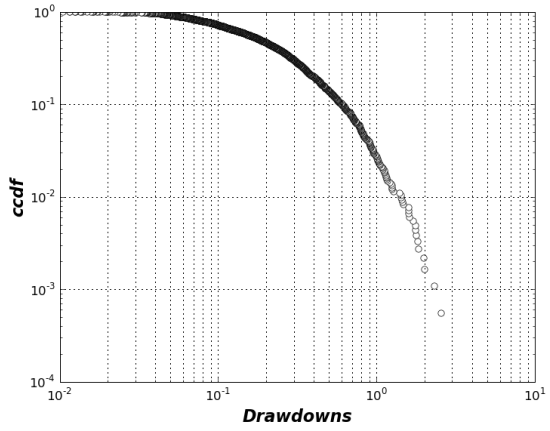

(c) German Government Bonds at 1-hour scale

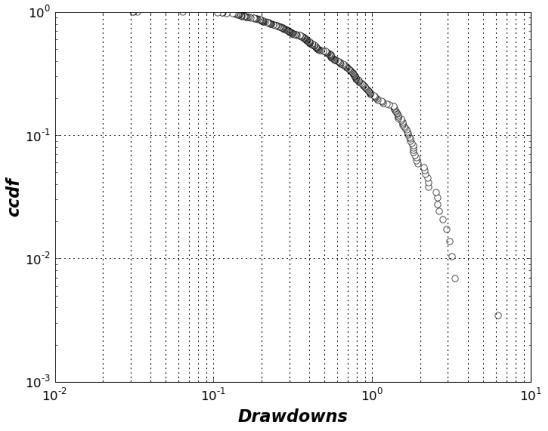

(d) German Government Bonds at 1-day scale

Fig. 50: Logarithmic plots of the complementary cumulative distribution of $\epsilon-$drawdowns ($\epsilon = 0.5\sigma$) for the price of futures on the German Government Bonds index at different time scales -from 1-min to 1-day-.

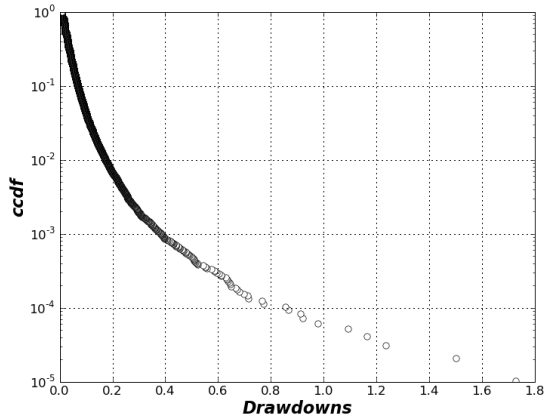

(a) German Government Bonds at 1-min scale

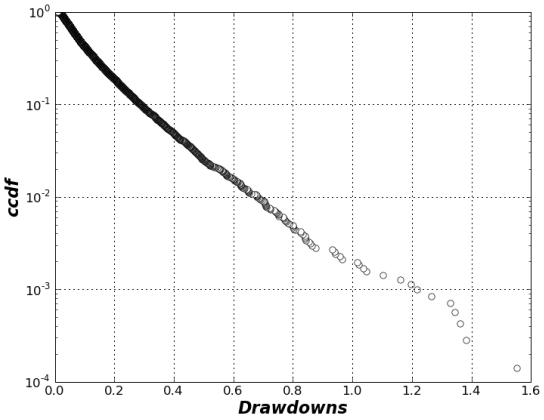

(b) German Government Bonds at 15-min scale

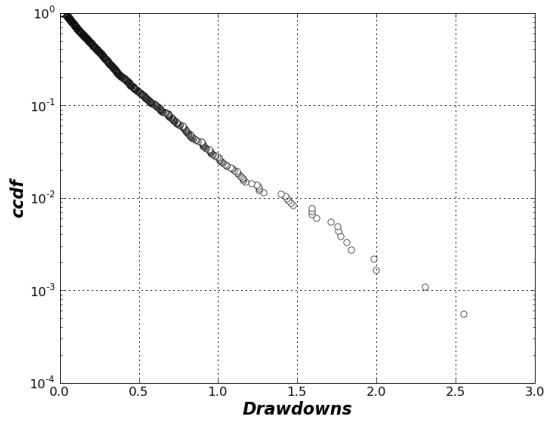

(c) German Government Bonds at 1-hour scale

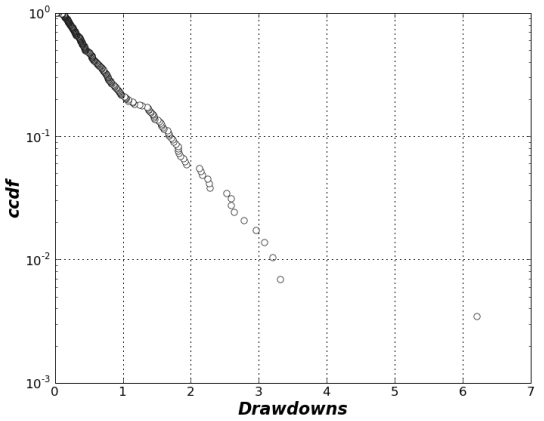

(d) German Government Bonds at 1-day scale

Fig. 51: Log-linear plots of the complementary cumulative distribution of $\epsilon-$drawdowns ($\epsilon = 0.5\sigma$) for the price of futures on the German Government Bonds index at different time scales -from 1-min to 1-day-.

C.3.2 Reshuffling returns

C.3.2.1 SP 500

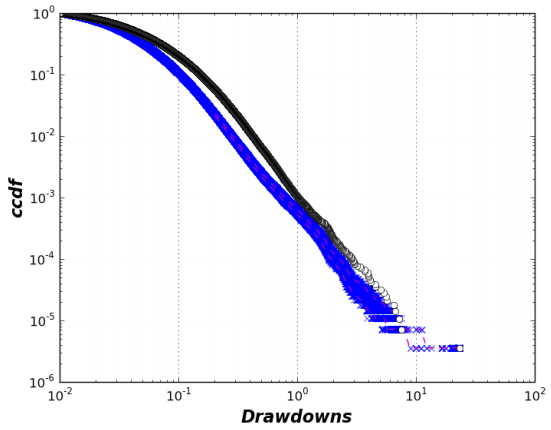

(a) SP 500 at 1-min scale

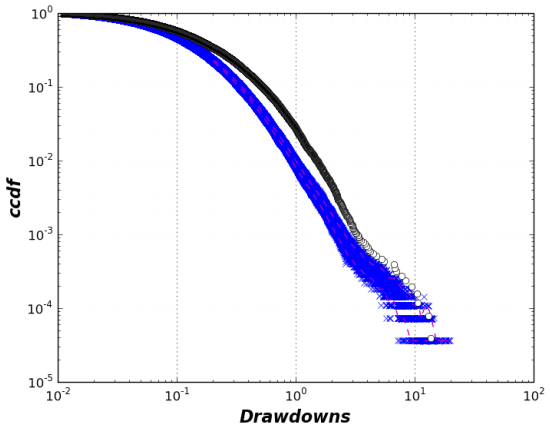

(b) SP 500 at 15-min scale

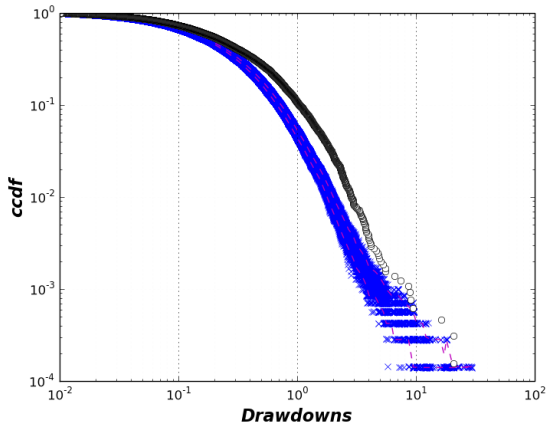

(c) SP 500 at 1-hour scale

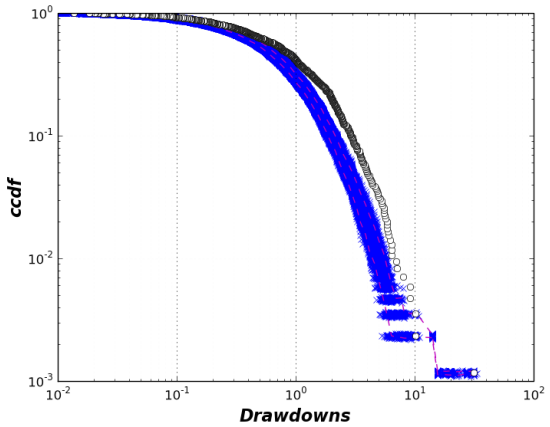

(d) SP 500 at 1-day scale

Fig. 52: Logarithmic plots of the complementary cumulative distribution of *pure* drawdowns ($\epsilon = 0$) for the SP 500 time series at different time scales -from 1-min to 1-day-. Plotted are the 0-DD ccdf of: (x) 500 samples of the reshuffled return time series, (-) the 95% confidence interval of the reshuffled realizations, (o) time series of the original SP 500 dataset.

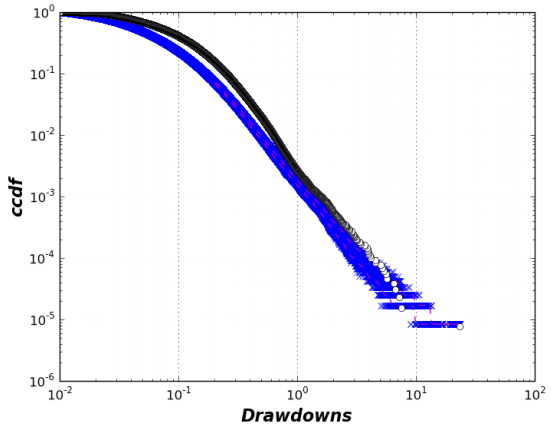

(a) SP 500 at 1-min scale

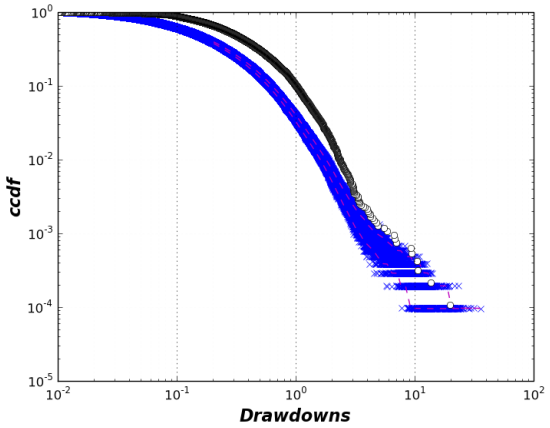

(b) SP 500 at 15-min scale

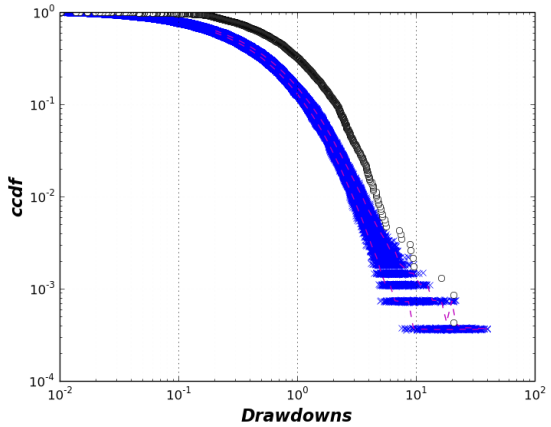

(c) SP 500 at 1-hour scale

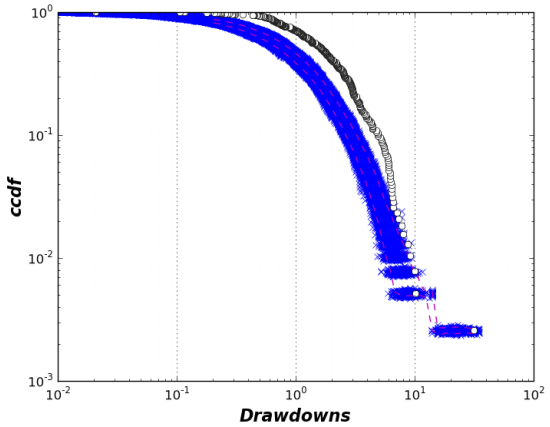

(d) SP 500 at 1-day scale

Fig. 53: Logarithmic plots of the complementary cumulative distribution of $\sigma/2$-Drawdowns ($\epsilon = 0.5\sigma$) for the SP 500 time series at different time scales -from 1-min to 1-day-. Plotted are the $\sigma/2$-DD ccdf of: (x) 500 samples of the reshuffled return time series, (-) the 95% confidence interval of the reshuffled realizations, (o) time series of the original SP 500 dataset.

C.3.2.2 FTSE 100

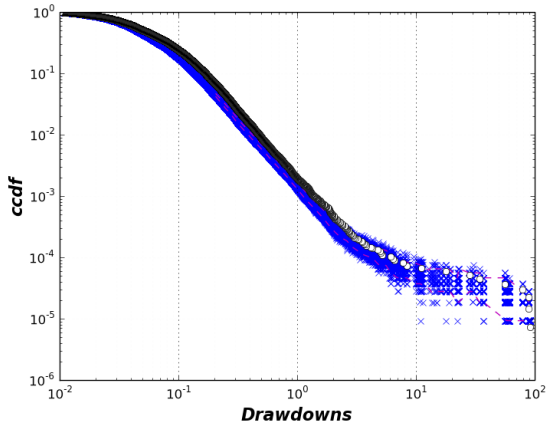

(a) FTSE 100 at 1-min scale

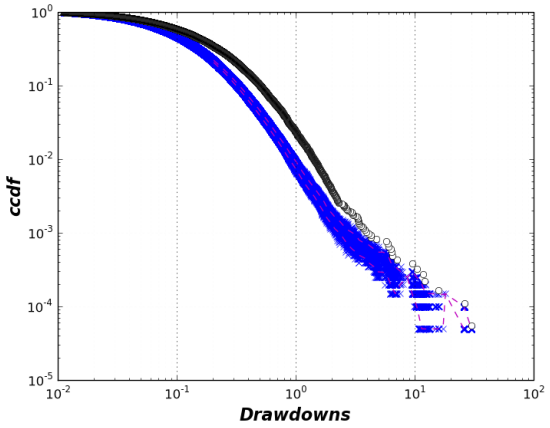

(b) FTSE 100 at 15-min scale

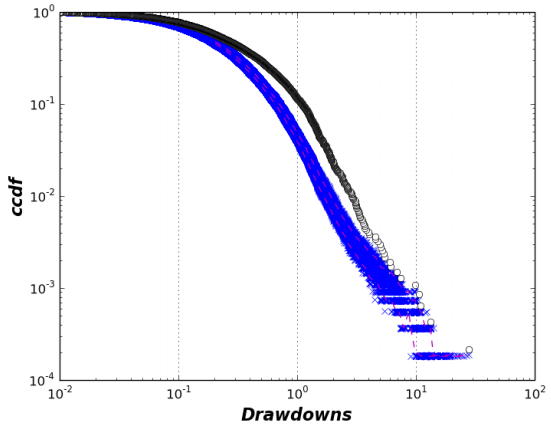

(c) FTSE 100 at 1-hour scale

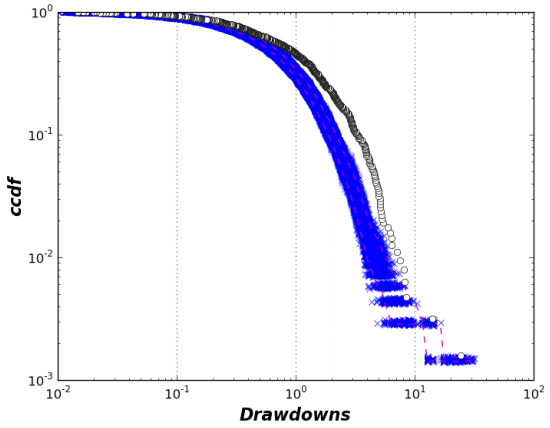

(d) FTSE 100 at 1-day scale

Fig. 54: Logarithmic plots of the complementary cumulative distribution of *pure* drawdowns ($\epsilon = 0$) for the FTSE time series at different time scales -from 1-min to 1-day-. Plotted are the 0-DD ccdf of: (x) 500 samples of the reshuffled return time series, (-) the 95% confidence interval of the reshuffled realizations, (o) time series of the original FTSE 100 dataset.

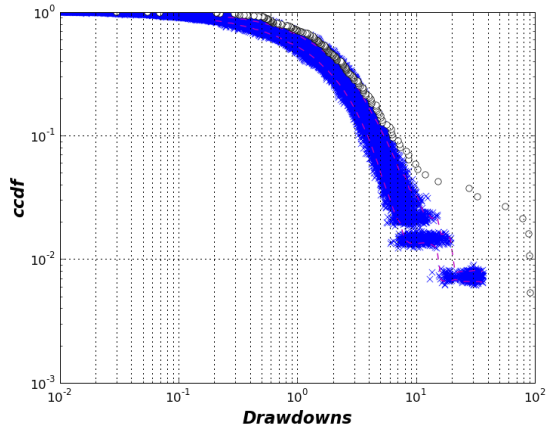

(a) FTSE 100 at 1-min scale

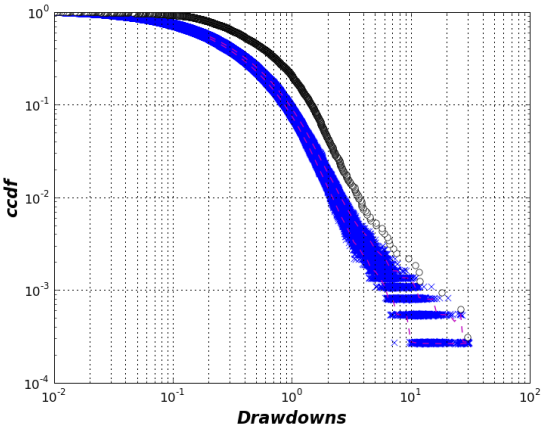

(b) FTSE 100 at 15-min scale

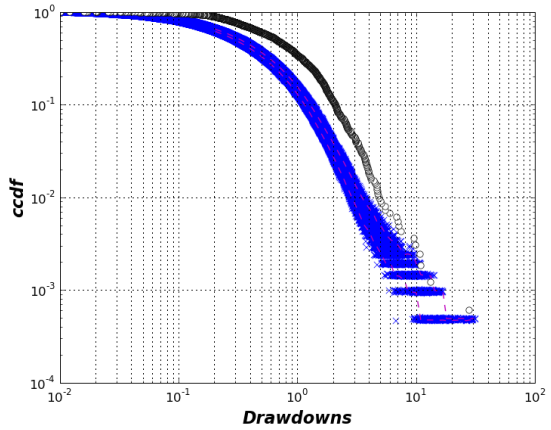

(c) FTSE 100 at 1-hour scale

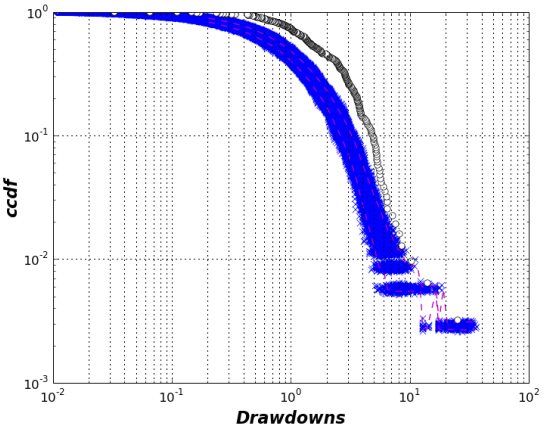

(d) FTSE 100 at 1-day scale

Fig. 55: Logarithmic plots of the complementary cumulative distribution of $\sigma/2$-Drawdowns ($\epsilon = 0.5\sigma$) for the FTSE 100 time series at different time scales -from 1-min to 1-day-. Plotted are the $\sigma/2$-DD ccdf of: (x) 500 samples of the reshuffled return time series, (-) the 95% confidence interval of the reshuffled realizations, (o) time series of the original FTSE 100 dataset.

C.3.2.3 Nikkei 225

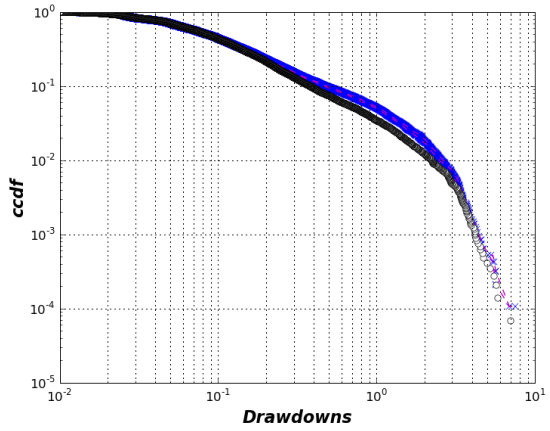

(a) Nikkei 225 at 1-min scale

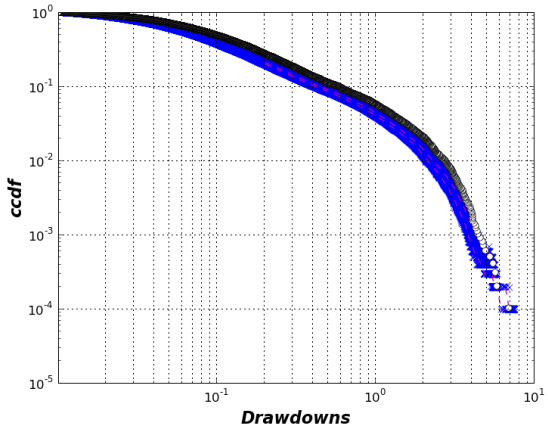

(b) Nikkei 225 at 15-min scale

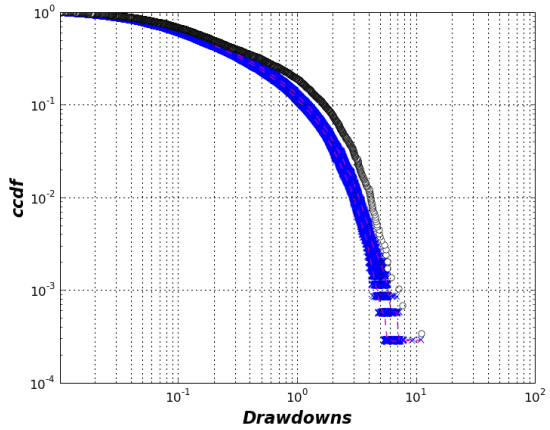

(c) Nikkei 225 at 1-hour scale

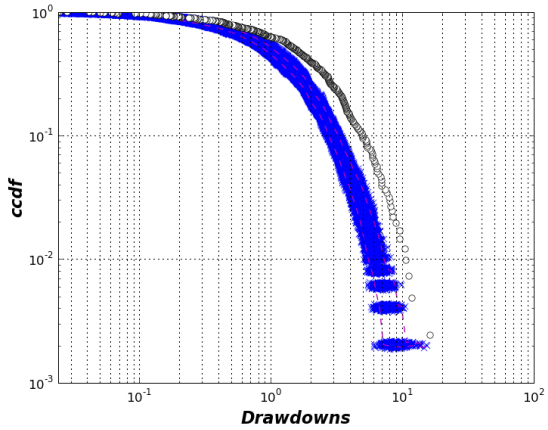

(d) Nikkei 225 at 1-day scale

Fig. 56: Logarithmic plots of the complementary cumulative distribution of *pure* drawdowns ($\epsilon = 0$) for the Nikkei 225 time series at different time scales -from 1-min to 1-day-. Plotted are the 0-DD ccdf of: (x) 500 samples of the reshuffled return time series, (-) the 95% confidence interval of the reshuffled realizations, (o) time series of the original Nikkei 225 dataset.

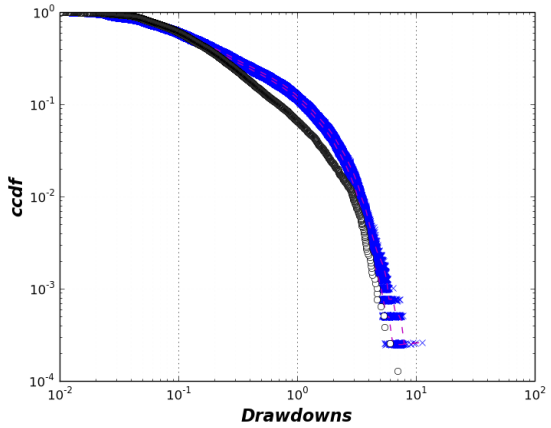

(a) Nikkei 225 at 1-min scale

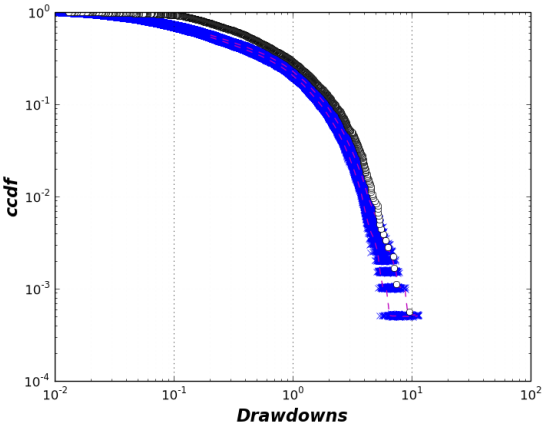

(b) Nikkei 225 at 15-min scale

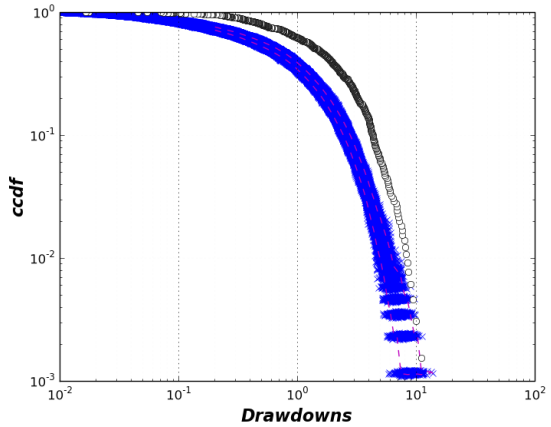

(c) Nikkei 225 at 1-hour scale

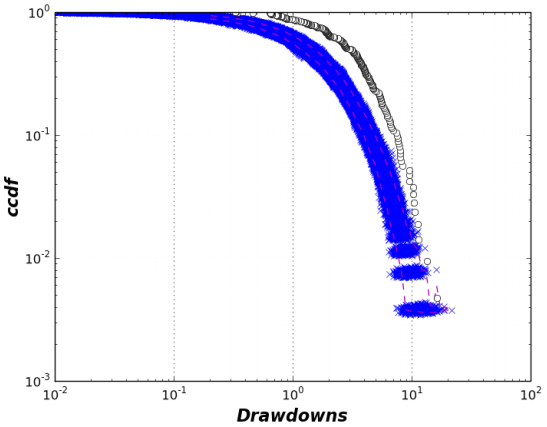

(d) Nikkei 225 at 1-day scale

Fig. 57: Logarithmic plots of the complementary cumulative distribution of $\sigma/2$-Drawdowns ($\epsilon = 0.5\sigma$) for the Nikkei 225 time series at different time scales -from 1-min to 1-day-. Plotted are the $\sigma/2$-DD ccdf of: (x) 500 samples of the reshuffled return time series, (-) the 95% confidence interval of the reshuffled realizations, (o) time series of the original Nikkei 225 dataset.

C.3.2.4 Japanese Yen

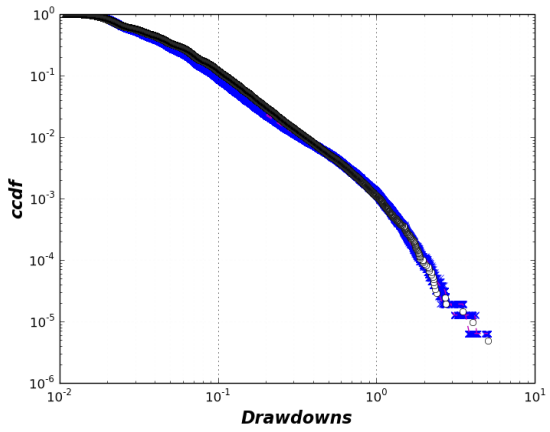

(a) Japanese Yen at 1-min scale

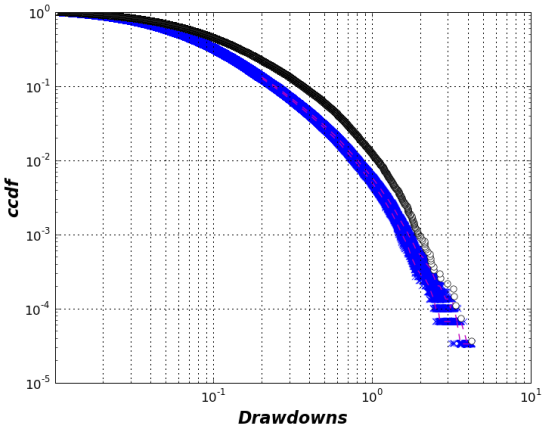

(b) Japanese Yen at 15-min scale

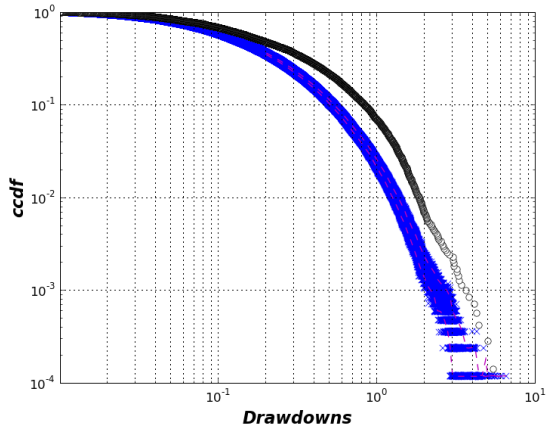

(c) Japanese Yen at 1-hour scale

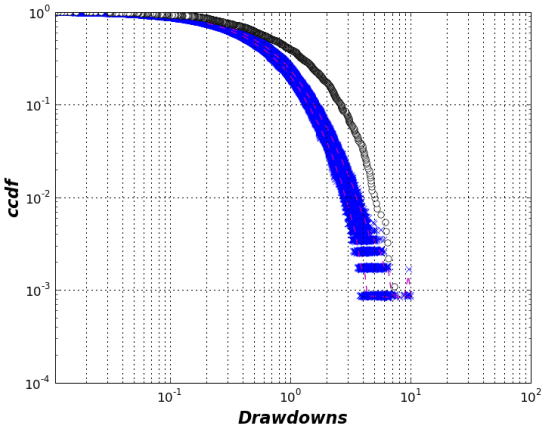

(d) Japanese Yen at 1-day scale

Fig. 58: Logarithmic plots of the complementary cumulative distribution of *pure* drawdowns ($\epsilon = 0$) for the Japanese Yen time series at different time scales -from 1-min to 1-day-. Plotted are the 0-DD ccdf of: (x) 500 samples of the reshuffled return time series, (-) the 95% confidence interval of the reshuffled realizations, (o) time series of the original Japanese Yen dataset.

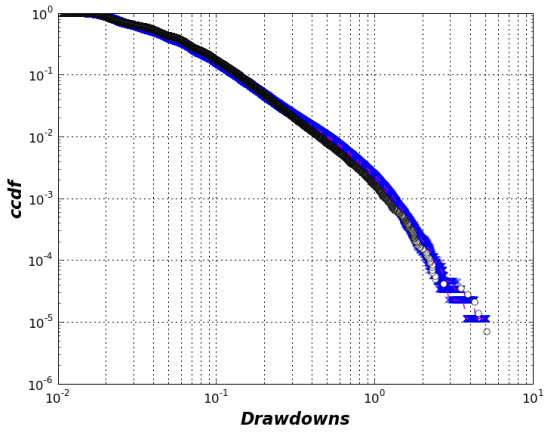

(a) Japanese Yen at 1-min scale

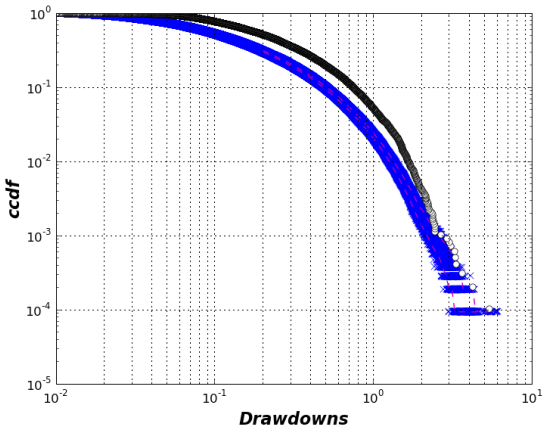

(b) Japanese Yen at 15-min scale

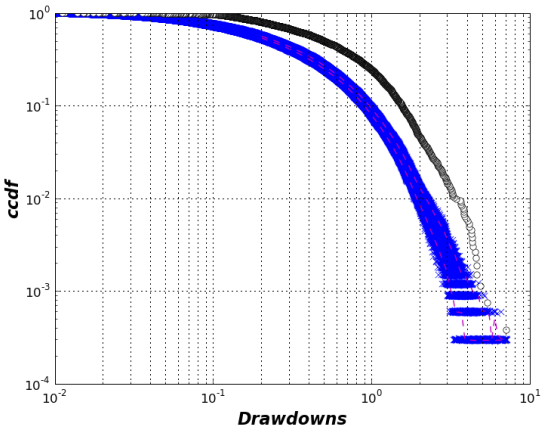

(c) Japanese Yen at 1-hour scale

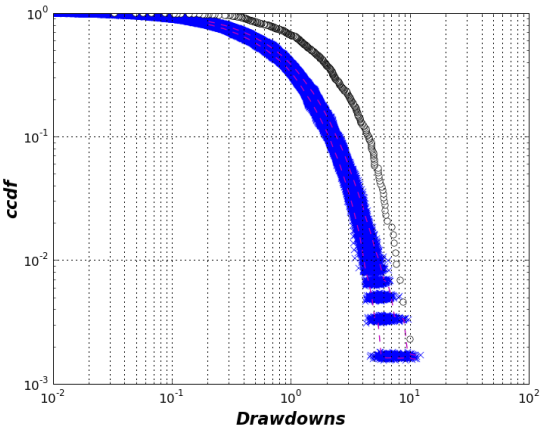

(d) Japanese Yen at 1-day scale

Fig. 59: Logarithmic plots of the complementary cumulative distribution of $\sigma/2$-Drawdowns ($\epsilon = 0.5\sigma$) for the Japanese Yen time series at different time scales -from 1-min to 1-day-. Plotted are the $\sigma/2$-DD ccdf of: (x) 500 samples of the reshuffled return time series, (-) the 95% confidence interval of the reshuffled realizations, (o) time series of the original Japanese Yen dataset.

C.3.2.5 Deutschmark

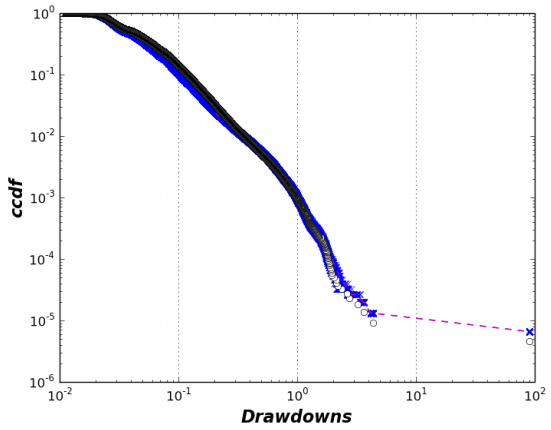

(a) Deutschmark at 1-min scale

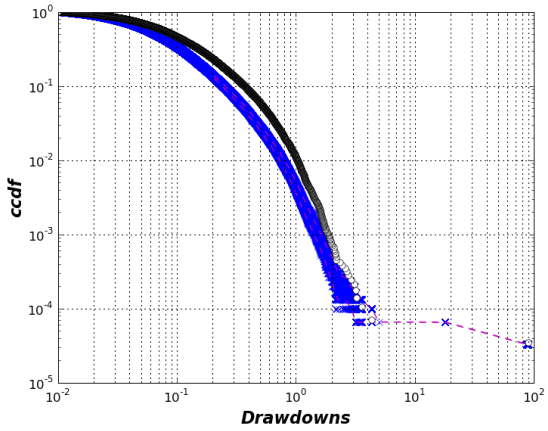

(b) Deutschmark at 15-min scale

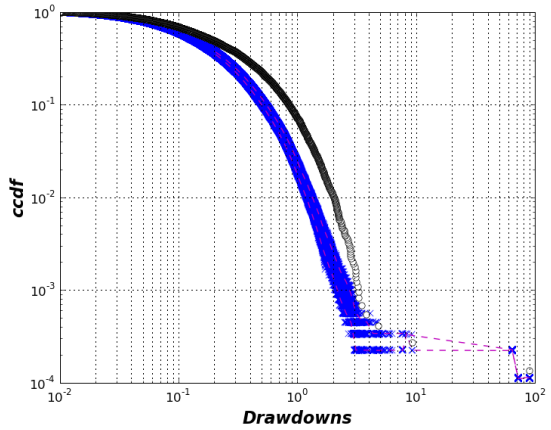

(c) Deutschmark at 1-hour scale

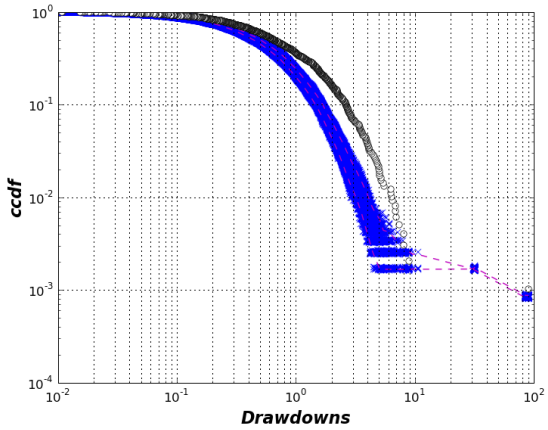

(d) Deutschmark at 1-day scale

Fig. 60: Logarithmic plots of the complementary cumulative distribution of *pure* drawdowns ($\epsilon = 0$) for the Deutschmark time series at different time scales -from 1-min to 1-day-. Plotted are the 0-DD ccdf of: (x) 500 samples of the reshuffled return time series, (-) the 95% confidence interval of the reshuffled realizations, (o) time series of the original Deutschmark dataset.

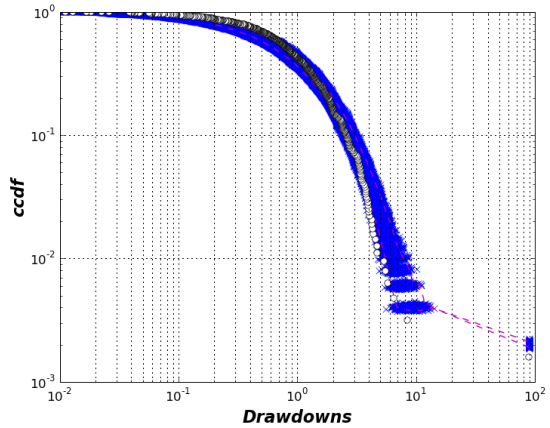

(a) Deutschmark at 1-min scale

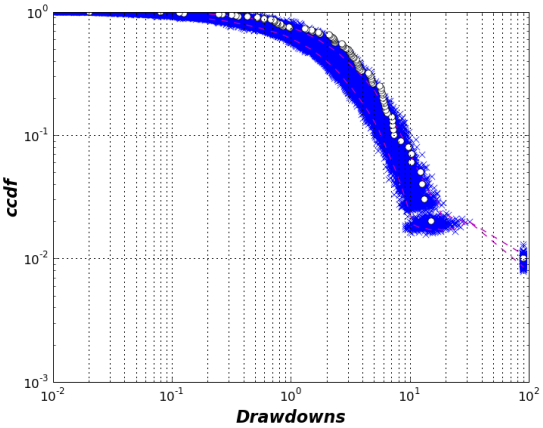

(b) Deutschmark at 15-min scale

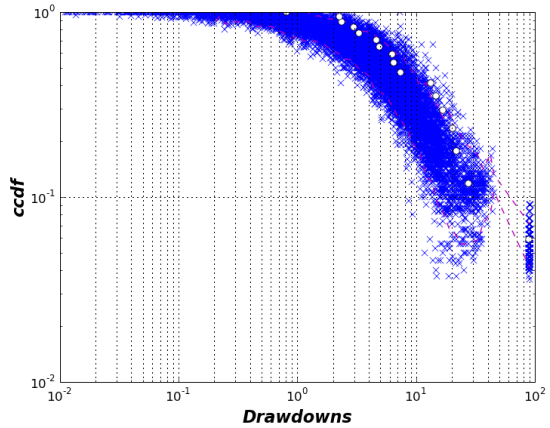

(c) Deutschmark at 1-hour scale

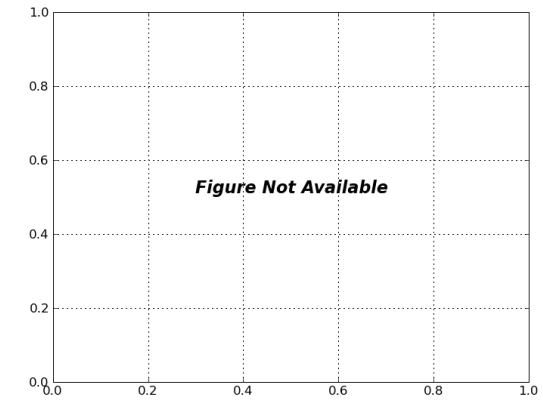

(d) Deutschmark at 1-day scale

Fig. 61: Logarithmic plots of the complementary cumulative distribution of $\sigma/2$-Drawdowns ($\epsilon = 0.5\sigma$) for the Deutschmark time series at different time scales -from 1-min to 1-day-. Plotted are the $\sigma/2$-DD ccdf of: (x) 500 samples of the reshuffled return time series, (-) the 95% confidence interval of the reshuffled realizations, (o) time series of the original Deutschmark dataset. Note: the $\sigma/2-$drawdown dataset was too small to perform the test

.

C.3.2.6 Japanese Government Bonds

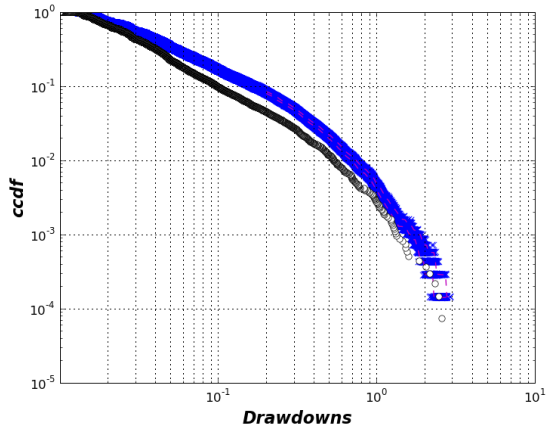

(a) Jap Government Bonds at 1-min scale

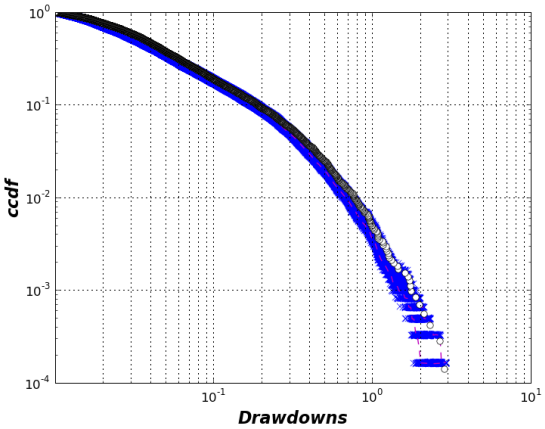

(b) Jap Government Bonds at 15-min scale

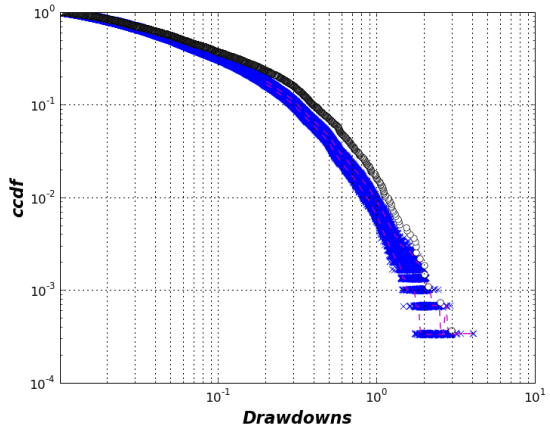

(c) Jap Government Bonds at 1-hour scale

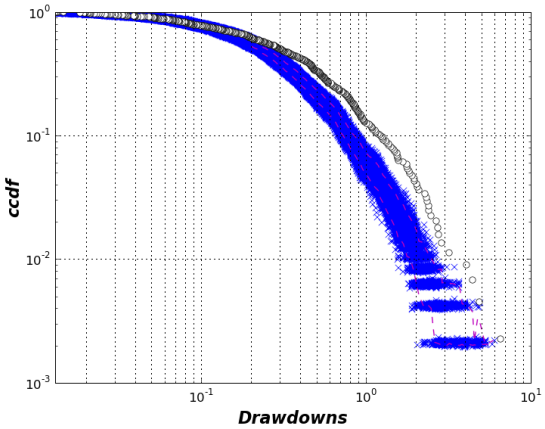

(d) Jap Government Bonds at 1-day scale

Fig. 62: Logarithmic plots of the complementary cumulative distribution of *pure* drawdowns ($\epsilon = 0$) for the Jap Government Bonds time series at different time scales -from 1-min to 1-day-. Plotted are the 0-DD ccdf of: (x) 500 samples of the reshuffled return time series, (-) the 95% confidence interval of the reshuffled realizations, (o) time series of the original Jap Government Bonds dataset.

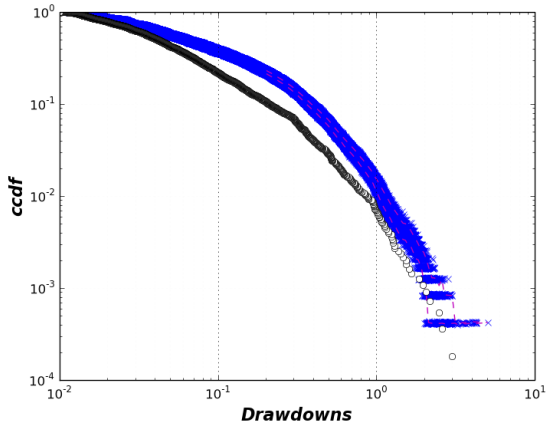

(a) Jap Government Bonds at 1-min scale

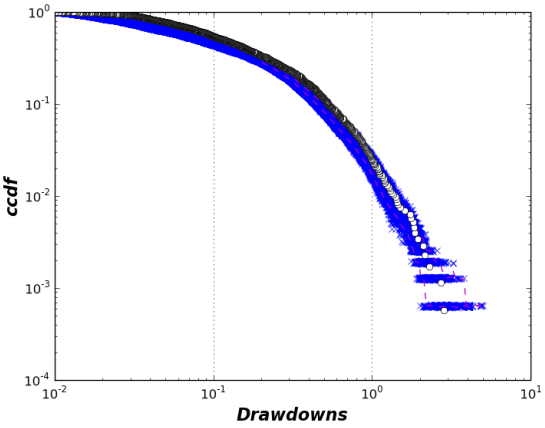

(b) Jap Government Bonds at 15-min scale

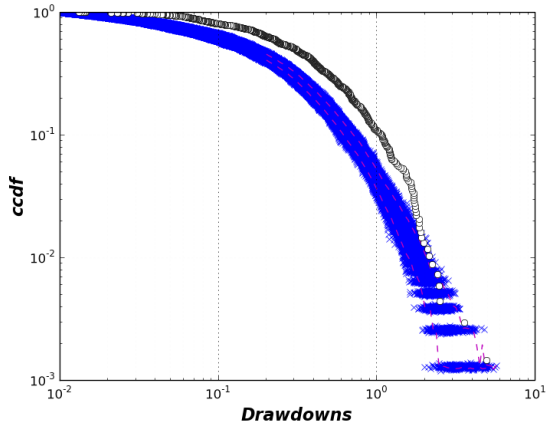

(c) Jap Government Bonds at 1-hour scale

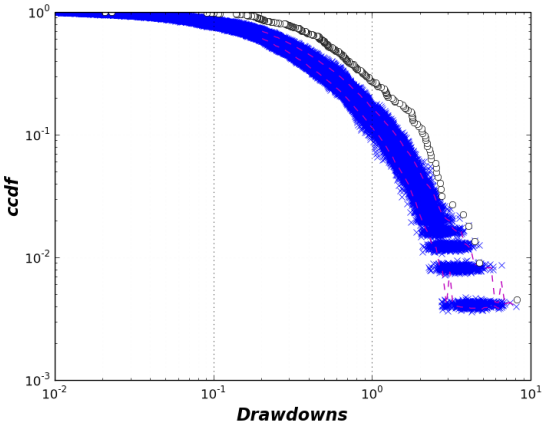

(d) Jap Government Bonds at 1-day scale

Fig. 63: Logarithmic plots of the complementary cumulative distribution of $\sigma/2$-Drawdowns ($\epsilon = 0.5\sigma$) for the Jap Government Bonds time series at different time scales -from 1-min to 1-day-. Plotted are the $\sigma/2$-DD ccdf of: (x) 500 samples of the reshuffled return time series, (-) the 95% confidence interval of the reshuffled realizations, (o) time series of the original Jap Government Bonds dataset.

C.3.2.7 US Treasury Bonds I

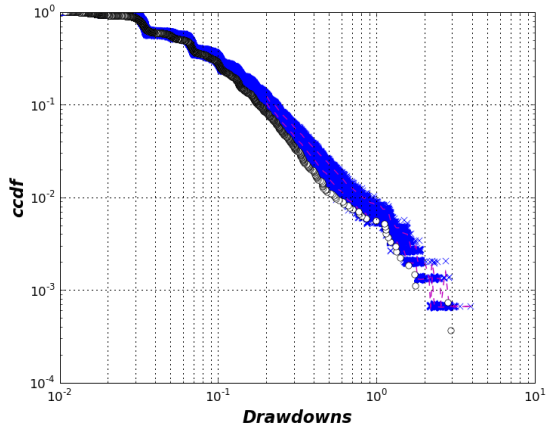

(a) US T-Bonds I at 1-min scale

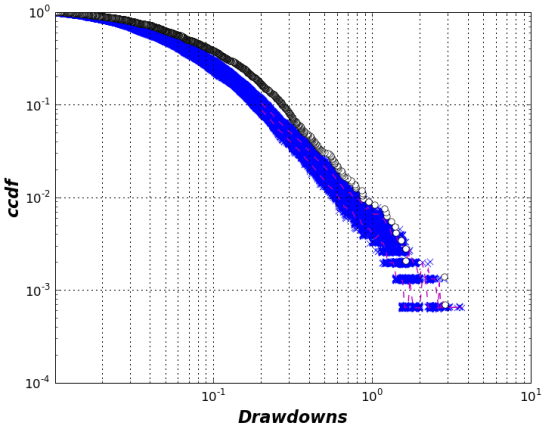

(b) US T-Bonds I at 15-min scale

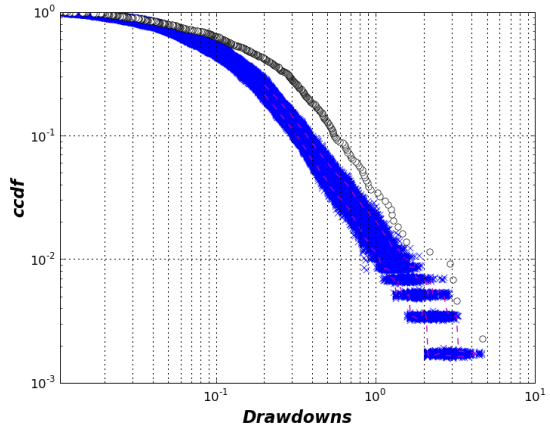

(c) US T-Bonds I at 1-hour scale

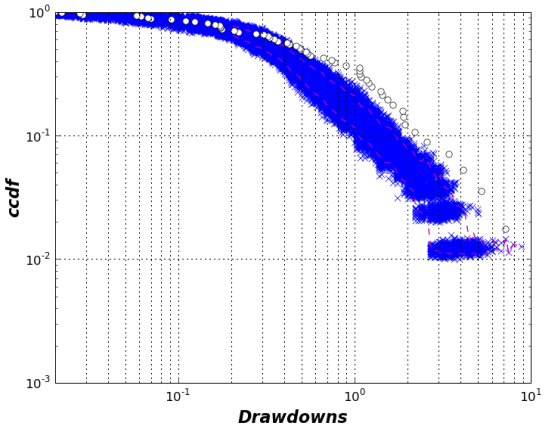

(d) US T-Bonds I at 1-day scale

Fig. 64: Logarithmic plots of the complementary cumulative distribution of *pure* drawdowns ($\epsilon = 0$) for the US T-Bonds I time series at different time scales -from 1-min to 1-day-. Plotted are the 0-DD ccdf of: (x) 500 samples of the reshuffled return time series, (-) the 95% confidence interval of the reshuffled realizations, (o) time series of the original US T-Bonds I dataset.

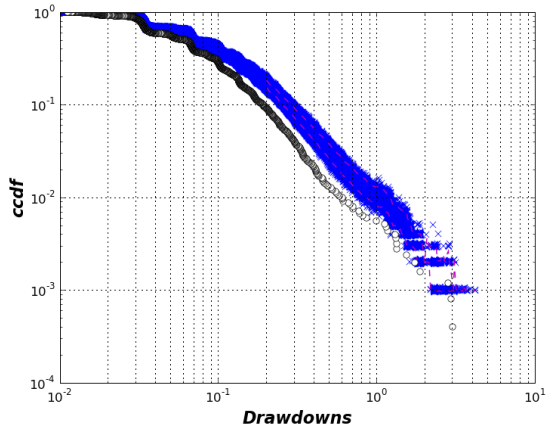

(a) US T-Bonds I at 1-min scale

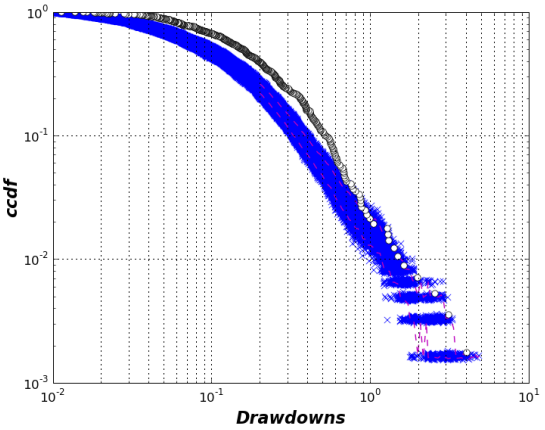

(b) US T-Bonds I at 15-min scale

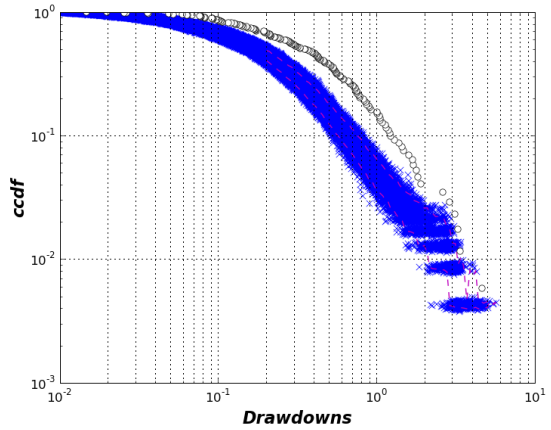

(c) US T-Bonds I at 1-hour scale

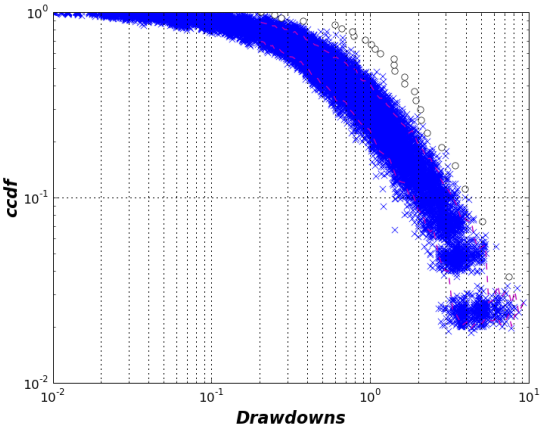

(d) US T-Bonds I at 1-day scale

Fig. 65: Logarithmic plots of the complementary cumulative distribution of $\sigma/2$-Drawdowns ($\epsilon = 0.5\sigma$) for the US T-Bonds I time series at different time scales -from 1-min to 1-day-. Plotted are the $\sigma/2$-DD ccdf of: (x) 500 samples of the reshuffled return time series, (-) the 95% confidence interval of the reshuffled realizations, (o) time series of the original US T-Bonds I dataset.

C.3.2.8 US Treasury Bonds III

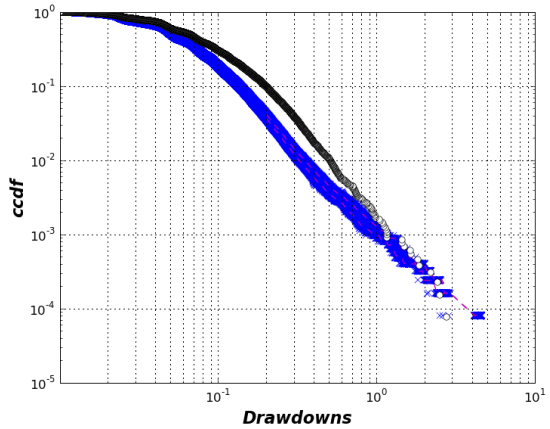

(a) US T-Bonds III at 1-min scale

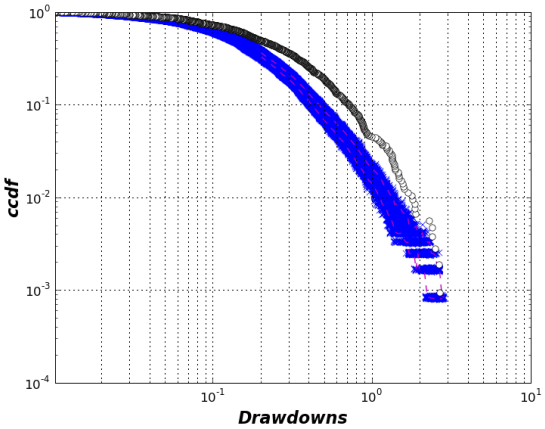

(b) US T-Bonds III at 15-min scale

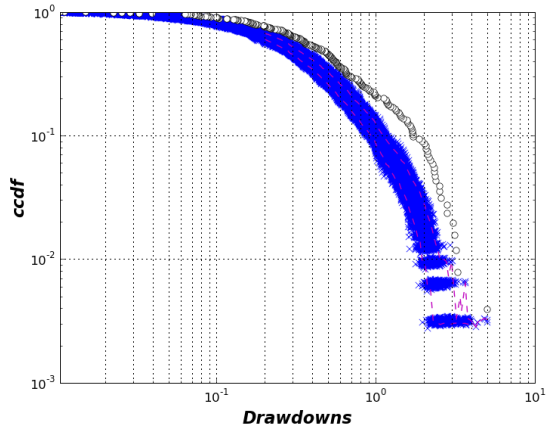

(c) US T-Bonds III at 1-hour scale

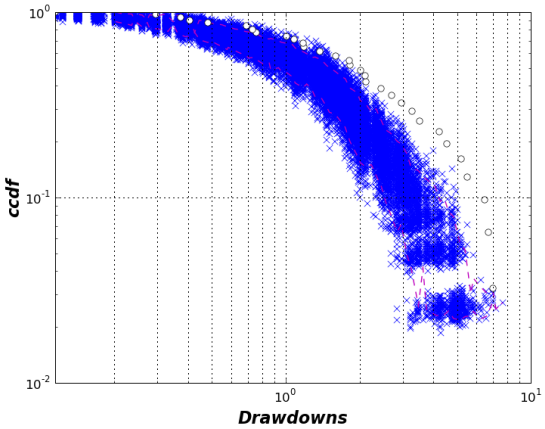

(d) US T-Bonds III at 1-day scale

Fig. 66: Logarithmic plots of the complementary cumulative distribution of *pure* drawdowns ($\epsilon = 0$) for the US T-Bonds III time series at different time scales -from 1-min to 1-day-. Plotted are the 0-DD ccdf of: (x) 500 samples of the reshuffled return time series, (-) the 95% confidence interval of the reshuffled realizations, (o) time series of the original US T-Bonds III dataset.

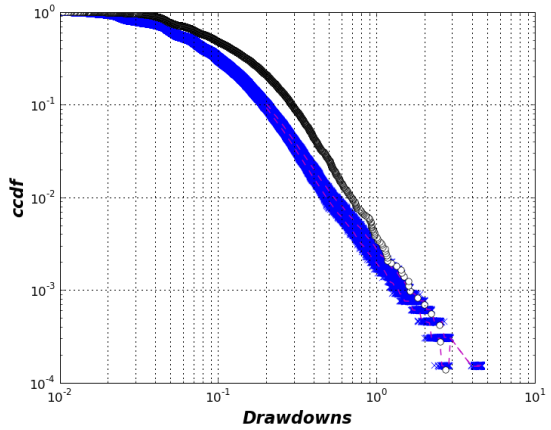

(a) US T-Bonds III at 1-min scale

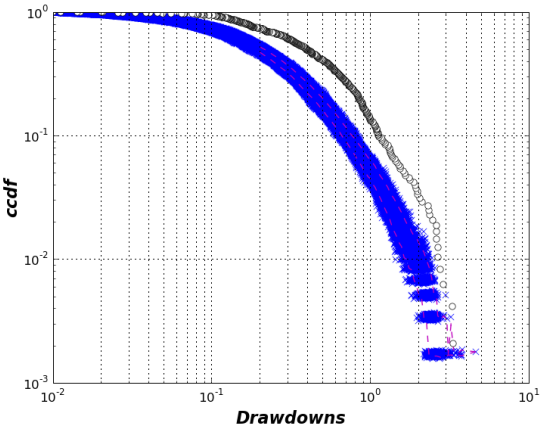

(b) US T-Bonds III at 15-min scale

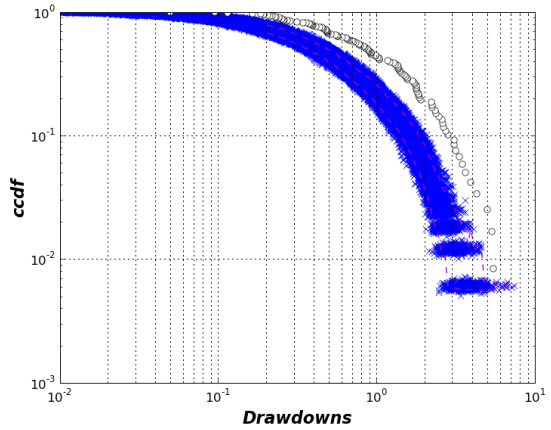

(c) US T-Bonds III at 1-hour scale

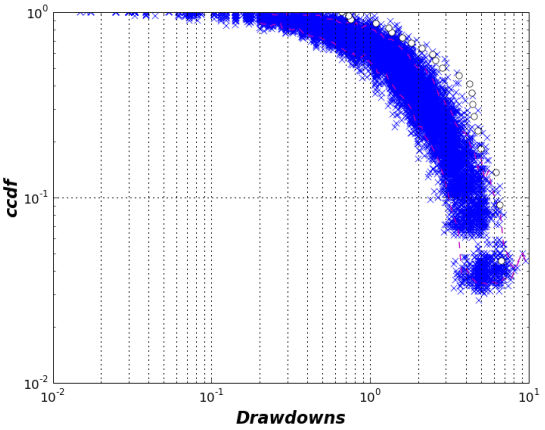

(d) US T-Bonds III at 1-day scale

Fig. 67: Logarithmic plots of the complementary cumulative distribution of $\sigma/2$-Drawdowns ($\epsilon = 0.5\sigma$) for the US T-Bonds III time series at different time scales -from 1-min to 1-day-. Plotted are the $\sigma/2$-DD ccdf of: (x) 500 samples of the reshuffled return time series, (-) the 95% confidence interval of the reshuffled realizations, (o) time series of the original US T-Bonds III dataset.

C.3.2.9 German Government Bonds

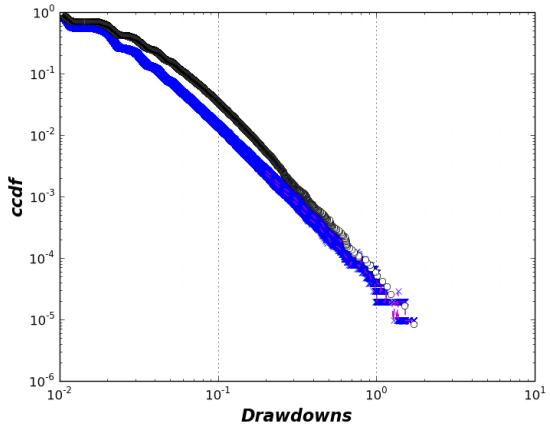

(a) German Government Bonds at 1-min scale

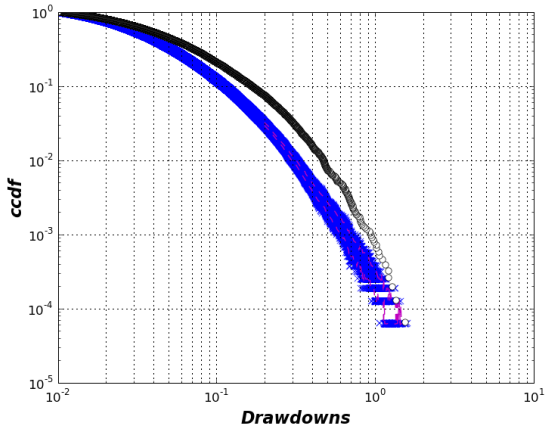

(b) German Government Bonds at 15-min scale

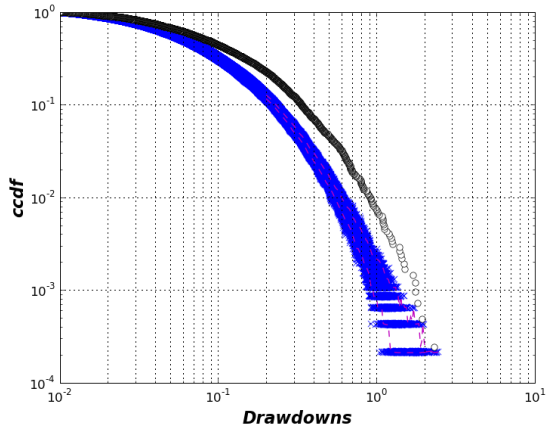

(c) German Government Bonds at 1-hour scale

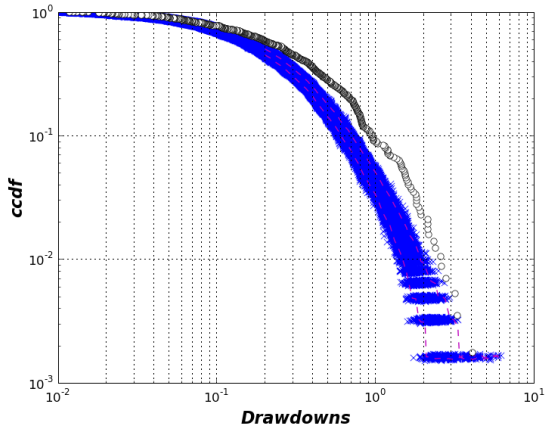

(d) German Government Bonds at 1-day scale

Fig. 68: Logarithmic plots of the complementary cumulative distribution of *pure* drawdowns ($\epsilon = 0$) for the German Government Bonds time series at different time scales -from 1-min to 1-day-. Plotted are the 0-DD ccdf of: (x) 500 samples of the reshuffled return time series, (-) the 95% confidence interval of the reshuffled realizations, (o) time series of the original German Government Bonds dataset.

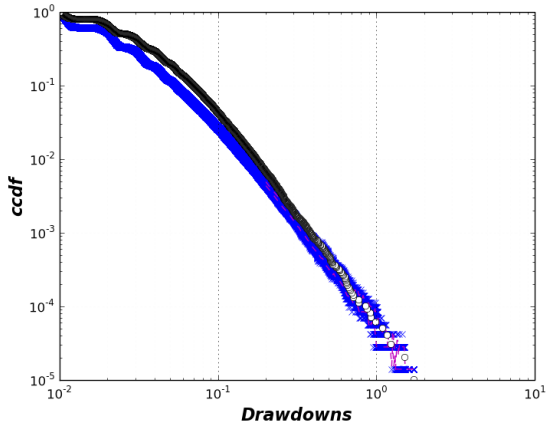

(a) German Government Bonds at 1-min scale

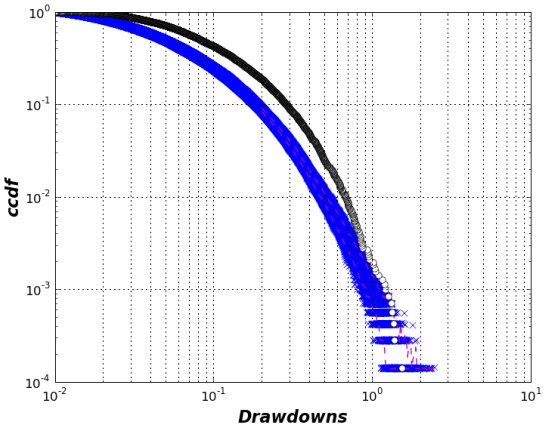

(b) German Government Bonds at 15-min scale

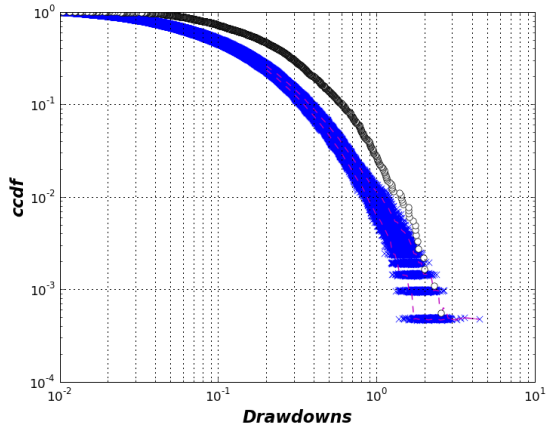

(c) German Government Bonds at 1-hour scale

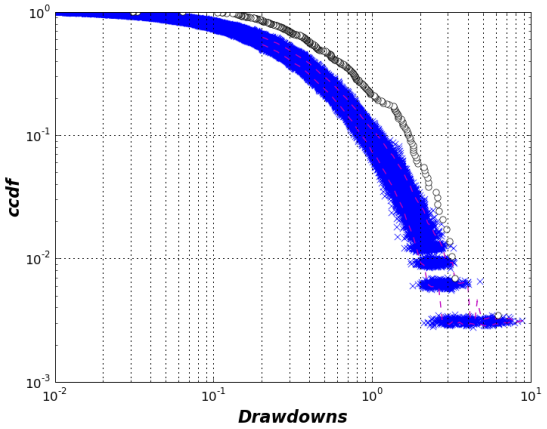

(d) German Government Bonds at 1-day scale

Fig. 69: Logarithmic plots of the complementary cumulative distribution of $\sigma/2$-Drawdowns ($\epsilon = 0.5\sigma$) for the German Government Bonds time series at different time scales -from 1-min to 1-day-. Plotted are the $\sigma/2$-DD ccdf of: (x) 500 samples of the reshuffled return time series, (-) the 95% confidence interval of the reshuffled realizations, (o) time series of the original German Government Bonds dataset.

C.3.3 $TE-$statistics tests

C.3.3.1 SP 500

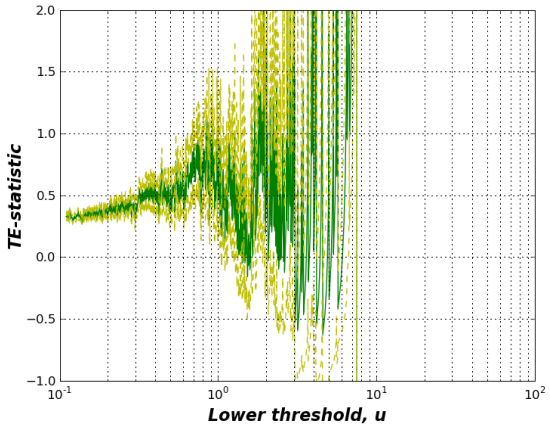

(a) SP 500 at 1-min scale

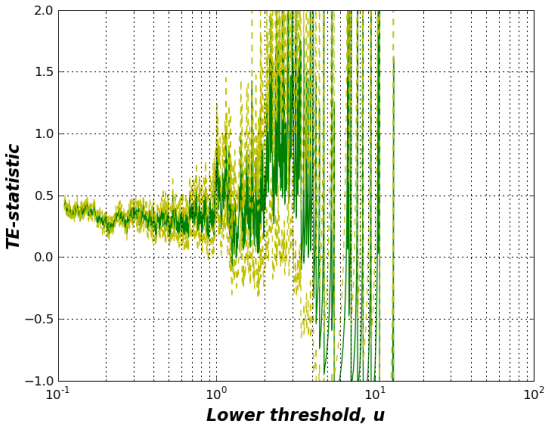

(b) SP 500 at 15-min scale

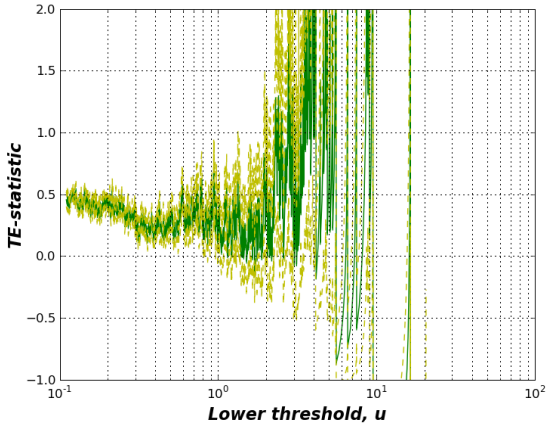

(c) SP 500 at 1-hour scale

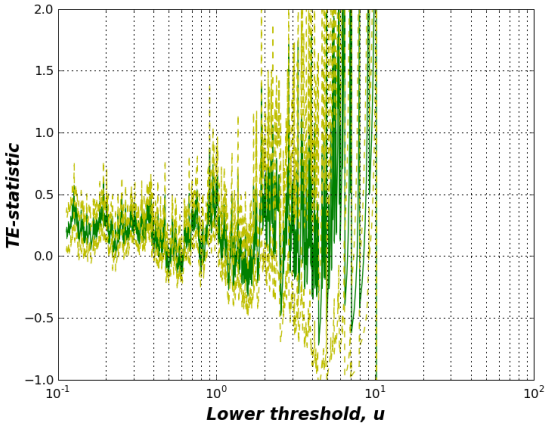

(d) SP 500 at 1-day scale

Fig. 70: $TE-$statistic (Eq.B.5) as a function of the lower threshold u, applied to the distribution of *pure*-drawdowns of the SP 500 dataset for each of the studied time scales - from 1-min to 1-day-. The two dashed lines represent plus and minus one standard deviation from the statistic.

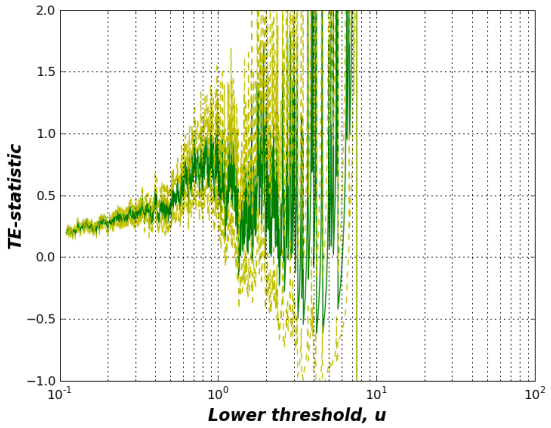

(a) SP 500 at 1-min scale

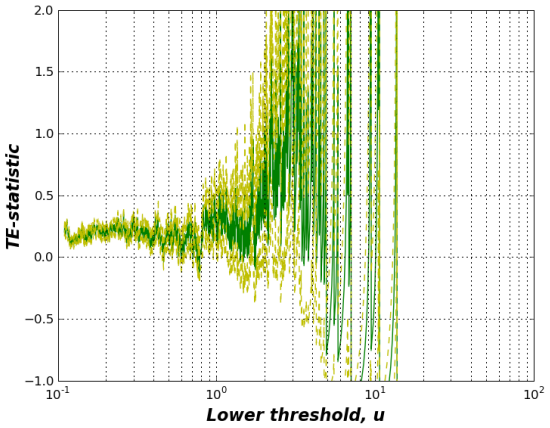

(b) SP 500 at 15-min scale

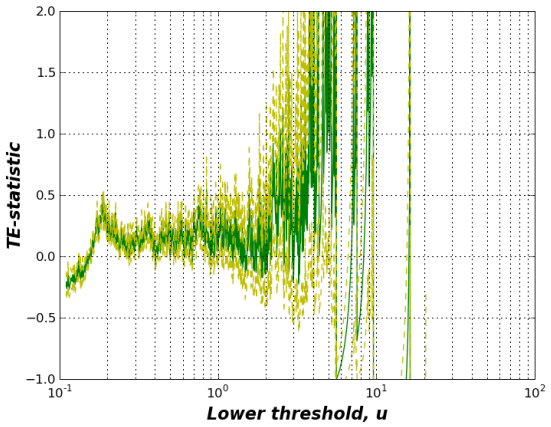

(c) SP 500 at 1-hour scale

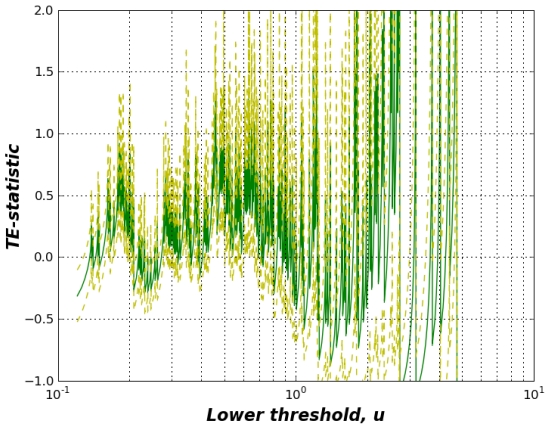

(d) SP 500 at 1-day scale

Fig. 71: $TE-$statistic (Eq.B.5) as a function of the lower threshold u, applied to the distribution of $\sigma/2$-drawdowns of the SP 500 dataset for each of the studied time scales - from 1-min to 1-day-. The two dashed lines represent plus and minus one standard deviation from the statistic.

C.3.3.2 FTSE 100

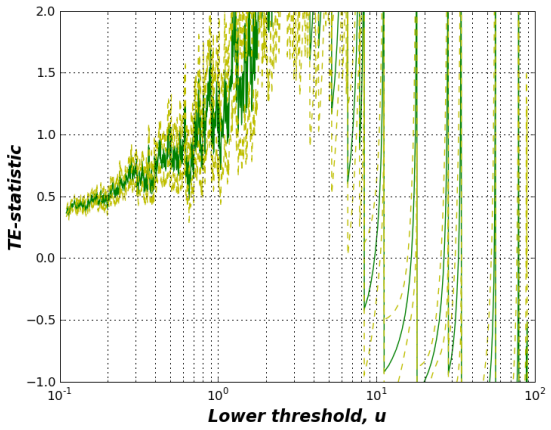

(a) FTSE 100 at 1-min scale

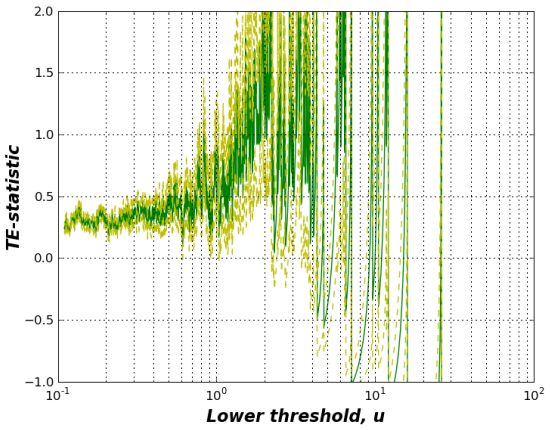

(b) FTSE 100 at 15-min scale

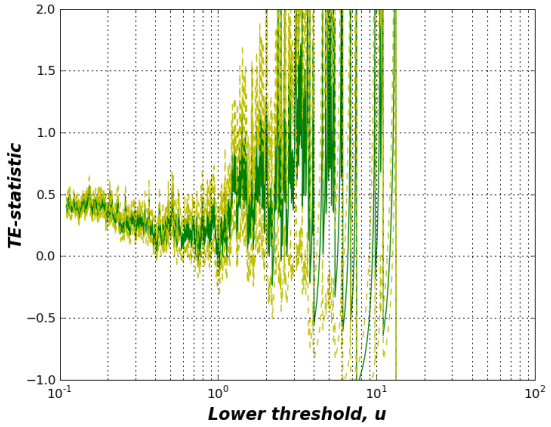

(c) FTSE 100 at 1-hour scale

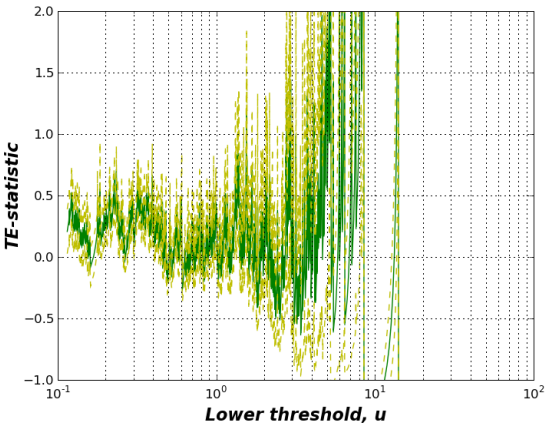

(d) FTSE 100 at 1-day scale

Fig. 72: $TE-$statistic (Eq.B.5) as a function of the lower threshold u, applied to the distribution of *pure*-drawdowns of the FTSE 100 dataset for each of the studied time scales - from 1-min to 1-day-. The two dashed lines represent plus and minus one standard deviation from the statistic.

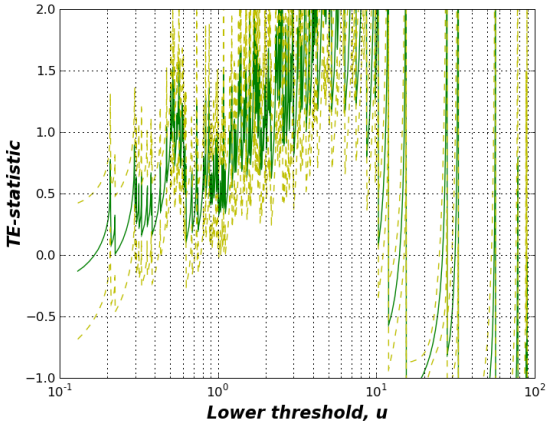

(a) FTSE 100 at 1-min scale

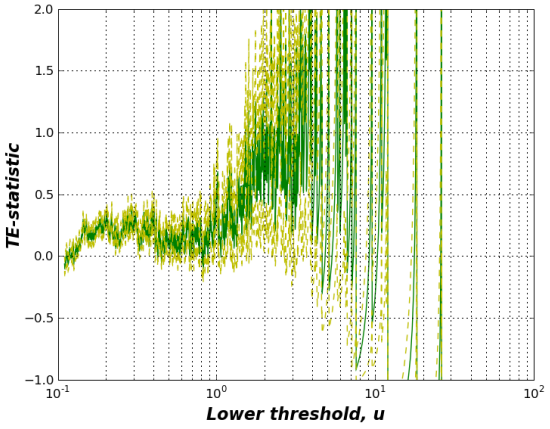

(b) FTSE 100 at 15-min scale

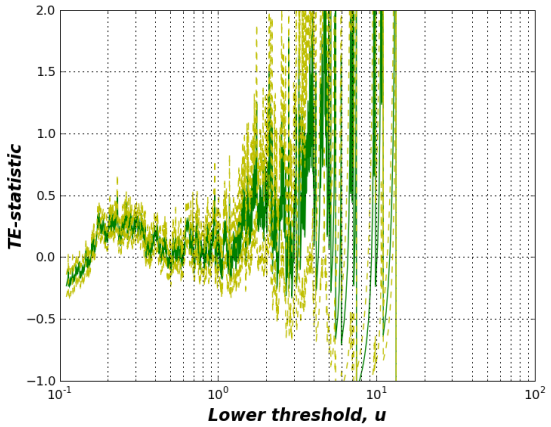

(c) FTSE 100 at 1-hour scale

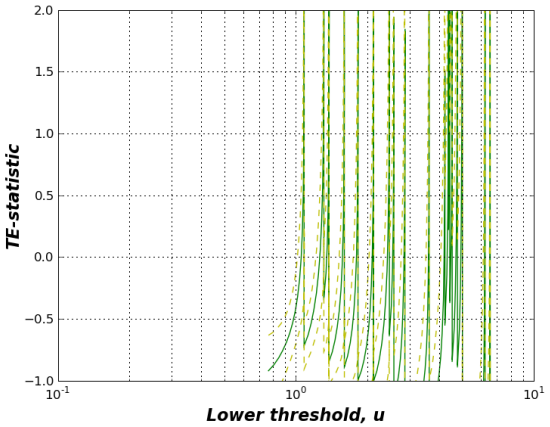

(d) FTSE 100 at 1-day scale

Fig. 73: $TE-$statistic (Eq.B.5) as a function of the lower threshold u, applied to the distribution of $\sigma/2$-drawdowns of the FTSE 100 dataset for each of the studied time scales - from 1-min to 1-day-. The two dashed lines represent plus and minus one standard deviation from the statistic.

C.3.3.3 Nikkei 225

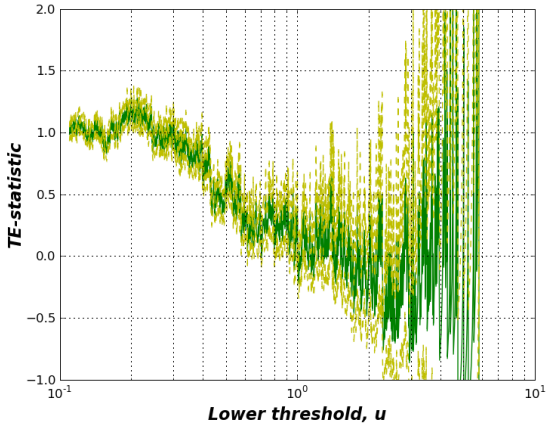

(a) Nikkei 225 at 1-min scale

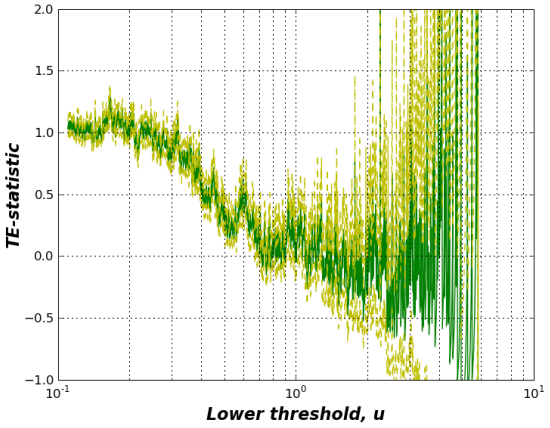

(b) Nikkei 225 at 15-min scale

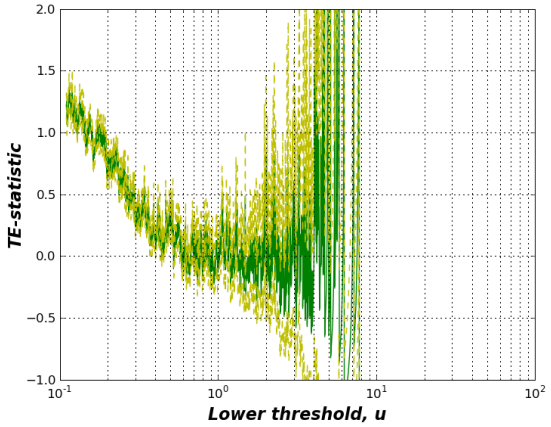

(c) Nikkei 225 at 1-hour scale

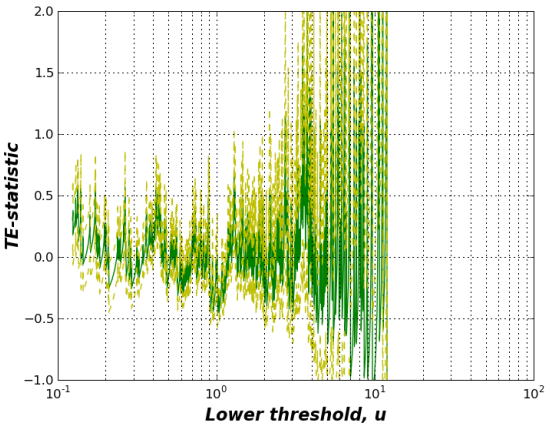

(d) Nikkei 225 at 1-day scale

Fig. 74: $TE-$statistic (Eq.B.5) as a function of the lower threshold u, applied to the distribution of *pure*-drawdowns of the Nikkei 225 dataset for each of the studied time scales - from 1-min to 1-day-. The two dashed lines represent plus and minus one standard deviation from the statistic.

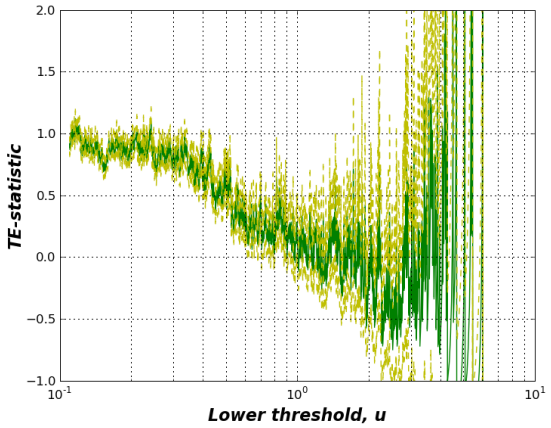

(a) Nikkei 225 at 1-min scale

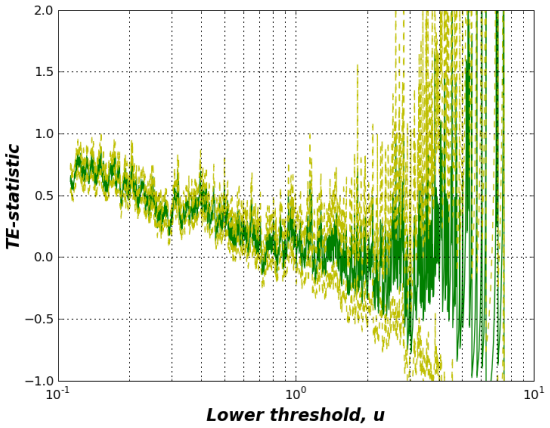

(b) Nikkei 225 at 15-min scale

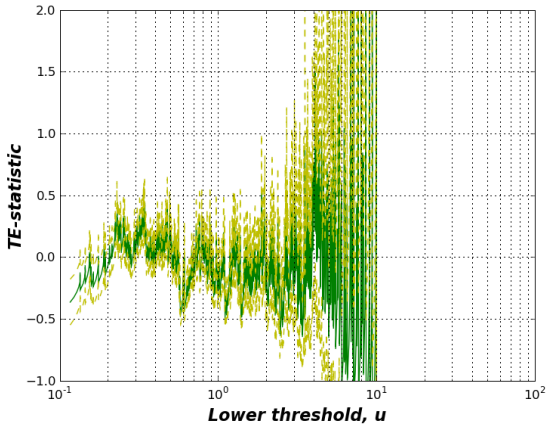

(c) Nikkei 225 at 1-hour scale

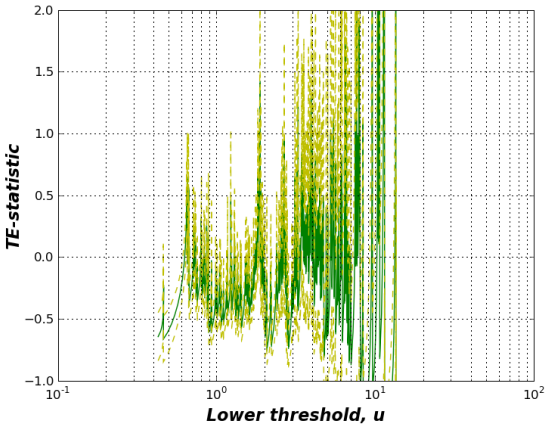

(d) Nikkei 225 at 1-day scale

Fig. 75: $TE-$statistic (Eq.B.5) as a function of the lower threshold u, applied to the distribution of $\sigma/2$-drawdowns of the Nikkei 225 dataset for each of the studied time scales - from 1-min to 1-day-. The two dashed lines represent plus and minus one standard deviation from the statistic.

C.3.3.4 Japanese Yen

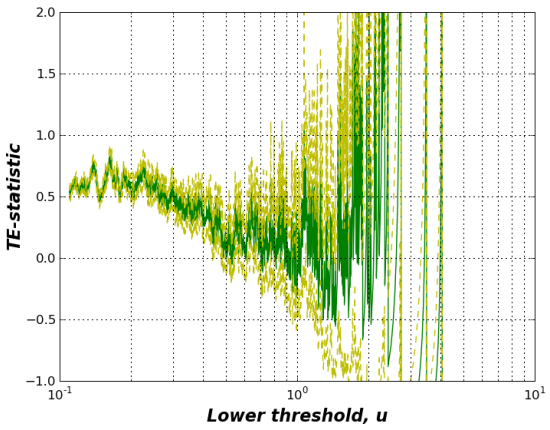

(a) Japanese Yen at 1-min scale

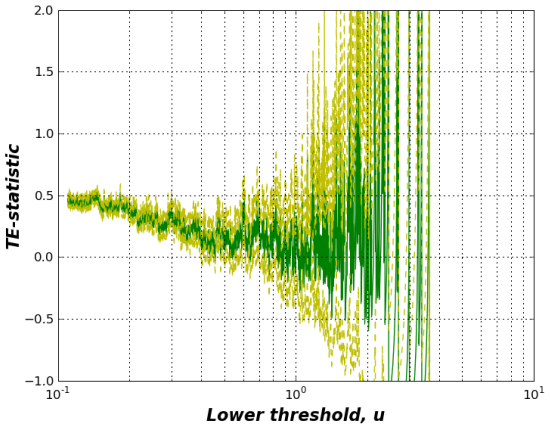

(b) Japanese Yen at 15-min scale

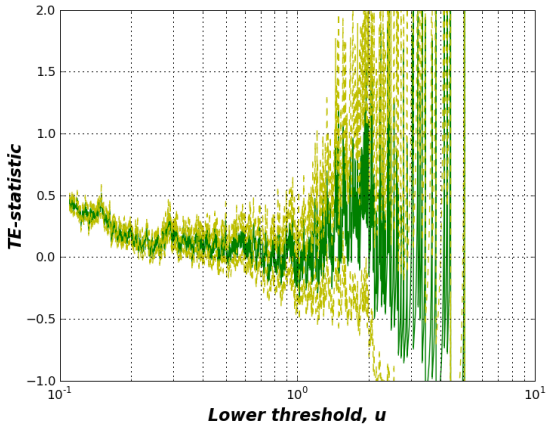

(c) Japanese Yen at 1-hour scale

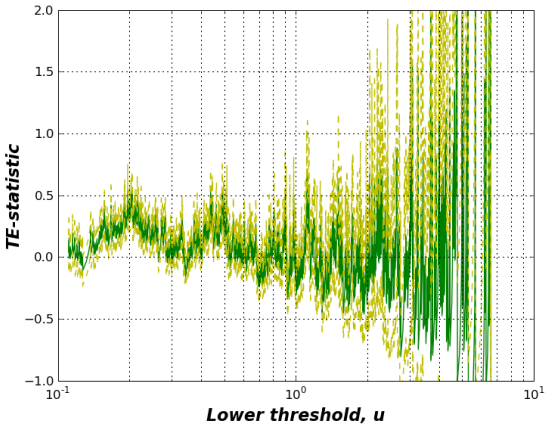

(d) Japanese Yen at 1-day scale

Fig. 76: *TE*−statistic (Eq.B.5) as a function of the lower threshold u, applied to the distribution of *pure*-drawdowns of the Japanese Yen dataset for each of the studied time scales - from 1-min to 1-day-. The two dashed lines represent plus and minus one standard deviation from the statistic.

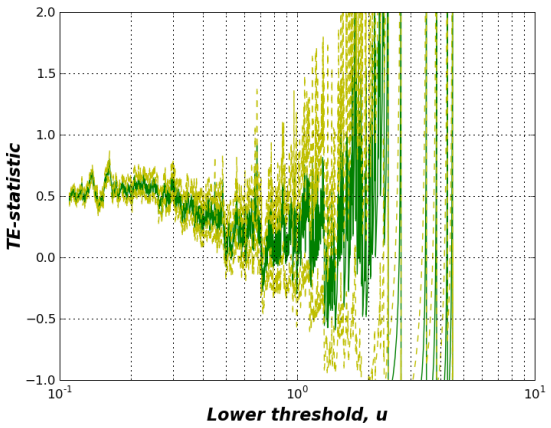

(a) Japanese Yen at 1-min scale

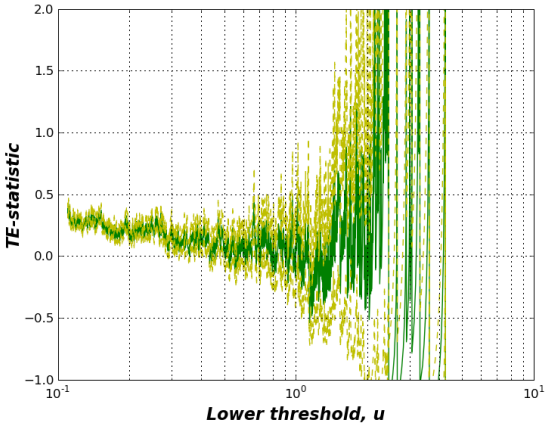

(b) Japanese Yen at 15-min scale

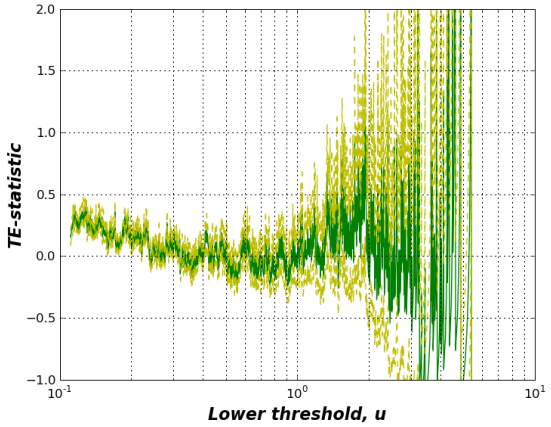

(c) Japanese Yen at 1-hour scale

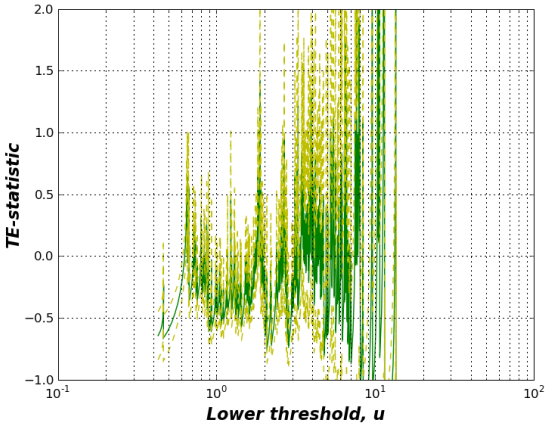

(d) Japanese Yen at 1-day scale

Fig. 77: $TE-$statistic (Eq.B.5) as a function of the lower threshold u, applied to the distribution of $\sigma/2$-drawdowns of the Japanese Yen dataset for each of the studied time scales - from 1-min to 1-day-. The two dashed lines represent plus and minus one standard deviation from the statistic.

C.3.3.5 Deutschmark

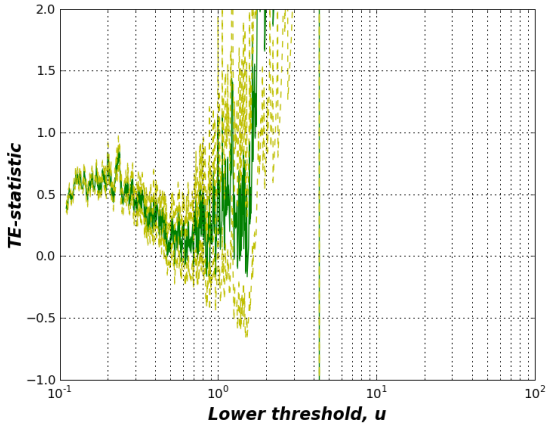

(a) Deutschmark at 1-min scale

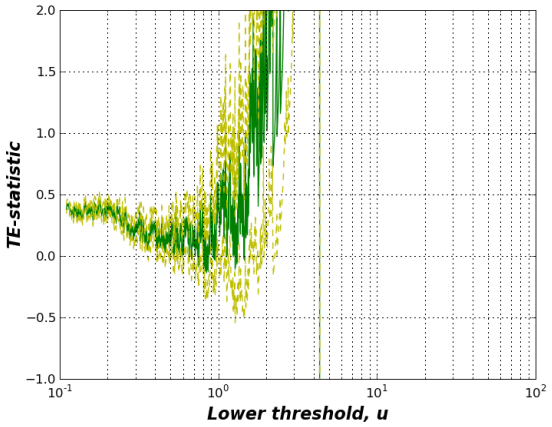

(b) Deutschmark at 15-min scale

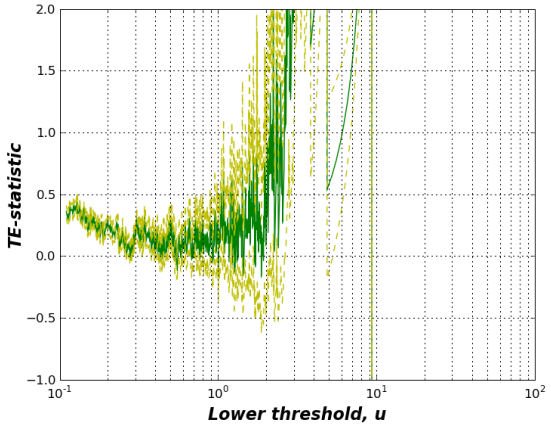

(c) Deutschmark at 1-hour scale

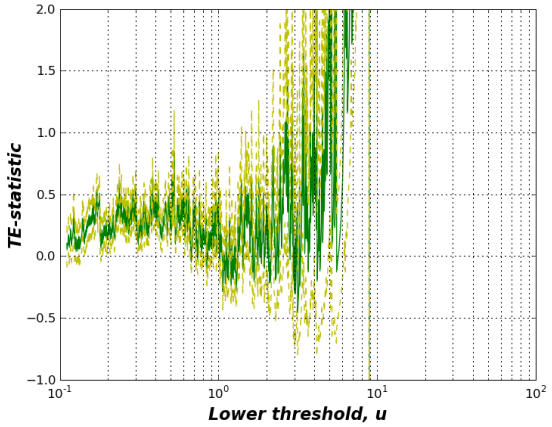

(d) Deutschmark at 1-day scale

Fig. 78: $TE-$statistic (Eq.B.5) as a function of the lower threshold u, applied to the distribution of *pure*-drawdowns of the Deutschmark dataset for each of the studied time scales - from 1-min to 1-day-. The two dashed lines represent plus and minus one standard deviation from the statistic.

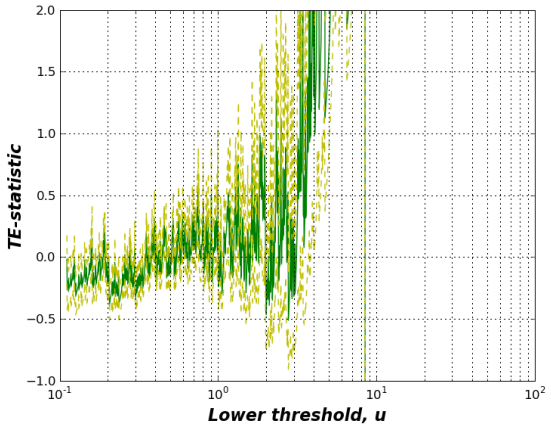

(a) Deutschmark at 1-min scale

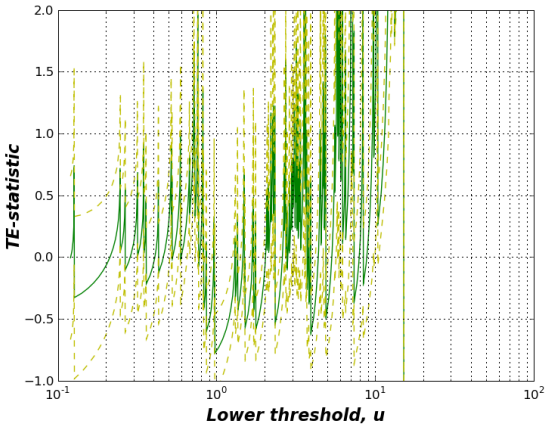

(b) Deutschmark at 15-min scale

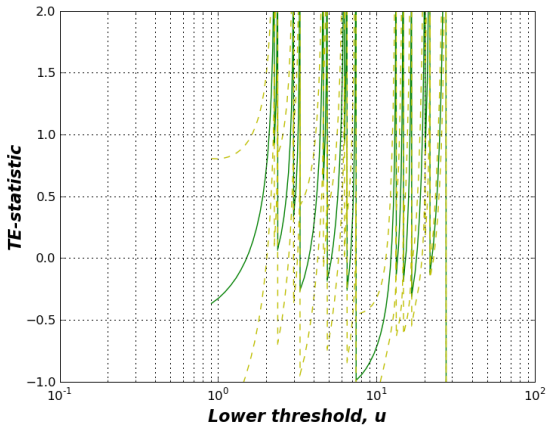

(c) Deutschmark at 1-hour scale

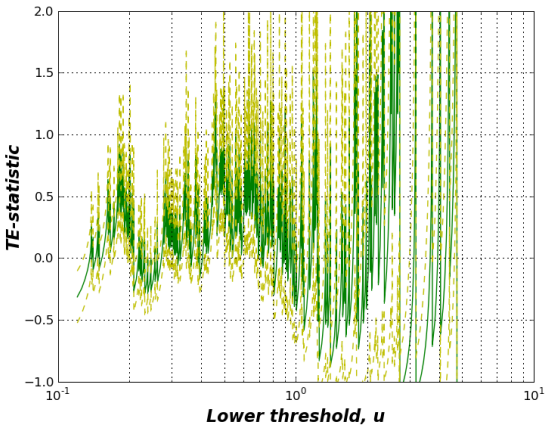

(d) Deutschmark at 1-day scale

Fig. 79: $TE-$statistic (Eq.B.5) as a function of the lower threshold u, applied to the distribution of $\sigma/2$-drawdowns of the Deutschmark dataset for each of the studied time scales - from 1-min to 1-day-. The two dashed lines represent plus and minus one standard deviation from the statistic.

C.3.3.6 Japanese Government Bonds

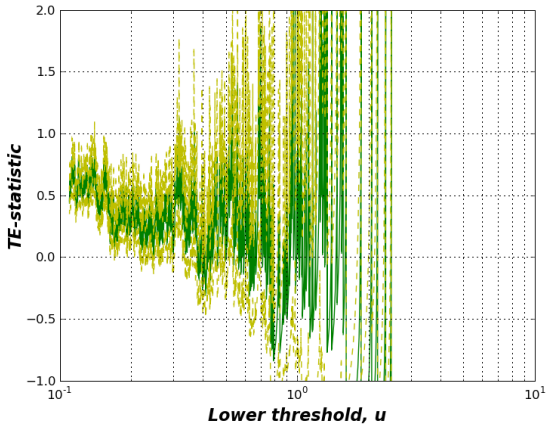

(a) Jap Government Bonds at 1-min scale

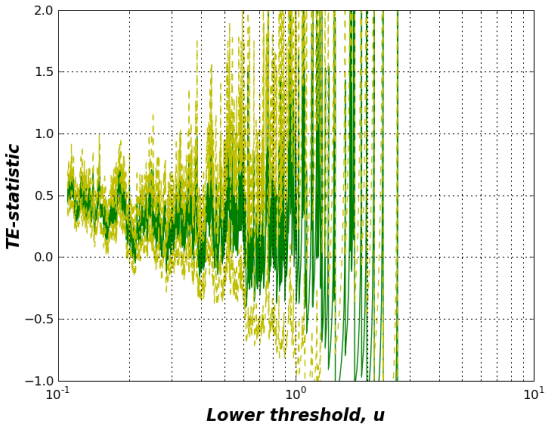

(b) Jap Government Bonds at 15-min scale

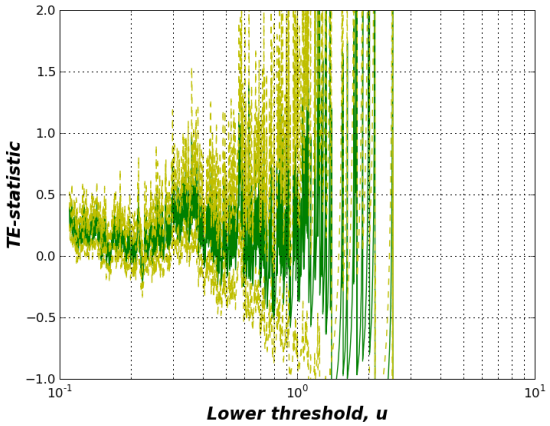

(c) Jap Government Bonds at 1-hour scale

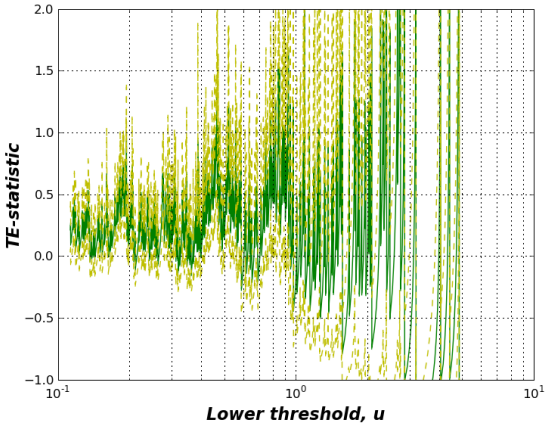

(d) Jap Government Bonds at 1-day scale

Fig. 80: $TE-$statistic (Eq.B.5) as a function of the lower threshold u, applied to the distribution of *pure*-drawdowns of the Jap Government Bonds dataset for each of the studied time scales - from 1-min to 1-day-. The two dashed lines represent plus and minus one standard deviation from the statistic.

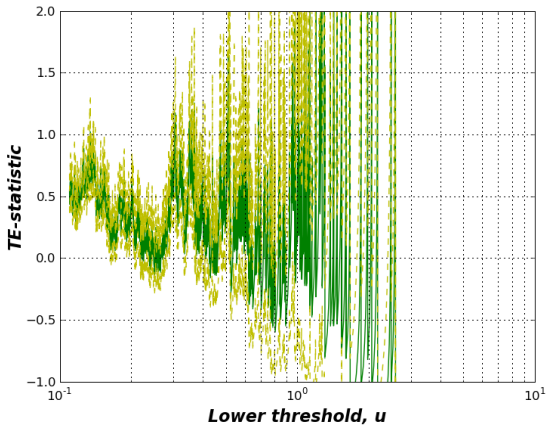

(a) Jap Government Bonds at 1-min scale

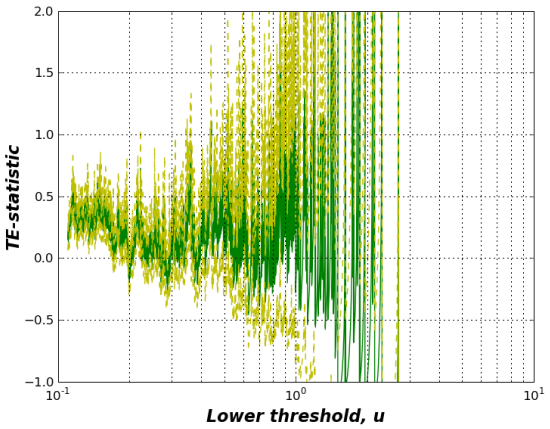

(b) Jap Government Bonds at 15-min scale

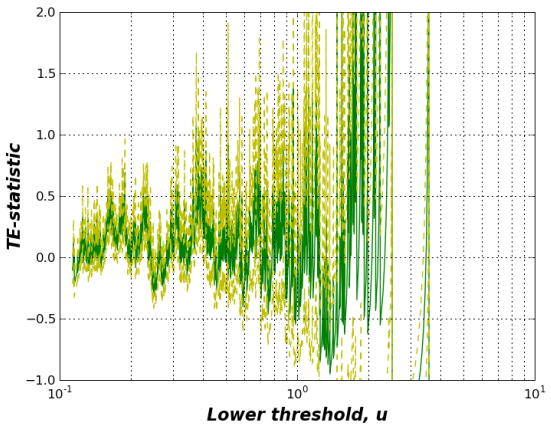

(c) Jap Government Bonds at 1-hour scale

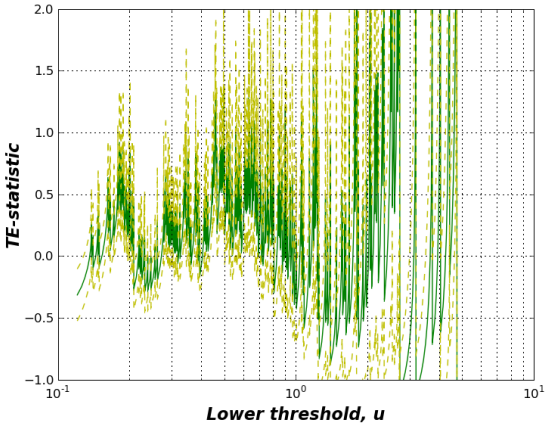

(d) Jap Government Bonds at 1-day scale

Fig. 81: $TE-$statistic (Eq.B.5) as a function of the lower threshold u, applied to the distribution of $\sigma/2$-drawdowns of the Jap Government Bonds dataset for each of the studied time scales - from 1-min to 1-day-. The two dashed lines represent plus and minus one standard deviation from the statistic.

C.3.3.7 US Treasury Bonds I

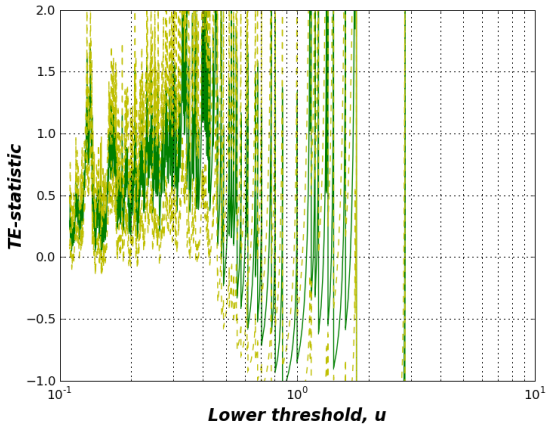

(a) US T-Bonds I at 1-min scale

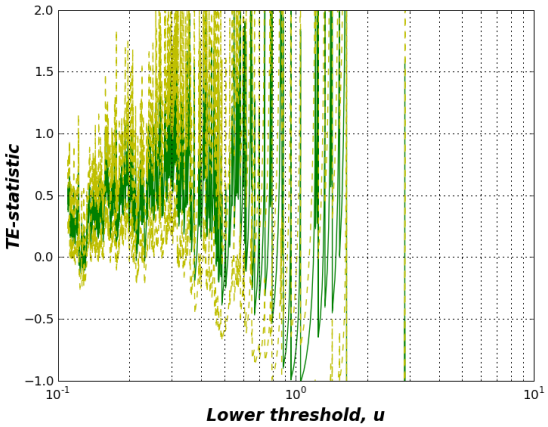

(b) US T-Bonds I at 15-min scale

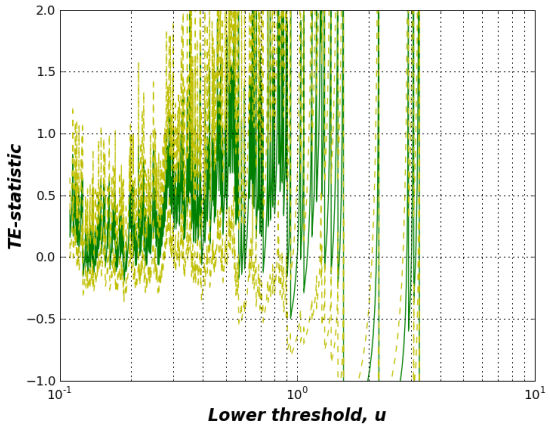

(c) US T-Bonds I at 1-hour scale

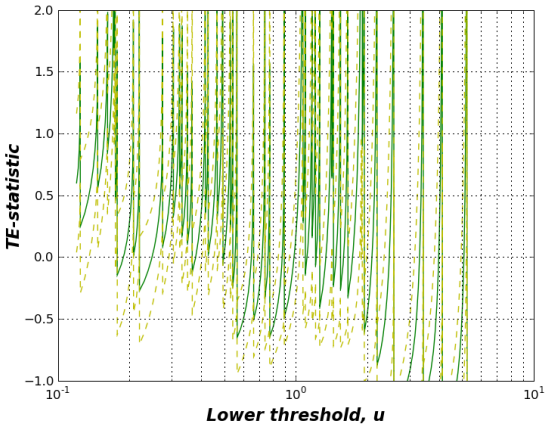

(d) US T-Bonds I at 1-day scale

Fig. 82: *TE*−statistic (Eq.B.5) as a function of the lower threshold u, applied to the distribution of *pure*-drawdowns of the US T-Bonds I dataset for each of the studied time scales - from 1-min to 1-day-. The two dashed lines represent plus and minus one standard deviation from the statistic.

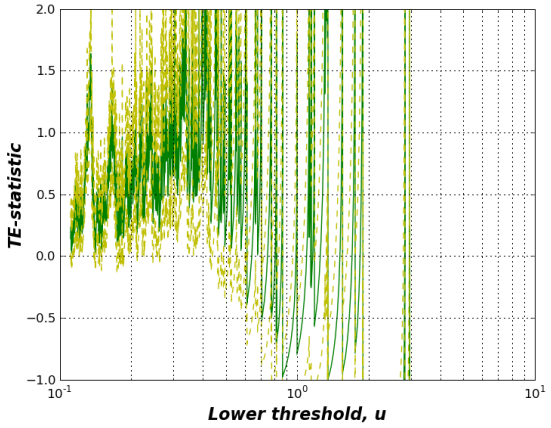

(a) US T-Bonds I at 1-min scale

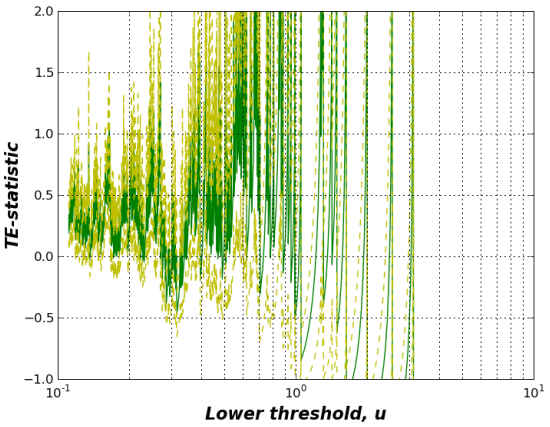

(b) US T-Bonds I at 15-min scale

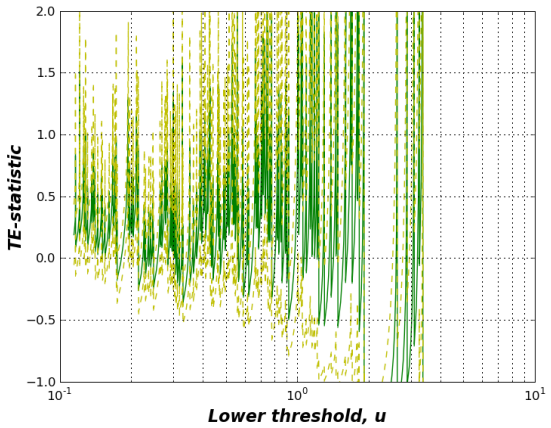

(c) US T-Bonds I at 1-hour scale

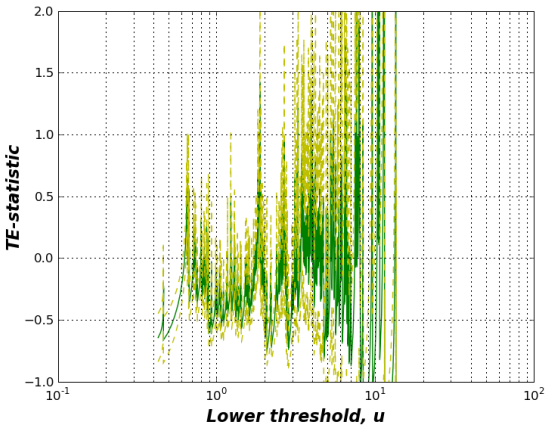

(d) US T-Bonds I at 1-day scale

Fig. 83: $TE-$statistic (Eq.B.5) as a function of the lower threshold u, applied to the distribution of $\sigma/2$-drawdowns of the US T-Bonds I dataset for each of the studied time scales - from 1-min to 1-day-. The two dashed lines represent plus and minus one standard deviation from the statistic.

C.3.3.8 US Treasury Bonds III

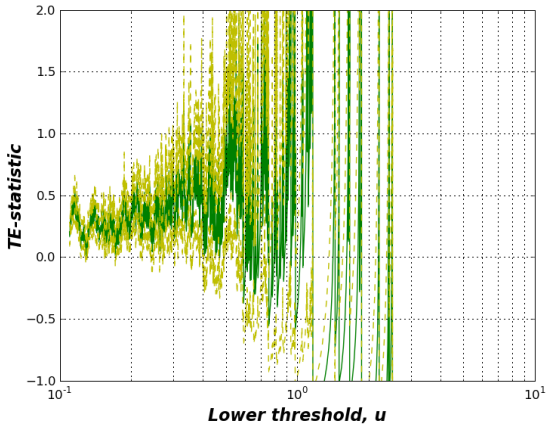

(a) US T-Bonds III at 1-min scale

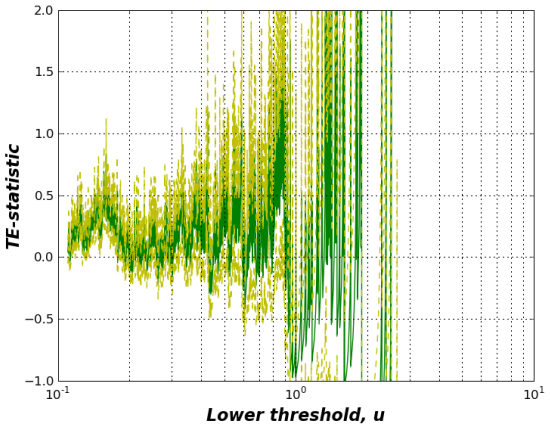

(b) US T-Bonds III at 15-min scale

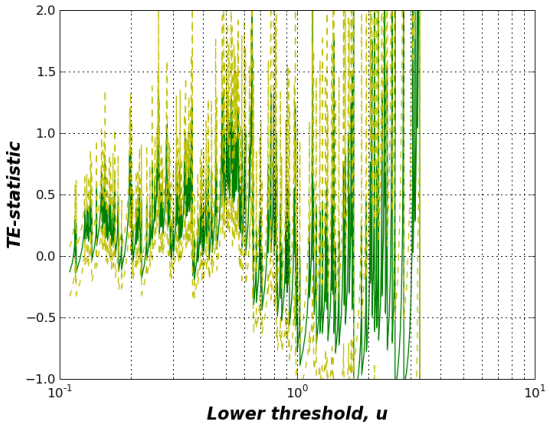

(c) US T-Bonds III at 1-hour scale

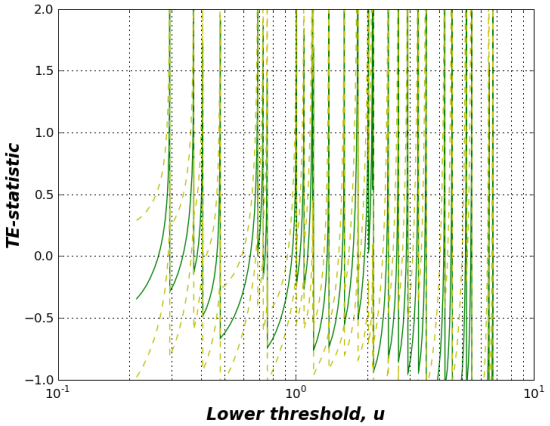

(d) US T-Bonds III at 1-day scale

Fig. 84: $TE-$statistic (Eq.B.5) as a function of the lower threshold u, applied to the distribution of *pure*-drawdowns of the US T-Bonds III dataset for each of the studied time scales - from 1-min to 1-day-. The two dashed lines represent plus and minus one standard deviation from the statistic.

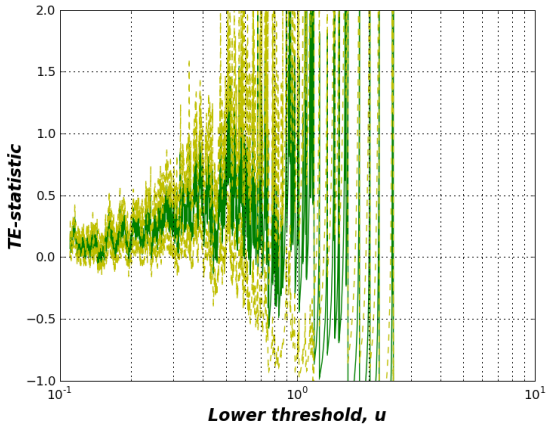

(a) US T-Bonds III at 1-min scale

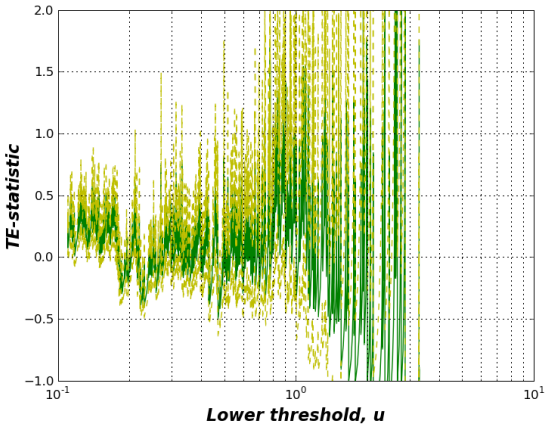

(b) US T-Bonds III at 15-min scale

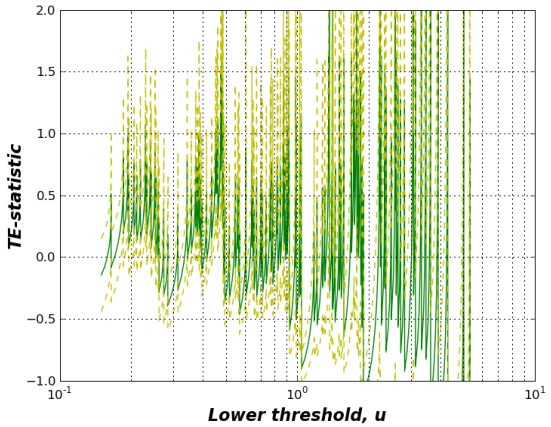

(c) US T-Bonds III at 1-hour scale

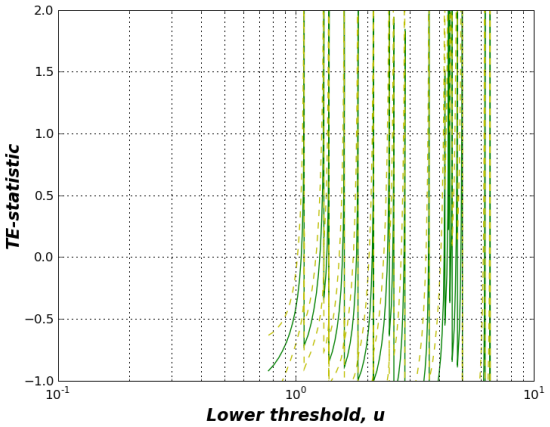

(d) US T-Bonds III at 1-day scale

Fig. 85: $TE-$statistic (Eq.B.5) as a function of the lower threshold u, applied to the distribution of $\sigma/2$-drawdowns of the US T-Bonds III dataset for each of the studied time scales - from 1-min to 1-day-. The two dashed lines represent plus and minus one standard deviation from the statistic.

C.3.3.9 German Government Bonds

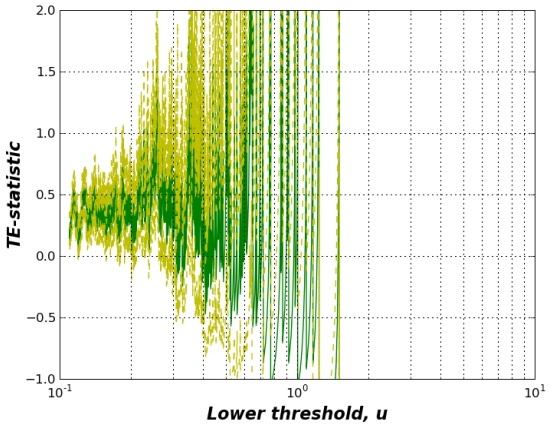

(a) German Government Bonds at 1-min scale

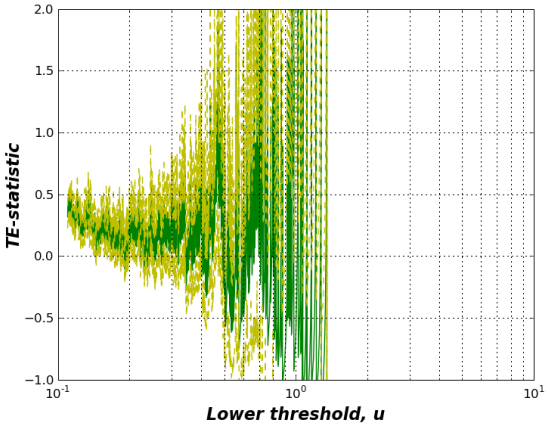

(b) German Government Bonds at 15-min scale

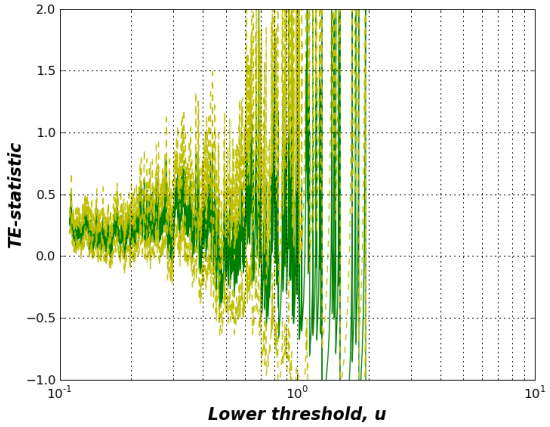

(c) German Government Bonds at 1-hour scale

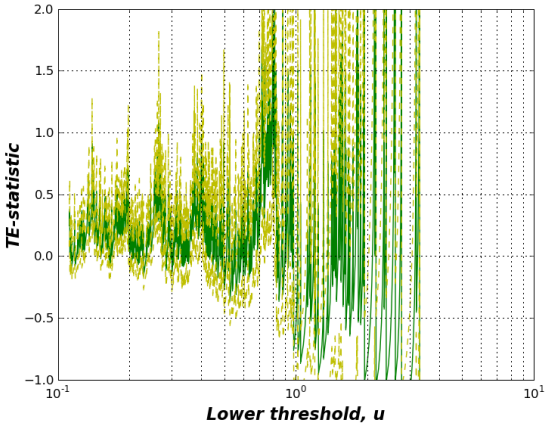

(d) German Government Bonds at 1-day scale

Fig. 86: $TE-$statistic (Eq.B.5) as a function of the lower threshold u, applied to the distribution of *pure*-drawdowns of the German Government Bonds dataset for each of the studied time scales - from 1-min to 1-day-. The two dashed lines represent plus and minus one standard deviation from the statistic.

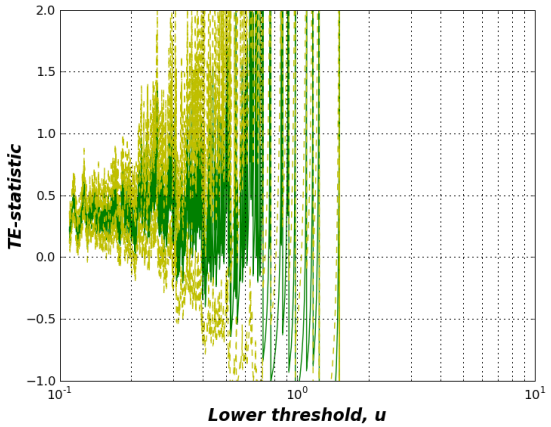

(a) German Government Bonds at 1-min scale

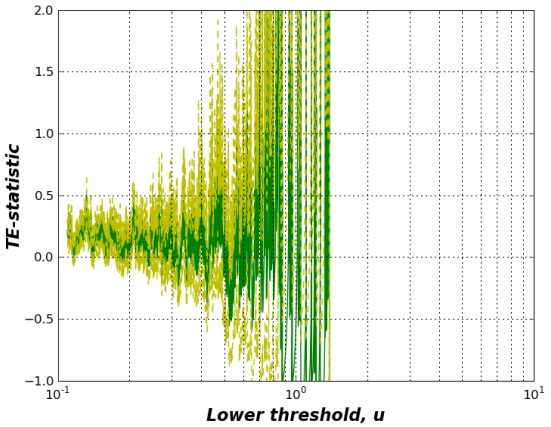

(b) German Government Bonds at 15-min scale

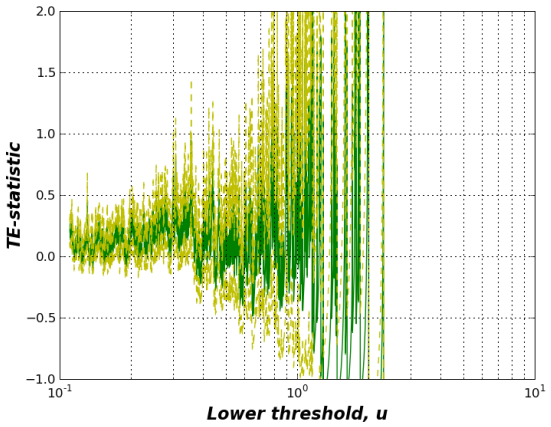

(c) German Government Bonds at 1-hour scale

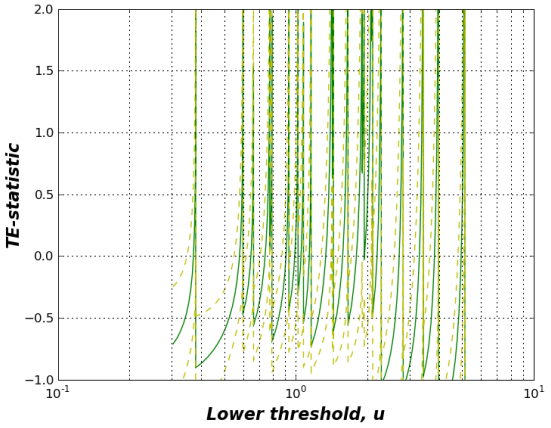

(d) German Government Bonds at 1-day scale

Fig. 87: $TE-$statistic (Eq.B.5) as a function of the lower threshold u, applied to the distribution of $\sigma/2$-drawdowns of the German Government Bonds dataset for each of the studied time scales - from 1-min to 1-day-. The two dashed lines represent plus and minus one standard deviation from the statistic.

C.3.4 $TP-$statistics tests

C.3.4.1 SP 500

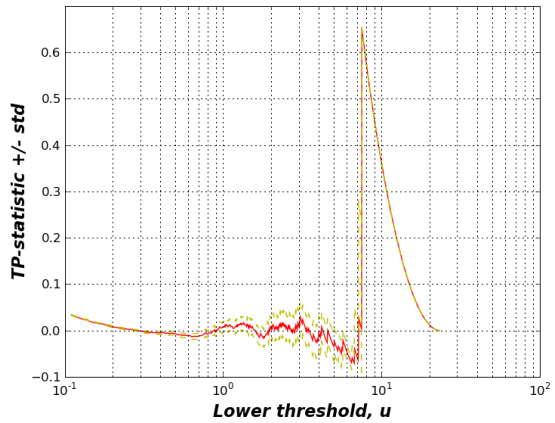

(a) SP 500 at 1-min scale

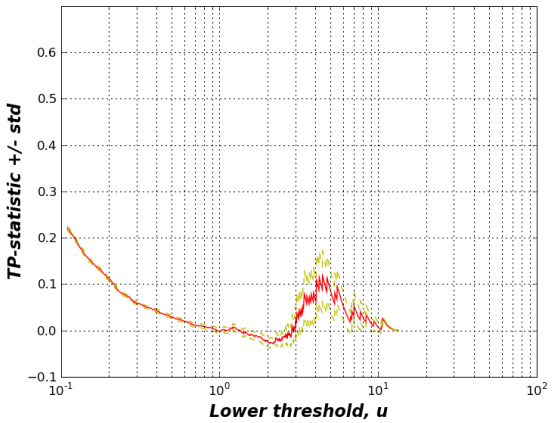

(b) SP 500 at 15-min scale

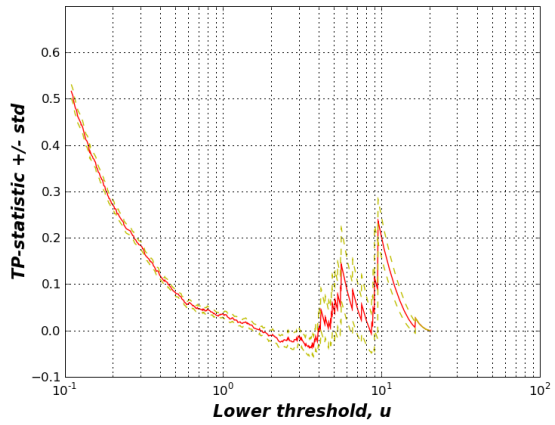

(c) SP 500 at 1-hour scale

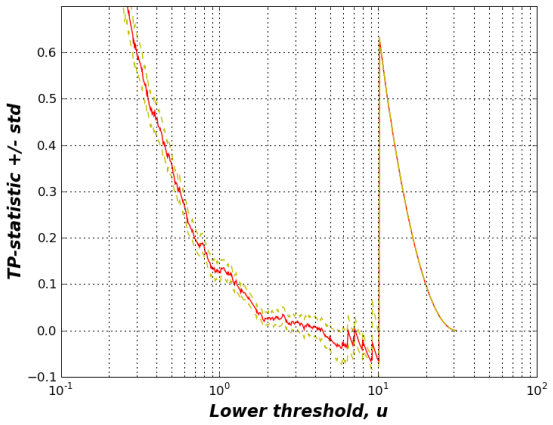

(d) SP 500 at 1-day scale

Fig. 88: $TP-$statistic (Eq.B.2) as a function of the lower threshold u, applied to the distribution of *pure*-drawdowns of the SP 500 dataset for each of the studied time scales - from 1-min to 1-day-. The two dashed lines represent plus and minus one standard deviation from the statistic.

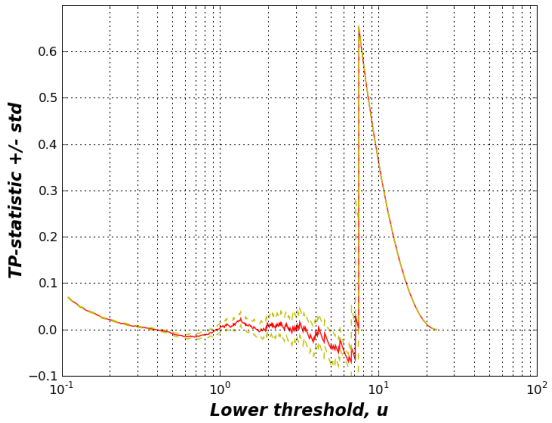

(a) SP 500 at 1-min scale

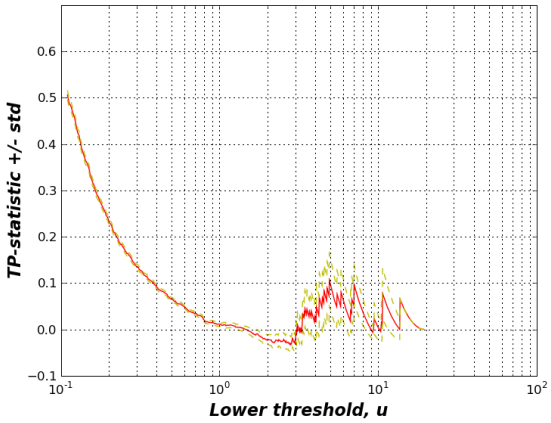

(b) SP 500 at 15-min scale

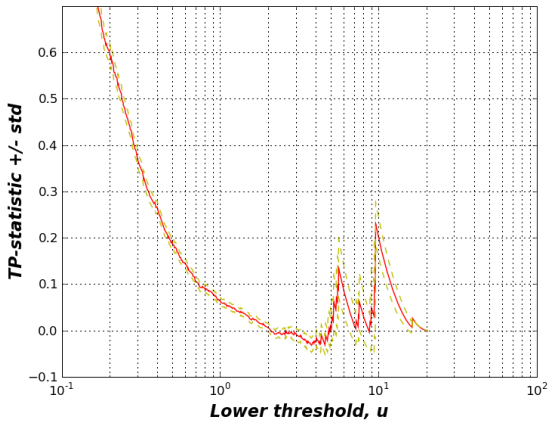

(c) SP 500 at 1-hour scale

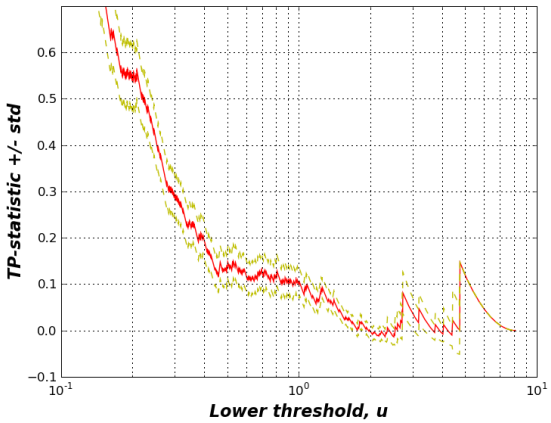

(d) SP 500 at 1-day scale

Fig. 89: $TP-$statistic (Eq.B.2) as a function of the lower threshold u, applied to the distribution of $\sigma/2$-drawdowns of the SP 500 dataset for each of the studied time scales - from 1-min to 1-day-. The two dashed lines represent plus and minus one standard deviation from the statistic.

C.3.4.2 FTSE 100

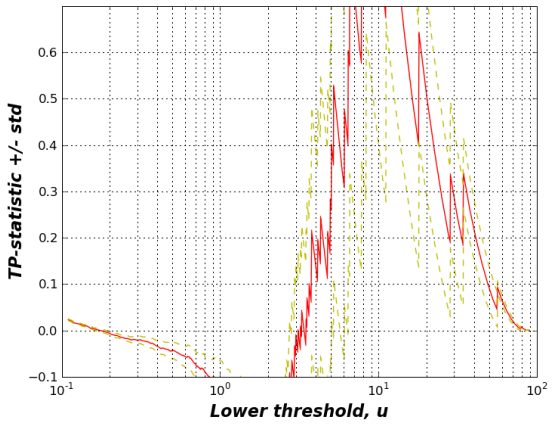

(a) FTSE 100 at 1-min scale

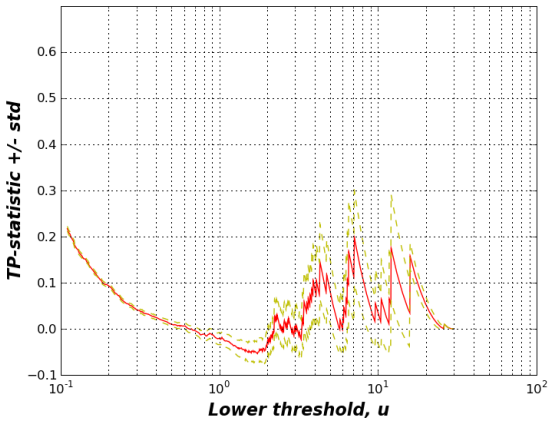

(b) FTSE 100 at 15-min scale

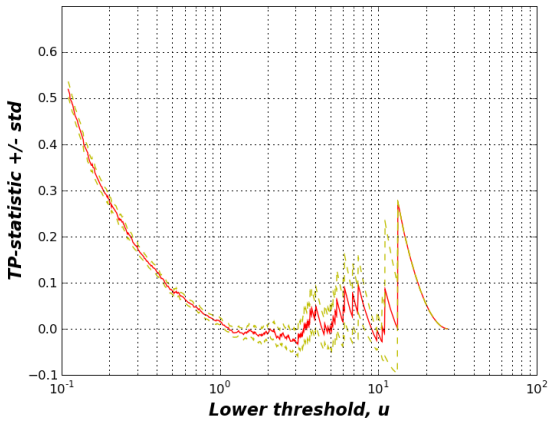

(c) FTSE 100 at 1-hour scale

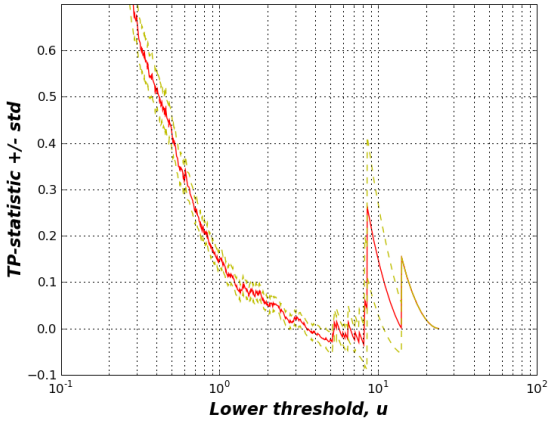

(d) FTSE 100 at 1-day scale

Fig. 90: *TP*−statistic (Eq.B.2) as a function of the lower threshold u, applied to the distribution of *pure*-drawdowns of the FTSE 100 dataset for each of the studied time scales - from 1-min to 1-day-. The two dashed lines represent plus and minus one standard deviation from the statistic.

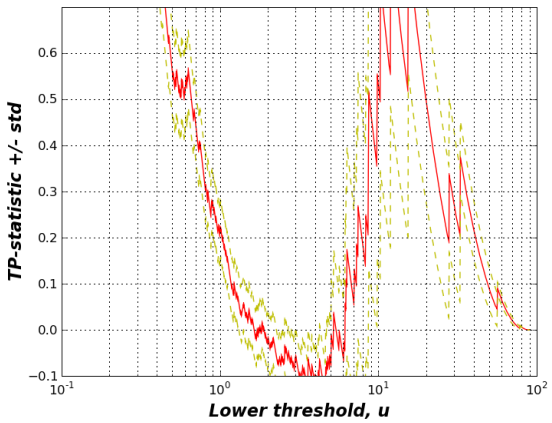

(a) FTSE 100 at 1-min scale

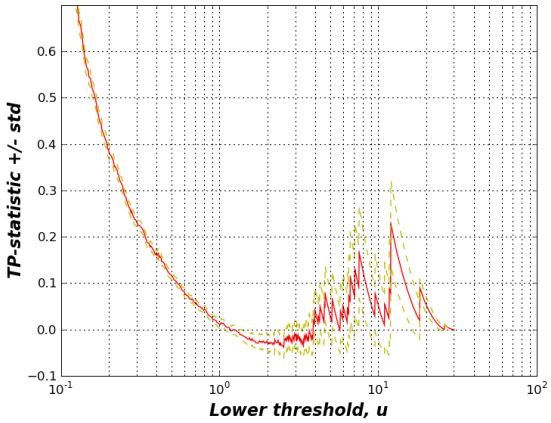

(b) FTSE 100 at 15-min scale

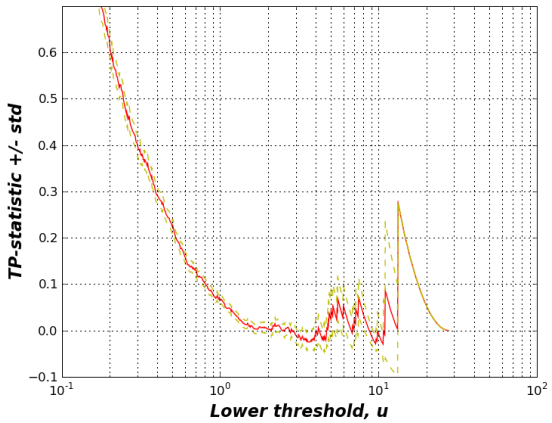

(c) FTSE 100 at 1-hour scale

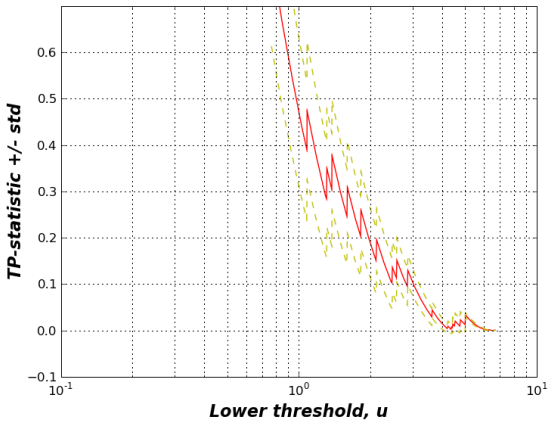

(d) FTSE 100 at 1-day scale

Fig. 91: $TP-$statistic (Eq.B.2) as a function of the lower threshold u, applied to the distribution of $\sigma/2$-drawdowns of the FTSE 100 dataset for each of the studied time scales - from 1-min to 1-day-. The two dashed lines represent plus and minus one standard deviation from the statistic.

C.3.4.3 Nikkei 225

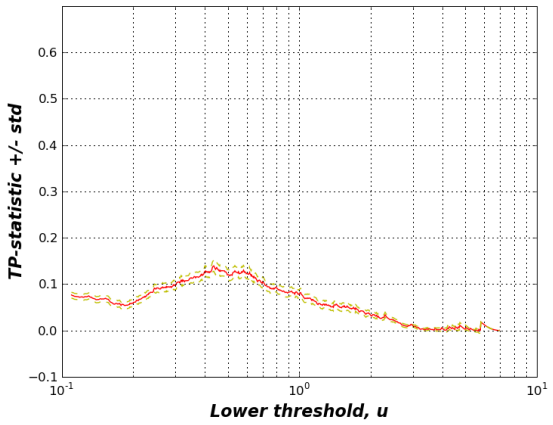

(a) Nikkei 225 at 1-min scale

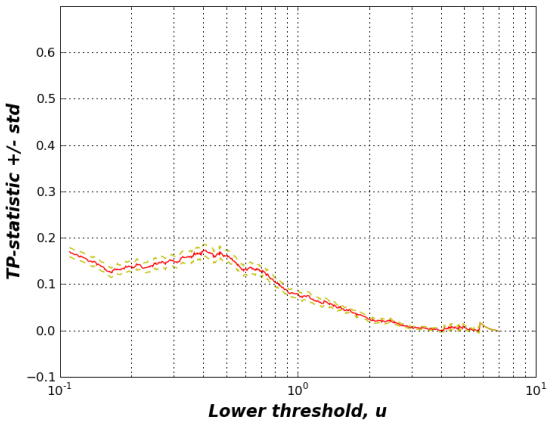

(b) Nikkei 225 at 15-min scale

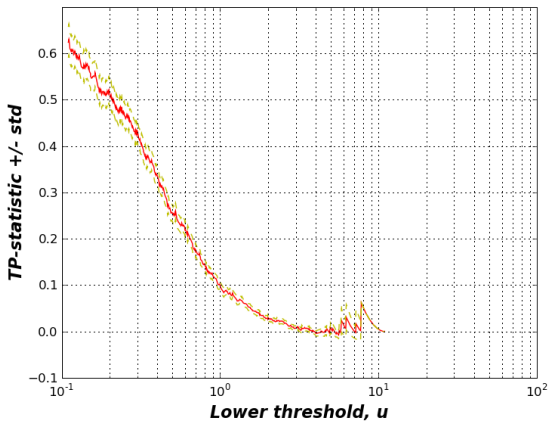

(c) Nikkei 225 at 1-hour scale

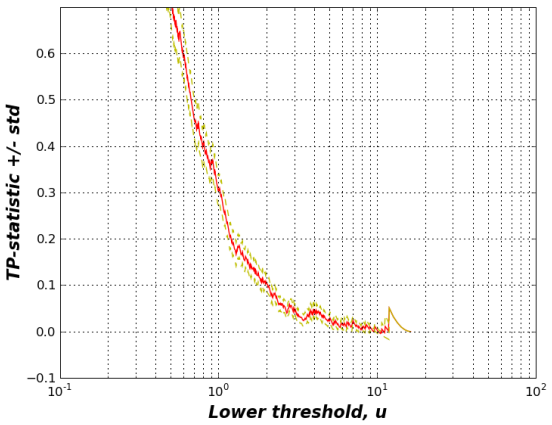

(d) Nikkei 225 at 1-day scale

Fig. 92: *TP*−statistic (Eq.B.2) as a function of the lower threshold u, applied to the distribution of *pure*-drawdowns of the Nikkei 225 dataset for each of the studied time scales - from 1-min to 1-day-. The two dashed lines represent plus and minus one standard deviation from the statistic.

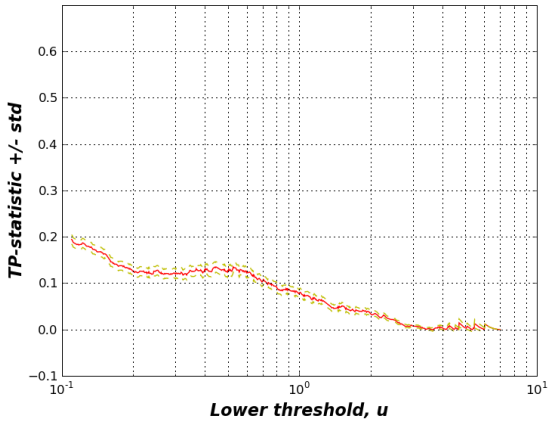

(a) Nikkei 225 at 1-min scale

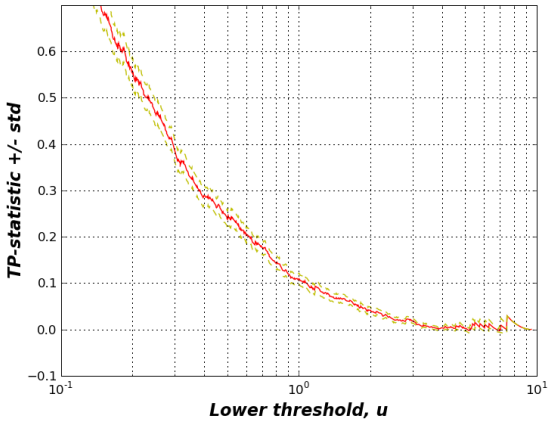

(b) Nikkei 225 at 15-min scale

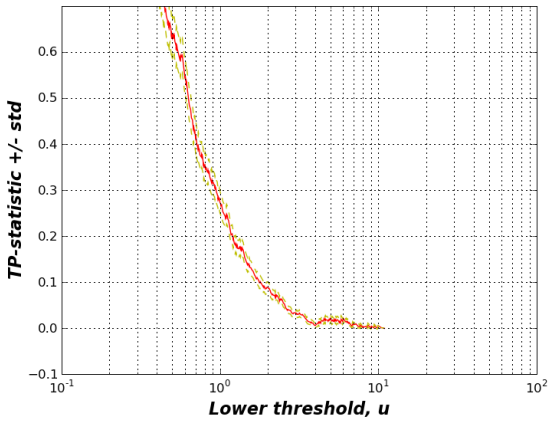

(c) Nikkei 225 at 1-hour scale

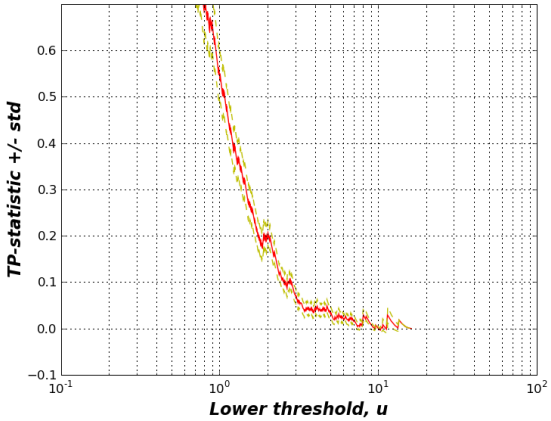

(d) Nikkei 225 at 1-day scale

Fig. 93: $TP-$statistic (Eq.B.2) as a function of the lower threshold u, applied to the distribution of $\sigma/2$-drawdowns of the Nikkei 225 dataset for each of the studied time scales - from 1-min to 1-day-. The two dashed lines represent plus and minus one standard deviation from the statistic.

C.3.4.4 Japanese Yen

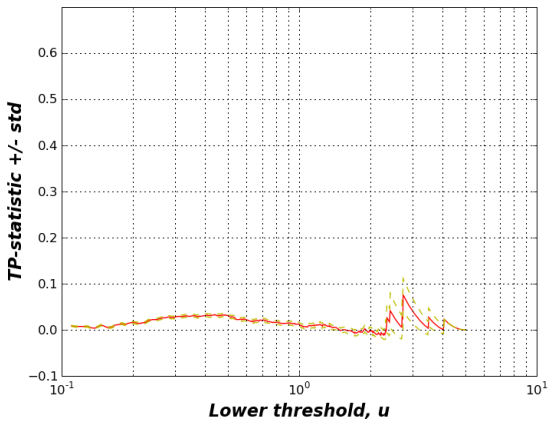

(a) Japanese Yen at 1-min scale

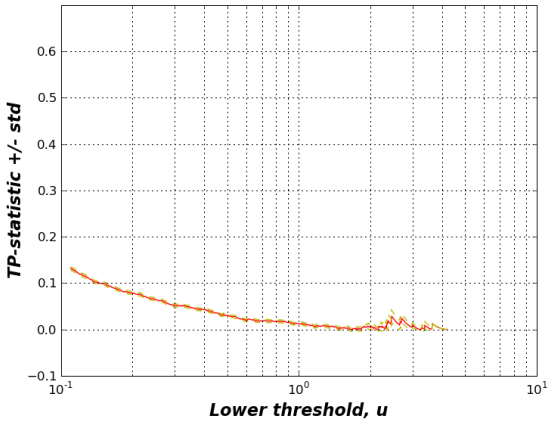

(b) Japanese Yen at 15-min scale

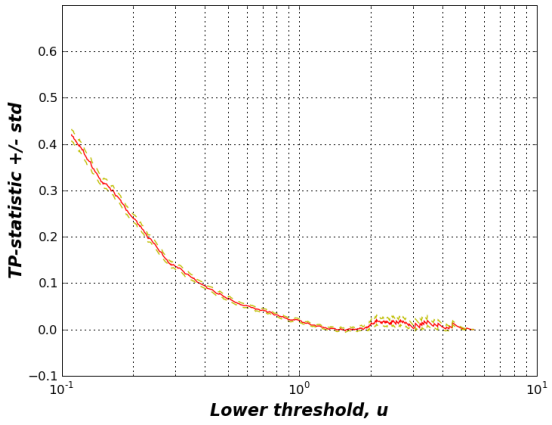

(c) Japanese Yen at 1-hour scale

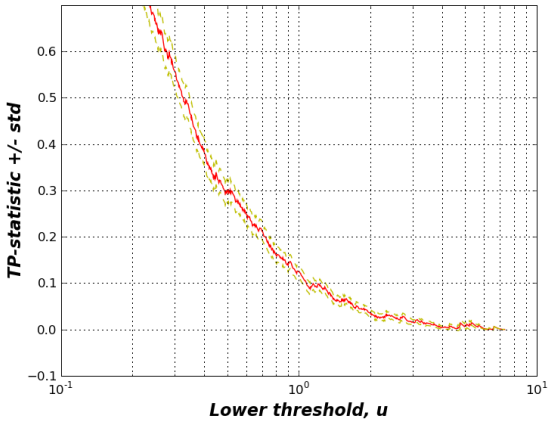

(d) Japanese Yen at 1-day scale

Fig. 94: *TP*−statistic (Eq.B.2) as a function of the lower threshold u, applied to the distribution of *pure*-drawdowns of the Japanese Yen dataset for each of the studied time scales - from 1-min to 1-day-. The two dashed lines represent plus and minus one standard deviation from the statistic.

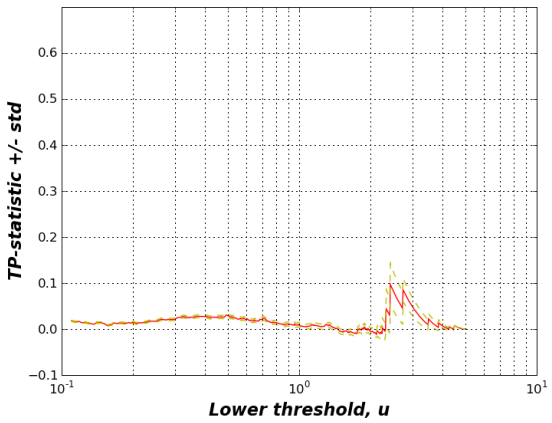

(a) Japanese Yen at 1-min scale

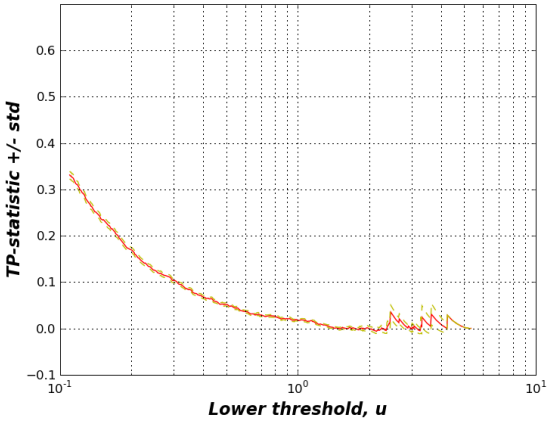

(b) Japanese Yen at 15-min scale

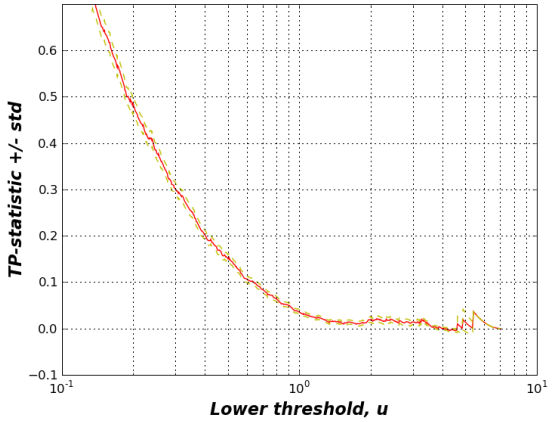

(c) Japanese Yen at 1-hour scale

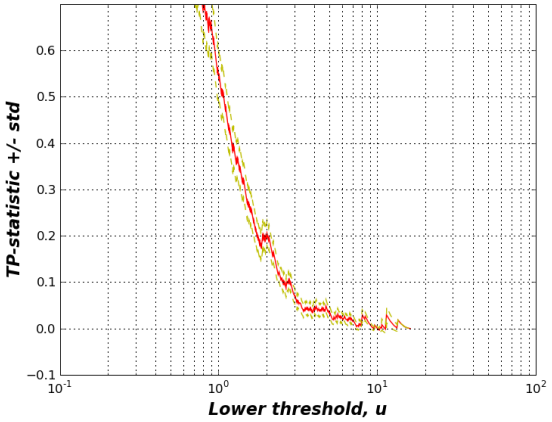

(d) Japanese Yen at 1-day scale

Fig. 95: $TP-$statistic (Eq.B.2) as a function of the lower threshold u, applied to the distribution of $\sigma/2$-drawdowns of the Japanese Yen dataset for each of the studied time scales - from 1-min to 1-day-. The two dashed lines represent plus and minus one standard deviation from the statistic.

C.3.4.5 Deutschmark

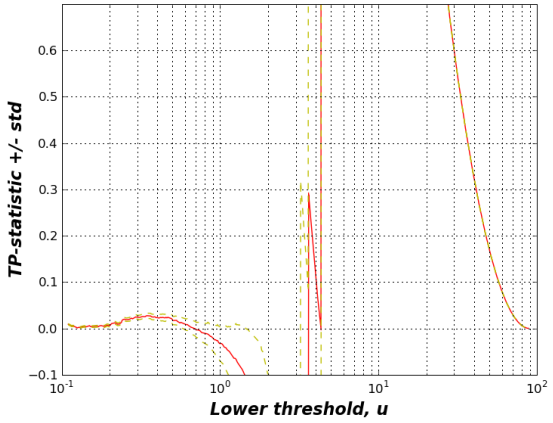

(a) Deutschmark at 1-min scale

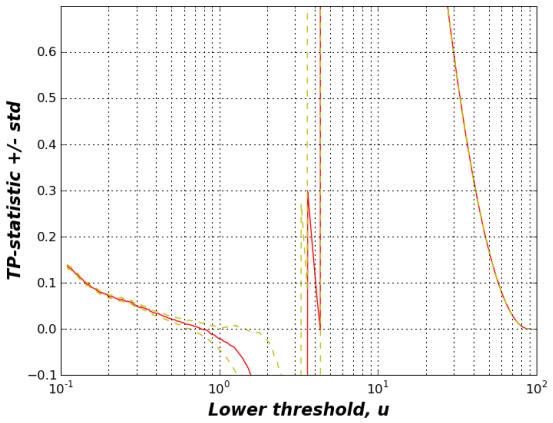

(b) Deutschmark at 15-min scale

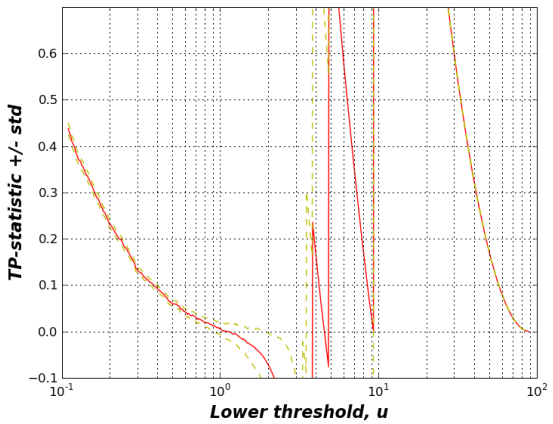

(c) Deutschmark at 1-hour scale

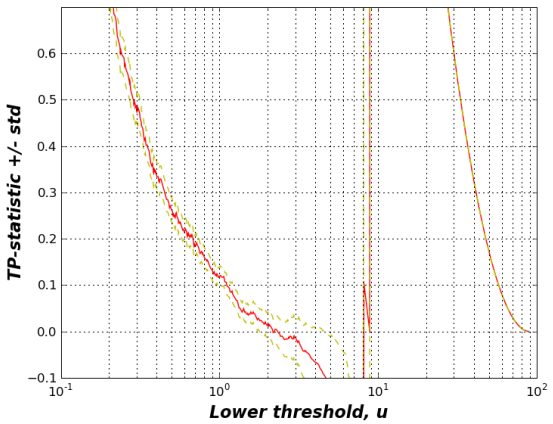

(d) Deutschmark at 1-day scale

Fig. 96: *TP*−statistic (Eq.B.2) as a function of the lower threshold u, applied to the distribution of *pure*-drawdowns of the Deutschmark dataset for each of the studied time scales - from 1-min to 1-day-. The two dashed lines represent plus and minus one standard deviation from the statistic.

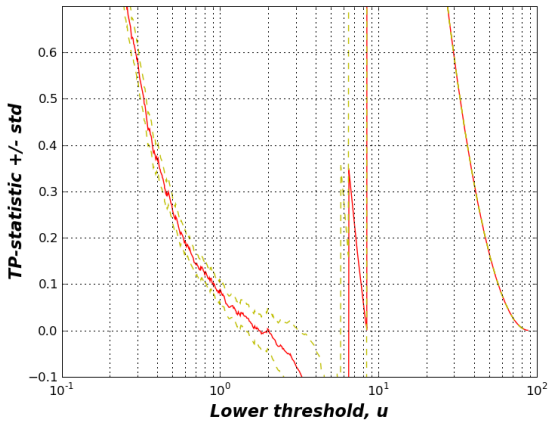

(a) Deutschmark at 1-min scale

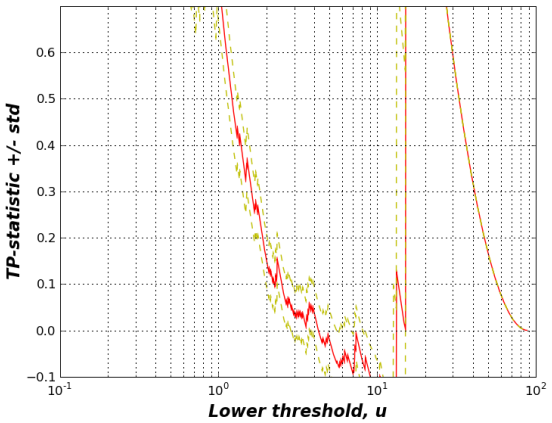

(b) Deutschmark at 15-min scale

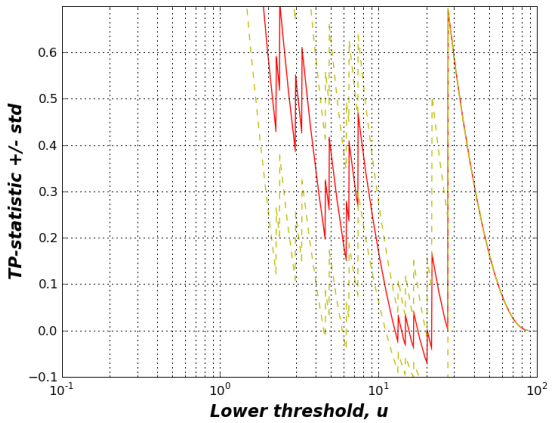

(c) Deutschmark at 1-hour scale

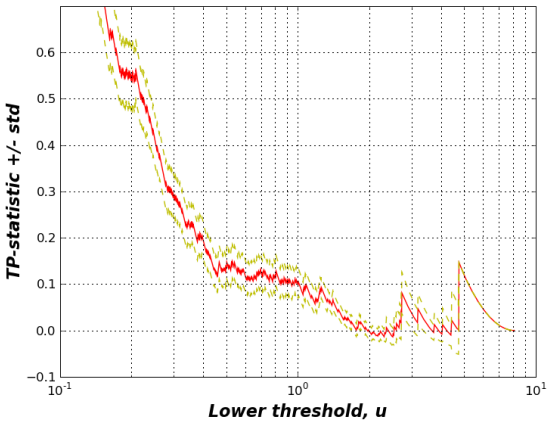

(d) Deutschmark at 1-day scale

Fig. 97: $TP-$statistic (Eq.B.2) as a function of the lower threshold u, applied to the distribution of $\sigma/2$-drawdowns of the Deutschmark dataset for each of the studied time scales - from 1-min to 1-day-. The two dashed lines represent plus and minus one standard deviation from the statistic.

C.3.4.6 Japanese Government Bond

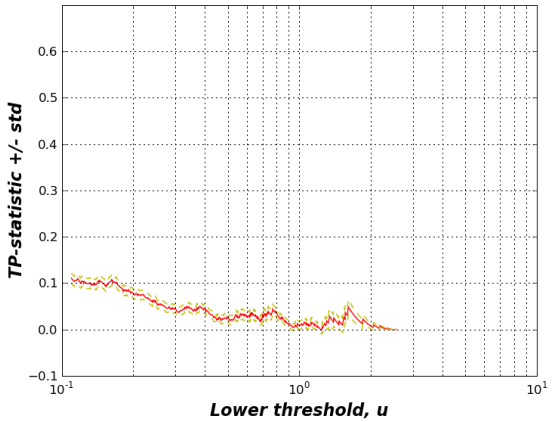

(a) Jap Gov Bonds at 1-min scale

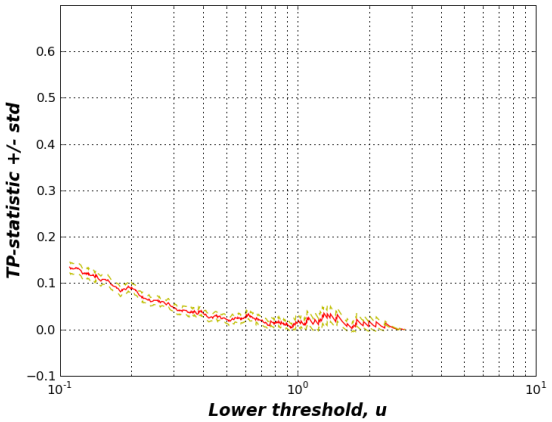

(b) Jap Gov Bonds at 15-min scale

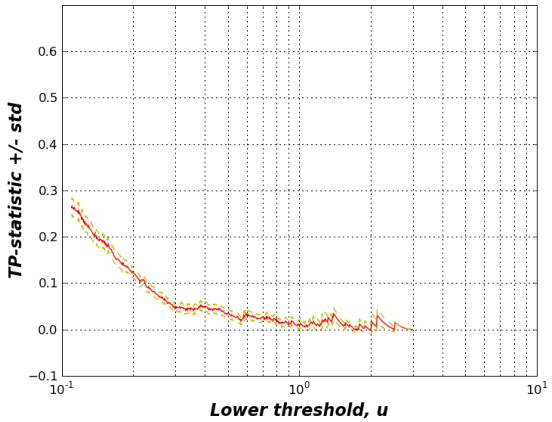

(c) Jap Gov Bonds at 1-hour scale

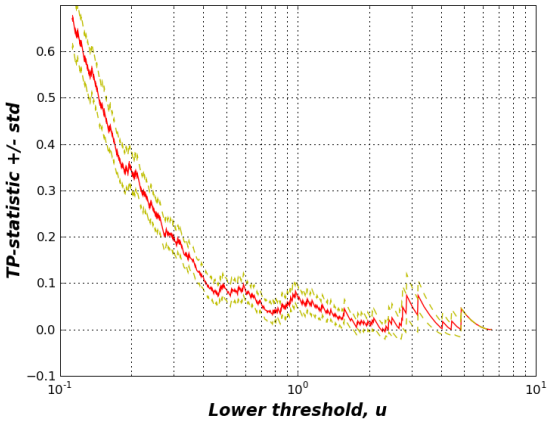

(d) Jap Gov Bonds at 1-day scale

Fig. 98: *TP*−statistic (Eq.B.2) as a function of the lower threshold u, applied to the distribution of *pure*-drawdowns of the Japanese Government Bond dataset for each of the studied time scales - from 1-min to 1-day-. The two dashed lines represent plus and minus one standard deviation from the statistic.

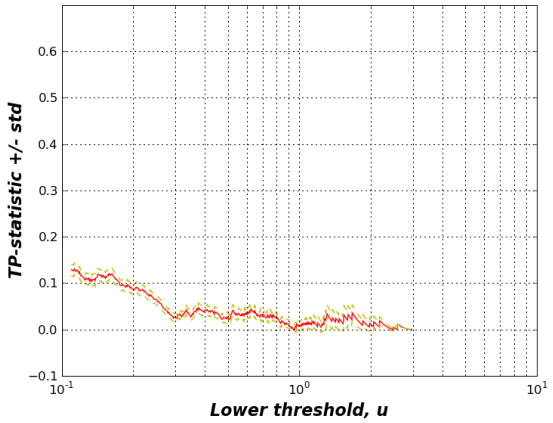

(a) Jap Gov Bonds at 1-min scale

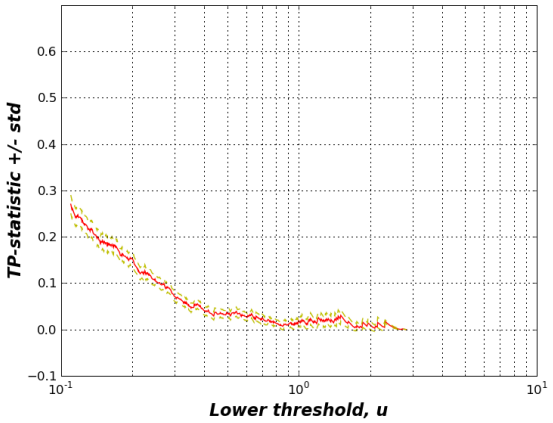

(b) Jap Gov Bonds at 15-min scale

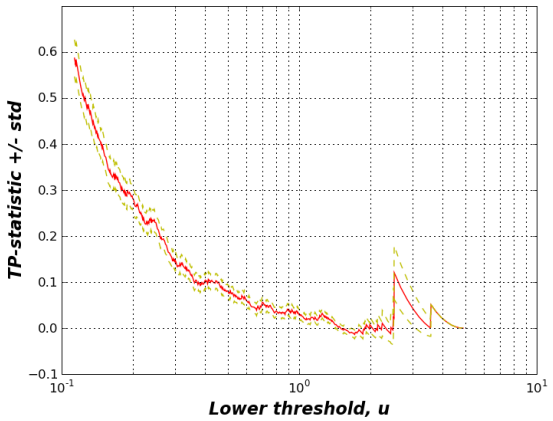

(c) Jap Gov Bonds at 1-hour scale

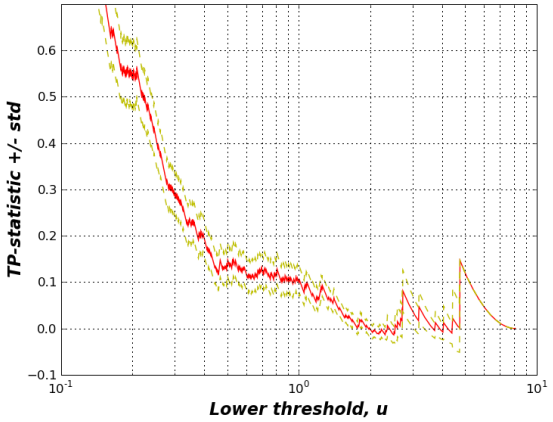

(d) Jap Gov Bonds at 1-day scale

Fig. 99: $TP-$statistic (Eq.B.2) as a function of the lower threshold u, applied to the distribution of $\sigma/2$-drawdowns of the Japanese Government Bond dataset for each of the studied time scales - from 1-min to 1-day-. The two dashed lines represent plus and minus one standard deviation from the statistic.

C.3.4.7 US Treasury Bond I

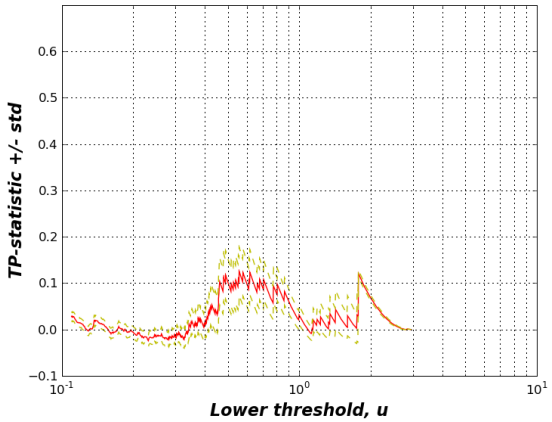

(a) US T-Bonds I at 1-min scale

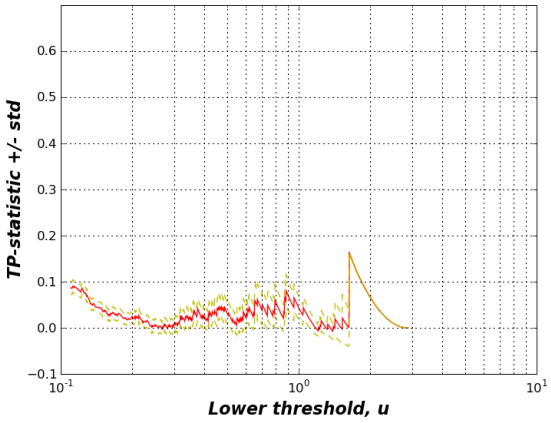

(b) US T-Bonds I at 15-min scale

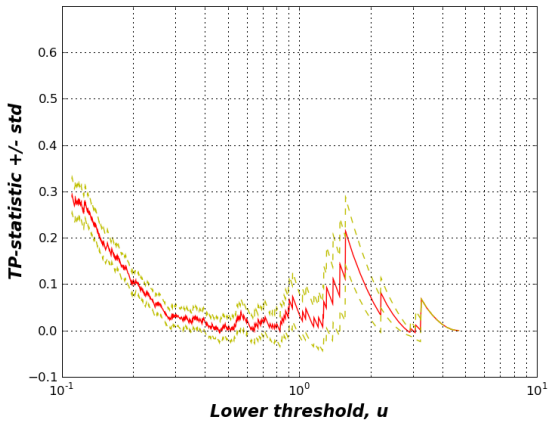

(c) US T-Bonds I at 1-hour scale

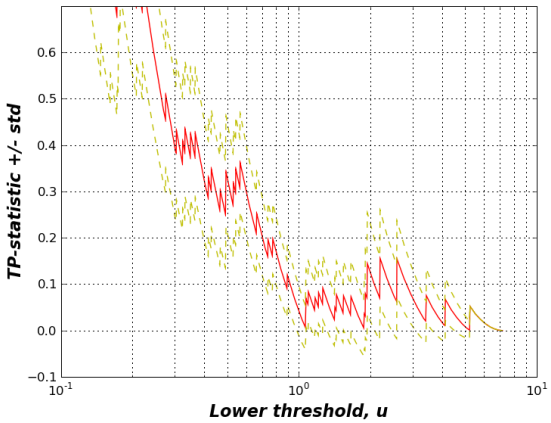

(d) US T-Bonds I at 1-day scale

Fig. 100: $TP-$statistic (Eq.B.2) as a function of the lower threshold u, applied to the distribution of *pure*-drawdowns of the US T-Bonds I dataset for each of the studied time scales - from 1-min to 1-day-. The two dashed lines represent plus and minus one standard deviation from the statistic.

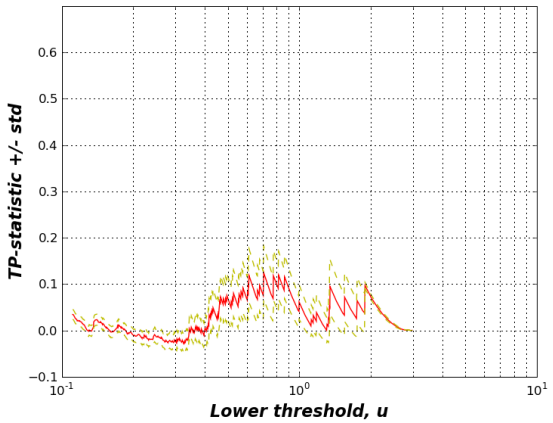

(a) US T-Bonds I at 1-min scale

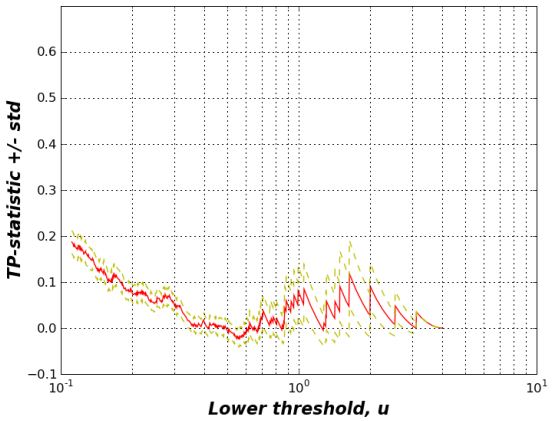

(b) US T-Bonds I at 15-min scale

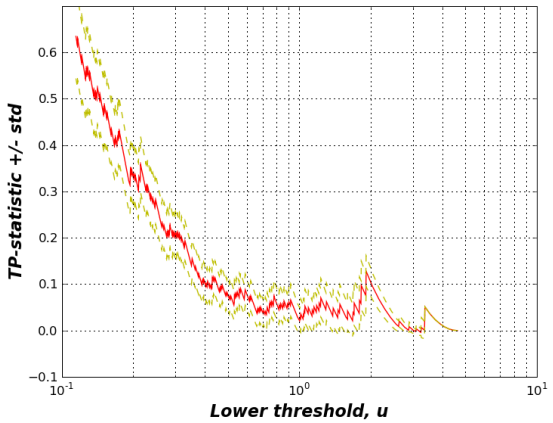

(c) US T-Bonds I at 1-hour scale

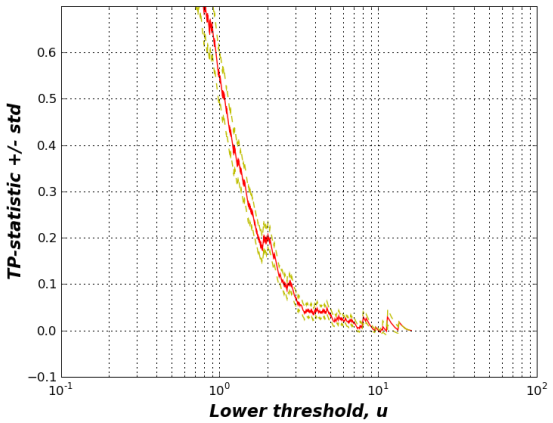

(d) US T-Bonds I at 1-day scale

Fig. 101: $TP-$statistic (Eq.B.2) as a function of the lower threshold u, applied to the distribution of $\sigma/2$-drawdowns of the US T-Bonds I dataset for each of the studied time scales - from 1-min to 1-day-. The two dashed lines represent plus and minus one standard deviation from the statistic.

C.3.4.8 US Treasury Bond III

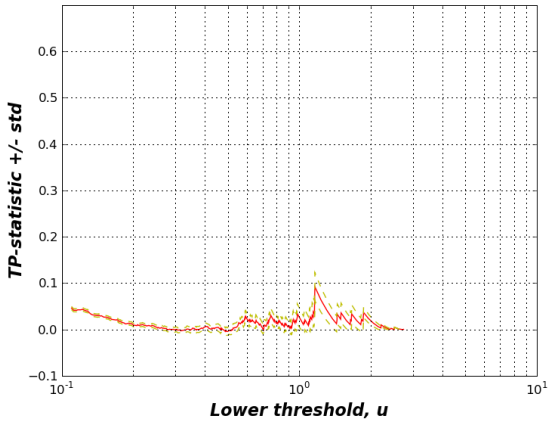

(a) US T-Bonds III at 1-min scale

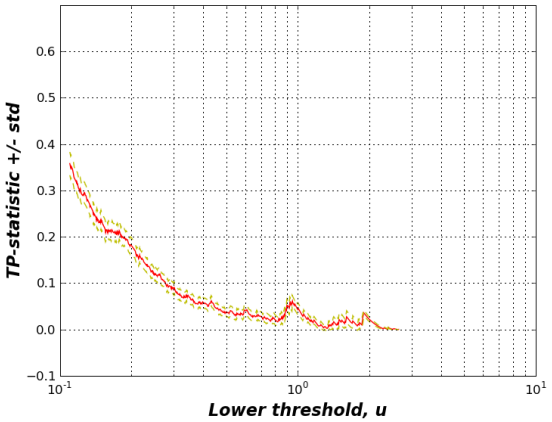

(b) US T-Bonds III at 15-min scale

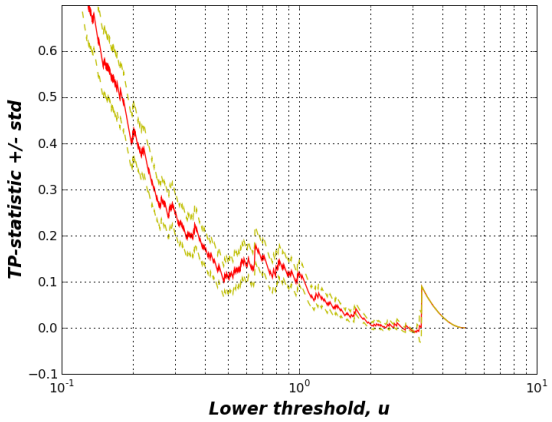

(c) US T-Bonds III at 1-hour scale

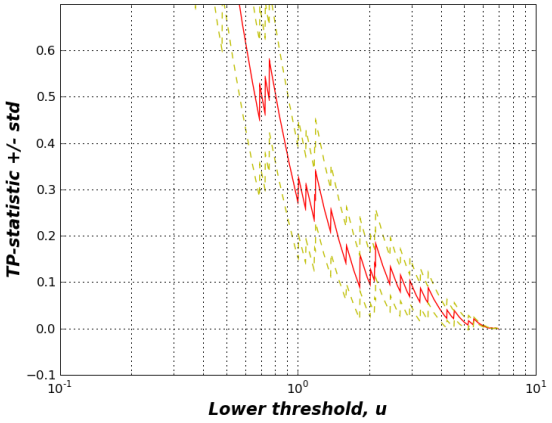

(d) US T-Bonds III at 1-day scale

Fig. 102: $TP-$statistic (Eq.B.2) as a function of the lower threshold u, applied to the distribution of *pure*-drawdowns of the US T-Bonds III dataset for each of the studied time scales - from 1-min to 1-day-. The two dashed lines represent plus and minus one standard deviation from the statistic.

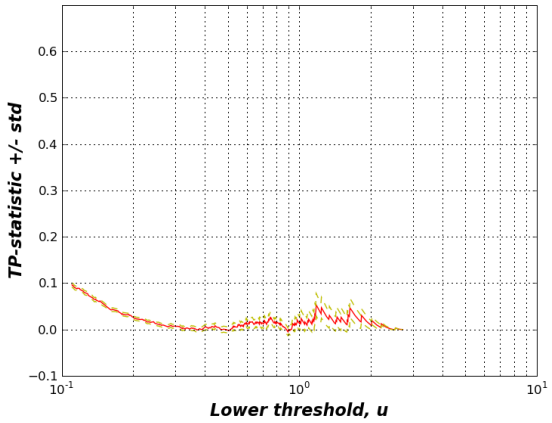

(a) US T-Bonds III at 1-min scale

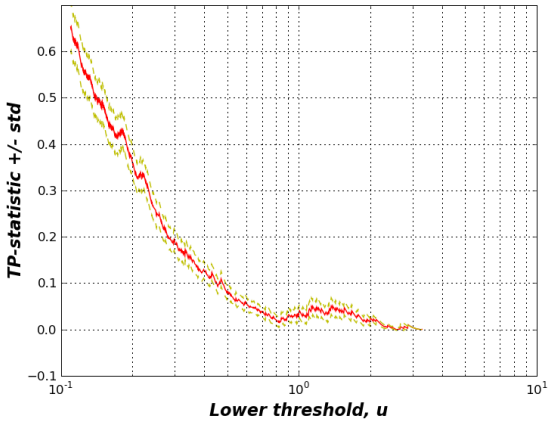

(b) US T-Bonds III at 15-min scale

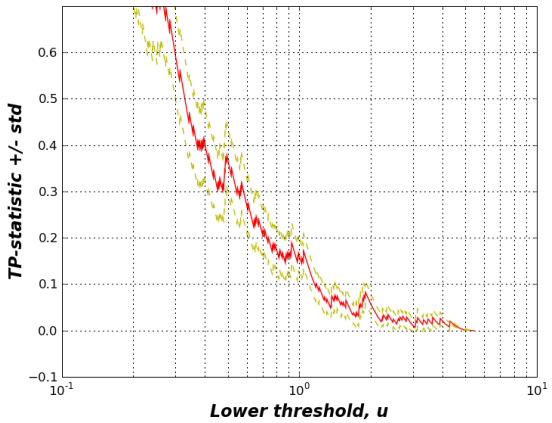

(c) US T-Bonds III at 1-hour scale

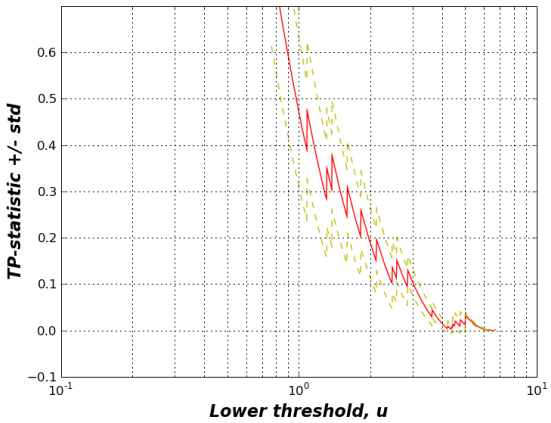

(d) US T-Bonds III at 1-day scale

Fig. 103: $TP-$statistic (Eq.B.2) as a function of the lower threshold u, applied to the distribution of $\sigma/2$-drawdowns of the US T-Bonds III dataset for each of the studied time scales - from 1-min to 1-day-. The two dashed lines represent plus and minus one standard deviation from the statistic.

C.3.4.9 German Government Bond

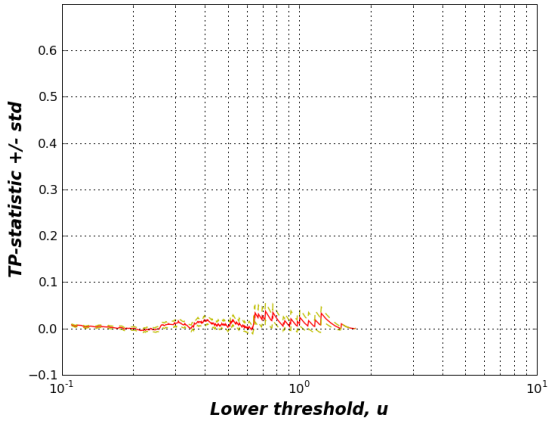

(a) German Gov Bonds at 1-min scale

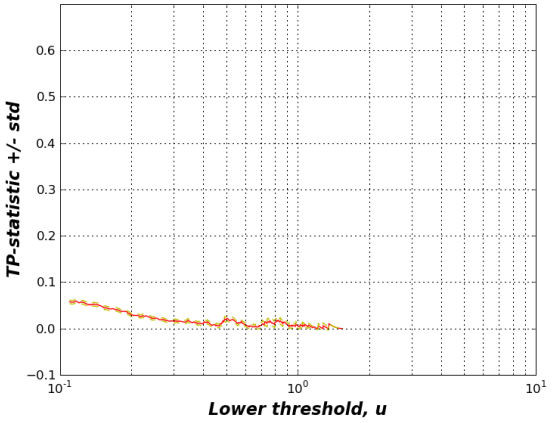

(b) German Gov Bonds at 15-min scale

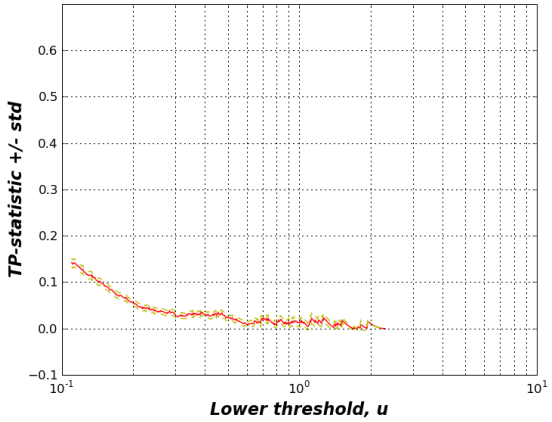

(c) German Gov Bonds at 1-hour scale

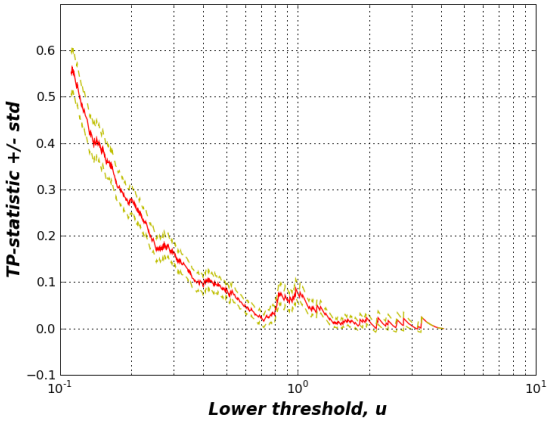

(d) German Gov Bonds at 1-day scale

Fig. 104: *TP*−statistic (Eq.B.2) as a function of the lower threshold u, applied to the distribution of *pure*-drawdowns of the German Government Bond dataset for each of the studied time scales - from 1-min to 1-day-. The two dashed lines represent plus and minus one standard deviation from the statistic.

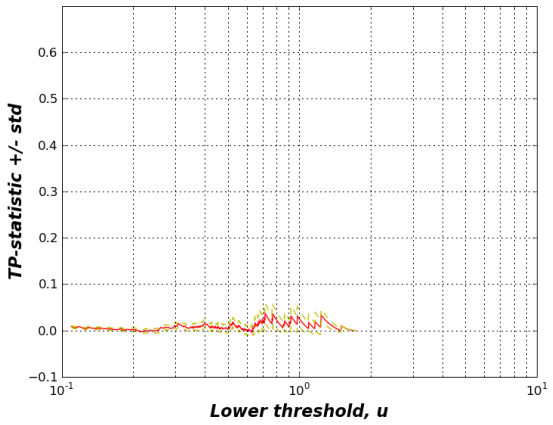

(a) German Gov Bonds at 1-min scale

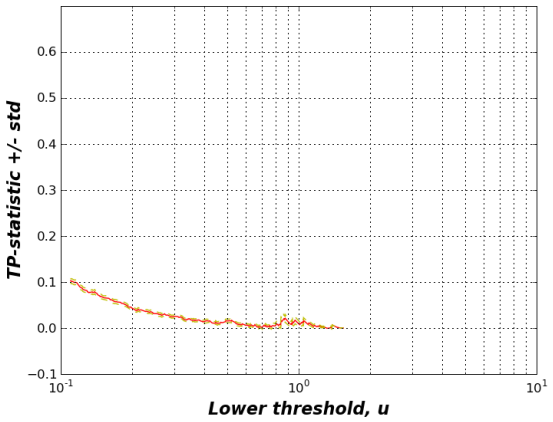

(b) German Gov Bonds at 15-min scale

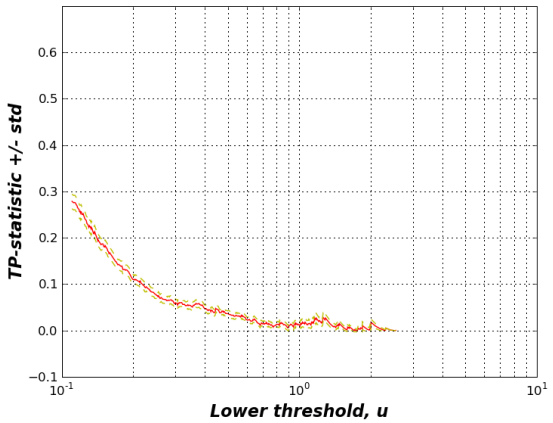

(c) German Gov Bonds at 1-hour scale

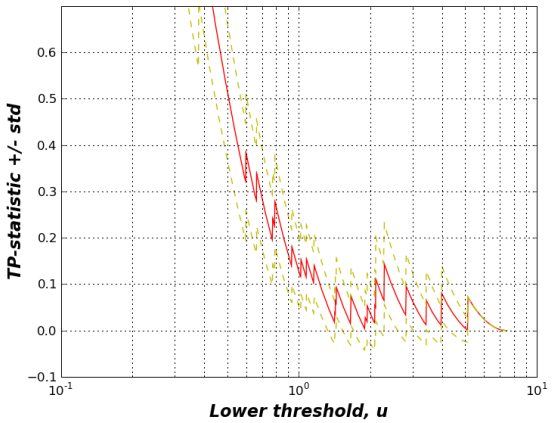

(d) German Gov Bonds at 1-day scale

Fig. 105: $TP-$statistic (Eq.B.2) as a function of the lower threshold u, applied to the distribution of $\sigma/2$-drawdowns of the German Government Bond dataset for each of the studied time scales - from 1-min to 1-day-. The two dashed lines represent plus and minus one standard deviation from the statistic.

C.3.5 Distributions at different scales

C.3.5.1 SP 500

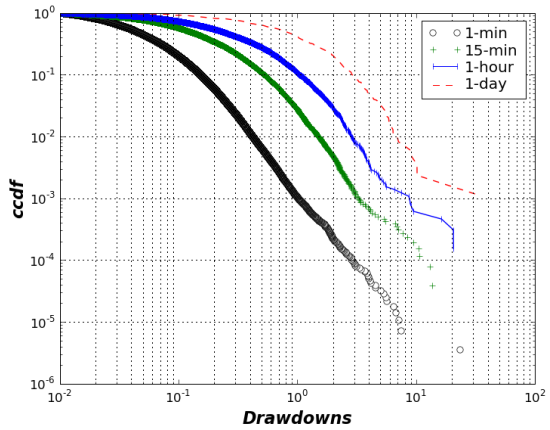

(a) SP 500 *pure*-DD, no normalization

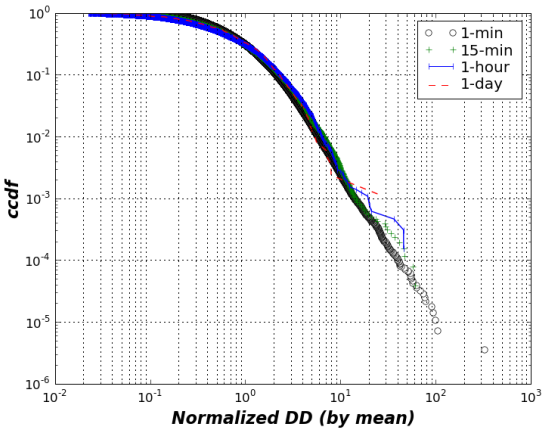

(b) SP 500 *pure*-DD, normalized

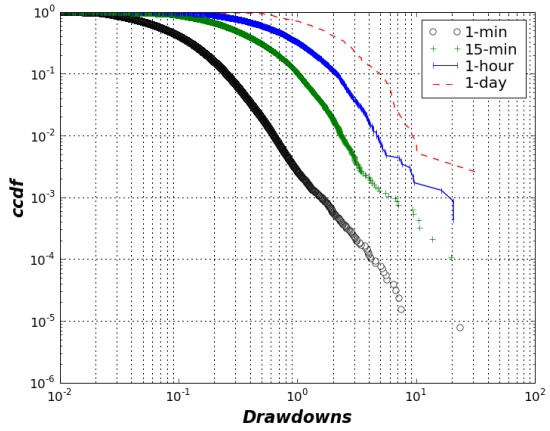

(c) SP 500 $\sigma/2$-DD, no normalization

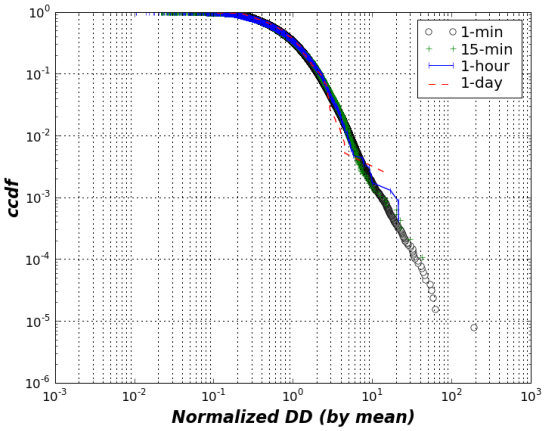

(d) SP 500 $\sigma/2$-DD, normalized

Fig. 106: Distributions of ϵ-drawdown ($\epsilon = 0, \sigma/2$) at all studied scales were collapsed to identify dissident behaviors in the tail. The left panels show the superposed original distributions and the right panels normalize the ϵ-DD by their mean.

C.3.5.2 FTSE 100

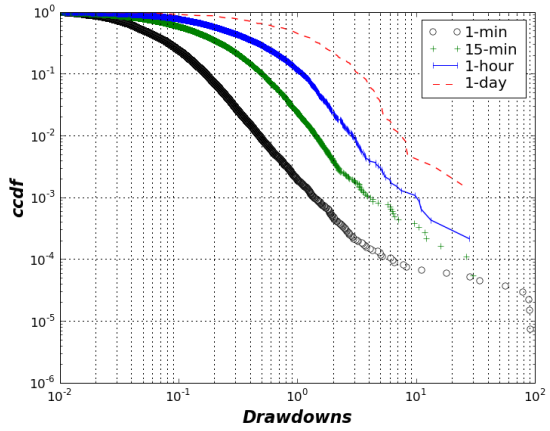

(a) FTSE 100 *pure*-DD, no normalization

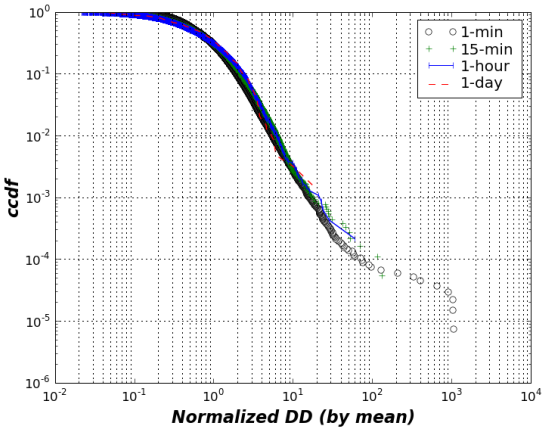

(b) FTSE 100 *pure*-DD, normalized

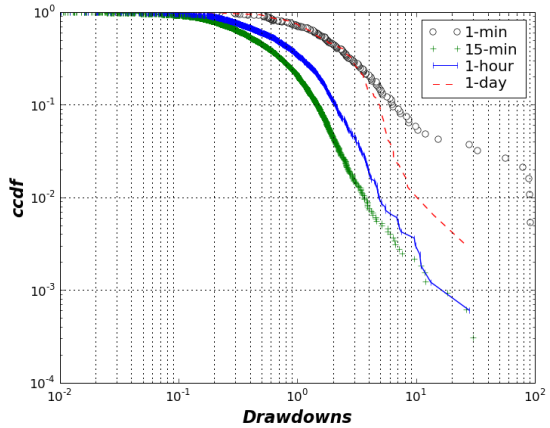

(c) FTSE 100 $\sigma/2$-DD, no normalization

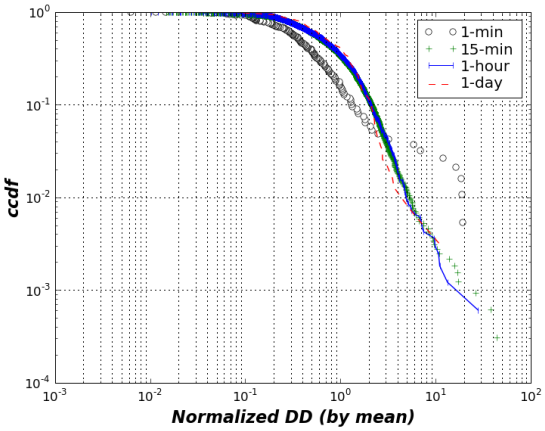

(d) FTSE 100 $\sigma/2$-DD, normalized

Fig. 107: Distributions of ϵ-drawdown ($\epsilon = 0, \sigma/2$) at all studied scales were collapsed to identify dissident behaviors in the tail. The left panels show the superposed original distributions and the right panels normalize the ϵ-DD by their mean.

C.3.5.3 Nikkei 225

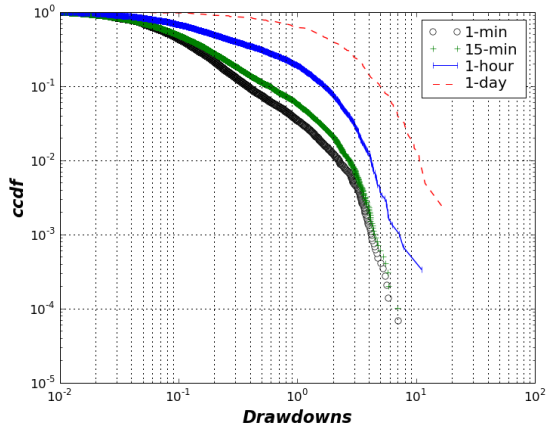

(a) Nikkei 225 *pure*-DD, no normalization

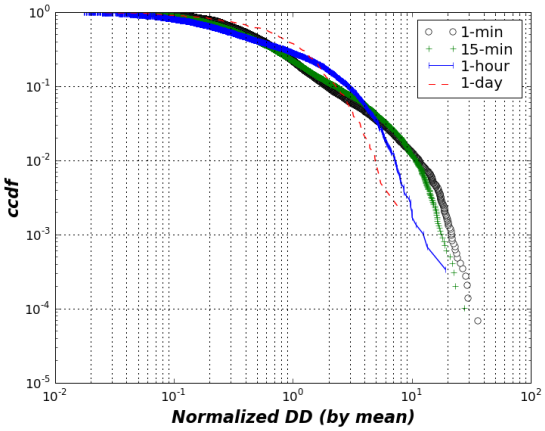

(b) Nikkei 225 *pure*-DD, normalized

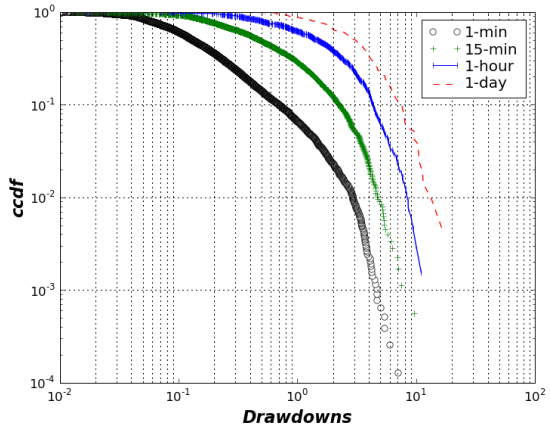

(c) Nikkei 225 $\sigma/2$-DD, no normalization

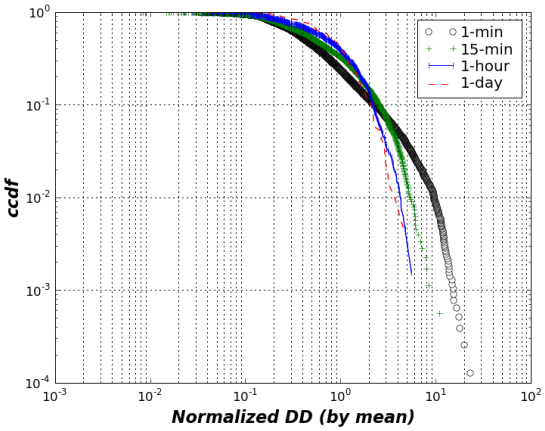

(d) Nikkei 225 $\sigma/2$-DD, normalized

Fig. 108: Distributions of ϵ-drawdown ($\epsilon = 0, \sigma/2$) at all studied scales were collapsed to identify dissident behaviors in the tail. The left panels show the superposed original distributions and the right panels normalize the ϵ-DD by their mean.

C.3.5.4 Japanese Yen

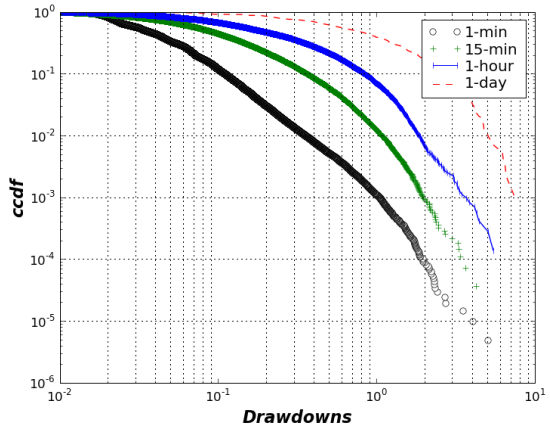

(a) JY *pure*-DD, no normalization

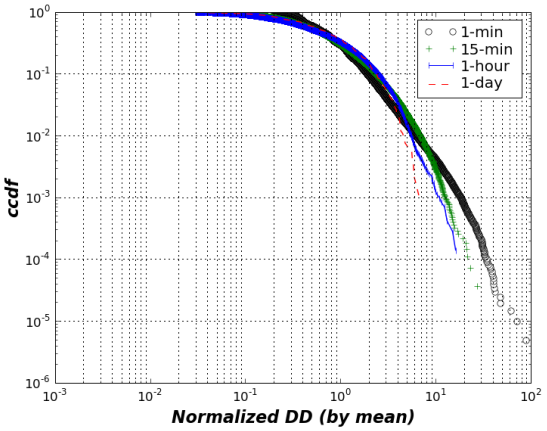

(b) JY *pure*-DD, normalized

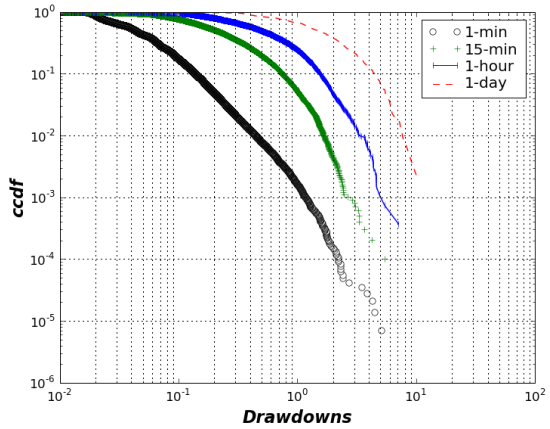

(c) JY $\sigma/2$-DD, no normalization

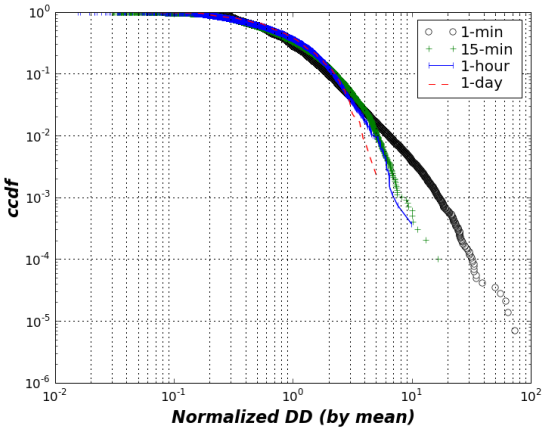

(d) JY $\sigma/2$-DD, normalized

Fig. 109: Distributions of ϵ-drawdown ($\epsilon = 0, \sigma/2$) at all studied scales were collapsed to identify dissident behaviors in the tail. The left panels show the superposed original distributions and the right panels normalize the ϵ-DD by their mean.

C.3.5.5 Deutschmark

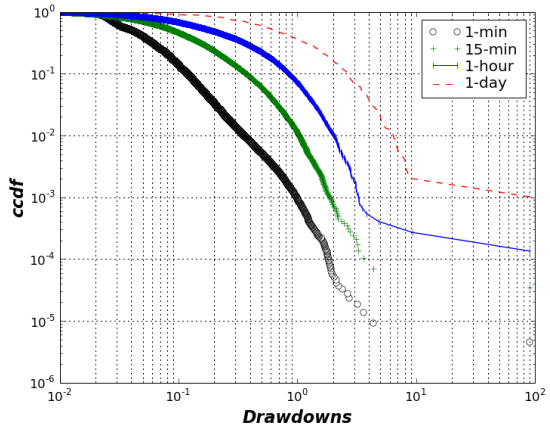

(a) DM *pure*-DD, no normalization

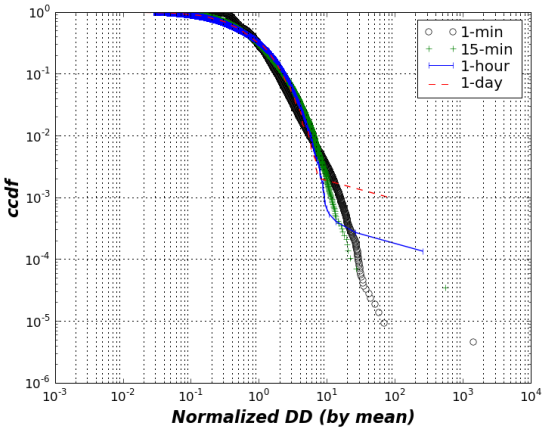

(b) DM *pure*-DD, normalized

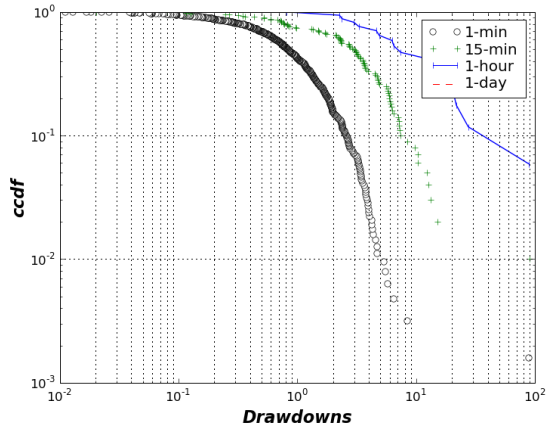

(c) DM $\sigma/2$-DD, no normalization

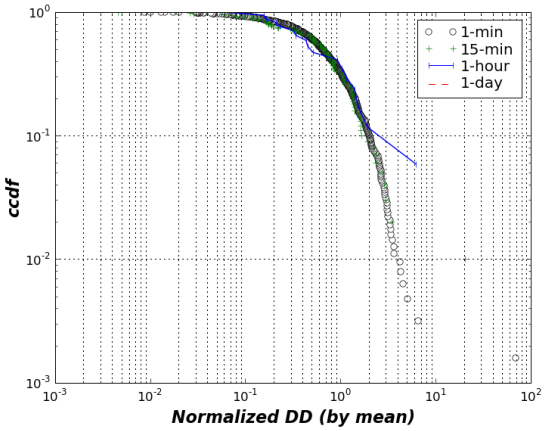

(d) DM $\sigma/2$-DD, normalized

Fig. 110: Distributions of ϵ-drawdown ($\epsilon = 0, \sigma/2$) at all studied scales were collapsed to identify dissident behaviors in the tail. The left panels show the superposed original distributions and the right panels normalize the ϵ-DD by their mean.

C.3.5.6 Japanese Government Bonds

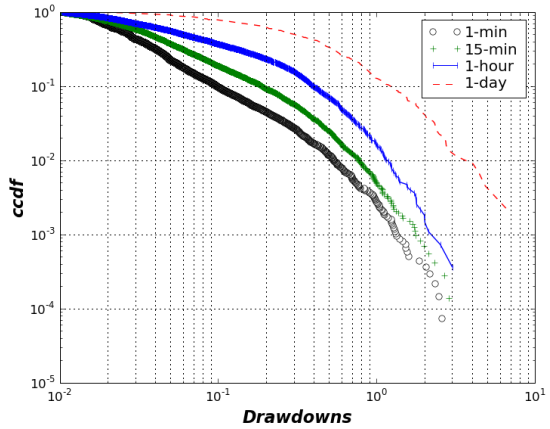

(a) IJ *pure*-DD, no normalization

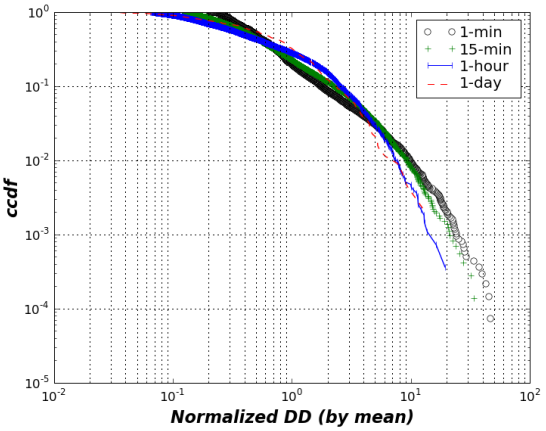

(b) IJ *pure*-DD, normalized

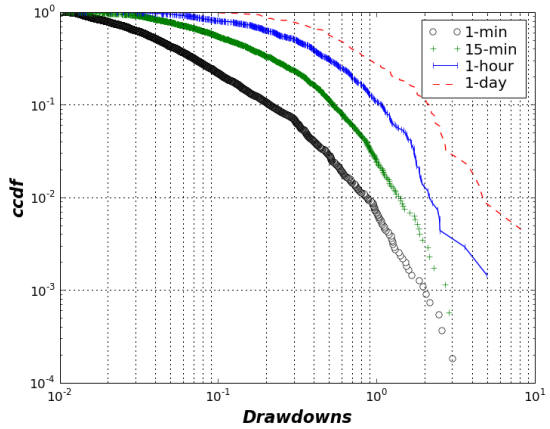

(c) IJ $\sigma/2$-DD, no normalization

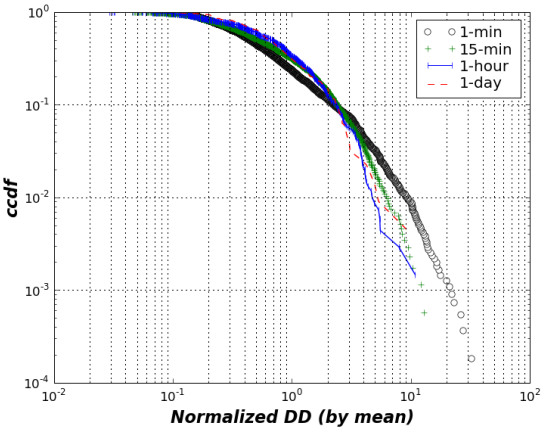

(d) IJ $\sigma/2$-DD, normalized

Fig. 111: Distributions of ϵ-drawdown ($\epsilon = 0, \sigma/2$) at all studied scales were collapsed to identify dissident behaviors in the tail. The left panels show the superposed original distributions and the right panels normalize the ϵ-DD by their mean.

C.3.5.7 US Treasury Bonds I

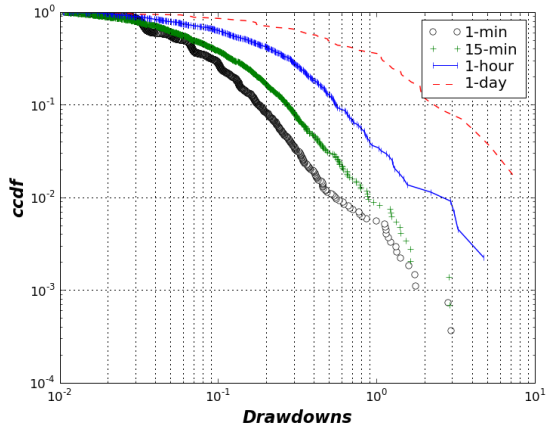

(a) US1 *pure*-DD, no normalization

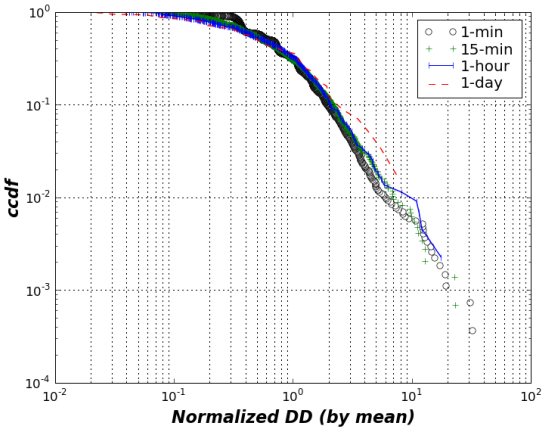

(b) US1 *pure*-DD, normalized

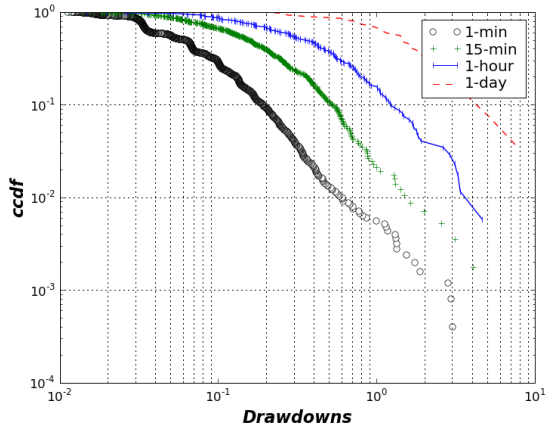

(c) US1 $\sigma/2$-DD, no normalization

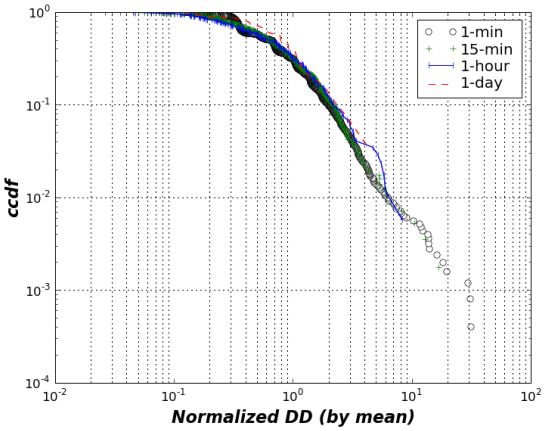

(d) US1 $\sigma/2$-DD, normalized

Fig. 112: Distributions of ϵ-drawdown ($\epsilon = 0, \sigma/2$) at all studied scales were collapsed to identify dissident behaviors in the tail. The left panels show the superposed original distributions and the right panels normalize the ϵ-DD by their mean.

C.3.5.8 US Treasury Bonds III

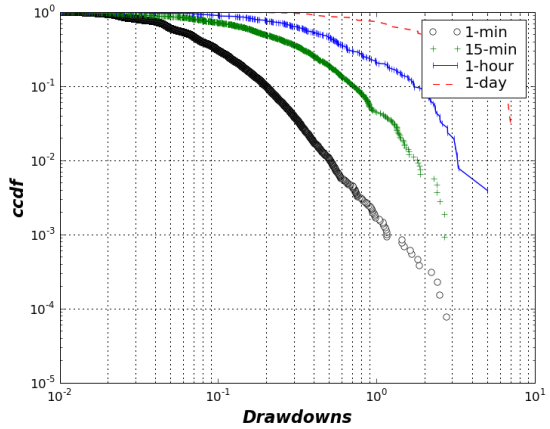

(a) US3 *pure*-DD, no normalization

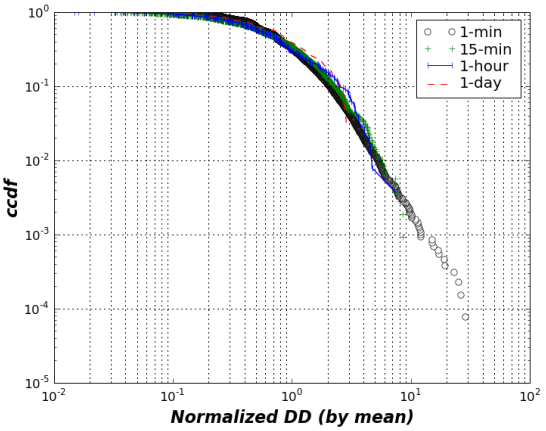

(b) US3 *pure*-DD, normalized

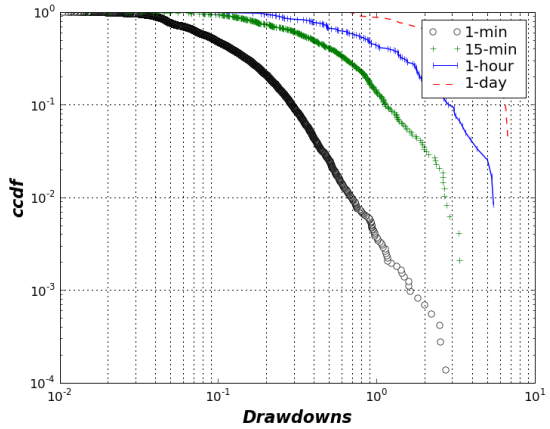

(c) US3 $\sigma/2$-DD, no normalization

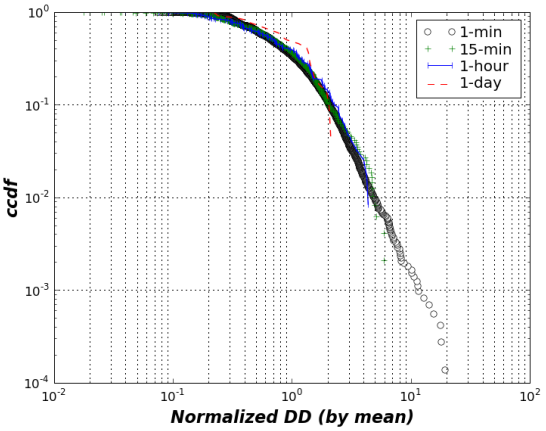

(d) US3 $\sigma/2$-DD, normalized

Fig. 113: Distributions of ϵ-drawdown ($\epsilon = 0, \sigma/2$) at all studied scales were collapsed to identify dissident behaviors in the tail. The left panels show the superposed original distributions and the right panels normalize the ϵ-DD by their mean.

C.3.5.9 German Government Bonds

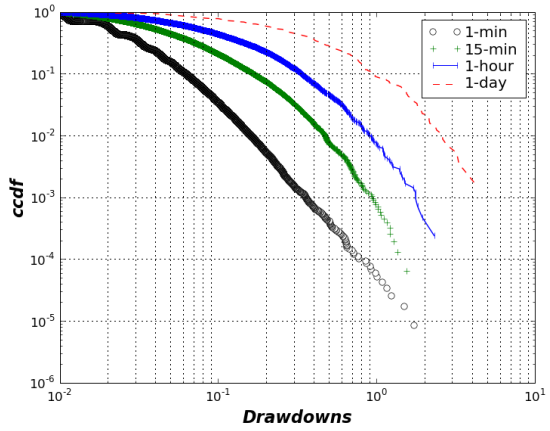

(a) IA *pure*-DD, no normalization

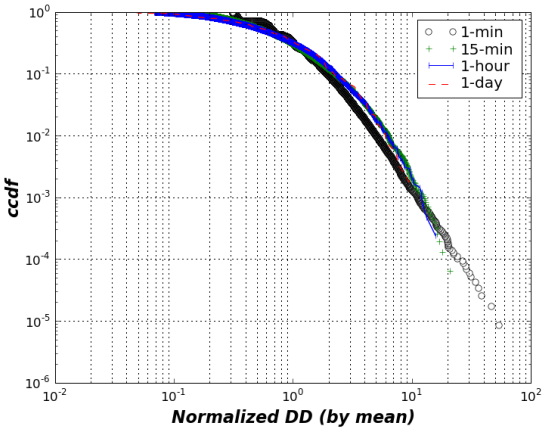

(b) IA *pure*-DD, normalized

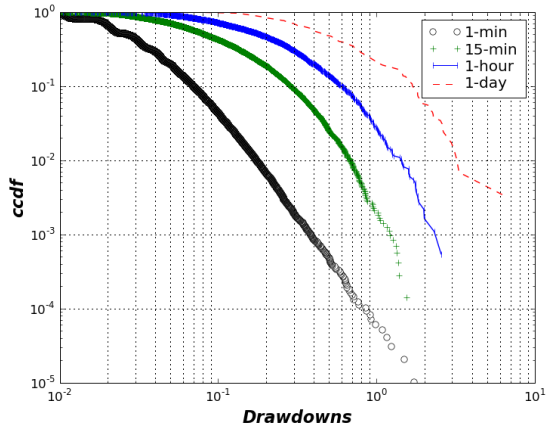

(c) IA $\sigma/2$-DD, no normalization

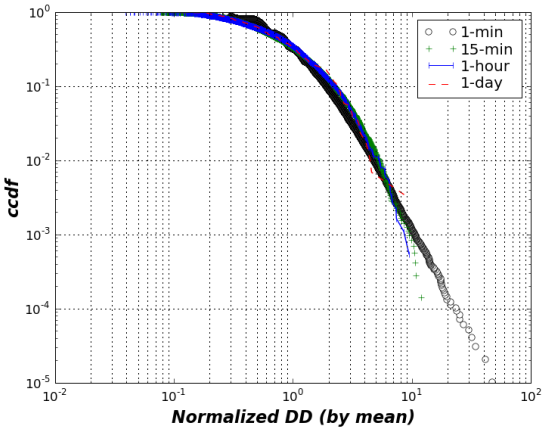

(d) IA $\sigma/2$-DD, normalized

Fig. 114: Distributions of ϵ-drawdown ($\epsilon = 0, \sigma/2$) at all studied scales were collapsed to identify dissident behaviors in the tail. The left panels show the superposed original distributions and the right panels normalize the ϵ-DD by their mean.

C.3.6 Maximum Likelihood Analysis

C.3.6.1 SP 500

	$\epsilon = 0.0$					$\epsilon = \sigma/2$				
Scales	$\mathbf{P}_{80}$	$\mathbf{P}_{90}$	$\mathbf{P}_{95}$	$\mathbf{P}_{99}$	$\mathbf{P}_{99.5}$	$\mathbf{P}_{80}$	$\mathbf{P}_{90}$	$\mathbf{P}_{95}$	$\mathbf{P}_{99}$	$\mathbf{P}_{99.5}$
1-min	2160	0.00	0.00	940.52	1734.12	NA	NA	NA	NA	NA
15-min	14.34	48.13	102.05	242.25	299.84	25.99	63.58	92.20	170.94	193.03
1-hour	6.90	15.29	21.64	51.58	56.90	6.57	14.40	23.88	38.02	43.66
1-day	1.22	2.07	2.56	5.50	5.76	1.33	1.93	5.08	6.38	NA

Tab. 5: SP 500, T-values (defined as Eq.4.5) resulting from comparing the two competing candidates (SE and MSE) at different fraction 'quantiles' of the ϵ-DD belonging to [0,u] for each of the studied scales. Results for ϵ-DD are obtained for $\epsilon = 0.0$ and $\epsilon = \sigma/2$. "NA" indicates a very poor fit of both candidates distributions, hence, rendering the test indecisive. "T=0.00" indicates that the maximization algorithm found that the additional term "C" does not improve the fit in any way.

C.3.6.2 FTSE 100

	$\epsilon = 0.0$					$\epsilon = \sigma/2$				
Scales	$\mathbf{P}_{80}$	$\mathbf{P}_{90}$	$\mathbf{P}_{95}$	$\mathbf{P}_{99}$	$\mathbf{P}_{99.5}$	$\mathbf{P}_{80}$	$\mathbf{P}_{90}$	$\mathbf{P}_{95}$	$\mathbf{P}_{99}$	$\mathbf{P}_{99.5}$
1-min	NA	NA	NA	NA	21700	0.03	1.03	2.66	2.07	2.07
15-min	0.00	8.17	0.00	10.64	44.08	4.41	9.75	16.88	28.87	42.57
1-hour	2.45	9.91	20.81	27.03	35.76	5.68	8.38	9.87	22.69	26.28
1-day	0.81	1.51	2.55	2.59	3.22	1.13	1.10	1.87	0.00	0.00

Tab. 6: FTSE 100, T-values (defined as Eq.4.5) resulting from comparing the two competing candidates (SE and MSE) at different fraction 'quantiles' of the ϵ-DD belonging to $[0,u]$ for each of the studied scales. Results for ϵ-DD are obtained for $\epsilon = 0.0$ and $\epsilon = \sigma/2$. "NA" indicates a very poor fit of both candidates distributions, hence, rendering the test indecisive. "T=0.00" indicates that the maximization algorithm found that the additional term "C" does not improve the fit in any way.

C.3.6.3 Nikkei 225

	$\epsilon = 0.0$					$\epsilon = \sigma/2$				
Scales	$\mathbf{P}_{80}$	$\mathbf{P}_{90}$	$\mathbf{P}_{95}$	$\mathbf{P}_{99}$	$\mathbf{P}_{99.5}$	$\mathbf{P}_{80}$	$\mathbf{P}_{90}$	$\mathbf{P}_{95}$	$\mathbf{P}_{99}$	$\mathbf{P}_{99.5}$
1-min	NA	663	611	0.00	0.00	0.18	48.64	151.11	302.18	331.33
15-min	87.70	0.00	45.73	241.84	278.94	7.59	13.14	18.73	27.07	27.82
1-hour	16.34	29.40	36.46	42.79	43.97	1.51	2.18	1.99	1.47	1.94
1-day	0.31	0.47	0.24	0.87	1.35	NA	NA	NA	NA	NA

Tab. 7: Nikkei 225, T-values (defined as Eq.4.5) resulting from comparing the two competing candidates (SE and MSE) at different fraction 'quantiles' of the ϵ-DD belonging to [0,u] for each of the studied scales. Results for ϵ-DD are obtained for $\epsilon = 0.0$ and $\epsilon = \sigma/2$. "NA" indicates a very poor fit of both candidates distributions, hence, rendering the test indecisive. "T=0.00" indicates that the maximization algorithm found that the additional term "C" does not improve the fit in any way.

C.3.6.4 Japanese Yen

	$\epsilon = 0.0$					$\epsilon = \sigma/2$				
Scales	$\mathbf{P}_{80}$	$\mathbf{P}_{90}$	$\mathbf{P}_{95}$	$\mathbf{P}_{99}$	$\mathbf{P}_{99.5}$	$\mathbf{P}_{80}$	$\mathbf{P}_{90}$	$\mathbf{P}_{95}$	$\mathbf{P}_{99}$	$\mathbf{P}_{99.5}$
1-min	NA	NA	NA	NA	NA	NA	NA	NA	NA	NA
15-min	11.12	0.47	69.83	305.27	382.69	39.67	79.45	115.95	191.77	209.33
1-hour	10.81	21.35	32.62	48.54	49.08	10.23	14.52	18.27	23.81	31.13
1-day	1.46	2.73	3.73	5.74	4.71	0.03	0.74	1.95	2.60	2.48

Tab. 8: Japanese Yen, T-values (defined as Eq.4.5) resulting from comparing the two competing candidates (SE and MSE) at different fraction 'quantiles' of the ϵ-DD belonging to [0,u] for each of the studied scales. Results for ϵ-DD are obtained for $\epsilon = 0.0$ and $\epsilon = \sigma/2$. "NA" indicates a very poor fit of both candidates distributions, hence, rendering the test indecisive. "T=0.00" indicates that the maximization algorithm found that the additional term "C" does not improve the fit in any way.

C.3.6.5 Deutschmark

	$\epsilon = 0.0$					$\epsilon = \sigma/2$				
Scales	$\mathbf{P}_{80}$	$\mathbf{P}_{90}$	$\mathbf{P}_{95}$	$\mathbf{P}_{99}$	$\mathbf{P}_{99.5}$	$\mathbf{P}_{80}$	$\mathbf{P}_{90}$	$\mathbf{P}_{95}$	$\mathbf{P}_{99}$	$\mathbf{P}_{99.5}$
1-min	NA	NA	NA	NA	NA	1.14	0.00	0.67	0.80	0.84
15-min	92.64	0.00	17.21	221.82	292.27	NA	NA	NA	NA	NA
1-hour	5.22	13.89	21.22	27.02	29.03	NA	NA	NA	NA	NA
1-day	0.75	2.21	3.08	5.49	6.89	NA	NA	NA	NA	NA

Tab. 9: Deutschmark, T-values (defined as Eq.4.5) resulting from comparing the two competing candidates (SE and MSE) at different fraction 'quantiles' of the ϵ-DD belonging to [0,u] for each of the studied scales. Results for ϵ-DD are obtained for $\epsilon = 0.0$ and $\epsilon = \sigma/2$. "NA" indicates a very poor fit of both candidates distributions, hence, rendering the test indecisive. "T=0.00" indicates that the maximization algorithm found that the additional term "C" does not improve the fit in any way.

C.3.6.6 Japanese Government Bonds

	$\epsilon = 0.0$					$\epsilon = \sigma/2$				
Scales	$\mathbf{P}_{80}$	$\mathbf{P}_{90}$	$\mathbf{P}_{95}$	$\mathbf{P}_{99}$	$\mathbf{P}_{99.5}$	$\mathbf{P}_{80}$	$\mathbf{P}_{90}$	$\mathbf{P}_{95}$	$\mathbf{P}_{99}$	$\mathbf{P}_{99.5}$
1-min	NA	NA	NA	NA	NA	0.00	15.16	89.50	186.06	209.20
15-min	NA	NA	578.43	0.00	0.00	5.13	12.82	16.38	25.45	26.90
1-hour	0.34	17.70	23.13	33.37	35.91	1.74	2.64	3.96	8.97	9.59
1-day	0.17	0.61	0.63	2.87	4.87	0.49	2.96	3.76	5.15	6.79

Tab. 10: Japanese Government Bonds, T-values (defined as Eq.4.5) resulting from comparing the two competing candidates (SE and MSE) at different fraction 'quantiles' of the ϵ-DD belonging to [0,u] for each of the studied scales. Results for ϵ-DD are obtained for $\epsilon = 0.0$ and $\epsilon = \sigma/2$. "NA" indicates a very poor fit of both candidates distributions, hence, rendering the test indecisive. "T=0.00" indicates that the maximization algorithm found that the additional term "C" does not improve the fit in any way.

C.3.6.7 US Treasury Bonds I

	$\epsilon = 0.0$					$\epsilon = \sigma/2$				
Scales	$\mathbf{P}_{80}$	$\mathbf{P}_{90}$	$\mathbf{P}_{95}$	$\mathbf{P}_{99}$	$\mathbf{P}_{99.5}$	$\mathbf{P}_{80}$	$\mathbf{P}_{90}$	$\mathbf{P}_{95}$	$\mathbf{P}_{99}$	$\mathbf{P}_{99.5}$
1-min	0.00	0.00	185.22	0.00	0.00	18.61	0.00	7.10	39.64	55.44
15-min	16.48	17.49	0.59	0.00	1.45	1.32	3.92	6.42	13.42	20.39
1-hour	0.54	0.68	0.21	3.85	8.67	0.37	0.76	1.55	5.00	5.00
1-day	0.21	0.24	0.67	0.67	0.67	0.00	0.43	0.87	0.87	0.87

Tab. 11: US Treasury Bonds I, T-values (defined as Eq.4.5) resulting from comparing the two competing candidates (SE and MSE) at different fraction 'quantiles' of the ϵ-DD belonging to [0,u] for each of the studied scales. Results for ϵ-DD are obtained for $\epsilon = 0.0$ and $\epsilon = \sigma/2$. "NA" indicates a very poor fit of both candidates distributions, hence, rendering the test indecisive. "T=0.00" indicates that the maximization algorithm found that the additional term "C" does not improve the fit in any way.

C.3.6.8 US Treasury Bonds III

	$\epsilon = 0.0$					$\epsilon = \sigma/2$				
Scales	$\mathbf{P}_{80}$	$\mathbf{P}_{90}$	$\mathbf{P}_{95}$	$\mathbf{P}_{99}$	$\mathbf{P}_{99.5}$	$\mathbf{P}_{80}$	$\mathbf{P}_{90}$	$\mathbf{P}_{95}$	$\mathbf{P}_{99}$	$\mathbf{P}_{99.5}$
1-min	NA	515.45	589.34	0.00	0.00	27.35	53.26	78.66	136.98	170.27
15-min	0.10	0.40	2.41	5.56	8.88	1.11	1.70	1.55	9.65	10.39
1-hour	0.42	2.14	3.42	4.36	3.57	0.66	0.99	1.33	2.19	2.19
1-day	0.12	0.22	0.23	0.23	0.23	NA	NA	NA	NA	NA

Tab. 12: US Treasury Bonds III, T-values (defined as Eq.4.5) resulting from comparing the two competing candidates (SE and MSE) at different fraction 'quantiles' of the ϵ-DD belonging to [0,u] for each of the studied scales. Results for ϵ-DD are obtained for $\epsilon = 0.0$ and $\epsilon = \sigma/2$. "NA" indicates a very poor fit of both candidates distributions, hence, rendering the test indecisive. "T=0.00" indicates that the maximization algorithm found that the additional term "C" does not improve the fit in any way.

C.3.6.9 German Government Bonds

	$\epsilon = 0.0$					$\epsilon = \sigma/2$				
Scales	$\mathbf{P}_{80}$	$\mathbf{P}_{90}$	$\mathbf{P}_{95}$	$\mathbf{P}_{99}$	$\mathbf{P}_{99.5}$	$\mathbf{P}_{80}$	$\mathbf{P}_{90}$	$\mathbf{P}_{95}$	$\mathbf{P}_{99}$	$\mathbf{P}_{99.5}$
1-min	NA	NA	NA	NA	NA	NA	NA	NA	NA	NA
15-min	0.00	10.48	65.56	212.27	255.88	28.83	63.95	95.36	156.47	173.79
1-hour	2.74	10.22	15.56	32.41	41.68	7.39	13.34	23.17	35.67	40.84
1-day	0.57	1.39	1.22	5.98	7.10	2.25	5.79	6.37	8.16	8.18

Tab. 13: German Government Bonds, T-values (defined as Eq.4.5) resulting from comparing the two competing candidates (SE and MSE) at different fraction 'quantiles' of the ϵ-DD belonging to [0,u] for each of the studied scales. Results for ϵ-DD are obtained for $\epsilon = 0.0$ and $\epsilon = \sigma/2$. "NA" indicates a very poor fit of both candidates distributions, hence, rendering the test indecisive. "T=0.00" indicates that the maximization algorithm found that the additional term "C" does not improve the fit in any way.

List of Tables

List of Figures

Abbreviations

PL	Power Law
bp	basis points or %,,
ODF	Outlier Detection Filter
CCDF	Complementary Cumulative Distribution Function
CDF	Cumulative Distribution Function
DK	Dragon-Kings
PDF	Probability Density Function
SE	Stretched Exponential
T-Bonds	Treasury Bonds
J&S	Johansen and Sornette
DD	Drawdown
GARCH	Generalized Autoregressive Conditional Heteroscedasticity
MLE	Maximum Likelihood Estimator
MSE	Modified Stretched Exponential
NA	Not Available
std	standard deviation
S&P	Standard and Poor's
FT-SE	Financial Times - London Stock Exchange
iid	Independent and identically distributed
DJIA	Dow Jones Industrial Average

Bibliography

[1] Amaral, L. A., et al. The distribution of returns of stock prices. *International Journal of Theoretical and Applied Finance 3*, 3 (2000).

[2] Bachelier, L. *Théorie de la spéculation*. PhD thesis, École Normale Supérieure, 1900.

[3] Bak, P. How Nature Works: the Science of Self-organized Criticality. *Copernicus*, 49 (1996).

[4] Barndorff-Nielsen, O., and Cox, D. Inference and Asymptotics, 1995.

[5] Bouchaud, J.-P., and Potters, M. *Theory of Financial Risks: From Statistical Physics to Risk Management*. Cambridge University Press, Cambridge, 2000.

[6] Clauset, A., Shalizi, C., and Newman, M. Power-law distributions in empirical data, 2007. `http://www.citebase.org/abstract?id=oai:arXiv.org:0706.1062`.

[7] Eguiluz, V. M., and Zimmermann, M. G. Transmission of Information and Herd Behavior: An Application to Financial Markets. *Physical Review Letters 85*, 26 (2000).

[8] Gopikrishnan, P., Meyer, M., Amaral, L. A., and Stanley, H. E. Inverse cubic law for the distribution of stock price variations. *The Eur. Phys. Journal B* (1998), 139 – 140.

[9] Hsieh, D. Testing for nonlinear dependence in daily foreign exchange rates. *Journal of Business*, 62 (1989), 339–368.

[10] Johansen, A., and Sornette, D. Stock market Crashes are Outliers. *European Physical Journal B*, 1 (1998), 141–143.

[11] Johansen, A., and Sornette, D. Large stock market price drawdowns are Outliers. *Journal of Risk 4*, 2 (2001), 69–110. `arXiv.org/abs/cond-mat/0010050`.

[12] Johansen, A., and Sornette, D. Shocks, Crashes and Bubbles in Financial Markets. *Brussels Economic Review (Cahiers economiques de Bruxelles)*, 49 (2006), 3/4. http://arXiv.org/abs/cond-mat/0210509.

[13] Laherrere, J., and Sornette, D. Stretched exponential distributions in nature and economy: Fat tails with characteristic scales. *European Physical Journal B*, 2 (1999), 525 – 539.

[14] Le Bris, D. What is a Stock Market Crash? 20 French Crashes since 1854. electroniccopyavailableat:http://ssrn.com/abstract=1328305, September 2009.

[15] Lee, M. Conversion of Time in Financial Data and the handling of Tick Data, 1999.

[16] L'vov, V., Pomyalov, A., and Procaccia, I. Outliers, Extreme Events and Multiscaling. *Physical Review E 6305*, 5 (2001), 158–166.

[17] Malevergne, Y., Pisarenko, V., and Sornette, D. Gibrat's law for cities: uniformly most powerful unbiased test of the pareto against the lognormal. Letter.

[18] Malevergne, Y., Pisarenko, V., and Sornette, D. Empirical Distributions of Log-Returns: between the Stretched Exponential and the Power Law? *Quantitative Finance 5*, 4 (2005), 379–401.

[19] Mitzenmacher, M. A Brief History of Generative Models for Power Law and Lognormal Distributions.

[20] Newman, M. Power laws, Pareto distributions and Zipf's law, 2005.

[21] Osorio, I., Frei, M., Sornette, D., and Milton, J. Pharmaco-resistant seizures: Self-triggering capacity, Scale-free properties and Predictability? *European Journal of Neuroscience 30* (2009), 1554–1558.

[22] Pisarenko, V., and Sornette, D. New statistic for financial return distributions: Power-law or exponential? *Physica A 366*, 387 - 400 (2006).

[23] Press, W., et al. Numerical recipes in C: The Art of Scientific Computing, 1992.

[24] Rao, C. *Linear statistical inference and its applications*. Wiley, N.Y., 1965.

[25] Robinson, P. The stimulation of a non-linear average model, stochastic model and their applications. *Journal of Business*, 5 (February 1979), 81–90.

[26] Saichev, A., Malevergne, Y., and Sornette, D. *Theory of Zipf's law and beyond*. Springer, November 2009.

[27] Sammis, S., and Sornette, D. Positive Feedback, Memory and the Predictability of Earthquakes. *Proceedings of the National Academy of Sciences USA 99* (2002), 2501–2508.

[28] Sornette, D. *Why stock markets crash, Critical events in Complex Financial Systems*. Princeton University Press, January 2003.

[29] Sornette, D. Dragon-kings, Black Swans and the Prediction of Crashes. *International Journal of Terraspace Science and Engineering 1*, 3 (2009), 1–17. http://arXiv.org/abs/0907.4290.

[30] Sornette, D. Probability Distributions in Complex Systems. Article for the Encyclopedia of Complexity and System Science, 2009.

[31] Sornette, D., and Johansen, A. Significance of log-periodic precursors to financial crashes. *Quantitative Finance 1* (2001), 452. http://www.citebase.org/abstract?id=oai:arXiv.org:cond-mat/0106520.

[32] Sornette, D., and Pisarenko, V. Properties of a simple bilinear stochastic model: Estimation and predictability. *Physica D*, 237 (2008), 429–445.

[33] Taleb, N. *The Black Swan: the Impact of the Highly Improbable*. Random House, 2007.